NASA Contractor Report **181617**

Some Operational Aspects of a Rotating Advanced-Technology Space Station for the Year 2025

M.J. Queijo, A.J. Butterfield, W.F. Cuddihy, C.B. King, R.W. Stone, J.R. Wrobel, and P.A. Garn

The Bionetics Corporation
Hampton, VA 23666

Contract NAS1-18267
June 1988

NASA
National Aeronautics and Space Administration
Langley Research Center
Hampton, Virginia 23665

DISPLAY 03/6/1

88N26397*# ISSUE 20 PAGE 2765 CATEGORY 18 RPT#: NASA-CR-181617 NAS 1.26:181617 CNT#: NAS1-18267 88/06/00 313 PAGES UNCLASSIFIED DOCUMENT

UTTL: Some operational aspects of a rotating advanced-technology space station for the year 2025 TLSP: Contractor Report, May - Nov. 1987

AUTH: A/QUEIJO, M. J.; B/BUTTERFIELD, A. J.; C/CUDDIHY, W. F.; D/KING, C. B.; E/STONE, R. W.; F/WROBEL, J. R.; G/GARN, P. A.

CORP: Bionetics Corp., Hampton, VA.

SAP: Avail: NTIS HC A14/MF A01

CIO: UNITED STATES

MAJS: /*ARTIFICIAL GRAVITY/*DESIGN ANALYSIS/*ROTATION/*SPACE MANUFACTURING/* SPACE STATIONS

MINS: / GAS DYNAMICS/ MANNED SPACE FLIGHT/ MARS (PLANET)/ MATERIALS HANDLING/ REDUCED GRAVITY/ SOLAR DYNAMIC POWER SYSTEMS/ SPACE COMMERCIALIZATION/ SPACE EXPLORATION/ SPACE POWER REACTORS/ TRADEOFFS

ABA: Author

TABLE OF CONTENTS

LIST OF TABLES

LIST OF FIGURES

ABSTRACT

This report continues the study of an Advanced-Technology Space Station which would utilize the capabilities of subsystems projected for the time frame of the years 2000 to 2025. The particular studies include trade-offs of nuclear versus solar dynamic power systems that produce power outputs of 2.5 megawatts and analyses of the dynamics of the spacecraft of which portions are rotated for artificial gravity. The design considerations for the support of a manned Mars mission from low Earth orbit are addressed. The studies extend to on-board manufacturing, internal gas composition effects, and locomotion and material transfer under artificial gravity forces. The report concludes with an assessment of technology requirements for the Advanced-Technology Space Station.

ABBREVIATIONS AND ACRONYMS

A	Total Area for Leakage Passages, m^2
a	Acceleration, m/sec^2 (ft/sec^2)
ACC	Aft Cargo Carrier
ATSS	Advanced-Technology Space Station
B^2	Buckling, Geometric Shape Parameter for Critical Mass, cm^{-2}
c	Sonic Velocity, m/sec (ft/sec)
c_p	Specific Heat at Constant Pressure, J/kg-K (Btu/lb-^oR)
CAD	Computer Aided Drawing
CAE	Computer Aided Engineering
CAM	Computer Aided Manufacture
CMG	Control Moment Gyro
D	Diameter, m (ft)
D_f	Hydraulic Diameter, m (ft) = $\frac{4(\text{Flow Passage Area})}{\text{Flow Passage Perimeter}}$
d	Distance in the Circumferential Direction, m (ft)
EVA	Extravehicular Activity
g	Gravitational Acceleration of the Earth, 9.8 m/sec^2 (32.2 ft/sec^2)
GEO	Geosynchronous Earth Orbit
GLOW	Gross Lift-Off Weight
GN_2	Gaseous Nitrogen
HEO	High Earth Orbit
HLLV	Heavy Lift Launch Vehicle
I	Moment of Inertia, $kg-m^2$ ($lb-ft^2$, $slug-ft^2$)
Isp	Specific Impulse, $\frac{\text{N-sec}}{\text{kg}}$, (sec)
$IDEAS^2$	Integrated Design Engineering Analysis Software - Interactive Design and Evaluation of Advanced Spacecraft

IOC	Initial Operating Capability
I/O	Input-Output
IPV	Interplanetary Vehicle
I^2R	Electrical Energy Loss Related to Material Conductivity
IVA	Intravehicular Activity
k	Thermal Conductivity, $kW/m^2-K/m$ ($Btu/hr-ft^2-{}^oR/ft$)
L	Length m, (ft)
L →	Stairway Landing, Direction Up
LaRC-SSO	Langley Research Center-Space Station Office
LAV	Lavatory
LEO	Low Earth Orbit
LH_2	Liquid Hydrogen
LO_2	Liquid Oxygen
LOX	Liquid Oxygen
M	Molecular Weight, kg (lb)
MDLL	Mass Driven Lunar Launcher
MIT	Massachusetts Institute of Technology
MT	Metric Ton, 1000 kg
NaK	Mixture of Sodium and Potassium Liquid at Ordinary Temperatures
NSTS	National Space Transportation System
OMV	Orbital Maneuvering Vehicle
OTV	Orbital Transfer Vehicle
P	Pressure, Pa (psi)
P-C	Pressure Cure
P/L	Payload
r	Radial Distance, m (ft)
R	Gas Constant, J/mol-K ($Btu/mol-{}^oR$)

s	Displacement Distance, m (ft)
S →	Stairs, Direction Up
SC-WAO	Supercritical Wet Air Oxidizers
SDSS	Self Deployed Space Station
SDV	Shuttle Derived Vehicle
SOC	Space Operating Center
SPRTR	Separator
T	Torque, N-m (lb-ft)
TAMU	Texas A&M University
U, V, W	Angular Displacements in Degrees for the Principal Axes away from their Reference Position
UTA	University of Texas at Austin
V	Velocity, m/sec (ft/sec) or Gas Volume, m^3 (ft^3)
X, Y, Z	Principal Axis of the ATSS
α	Angular Position Degrees
γ	Ratio of Specific Heats at Constant Pressure and Constant Volume
δ	Solar Position Degrees
θ	Orbit Angular Position Relative to Solar Zenith
θe, Φe, Ψe	Euler Angles Relative to Inertial Axes, Radians
μ	Viscosity, $\frac{\text{N-sec}}{m^2}$ $\left(\frac{\text{lb}}{\text{hr-ft}}\right)$
ρ	Density, kg/m^3 (lb/ft^3)
Σ	Sum of Elements
σ	Stress, Pa (psi)
τ	Element of Mass, kg (lb)
ω	Angular Velocity, rad/sec

PARTICULAR SUBSCRIPTS

F	Position of Release for Free Fall
H_S	Hydrostatic
h	Head
m	Meridional
N	Nitrogen
NO	Nitrogen at 1 Atmosphere Pressure
o	Initial, Standard, or Stagnation Condition
O	Final Conditions
O_2	Oxygen
T	Total
v	Torus Rotating Velocity
w	Velocity within the Torus or Working Level

A Dot Indicates a Time Derivative

1.0 INTRODUCTION

One of the goals of the United States Space Program is the establishment of permanent space stations. The design of the first "IOC Space Station" is still evolving, but will probably have the general appearance of the configuration shown in Figure 1.0-1. References 1-1 and 1-2 present some details for that configuration. The IOC Space Station is nadir-pointing, and causes a rotation about its transverse axis at the rate of one revolution per orbit. Current plans are to have such a space station in low Earth orbit by about the year 1994.

Studies of space stations are under way for the more distant future, utilizing advanced technology and performing functions in support of future space missions. One series of studies is concerned with examining various aspects of a space station for the time period around the year 2025. Two reports have been published in this series of studies (References 1-3 and 1-4). The first study (Reference 1-3) led to the conceptual configuration shown in Figure 1.0-2, which is basically a rotating space station with an inertially oriented central section. The second study (Reference 1-4) used that configuration as a starting point to examine the configuration and its functions in some detail and to identify pacing technology areas.

The rotating Advanced-Technology Space Station (ATSS) provides an artificial gravity field, which reduces medical and physiological problems associated with weightless long-duration space flight (see References 1-4 and 1-5).

The present study uses the rotating ATSS configuration described in References 1-3 and 1-4 (and summarized in Section 2 of this report) for more in-depth analyses with emphasis on the following tasks:

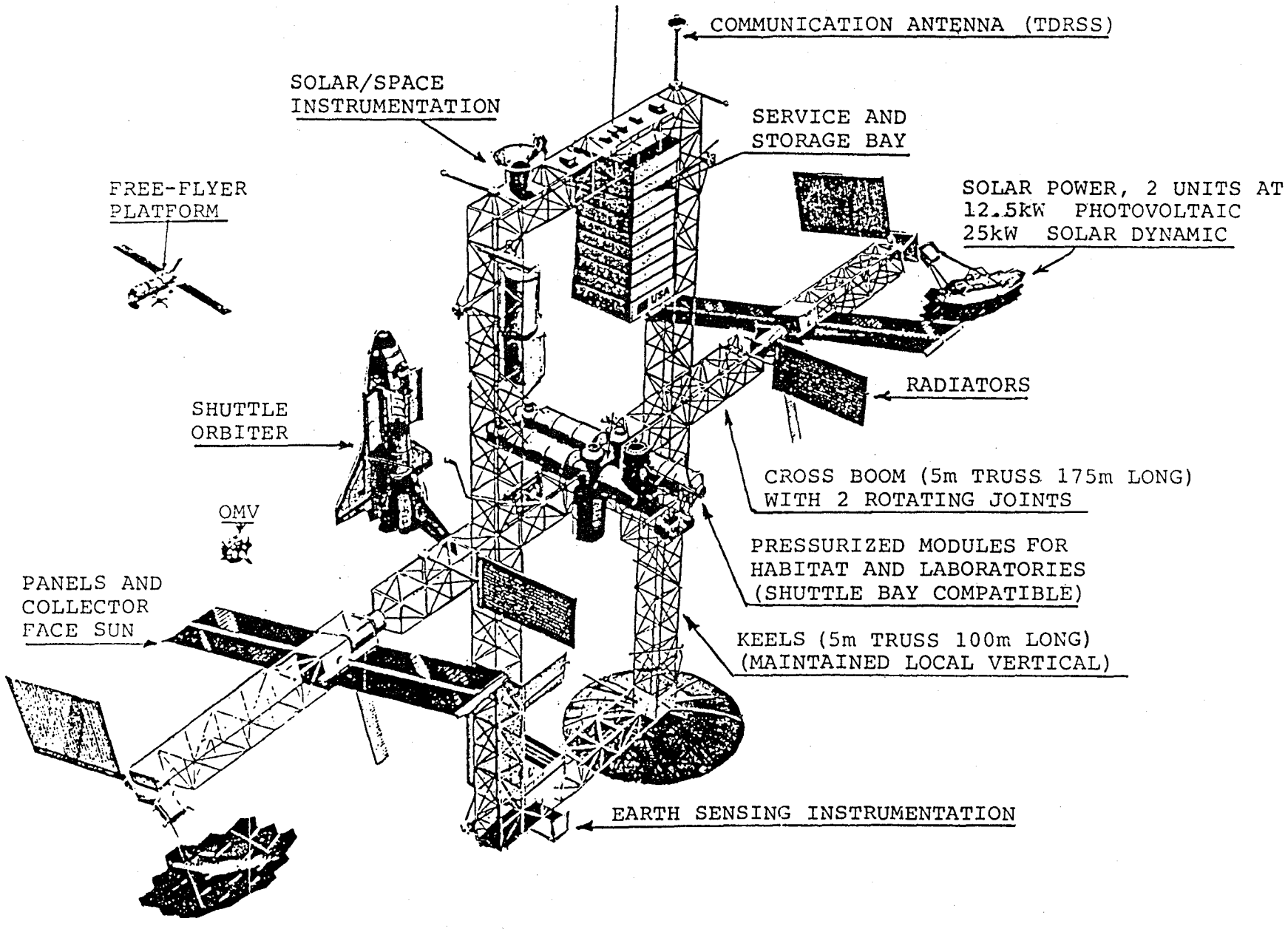

Figure 1.0-1 Baseline Configuration Dual-Keel Space Station, Principal Features

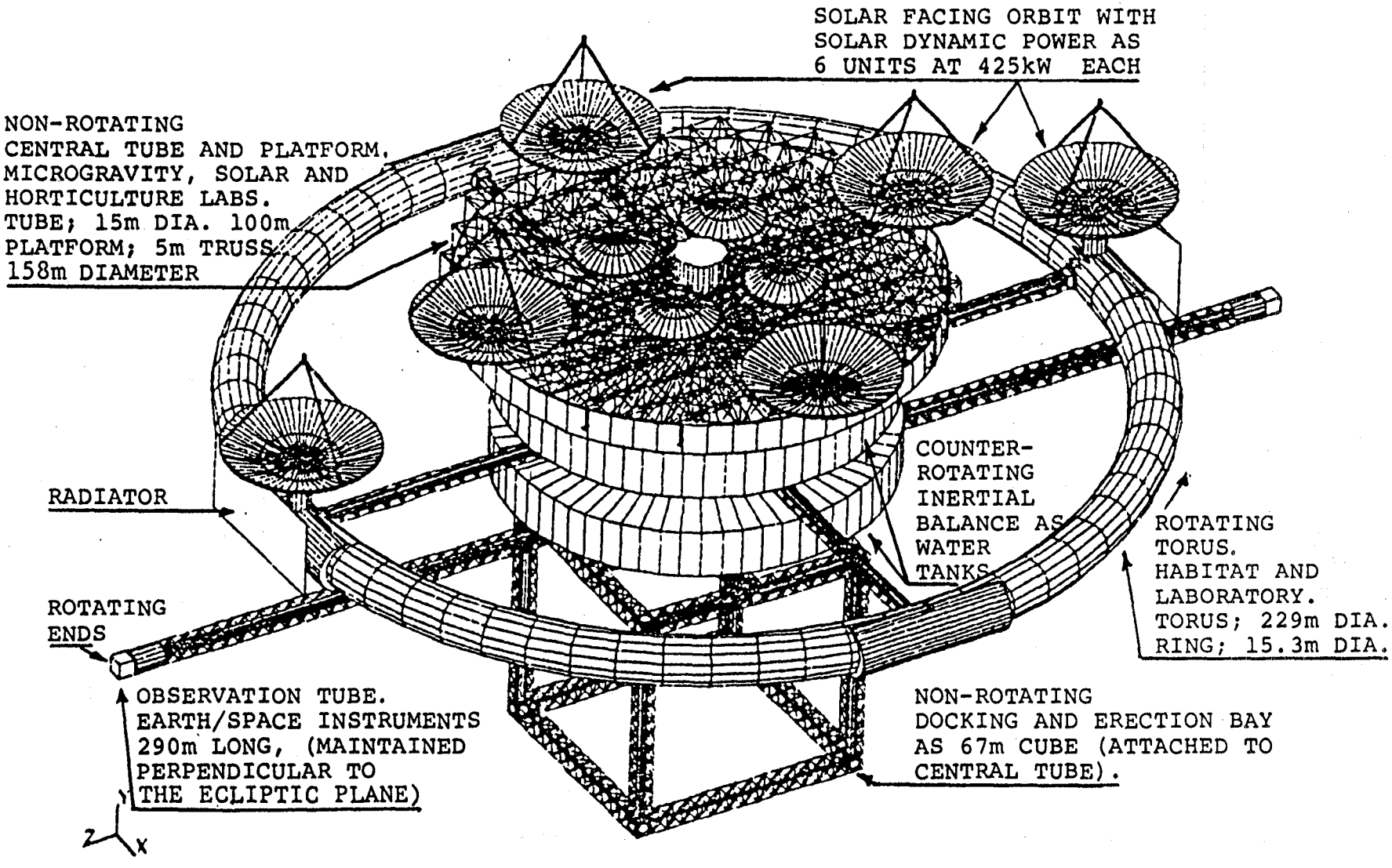

Figure 1.0-2 Advanced-Technology Space Station Concept, Principal Features of Reference Configuration

1. Perform comparative system analyses of baseline concepts, such as power generation and storage (reported in Section 3).
2. Examine operational aspects, such as orbital lifetime and control requirements (reported in Section 4).
3. Assess the effects of artificial gravity (generated by rotation) on subjects and on material transfer (reported in Section 5).
4. Examine the rigid body dynamics of the rotating ATSS (reported in Section 6).
5. Assess the feasibility of on-board manufacturing of spacecraft components for planetary missions (reported in Section 7).
6. Assess effects of reduced pressure on ATSS operations (reported in Section 8).
7. Consider the role(s) of the ATSS in support of Mars missions, using three Mars mission scenarios provided from studies by the Langley Research Center, Massachusetts Institute of Technology, and Texas A&M at Austin (reported in Section 9).
8. Identify and assess pacing technologies (reported in Section 10).

REFERENCES

1-1 Space Station Reference Configuration Description. NASA Report JSC 19989, August 1984.

1-2 Architectural Control Document. Preliminary Report, NASA JSC Space Station Office, June 1986.

1-3 Queijo, M. J. et al.: An Advanced-Technology Space Station for the Year 2025. Study and Concepts, NASA CR-178208, March 1987.

1-4 Queijo, M. J. et al.: Analysis of a Rotating Advanced-Technology Space Station for the Year 2025, NASA CR-178345, January 1988.

1-5 De Campli, William M.: The Limits of Manned Space Flight. The Sciences, September - October 1986.

2.0 ROTATING ADVANCED-TECHNOLOGY SPACE STATION CONFIGURATION

The configuration used as a starting point is described in some detail in Reference 1-4, and the major features are repeated for convenience and reference. Relevant weights and dimensions for elements of the Space Station are given in Figures 2.0-1 and 2.0-2, respectively.

The ATSS has a large rotating torus which provides artificial gravity (centrifugal force) and is the primary habitat and work area for the crew and also provides gas (O_2 and H_2) storage. An artificial gravity of one Earth g, 9.8 m/sec^2 (32.2 ft/sec^2), can be obtained at 2.8 revolutions per minute. Two solar dynamic units on the torus provide electrical power for use in the torus.

The other components of the ATSS are attached to a central tube which remains Sun-pointing and does not rotate with the torus. These units include a celestial observatory, an Earth observatory, a platform with horticultural domes and four solar dynamic units, and a section for berthing, loading, and unloading spacecraft. The entire ATSS is Sun-pointing, and therefore, precesses at the rate of one revolution per year.

The baseline configuration had two alternatives. It was examined briefly with and without storage tanks that rotated counter to the torus. Reasons for considering use of counterrotating tanks are discussed in Section 5 of Reference 1-4. Tanks could be used for fluid (water) storage and also to reduce the net angular momentum of the Space Station.

In reference to the baseline configuration, the studies described in this report provide additional information regarding "some operational aspects" and pacing technologies pertinent to a rotating Advanced-Technology Space Station for the year 2025.

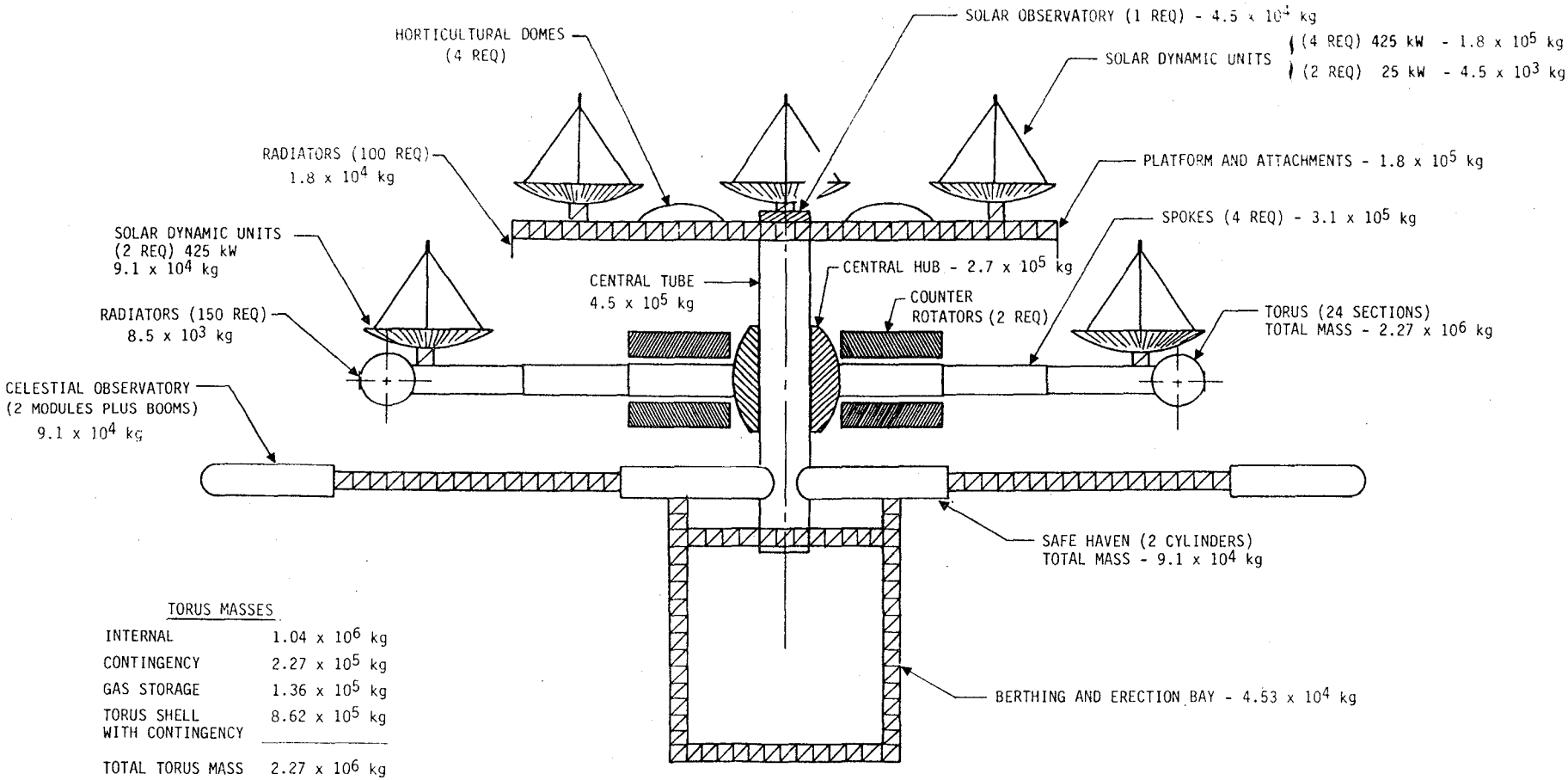

Figure 2.0-1 Space Station Subassembly Masses

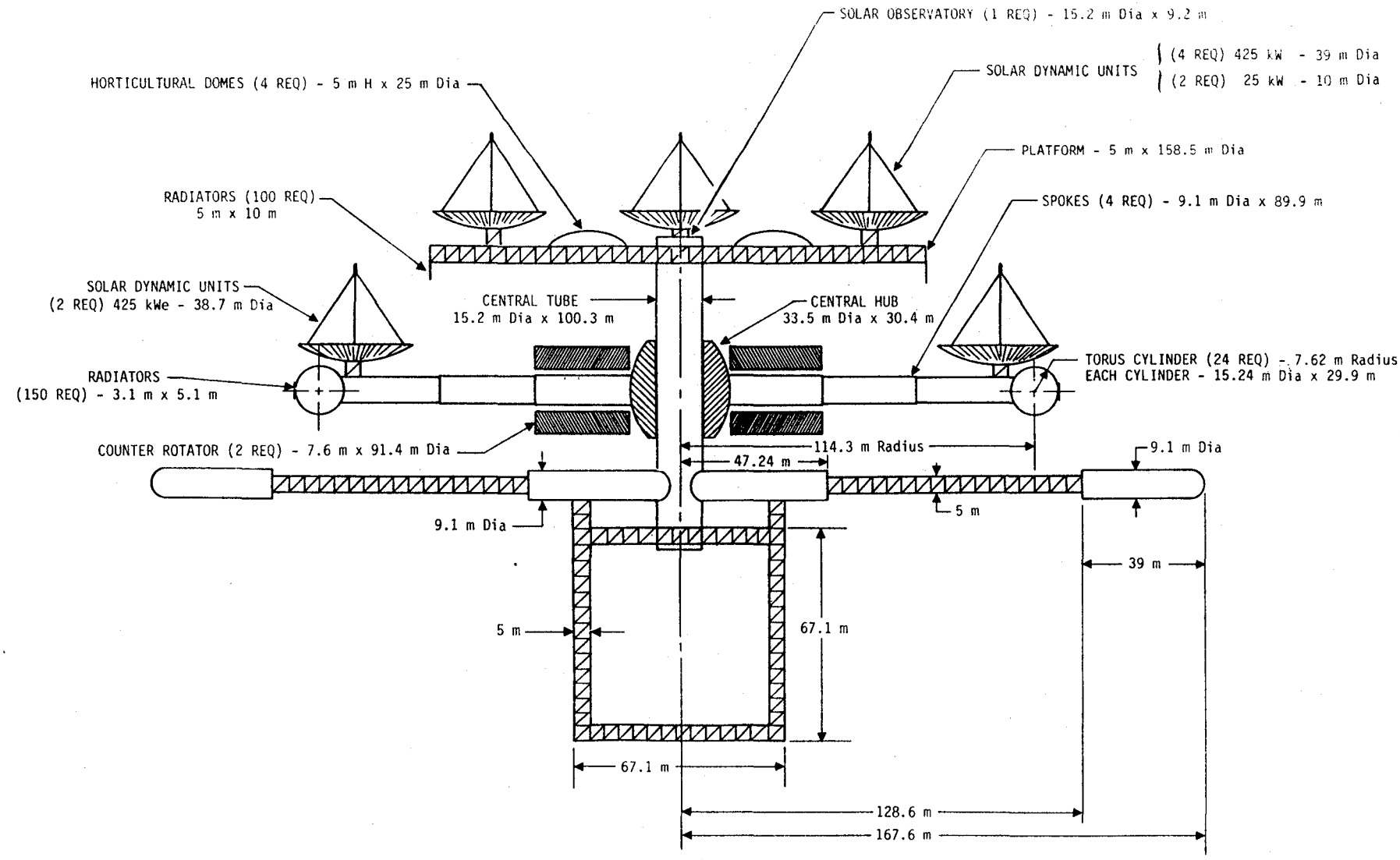

Figure 2.0-2 Space Station Dimensions

3.0 ON-BOARD POWER GENERATION - A COMPARISON OF SOLAR DYNAMIC AND NUCLEAR FISSION HEAT SOURCES

Operating the subsystems within the rotating Advanced-Technology Space Station (ATSS) and performing some of the different, unique tasks, such as on-board generation of oxygen and hydrogen for atmospheric replenishment and additional propellant fuel, will place large demands on the electrical power system. The ATSS concept utilizes about 2550 kW of electric power supplied by a solar dynamic system considered fundamentally more efficient than a photovoltaic system. The solar dynamic system consists of six identical units, of 425 kW output each, as the baseline electric power system. Solar dynamic systems experience long shadow times during each orbit, and their structures are still relatively large compared to other continuous heat sources. A comparison and evaluation of alternative heat sources for power generators appears prudent.

Alternative types of heat sources are radioisotope decay, nuclear fission, and potentially, nuclear fusion. Both radioisotope decay and nuclear fission sources have experienced space flight (References 3-1 through 3-3) but not at the power levels or in the configurations required by the ATSS. Therefore, a careful comparison is required of the parameters governing the design of each alternative. Nuclear fission represents the principal heat alternative; consequently, this effort compares the nuclear fission alternative to the solar dynamic baseline system.

3.1 Comparison Evaluation Approach and General Results

3.1.1 Approach

The comparison first generates a baseline configuration for the ATSS solar dynamic units as the reference for comparison evaluations of the alternates in terms of mass, control requirements, and configuration-related elements.

The evaluation proceeds in a sequence of four steps with each step making contributions to those which follow:

A. Define a Thermal Cycle for Energy Conversion

The initial step defines the operating thermodynamic parameters for a closed-cycle gas turbine as the input to an electrical generator. The selection of a closed-cycle gas turbine was influenced by its independence from local gravity effects. The Space Station has four platform-mounted units operating in microgravity and two torus-mounted units operating in a rotation-induced field which can range up to a one Earth gravity equivalent. The operating parameters for the cycle are drawn from previous definitions (Reference 3-4) and include a 320 K radiator temperature and a 40 percent energy throughput conversion efficiency.

B. Define the Baseline Solar Dynamic Unit

The definition for the baseline solar dynamic unit includes conceptual configurations for the concentrator, collector, converter, and radiator, plus the mounting and the pointing control elements. The detail of definition extends to a level which allows an estimate of mass, an estimate of control requirements, and an assessment of specific constraints or operational considerations.

C. Define a Nuclear Fission Heat Source

A concept which employs nuclear fission reactors as the heat source for six converter-radiator units is generated and compared with the baseline solar dynamic system. The comparison includes a range of reactor shield material options in addition to the control requirements and configuration-related considerations. The comparison of shield weights and shield options provides a degree of insight for the conditions which would determine a minimum power threshold for application of fission reactors to space power systems.

D. System Comparisons and Evaluations

The mass estimates provide the first and most objective comparisons for the system. The comparison of control requirements assesses the number of parameters, required accuracy, range, and operating frequencies to make a general comparison of relative complexity or difficulty. The comparison of particular features makes a generalized assessment of relative difficulty in responding to entirely different sets of requirements.

3.1.2 General Results

Section 3.5 contains the comparisons and assessments which lead to the following specific conclusions and results relative to each of the pertinent features.

A. Energy Conversion Efficiency

A 40 percent energy conversion efficiency appears achievable through performance improvements in rotating machinery and heat recovery techniques (regenerators for Brayton cycles or co-generation for Rankine cycles). The cycle calculations show that for any combination of

rotating components, the performance of the heat exchanging elements defines the practical operating efficiency. High efficiency turbines or compressors cannot compensate for performance losses within heat exchangers.

B. Solar Dynamic Power Systems

The concentrators for 425 kW power systems were recognized as large area structures and priority candidates for both materials development and configuration development for reduced mass. The 40 percent throughput efficiency results in a near equal area for radiators and underscores the need for their low mass configurations. The size of the elements leads to a system configuration which effectively becomes a non-interruptable continuous power generator. Modulation of the solar input appears to require movement (or masking) for portions of the concentrator area and thereby introduces complexities to the control functions. Energy storage in phase change material adds a significant thermal inertia to the collection and conversion sequence. The masses associated with a 425 kW power unit and the thermal inertia of the system combine in a manner that only permits slow changes; an emergency or uncontrolled shutdown could damage portions of the system.

C. Nuclear Fission Reactors

The evaluation confirmed shield weight as the dominating element for the system. The evaluation of candidate materials for a shield revealed a factor of five in the range of shield weights and indicated an overall mass advantage by using shield materials of high density. The comparison of shield mass as a function of core size and output power indicates a decreasing mass-to-power ratio with increased output and suggests that a

thermal output of 3 MW is a practical lower limit for an individual reactor in this type of an application.

D. Comparison of Systems

The comparisons revealed similar system masses, system controls, and specific operational conditions. The estimate of masses showed one shield option (lead) for a nuclear system at a lower value than the baseline solar dynamic system. The control requirements showed near equal complexities in addressing the functions with different parameters (converter controls are the same for both systems). The particular considerations traded complexities in assembly and start-up for the solar dynamics with recovery of radioactive components after reactor operation and did not show a decisive difference. This comparison indicates that the selection of a heat source for power generation should be decided by mission requirements rather than power system features or complexities.

3.1.3 Continuing Evaluations

The results from comparing solar dynamic and nuclear fission heat sources indicate the need for extending the comparison to include radioisotope decay and estimating nuclear fusion potentials. In addition, the comparisons will benefit from including the option for advanced photovoltaics coupled with advanced energy storage elements, such as batteries, fuel cells, or flywheels.

3.2 Definition of the Thermodynamic Cycle for Energy Conversion

The thermodynamic cycle defined for converting heat energy into an electrical output draws upon the previously established values of 320 K (576^{o}R) for the radiator temperature and a 40 percent throughput

efficiency for energy conversion (Reference 3-4). The cycle selected utilizes GN_2 as the working fluid and produces 450 kW. The added increment of power recognizes the system need for internal fluid pumping and the operation of system controls without diminishing the energy delivered for Space Station functions. Table 3.2-1 summarizes the thermal cycle for temperatures, pressures, and energies using GN_2 at a flow rate of 4.08 kg/sec (9 lb/sec). The specific features of the cycle include or reflect the following considerations:

3.2.1 Compressor Conditions

Within the Carnot equation for maximum theoretical efficiency, the compressor inlet represents the low temperature limit for a closed cycle gas turbine application. Here, the inlet temperature is fixed by a 320 K (576^{o}R) radiator surface temperature. A working margin of 2.5 K (5^{o}R) above the metal temperature plus a 27.5 K (50^{o}R) temperature difference from the inlet GN_2 yields the 350 K (631^{o}R) value for the compressor inlet. The establishment of the inlet pressure and compression ratio must recognize that an optimum compression ratio will exist for any combination of component efficiencies and turbine inlet temperature (Reference 3-5). Here, the optimum compression ratio must fall between 2.7 and 2.8 to yield a cycle efficiency above 42 percent. This compression ratio and a compression efficiency of 0.93 can be achieved by a single stage centrifugal design. The selection of pressure levels relates to the creep-stress limits for high temperature materials in the heat exchangers. This cycle has the potential for increasing the energy throughput by increasing the pressure levels. Operation at a maximum pressure of 13.788 MPa (2000 psi), with increased velocities in the heat

TABLE 3.2-1 SUMMARY OF THE CONVERTER THERMODYNAMIC CYCLE

Flow GN_2 at 4.08 kg/sec (9.0 lb/sec)

1. Compressor	Inlet	Outlet
Temperature, K (^{O}R)	350 (631)	471 (849)
Pressure, MPa (psia)	2.07 (300)	5.52 (800)
Energy in, kW (Btu/sec)	514 (490)	
Efficiency	0.93	
2. Regenerator - High Pressure		
Temperature, K (^{O}R)	471 (849)	783 (1410)
Pressure, MPa (psia)	5.52 (800)	5.45 (790)
Energy exchange, kW (Btu/sec)	1326 (1263)	
3. Source Heat Exchanger (NaK Counterflow)		
NaK Temperature, K (^{O}R)	1048 (1887)	1076 (1937)
NaK Flow, kg/sec (lb/sec)	39.41 (86.90)	
GN_2 Temperature, K (^{O}R)	783 (1410)	1047 (1886)
GN_2 Pressure, MPa (psia)	5.45 (790)	5.42 (785)
Energy Exchange, kW (Btu/sec)	1124 (1069)	
4. Turbine - Alternator		
Temperature, K (^{O}R)	1047 (1886)	815 (1468)
Pressure, MPa (psia)	5.42 (785)	2.14 (310)
Energy out, kW (Btu/sec)	987 (940)	
Efficiency	0.95	
Alternator:		
Energy In, kW (Btu/sec)	472.5 (450)	
Electrical Energy Out, kW	450	
Efficiency	0.95	

TABLE 3.2-1 SUMMARY OF THE CONVERTER THERMODYNAMIC CYCLE (concl.)

5. Regenerator Low Pressure	**Inlet**	**Outlet**	
Temperature, K (^{o}R)	815 (1468)	502 (906)	
Pressure, MPa (psia)	2.14 (310)	2.10 (305)	
Energy Exchange, kW (Btu/sec)	1326 (1263)		
6. Precooler Heat Exchanger, Water Counterflow			
Temperature, K (^{o}R)	502 (906)	350 (631)	
Pressure, MPa (psia)	2.10 (305)	2.07 (300)	Compressor Inlet
Energy Exchanged, kW (Btu/sec)	650 (619)		
Water/Radiator:			
Temperature, K (^{o}R)	350 (631)	322 (581)	
Flow, kg/sec (lb/sec)	5.58 (12.3)		
Radiator Surface, K (^{o}R) Temperature	322 (581)		

exchangers could double the energy throughput (at some sacrifice in cycle efficiency).

3.2.2 Regenerator Considerations

Overall cycle efficiency of 40 percent involves the recovery of waste heat (Reference 3-6) either as regeneration or cogeneration. The performance of the regenerator in gas turbines effectively establishes the source heat input requirement and the heat rejection requirement for the radiator. Regeneration with a 32.2 K (58°R) temperature difference and a minimum pressure loss requires a performance improvement from contemporary practices.

3.2.3 Turbine Conditions

The energy required to drive the generator combined with the energy required to drive the compressor and overcome the turbine losses establish the required turbine inlet temperature. The defining equation has the form (from Reference 3-6):

$$\frac{\text{Turbine Total Work}}{\text{Mass Flow (Specific Heat)}} = \text{Turbine Inlet Temp.} \left(1 - (\text{Expansion Ratio})^{\frac{\gamma - 1}{\gamma}}\right)$$

γ = Ratio of Specific Heats, 1.4 for Diatomic Gasses

The turbine inlet temperature at 1047 K (1886°R) falls within the capability of existing materials, but represents a practical upper limit for heat obtained from a liquid metal combination that remains a liquid at ordinary temperatures. This application uses a 60 Na-40 K mix which melts at 292 K (527°R) and boils at 1080 K (1960°R). The turbine at an efficiency of 0.95 represents a small increment of improvement from present radial in-flow configurations.

3.2.4 Heat Exchangers

The two heat exchangers show the least requirement for additional development. The high temperature heat exchanger would require development of a coating or alloy which would provide a ten-year life against erosion by liquid metal. Any increase in the operating pressure would add creep stability to the development requirement. The low pressure heat exchanger appears conventional, and water provides the coolant for the temperature range described. Water offers the synergy for sharing with other subsystems (it can operate with reclaimed water) and the use of the hot water as a supplemental ATSS heat source. The inherent flexibility of a water-cooled heat exchanger, where the energy transfer is a function of the local velocity, allows a flow versus temperature trade evaluation for any outlet temperature below boiling conditions. This comparison assumes one atmosphere pressure with boiling at 370 K ($672^{o}R$).

3.2.5 Other Considerations

Alternate thermal cycles could be defined using other gases and other flows. An initial evaluation using CO_2 as the other "on-board" gas option revealed a need for either an increased flow (regenerator size) or a higher turbine inlet temperature (liquid metal limits). The difference stems from the ratio of specific heats at 1.4 for diatomic GN_2 against 1.28 for triatomic CO_2. The noble monatomic gases with specific heat ratios of 5/3 (1.666) offer significant thermodynamic advantages and most of the current experimental systems utilize a heavy noble gas (A, Kr, Xe) (References 3-2 and 3-3). Since these gasses would not occur or be

utilized otherwise in the ATSS operations, they were not selected for the comparison.

The selection of GN_2 underscores the basic physical constraints associated with any cycle that generates electrical energy from a heat source. The low temperature limit for the cycle defines a radiator area. The high temperature requirement must address material limits in both structure and heat transfer media. Waste heat must be recovered without an undue compromise of the flow parameters. Thermal cycle efficiency stands as the effective countermeasure to overall system weight, and a 40 percent throughput efficiency presents a technical challenge for space power systems.

3.3 Solar Dynamic Baseline Configuration

A solar reflecting surface configured as a full paraboloid of revolution characterizes the six identical solar dynamic units selected as the baseline. The principal features and dimensions of the system appear in Figure 3.3-1 which illustrates one of four units mounted on the platform. The system configuration places the concentrator focus at the collector aperture. The collector and converter are mounted as an assembly supported on a tripod. A central pedestal-type mounting with actuators allows local pointing and tracking. The descriptions and discussions which follow address the concentrator and its mounting, the collector, the converter, and the radiator. These descriptions lead into a summary of masses, control complexities, and an assessment of other pertinent considerations.

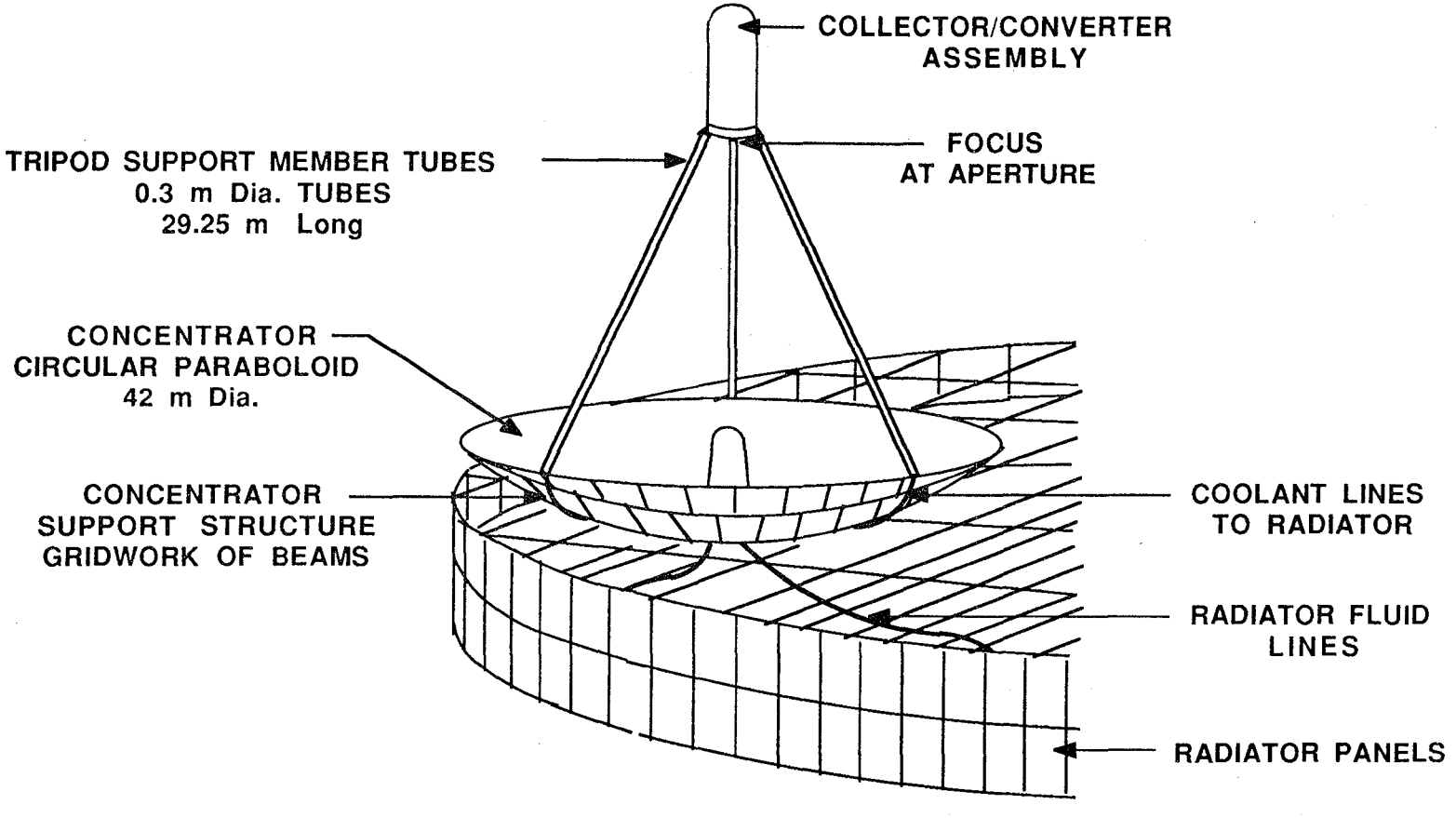

Figure 3.3-1 Solar Dynamic Power System, Platform Installation

3.3.1 The Solar Concentrator and Mount

The paraboloid of revolution provides a surface area and reflecting efficiency sufficient to provide a continuous output of 450 kW. An earlier study (Reference 3-4) required a 39 m (128 ft) diameter concentrator; however, the present baseline for evaluation uses a diameter of 42 m (137 ft) with a 3 m (10 ft) diameter opening at the center for the mounting cone. A solar input of 1.35 kW/m^2 and a 0.9 reflecting efficiency provides 1684 kW at the focus as the thermal input energy requirement for a 90 minute orbit period with 0.66 period illumination. An analytic expression for a parabola which generates such a reflector surface has the form:

$$y = 0.01x^2 \qquad \text{(x, y in meters with origin at the vertex)}$$

Construction of the reflecting surface will use a mosaic of elements. The surface is divided into concentric rings or zones, and each zone is further divided into a number of segments. Each segment within a zone would be identical. The mounting structure becomes a corresponding array of rings and radials that support and align the individual reflective elements. Requirements for surface accuracy and structural support stem from the dispersion limit of a 0.3 degree footprint envelope for the solar beam at the focus. Angular deviations of a reflected beam are double the angular error at the reflecting surface; therefore, the requirement on contour relates to an angular limit of 0.15 degree. In effect, a smooth curved surface must not deviate from the parabolic model by more than 2.5 parts per thousand (sin 0.15 degrees) in any direction along the reflecting surface. Specifically, if 2 points, 20 cm (8 in) apart, are defined as "on" the

parabola, then a smooth curve which joins them cannot deviate from the parabola by more than 0.5 mm (0.02 in) at the center, either as a bump or dimple. These limits appear stringent, but are developmentally achievable.

In operation, the collector-converter housing masks the center of the concentrator; A mounting installation makes use of the masked area. Figure 3.3-2 illustrates the concept. A cylindrical pedestal 2 m (6.6 ft) in diameter, with a hemispherical cap provides a mount and a pivot for pointing. A cone faired from the 3 m (10 ft) inner ring of the concentrator to a conforming hemisphere carries the concentrator, tripod, and collector-converter assembly. Pointing is accomplished by a pair of orthogonally placed actuators. Pointing range and accuracy define the stroke and position resolution requirements for the actuators. A one degree pointing range equates to approximately one day's change (or error) in a solar facing one-per-year revolution. At the inner ring of the concentrator, a one-degree range equates to a total actuator stroke capability of 15 cm (6 in) with instantaneous positions kept within a 2.5 cm (1 in) tolerance band. These requirements are not severe. Actuator force levels are specific to the installation. Platform mounted units would require forces sufficient to overcome low speed friction and static friction effects. Actuators for units on the torus would have to operate cyclically in synchronization with rotation, and these considerations are discussed as part of the particular considerations. (See paragraph 3.3.8.)

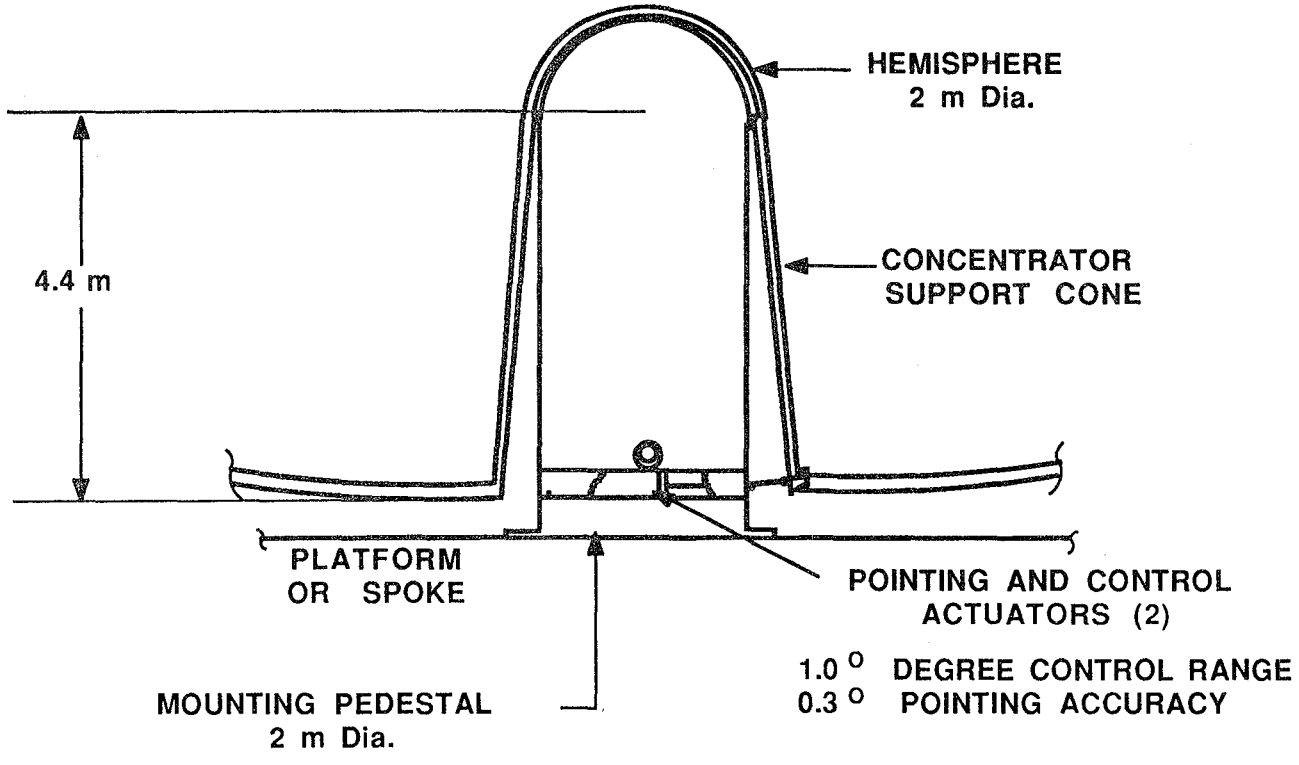

Figure 3.3-2 Concept for the Pointing Control and Mount

3.3.2 The Collector Concept

During each 90-minute orbit, the collector accepts a thermal solar flux of 1684 kW (1604 Btu/sec) for 60 minutes and converts the energy into a fusion phase change of which 558.3 kW (532 Btu/sec) is stored in the fusion phase change in order to provide a 1124 kW (1069 Btu/sec) continuous output. The concept for the collector employs a eutectic mixture consisting of 0.774 sodium fluoride plus 0.226 magnesium fluoride which melts at 1103 K (1985^{o}R) with a latent heat of 656 kJ/kg (281 Btu/lb). The flow of energy through the collector utilizes two liquid metal loops. A primary loop accepts the solar input and melts phase change material. A second loop supplies heat energy to the converter by solidifying phase change material. Figure 3.3-3 shows the principal features for the collector-converter assembly, and Figure 3.3-4 shows the principal details of the collector. These are described below in terms of the aperture and cavity, the phase change material, insulation requirements, and the liquid metal pumps.

A. The Aperture, Cavity, and Aperture Doors

The focal point for the concentrator is at the midpoint of the aperture both radially and axially. A perfect surface and perfect alignment would present the solar energy as an 89-degree cone on either side of the focal point. At the focal distance, a 0.3-degree tolerance for collector contour results in an energy footprint with an 11.5-cm (4.5 in) radius. The pointing accuracy limit of 0.3 degree doubles the footprint radius to 23 cm (9 in). This aperture doubles that radius for margin to prevent any portion of the solar beam from contacting either the aperture liner or insulator, thus generating an aperture with a nominal diametrical opening of 1 m (40 in).

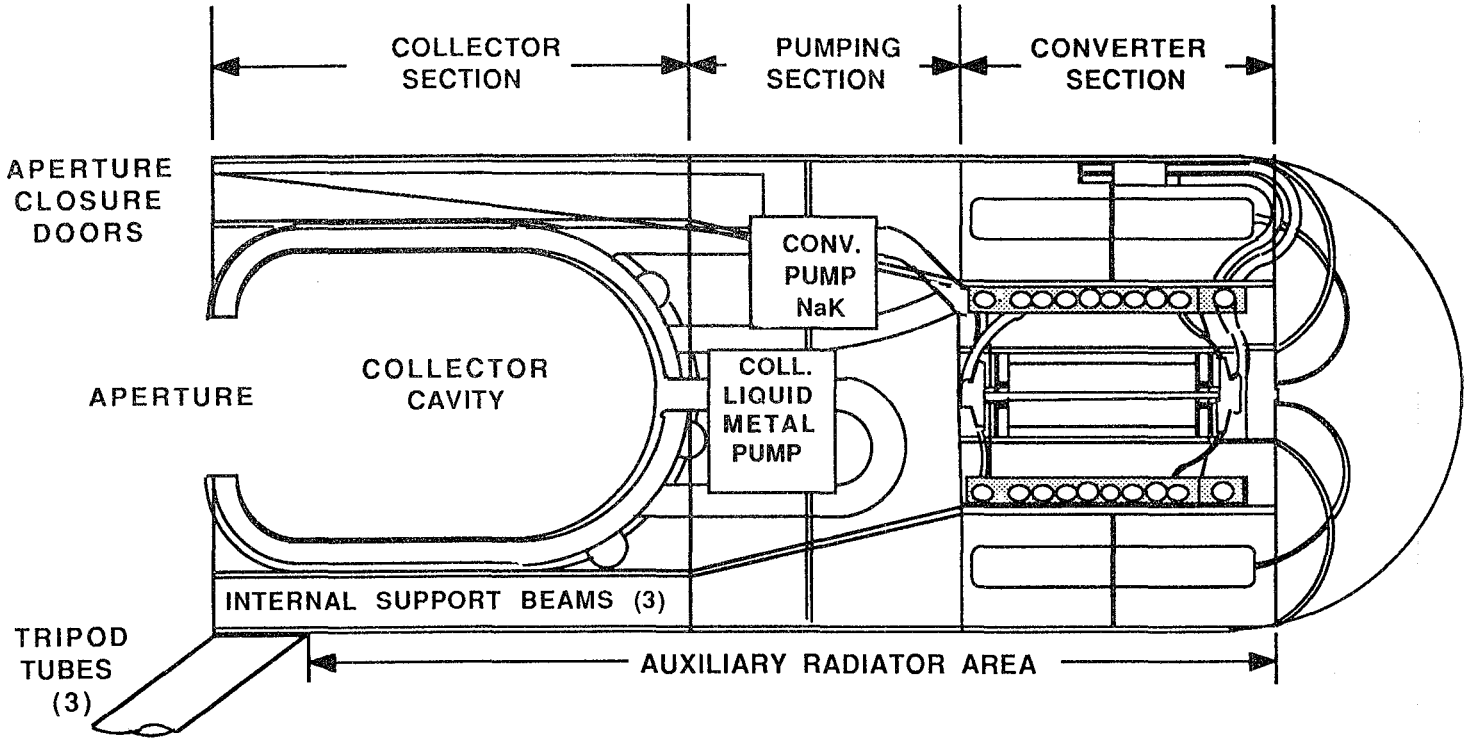

Figure 3.3-3 Collector/Converter Assembly Concept

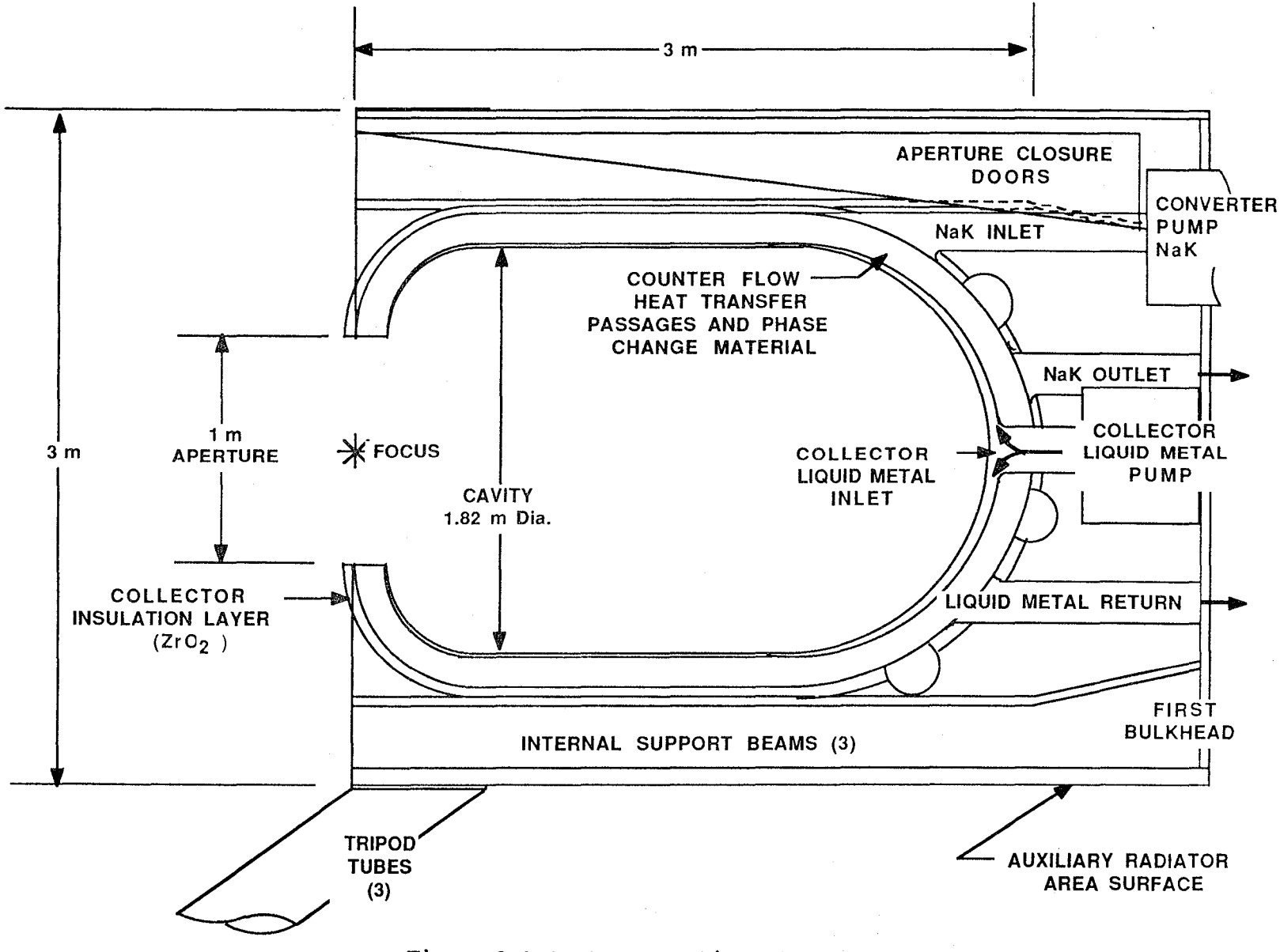

Figure 3.3-4 Cross Section of the Collector

Heat flux through the walls and the required volume of phase change material established the cavity size and shape. A heat flux of 128 kW/m^2 (11 Btu/ft^2 sec) yielded the 1.82 m (6 ft) diameter for the hemisphere, cylinder, torus-quadrant shaped cavity (cylinder L = 1.5 D) and accommodated the phase change material in a layer 15.2 cm (6 in) thick.

Within the cavity, liquid metal first cools the hemisphere and then flows along the cylinder toward the aperture. Liquid metal then returns through passages within the phase change material. Liquid metal flow conditions have an inlet temperature of 1157 K ($2086^{o}R$) which is 55 K ($100^{o}R$) above the melting temperature of the phase change material and a temperature rise of 41.6 K ($75^{o}R$) at the aperture. A cavity wall of 3 mm (0.125 in) nickel based alloy (79 Ni, 13 Cr, 7 Fe) results in a maximum cavity liner temperature of 1225 K ($2205^{o}R$) near the aperture. These temperatures are in the "orange" color range. To conserve energy, the aperture must close at sunset and reopen during sunrise. The three aperture doors are elements of a right circular cylinder with edges contoured to make a closure at full extension. In a closed position, the doors must reflect any incident sunlight away from the ATSS. A limiting condition occurs for rays from the periphery of the concentrator. A twenty-two degree half-cone for the doors results in a reflection just above the aperture plane.

B. Heat Transfer Materials, Exchange of Heat

The thermal storage requirement amounts to a phase change for 3115 kg (6869 lb) of 0.774 NaF-0.226 MgF salt. A margin of 15 percent results in a total phase change inventory of 3600 kg (8000 lb). The phase change material is carried in three layers separated by heat

transfer passages containing liquid metal; Figure 3.3-5 illustrates the concept. From the inlet, the liquid metal collector coolant flows along the liner wall within a ribbed passage that transfers heat into the phase change material. Liquid metal flow in a return passage completes the heat transfer into the melted phase change material. The NaK liquid metal from the converter heat exchanger enters in a ribbed passage along the outer shell of the collector. The NaK inlet temperature is 55 K (100^{o}R) below phase change and increases by 27.5 K (50^{o}R) as it flows through the inlet and return passages. In operation, the converter extracts heat through a phase change interface which continuously moves in an orbit-related cycle. The NaK passages always have a rime of solid phase change material. Collector liquid metal coolant passages maintain a layer of molten phase change material. The thickness of phase change material between passages does not exceed 2.5 cm (1 in) and thereby minimizes any differences in the output heat transfer.

C. Thermal Insulation

The outer surface of the collector operates "full red" and therefore requires an insulation blanket that combines low conductivity with high temperature compatibilities. Ceramics such as MgO, Al_2O_3, and ZrO_2 are the candidates; Reference 7 lists their melting temperatures and thermal conductivities. Zirconium oxide offers the best combination, it melts at 2973 K (5350 ^{o}R) and has the lowest thermal conductivity at 1.672 W/m^{2}K/m (0.97 Btu/hr ft^{2o}R/ft); in addition CaO stabilized ZrO_2 has an established compatibility with high temperature nickel and iron based alloys. The collector has an insulation layer 12 cm (4.75 in) thick of 50 percent density ZrO_2. External cooling is required to maintain the thermal gradient, and that heat becomes part of the load for

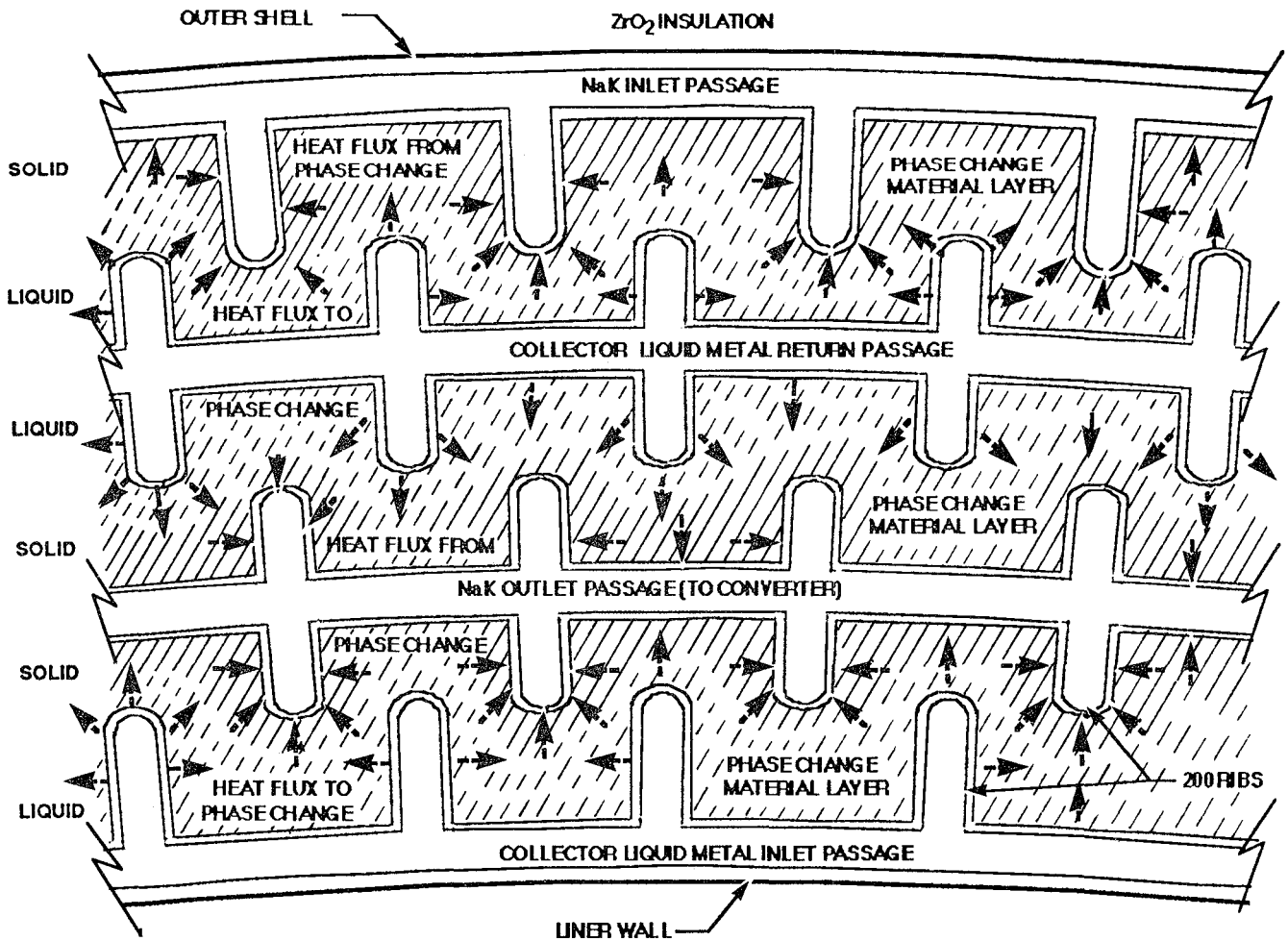

Figure 3.3-5 Cross Section through the Collector Wall Showing the Heat Transfer Passages and the Phase Change Material

a secondary radiator formed into the cylindrical walls of the collector-converter housing structure.

D. Liquid Metal Pumps

Liquid metal in both loops will be driven by electromagnetic pumps; Figure 3.3-6 illustrates the concept. The pump utilizes the electrical conductivity of the metal stream to produce a force by passing a current through a magnetic field. Current through the liquid metal is perpendicular to the field and thereby generates a pumping force within the liquid metal. There are no moving elements. The application indicates a flow passage 12 by 25 cm (4.75 by 9.5 in) operating with a 10,000-gauss field and up to 1,000 amperes. A 5 kW power consumption has been allotted for coils and leads.

3.3.3 The Converter Section

The converter concept implements the closed gas turbine thermal cycle described above (Section 3.2); Figure 3.3-7 shows the overall layout and follows the same general approach described for units presently in development (Reference 3-3).

Rotating elements consist of a centrifugal compressor and a 400-Hz alternator driven by a radial in-flow turbine, all on a common shaft. Heat exchangers and a regenerator surround the rotating section. Control-related elements and the lines to the radiator are carried by surrounding support structure. Pertinent details are summarized for the turbine-alternator, the heat exchangers, and the control elements.

A. The Turbine-Alternator Section

The 400-Hz alternator establishes rotational characteristics. The selected alternator follows established practice and consists of a four-

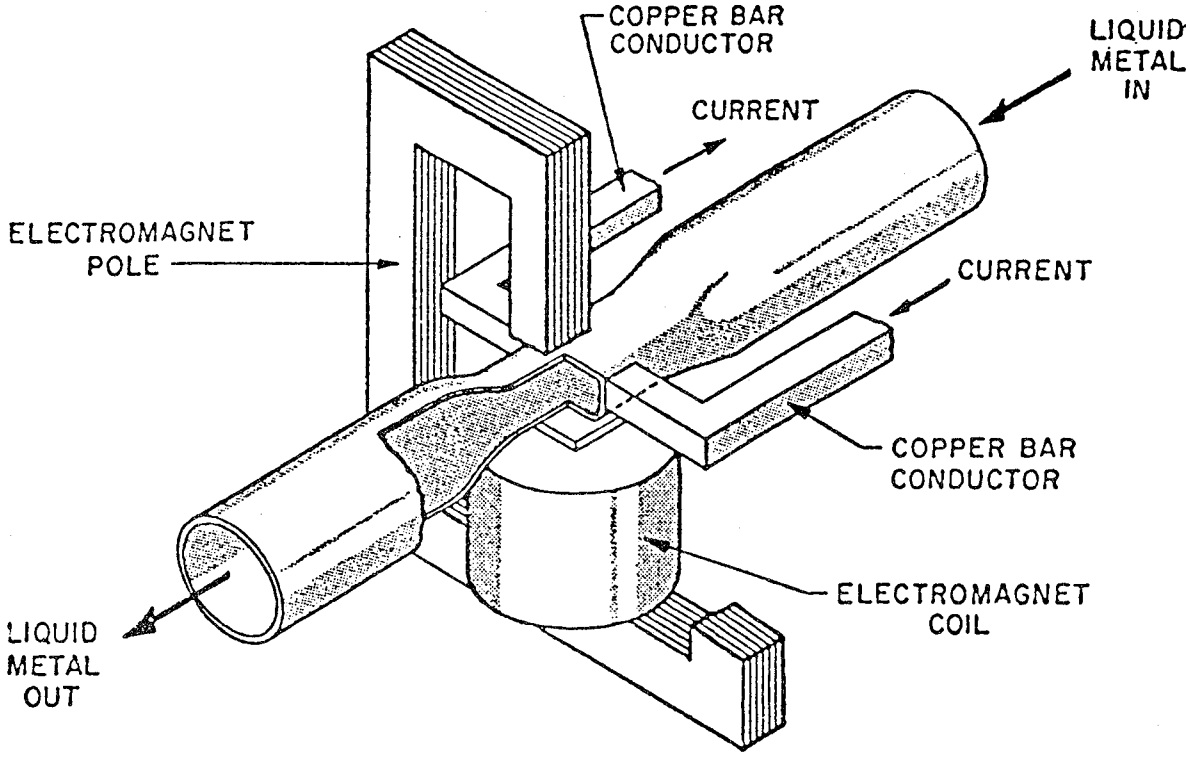

Figure 3.3-6 Concept for a Liquid Metal Electromagnetic Pump
(from Reference 3-7)

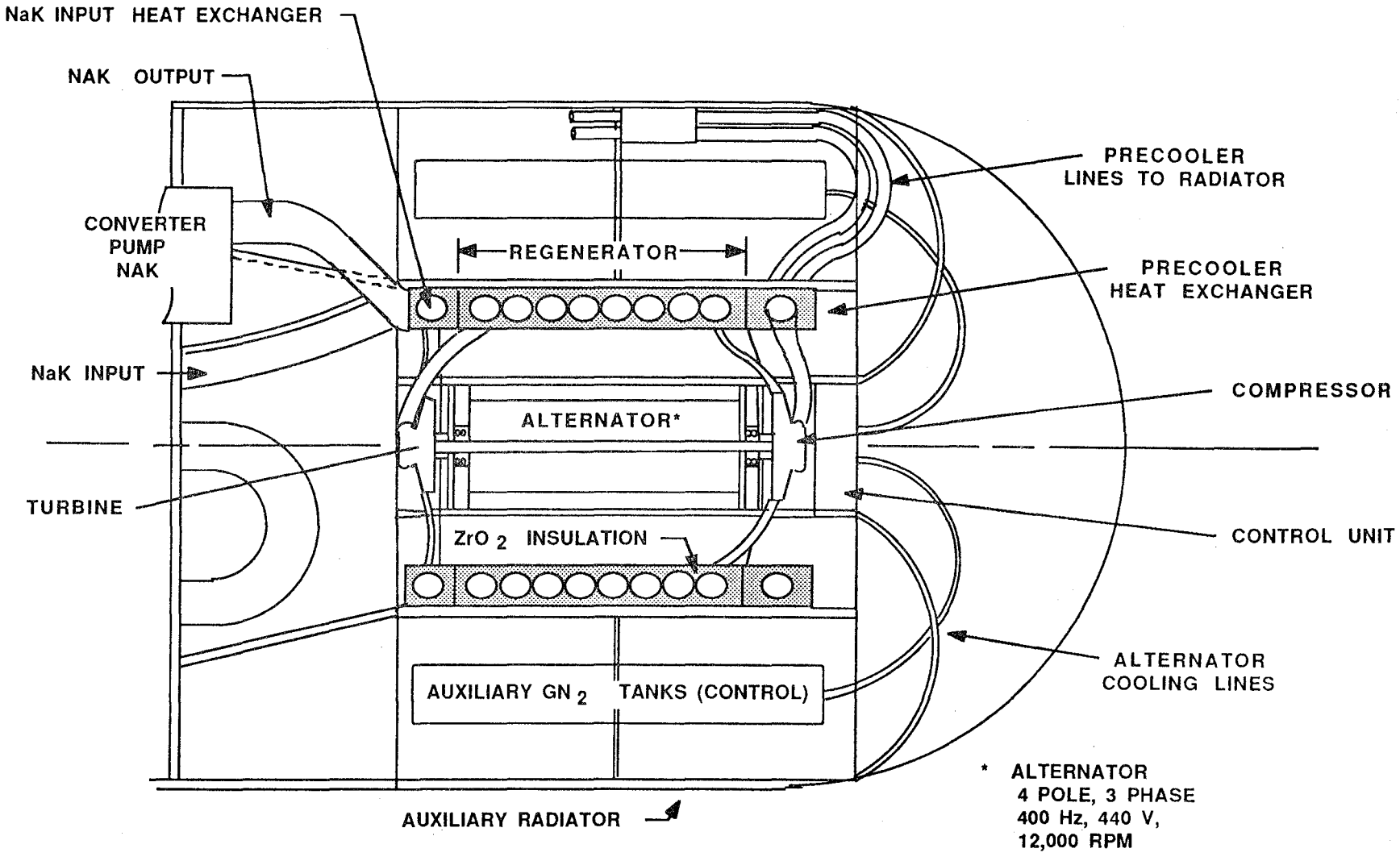

Figure 3.3-7 Converter Section Concept

pole magnet rotating at 12,000 rpm to deliver 400 Hz, 440 V, three phase alternating current from stationary armature coils. Electrical conditions dictate a single rotating speed and a constant armature excitation current to provide a rotating magnetic field. A compression ratio of 2.666 at a thermal efficiency of 0.93 requires a rotating peripheral velocity of 365.8 m/sec (1200 ft/sec) and results in an impeller diameter of 58.4 cm (23 in). This dimension effectively establishes an outer diameter for the support casing. A radial in-flow turbine drives the unit. The configuration requires two sets of bearings, electrical slip rings for armature current, and some form of heat extraction. Figure 3.3-7 shows a pressure shell which provides bearing supports, electrical access, a magnetic flux return through generator coils, and a cooling jacket. Bearing supports indicate ball types, although gas film bearings (air bearings) are preferred. The alternator is a candidate application for low loss (superconducting) electrical leads for rotating magnet coils and for stationary generating coils.

B. The Heat Exchangers and Regenerator

Heat exchangers and the regenerator are configured as a ten turn helical coil consisting of a 29 tube bundle inside an elliptical casing; Figure 3.3-8 illustrates the cross section. In operation, high pressure GN_2 leaves the compressor housing in 29 tubes of 1.27 cm (0.5 in) diameter and enters an elliptical casing to form a counterflow regenerator. These tubes continue through the NaK high temperature heat exchanger and become turbine inlet passages. A low pressure discharge from the center of the turbine flows as a single duct to become a return flow around the tubes inside the regenerator housing. Return flow

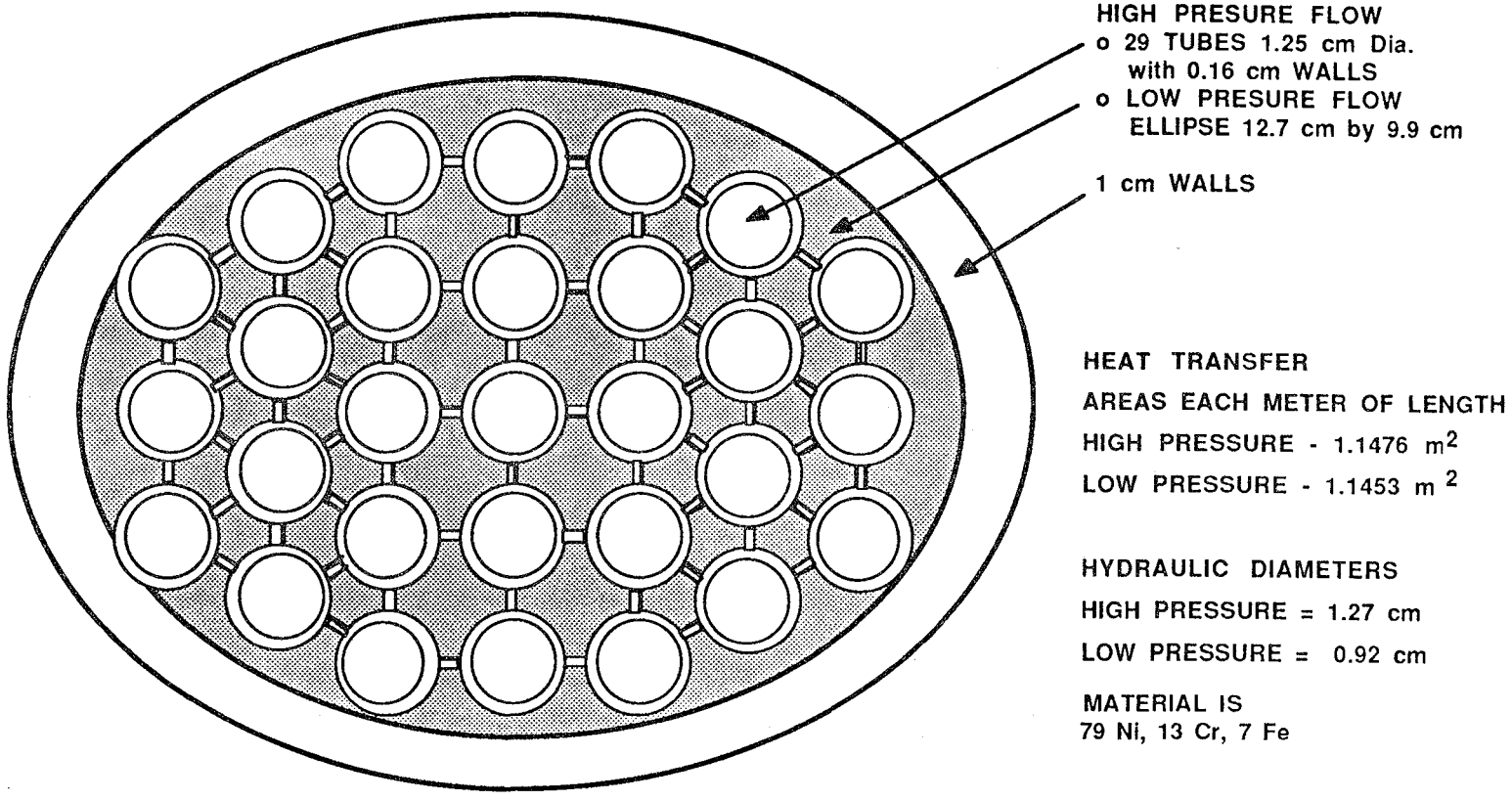

Figure 3.3-8 Converter Regenerator and Heat Exchanger Cross Section

continues into the precooler and passes over a water cooled tube bundle and then into the compressor inlet. Heat transfer predictions were based on the established dimensionless ratio equations using Dittus-Boelter for gases and Lyon for liquid metals (Reference 3-7):

For gasses flowing in tubes:

$$Nu = 0.023\ (Re)^{0.8}\ (Pr)^{0.4}$$

$$\frac{hD_f}{k} = 0.023 \left(\frac{D_f V \rho}{\mu}\right)^{0.8} \left(\frac{c_p \mu}{k}\right)^{0.4}$$

D_f = Hydraulic diameter
c_p = Specific heat at constant pressure
h = Film transfer coefficient
k = Thermal conductivity
V = Velocity
ρ = Density
μ = Viscosity

For liquid metal flowing in tubes:

$$Nu = 7 + 0.025\ (Pe)^{0.8}$$

$$\frac{hD_f}{k} = 7 + 0.25 \left(\frac{D_f V \rho c_p}{k}\right)^{0.8}$$

The film transfer coefficient for water employs an empirical equation that includes effects of temperature and has the general form:

$$h = A \quad f(t) \left(\frac{V^{0.8}}{D_f^{0.2}}\right)$$

The constant A and the coefficients in the temperature function have dimensional dependence (Reference 3-7). The relationship that determined the lengths for the exchangers and regenerator involved the film transfer coefficient, area as a function of length, and the wall-to-gas temperature balanced against flow, specific heat, and temperature rise in the gas stream. Within each heat exchanger, the length was constructed as a sum of two or more elements representing inlet, mid, and exit flow conditions.

Lengths for each of the three individual heat exchanging sections appeared as multiples of 3.5 m (11.5 ft) and thereby established a center line diameter of 1.1 m (44 in) for the helical wraps. Since heat

conservation is a primary consideration, all ten loops are imbedded in a ZrO_2 insulation matrix.

C. Control and Auxiliaries

Control requirements are derived from a continuous heat input that generates a 400 Hz alternating current at 440 V. Solar energy delivered to the collector must be converted into electrical energy. Therefore, an alternator must operate into a closely matched, near-constant load. Small changes in energy throughput are accomplished by corresponding small changes of compressor inlet pressure. An inherent lag in response for closed cycle gas turbines dictates slow changes over a narrow range of power output. A control system, therefore, requires some reserve gas supply and pumps for managing reserves. The control system will also need to perform "housekeeping" functions that provide coolant flows to the insulation blankets, the alternator, and the bearings. In addition, the control must provide signals for opening and closing aperture doors and signals to pointing-tracking elements. (The obvious location for the Sun sensor is at the apex of the collector-converter housing.)

3.3.4 The Radiator

Radiating area and radiator operating temperatures combine to determine an overall heat rejection capability. A 320 K (576^{o}R) radiator metal temperature and water with a 27.5 K (50^{o}R) temperature rise sets the flow rate at 5.62 kg/sec (12.4 lb/sec). Dissipation of 650 kW (619 Btu/sec) results in 1102 m^2 (11,864 ft^2) of radiator area. The actual radiating surface consists of individual panels; Figure 3.3-9 shows the principal features for a panel. Panel installations on the platform consist of two complete rings with each converter connected to a quadrant

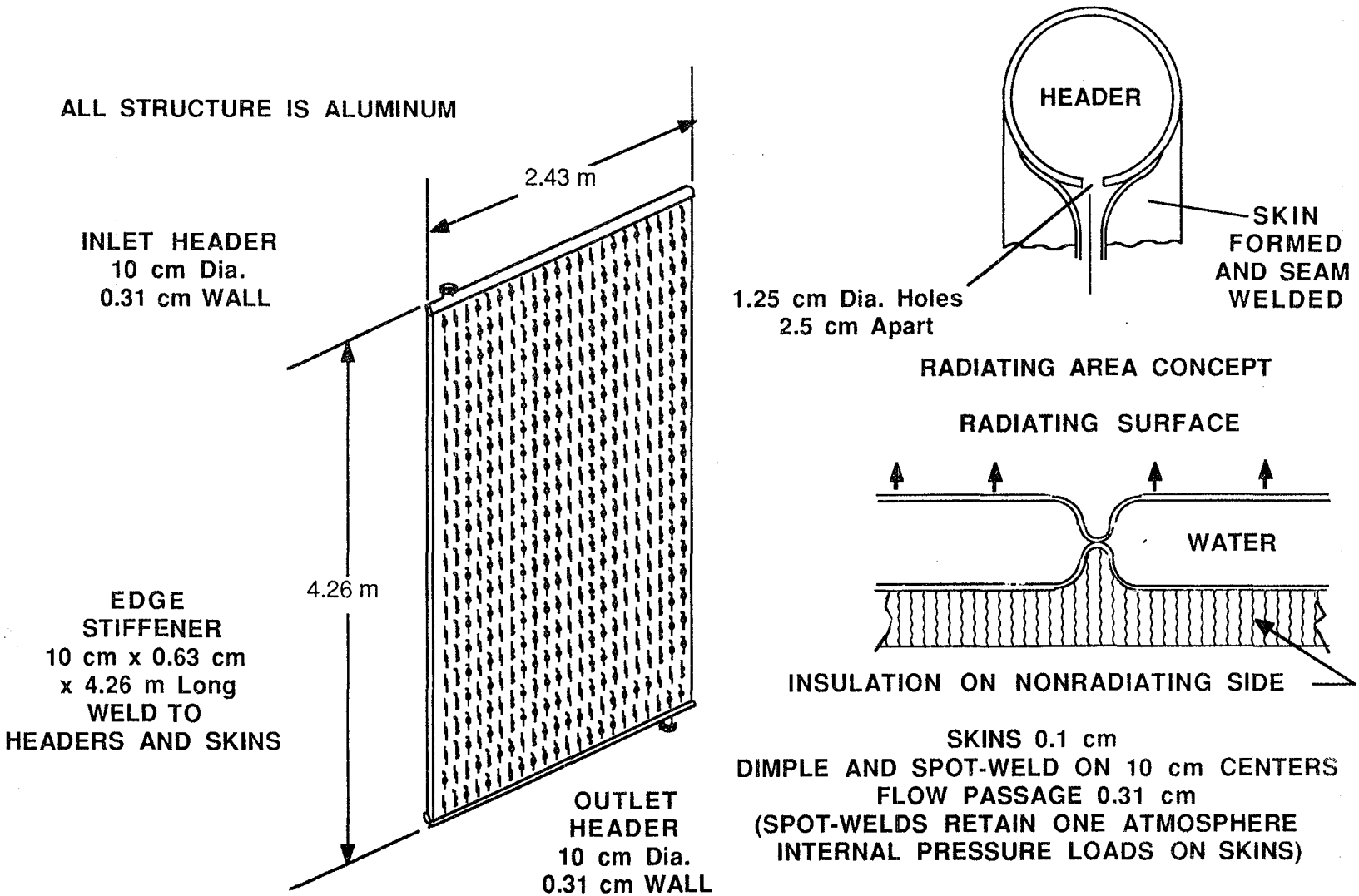

Figure 3.3-9 Radiator Panel Concept (102 for Each Converter)

containing 51 panels in each row for a total of 102. Radiator panels on the torus are set in a single row and extend around two-thirds of the periphery. The 102 panels total 1061 m^2 and require a radiation rate of 0.613 kW/m^2. An equivalent radiation temperature is 323.67 K (582°R), which is acceptable considering a 27.5 K (50°R) actual temperature difference between the two headers on each panel. Flow in each panel amounts to 0.055 kg/sec (0.12 lb/sec) and represents 0.16 percent of the total radiator flow volume. The flow equates to about a 10.4 minute transit time through a panel and, thereby, shows some margin in the radiator area. For example, operation at the median temperature of 334 K (601°R) would require a radiator area of 933.2 m^2 (10045 ft^2), or 12 percent less than the value stated. On the other hand, each radiator panel will spend up to 40 percent of an orbit with the Earth in view and operate with a reduced radiant heat transfer. The margin will be retained and include cross-feed between radiator sections on the platform.

3.3.5 Summary of Masses for the Solar Dynamic Units

The summary of estimated masses for the principal elements of a solar dynamic power unit is given in Table 3.3-1. The summary is divided into elements subject to pointing and tracking movements and elements which are fixed to the ATSS. Considerations and bases for masses are as follows.

A. Concentrator

The concentrator structure masses represent 2024 alloy aluminum as plates, beams, and tubes. The concentrator surface, as a mosaic of reflectors, has 3 mm (0.125 in) plates in segments nominally 3 m (10 ft)

TABLE 3.3-1 SOLAR DYNAMIC SYSTEM MASS SUMMARY

	kg		(lb)	
MOVEABLE ELEMENTS (Subject to Solar Pointing and Tracking Motions)				
Concentrator Elements:				
Reflecting Surface	9115		(20098)	
Supporting Structure	7679		(16932)	
Support Tripods	2214		(4881)	
Electrical Leads and Coolant Lines	1834		(4043)	
Total Each Concentrator		20842		(45954)
Collector Elements:				
Lines, Heat Transfer Passages	4469		(9854)	
Phase Change Material	3268		(7205)	
Liquid Metal	544		(1119)	
Liquid Metal Pumps	453		(999)	
Aperture Doors, Drives	1088		(2399)	
Insulations (ZrO_2)	4438		(9786)	
Internal Structure	704		(1552)	
Secondary Radiator	682		(1503)	
Total Each Collector, Assy.		15646		(34417)
Converter Elements:				
Turbine Alternator Unit	846		(1865)	
Heat Exchangers	1663		(3667)	
Insulation	1059		(2335)	
Controls and Auxiliaries	268		(591)	
Total Each Converter, Assy.		3836		(8458)
Mass Subject to Motion		**40324**		**(88914)**
FIXED ELEMENTS				
Radiator Elements:				
Radiator Panels (102)	10549		(23260)	
Radiator Fluid Lines	2200		(4851)	
Total Radiator Structure		12749		(28111)
Panel Coolant Fill (102)	8033		(17712)	
Fluid Line Fill	6474		(14275)	
Total Coolant Fill		14507		(31987)
Concentrator Mount and Actuators		1663		(3667)
Total Fixed Mass		**28919**		**(63766)**
Total Each Unit		69243		(152680)
TOTAL SPACE STATION (6 Units)		415458		(916084)

squares or equivalent. Supporting structure consists of rectangular box beams 0.2 m by 0.4 m (8 in x 16 in) formed from 2 mm (0.08 in) plate. Supports consist of seven rings joined by radials along the edge of each reflecting panel. Tripod legs are tubular 0.3 m (12 in) in diameter with 10 mm (0.40 in) walls and 29.25 m (96 ft) long.

Electrical leads are copper transmission lines sized for 3 phase 440 V and 450 kW. Water lines are 10 cm (4 in) diameter tubes with 3 mm walls (0.125 in) which extend from the collector-converter assembly down to a flexible joint at the mounting pedestal.

B. The Collector Assembly

Flow passages and the collector structure utilize 89 Ni, 13 Cr, 7 Fe alloy throughout. The cavity liner and shell utilize 3 mm (0.125 in) thickness; flow passages within phase change material utilize 1.5 mm (0.06 in) thickness. Phase change material has a 15-percent margin above that quantity which changes phase during each cycle. Liquid metal fills the flow inlet and flow return passages for both the collector and the NaK loops. The mass represents a 0.56 Na - 0.44 K mix in both loops plus a small margin; however, the collector loop operates above the temperature limit for NaK, and would probably utilize a Na-Li mix.

Masses for the pumps are estimates for iron required in the magnet plus a 25-percent allowance for windings and electrical conductors. Aperture doors utilize a reflecting surface based upon a series 310 or equivalent stainless steel structure plus a 40-percent addition for the actuation mechanism. Insulation utilizes stabilized ZrO_2 at a density of 50 percent of theoretical maximum (porous sintered ZrO_2). Supporting structure consists of three longitudinal I-beams with two circumferentials plus an auxiliary circumferential ring at the tripod

joints. The cylindrical housing and hemispherical cap are assumed to be 1.5 mm (0.06 in) thick aluminum. An auxiliary 1 mm (0.040 in) skin covers the cylindrical section and has dimples and welds to form the flow passages in the same manner as the main radiator panels.

C. The Converter Assembly

A mass estimate for the turbo-generator represents extrapolation from published studies and a comparison with present masses for aircraft on-board power units. The major element of mass results from the heat exchanger configuration which consists of 89 Ni, 13 Cr, 7 Fe alloy throughout. Insulation masses are based upon 50 percent porous ZrO_2. Auxiliaries consist of a pressure control unit plus storage tanks for GN_2 used to adjust system operating pressures.

D. Concentrator Mount and Actuators

The mounting pedestal is assumed to be an aluminum cylinder formed from 3 mm (0.125 in) plate with stiffeners of equal thickness. Actuators and reaction members allow for either a hydraulic unit or an electrically driven ball screw (e.g., like flap actuators for transport aircraft).

E. The Radiators

Radiator mass estimate considers individual panels as structural elements and adds the length of lines. Lengths for fluid lines assume a distributor feed line with a length of 102 panel widths plus an identical collector line. Both the feed and collector lines will require supplemental lengths to reach connections at the mounting pedestal. All lines are considered as 0.1 m (4 in) diameter aluminum with 3 mm (0.125 in) walls. Filled mass assumes water throughout the entire system of lines, headers, panels, and returns.

3.3.6 Control Parameters

The control-related features for a solar dynamic unit are in Table 3.3-2. Control will utilize a dedicated computer with five sub algorithms working in concert. Pertinent conditions or governing features for each are as follows:

A. Solar Pointing

Solar pointing has to be maintained throughout an orbit to assure an energy input and to prevent damage. A ZrO_2 insulation layer cannot withstand prolonged exposure to the concentrated (6000 K) solar input. Presently available Sun sensors have the required acquisition and sensing capability and pointing actuators with the required force range presently exist. Cycling requirements for units on the platform appear modest and could typically be accommodated by a Sun sensor with an expanded (e.g., 3 degree) field of view. Signals for the aperture doors can be derived from the Sun sensor supplemented by temperature monitors in the liquid metal streams of the collector.

B. Liquid Metal Loops

The liquid metal loops perform the energy transfers and require precise controls. The control system will modulate relatively large currents in the electromagnetic pumps. Such controls and precisions have been developed for the nuclear power industry and could be adapted for these applications. Controlled liquid metal flows must continue during the dark portion of an orbit. The collector liquid metal flow will need to be maintained but temperatures must not drop below the solidification point at 1103 K (1985^{o}R) for the phase change material. The NaK loop must operate at near-constant temperature and flow; and stored solar input energy must be removed from phase change material before reheating.

TABLE 3.3-2 SUMMARY OF CONTROL REQUIREMENTS FOR A SOLAR DYNAMIC POWER SYSTEM

Control Function or Element	Output or Action	Range	Precision	Rate/ Frequency
Solar Pointing Algorithm				
· Sun Sensor	Error Signal to Actuator, 2 axes	1^{o} Half Cone	0.15^{o} Circular	Steady or 0.5 Hz
· Concentrator Pointing	2 Axis Position	1^{o} Half Cone	0.3^{o} Circular	Steady
· Solar Tracking (Torus Unit only)	2 Axis Cyclic Positioning	1^{o} Half Cone Cyclic	0.3^{o} Circular	0.05 Hz
· Aperture Door Actuator Close, Open	Door Movement During Sunset/Sunrise	3.5 m Stroke (11.5 ft)	0.2 cm Limits (1 in)	Close-Open and Orbit
Liquid Metal Loops Algorithm				
· Collector Coolant Pump Flow	Pump Current Modulation	300-1000A	0.5A	Cyclic with Orbit
· Collector Coolant Temperature	Signal for Pump Control	320 to 1222 K (560 to 2200^{o}R)	3^{o} K (9^{o}R)	Cyclic with Orbit
· NaK Coolant Pump, Flow	Pump Current Modulator	300-1000A	0.5A	Steady
· NaK Temperature	Signal for Pump Modulator	320 to 1083 K (560 to 1950^{o}R)	2 K (3^{o}R)	Steady
Heat Rejection Radiator Algorithm				
· Water Flow Pump	Pumping Volume and Pressure	0 to 10 kg/sec (0 to 22 lb/sec)	0.1 kg/sec (0.25 lb/sec)	Steady
· Water Temperature	Signal to Pump Control and Valve Control	273 to 373 K (520 to 680^{o}R)	2 K (3^{o}R)	Steady
· Radiator Temperature	Signal to Pump Control	273 to 373 K (520 to 680^{o}R)	2 K (3^{o}R)	Steady
· Cross-over Valves, Operation	Signal from Water Temperature	Open Close	1 Percent of Position	Cycle During Part of Orbit

TABLE 3.3-2 SUMMARY OF CONTROL REQUIREMENTS FOR A SOLAR DYNAMIC POWER SYSTEM (continued)

Control Function or Element	Output or Action	Range	Precision	Rate/ Frequency
Converter Operating Algorithm				
· Rotation Speed	Error Signal to Input Valves and Electric Load Balance	0-12200 rpm	0.1 rpm	Steady
· Magnet Current	Error Signal to Electric Load	0-500A	0.1A	Steady
· Electrical Load and Phase Balance Volts, Amperes for Each Phase	Signal to Valves Switching Signals to Internal Load Leveling Elements	0-500A	0.1A	Steady
· Compressor Inlet Control and Resevoir Valves	Feed or Bleed to Maintain Speed	Open-Close Profile	0.01 of Profile	Steady
· Regenerator Temperature (multiple)	Signal to Valves	320-1083 K (560-1950^{o}R)	2 K (3^{o}R)	Steady
· Liquid Metal Heat Exchanger Temperatures (Multiple)	Signal to Valves	320-1083 K (560-1950^{o}R)	2 K (3^{o}R)	Steady
· Precooler Heat Exchanger Temperatures	Signal to Valves	273 to 555 K (560 to 1000^{o}R)	2 K (3^{o}R)	Steady
· Gas Stream Temperatures (Compressor, Regenerator Turbine)	Signal to Valves	320 to 1083 K (560 to 1950^{o}R)	2 K (3^{o}R)	Steady
· Gas Stream Pressures (Compressor Regnerator Turbine)	Signal to Valves	0 to 6894 mPa (0 to 1000 psia)	34.5 kPa (5 psi)	Steady
· Bearing, Lube or Gas Supply Temperature Pressure Flow	Signal to Control Valves	Configuration Particular Each Case	0.01	Steady

TABLE 3.3-2 SUMMARY OF CONTROL REQUIREMENTS FOR A SOLAR DYNAMIC POWER SYSTEM (concluded)

Control Function or Element	Output or Action	Range	Precision	Rate/ Frequency
Collector Converter Housekeeping Algorithm				
• Component and Structure Temperatures, Multiple (Heat Transfer through Insulation, etc.)	Signal to Coolant Pump and Flow Control Valve	320-555 K (576-1000°R)	2 K (3°R)	Steady
• Component and Structure Coolant Temperatures, Multiple	Signals to Coolant Pump and Flow Control Valves	273 to 473 K (520 to 850°R)	2 K (3°R)	Orbit Cycle
• Secondary Radiator Temperatures, Multiple	Signals to Coolant Pumps and Flow Control Valves	273 to 473 K (520 to 850°R)	2 K (3°R)	Orbit Cycle
• Secondary Radiator Coolant Flow Rates, Multiple	Signal to Flow Control Valves	0 to 10 kg/sec (0 to 25 lb/sec	0.1 kg/sec (0.25 lb/sec)	Orbit Cycle
• Secondary Coolant Flow Control Valves, Actuators	Position in Response to Signal	Close to Open	0.01 Stroke	Orbit Cycle
• Secondary Coolant Pump Flows	Output in Response to Signal	0 to 10 kg/sec (0 to 25 lb/sec)	0.01 Flow	Orbit Cycle

As a control measure, the NaK velocity could be increased to offset effects of a thickening layer of phase change material. An increased velocity in the converter heat exchanger would improve heat transfer from the NaK metal and retain the turbine inlet at the desired temperature.

C. Heat Rejection Radiators

Heat rejection radiators provide a near-constant heat sink for the system. The radiator area has some inherent margin, and the rotating radiators on the torus will use that margin to offset reduced radiation when the Earth is in the field of view. A cross-linking of the radiator panels on the platform will provide a common radiator for all four units and thereby offset any reduced effectivity for that portion which sees the Earth.

D. Converter Operation

Converter control has critical requirements. Tolerances on frequency (rotation) and output voltages (magnet current) are small; load-leveling becomes a significant requirement. In this context, electrolytic decomposition of water plays the major load-leveling role. Half of the available power can be fed into electrolysis should the need arise. More significantly, currents and allocated power can be varied continuously and smoothly over the entire range. Electrolytic cells provide the energy buffer necessary for operation of a solar dynamic system based upon large area concentrators.

E. Housekeeping

Housekeeping functions perform an environmental control within the confines of the collector-converter assembly. The heat rejection capabilities of the structural surface will vary with position around the orbit and require a control algorithm which accommodates the variables

due to orbit position while maintaining an acceptable operating environment. In effect, improved heat rejection in the cold shadow of the Earth must offset temperature rise from direct sunlight. Housekeeping controls must provide the means for accomplishment.

3.3.7 Particular Considerations

Installation and operation of a 450 kW solar dynamic power unit identify two areas of particular impact. The first consideration relates to the assembly, servicing, and eventual dismantling of the units, and a second consideration relates to operation on the torus in a rotationally induced gravity field.

A. Considerations for Assembly, Servicing, and Dismantling

Concepts for transport and on-orbit assembly of the solar dynamic units have been addressed in previous studies (Reference 3-8). Assembly of the concentrator and placing of the collector require long-reach booms and manipulators. A complicating detail appears in the start-up sequence for a unit. Each reflecting element of the concentrator will require a final adjustment-to-focus as part of the on-orbit assembly. During this phase, each element will need a radiation-rejecting cover that does not compromise the reflecting surface by either contamination or transfer of heat. In addition, exterior surfaces of protective covers must not focus incoming solar energy. After all concentrator reflective elements have received final alignment, removal of the covers must proceed in an orderly manner. The collector will be cold and the collector liquid metal (if in place) will be solid. A gradual warming start will build up to full operation. Some kind of auxiliary power will be required to spin the turbine-alternator to a point where the cycle can

maintain itself. Once operational, the system has no easy means for shutdown. Radiation input has to be interrupted such as reapplying the covers during a transit of the Earth shadow. Shutdown for servicing, replacement, or dismantling becomes a preplanned event. Emergency shutdown implies a technique for flipping mirror segments into an edge-on solar alignment and accepting some potential for harm to elements in the collector-converter assembly or ice forming in radiator panels.

B. Operation on the Rotating Torus

Operation on the rotating torus introduces two particular dynamic effects which are a steady-state moment reaction and a low frequency oscillation. The masses of the concentrator and the collector-converter assembly introduce substantial torque moments relative to the mounting plane and they must be reacted against equilibrators aligned with the tripod legs. The mass of the collector assembly in an Earth-equivalent gravity field will result in a tension force of 199646N (44,564 lb) parallel to a tripod leg oriented radially and a compression force of 99823N (22,282 lb) in each of the two other legs. (The tripod tubes, as defined, will accept this load without buckling.) Rotational effects for the concentrator may be reacted at the mounting point and could involve an equilibrator force of 204414 N (45956 lb) if applied radially in the plane of the center ring (Figure 3.3-2).

The oscillatory forces relate to solar tracking as the torus rotates in a plane 1 degree off-Sun. For a unit on the torus rotating 3 rpm (π/10 rad/sec) the maximum oscillatory motion can be expressed as:

$$s = R \sin 1^{o}(\sin \pi/10\ t)$$

$$s = 0.3485(\sin 0.31416\ t)$$

s = displacement distance m
R = radius of rotation, 20.5 m
t = time

The maximum angular acceleration then becomes:

$$\ddot{s} = 0.3485\ (0.31416)^2 = 0.0344\ \text{rad/sec}^2$$

The maximum torque required becomes:

$T = I\ddot{s}$

$I = \Sigma\ \tau r^2$

T = Torque
I = moment of inertia
τ = mass of an element
r = element distance from center of rotation

An approximation for the total moment of inertia would be the collector mass times the square of its distance from the point of rotation plus the inertia for a disc of mass equal to the concentrator.

$$I \text{ total} = 1.0629\ (10^7)\ \text{kg-m}^2$$

$$T = 0.0344\ (1.0629)10^7 = 3.66 \times 10^5\ \text{N-m}$$

If this force is applied at the inner ring of the collector, 4.41 m from the point of rotation, then:

$$\text{Force} = \frac{3.66 \times 10^5}{4.41} = 8.302 \times 10^4\ \text{N (18531 lb)}$$

In operation, the torus-mounted units will require application of this force from a pair of orthogonally mounted actuators that have a 15 cm (6 in) stroke position controllable within 2 cm (1 in) at all times.

3.4 Nuclear Fission Heat Source

A nuclear fission reactor represents a controllable heat source with a temperature capability sufficient to supply the heated NaK required for the converter thermal cycle. Description and comparisons for a nuclear fission based system begin with an assessment of requirements, proceeds through a description of system elements, and leads to an assessment of

masses. The mass assessments provide an estimate for a lower power limit as the threshold for application of nuclear reactors to the ATSS.

3.4.1 Assessment of Reactor Requirements

An application of nuclear fission reactors will provide a 10 year uninterrupted power supply for the ATSS. A reactor system also must have redundancy to assure continuity of power. Therefore, the configuration will need two independent reactor cores, with each core capable of supplying the heat requirement for three convertors of 450 kW each. The configuration can share shielding for weight benefit; however, the system arrangement must permit either core to supply heat to any three converters. The ATSS can accept a single, centralized location for generation of power.

A reactor design for the ATSS has to include adequate fuel, moderator material, a capability for high temperature operation, a means for extracting heat, and a control system. Fissionable material such as uranium of mass number 235 is a consumable fuel that produces about 200 MeV per fission or 7.94×10^{10} kJ/kg. The heat input requirements for three converters of 450 kW each will consume 13 kg of U235 over a ten-year period. This is more than an order of magnitude above the minimum required to sustain a fission reaction. The fuel requirement, therefore, must be defined in terms of an allowable burn fraction of the initial inventory. Power reactors can consume up to 10 percent of their total inventory. For this comparison, the fuel inventory will be established at 130 kg of U235 in combination with a supplemental quantity of U238; the core will require U235 enrichment. Since this core will operate at elevated temperatures and contain a quantity of metal that

tends to absorb neutrons, the enrichment selected will be 92 percent (near maximum). The total uranium inventory within each core becomes 141 kg provided as 161 kg of UO_2 in a volume of 14.66 liters. The fission reaction produces neutrons at average energies of 2 MeV; for power generation reactors, these neutrons must be slowed (moderated) by elastic collisions down to energies of 0.2 eV (thermal) range. Light elements are required and beryllium oxide (BeO) represents the practical compound. The reactor needs moderator atoms at a ratio of 100 or more per atom of fuel; therefore, each core will use 1461 kg of BeO in a volume of 566.5 liters. The neutrons produced during fission are absorbed to some degree by all materials present within the core including the primary coolant. Consequently, power reactors have separate loops for the core coolant and the heat transfer fluid. For this configuration, liquid sodium (Na) operates at 55.5 K (100°R) above the temperature of the converter NaK stream, and flows through heat exchangers which are outside the core and neutron environment, but inside the main radiation shield. (The NaK does not see neutrons, and radioactive Na stays within the shield.) Neutrons are generated at the rate of 2.5 per fission with about 0.7 percent having a delayed release from fission fragments. They appear over a period ranging from seconds to hours. The sustaining of a fission reaction at any power level requires that just one neutron from the fission release be absorbed to cause another fission and involve the delayed neutrons. The control system must maintain that balance, particularly during changes in power levels. The divergence from equilibrium must continue to require participation by the delayed neutrons (bombs "go critical" on prompt neutrons, power stations do not). Finally, the system must have a capability for shutdown and hold-

down which implies an absorber which effectively dries up any neutron population created within the core. The emergency or "scram" portion of the control system must provide that capability.

3.4.2 Reactor System Concept and Core Features

The reactor system concept uses two identical cores with a thermal output of 3367 kW each and two sets of three heat exchangers all contained within a common radiation shield. Figure 3.4-1 shows the overall concept. The fueled portion of the core is a right circular cylinder 1 m in diameter and 1 m long. Each core has a BeO neutron reflector 10 cm thick. A ZrO_2 thermal insulation layer 10 cm thick surrounds the core and reflector and is backed by a neutron barrier of either borated steel or borated aluminum. The high energy gamma radiation shield considers four options: lead, steel, concrete, or water. The pertinent features of the core are described further as core construction, control considerations, and coolant-heat transfer.

A. Core Construction

The concept for core construction is shown in cross section as Figure 3.4-2. The UO_2 fueled heat-generating section is provided as 282 hexagonal elements with a center hole for the heat transfer passage. Figure 3.4-3 shows the nesting of the hexagons and the accommodation of the control rods together with the detail for accommodating the reflector over the ends of the core. Fuel assemblies must contain fission fragments; therefore, the hexagons have a 1 mm cladding of an alloy compatible with liquid Na, (79 Ni, 13 Cr, 7 Fe). Because the local neutron flux (or population) density within a core determines the local heat generation rate, a near-uniform neutron distribution becomes

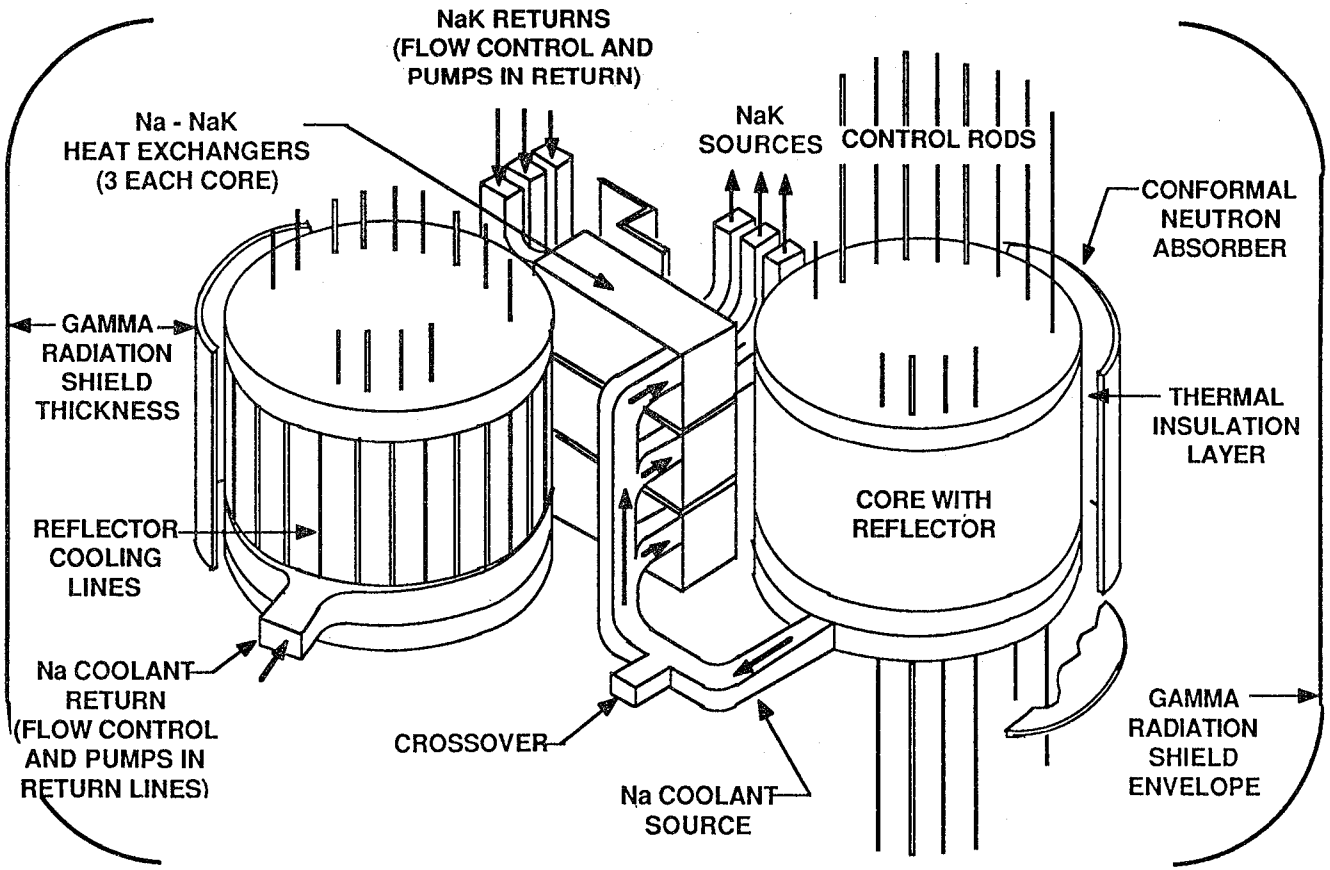

Figure 3.4-1 Nuclear Fission Power Reactor Concept for the 2025 Space Station

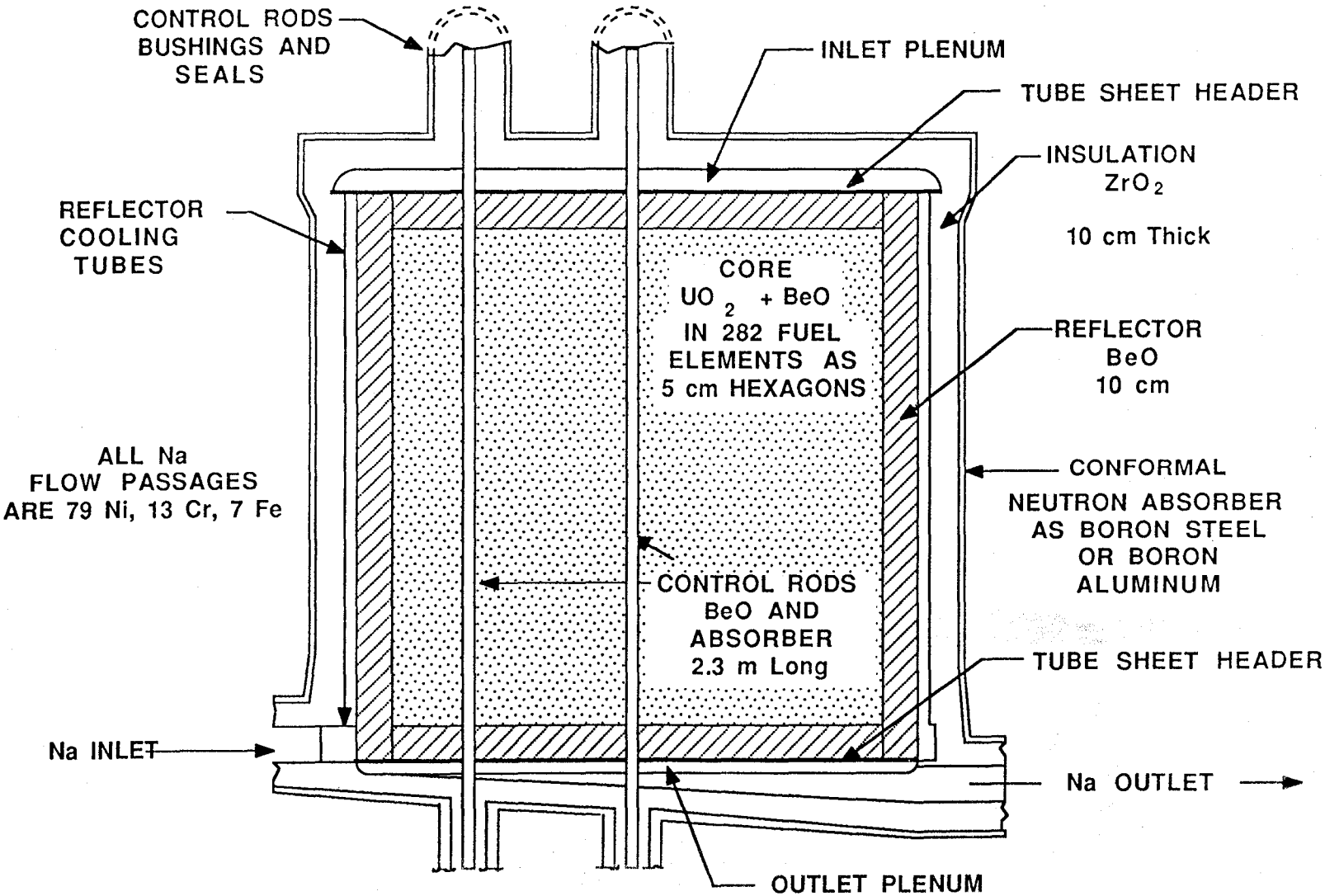

Figure 3.4-2 Reactor Core Concept, Cross Section

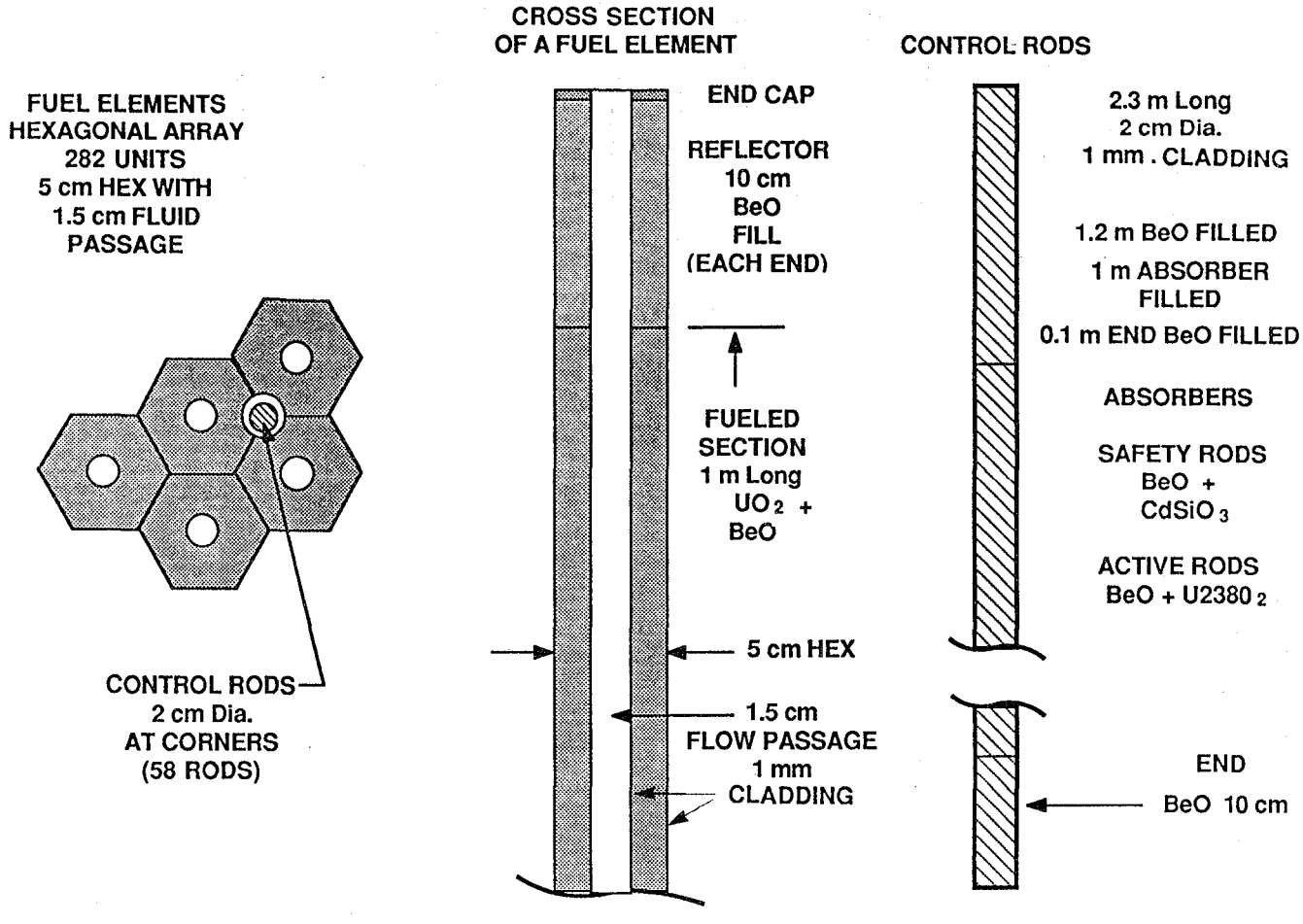

Figure 3.4-3 Core Internal Element Configuration Details

desirable; therefore, a BeO reflector surrounds the core (Figure 3.4-2). Figure 3.4-4 illustrates the effect of a reflector on the neutron distribution. Extraction of heat from the core uses liquid Na. Liquid metal enters in a manifold near one end of the assembly and flows to the other end through tubes in contact with the reflector. The Na flow absorbs heat from the reflector before entering a plenum that feeds the main heat transfer passages through the fuel elements. The Na leaves the core through an exit plenum into distribution manifolds that feed an array of heat exchangers (Figure 3.4-1).

The flow passages, plenums, and tube sheet headers that retain the fuel elements provide structural support. The ZrO_2 is formed as fitted segments which in turn are backed by the neutron absorber as a conformal metal structure. Nickel-based high temperature alloys as cladding and structure introduce a quantity of material which has significant neutron absorption characteristics; therefore, critical mass limits must be considered. The critical mass limits for a core have a geometrical shape dependency defined as "Buckling" (B^2), with dimensions of cm^{-2}. The bare core critical mass limits for typical moderator materials are shown in Figure 3.4-5 in terms of the geometric buckling and the ratio of moderator atoms to U235 atoms. Values for B^2 are defined from a relationship particular to a shape; the equation for a right circular cylinder is shown. A core using Be as a moderator at a ratio near 100 requires $B^2 = 0.008\ cm^{-2}$ or less, to achieve criticality. A right circular cylinder of 50-cm radius by 100-cm long has $B^2 = 0.0032\ cm^{-2}$ and thereby indicates a criticality margin for the concept.

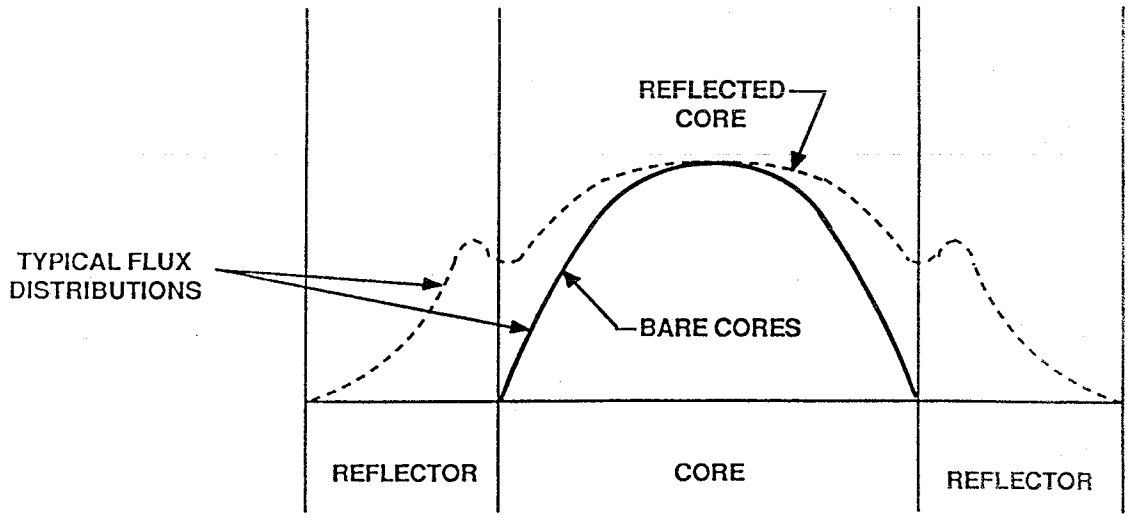

Figure 3.4-4 Comparison of Typical Thermal-Neutron Flux Distributions for Bare and Reflected Reactor Cores (from Reference 7)

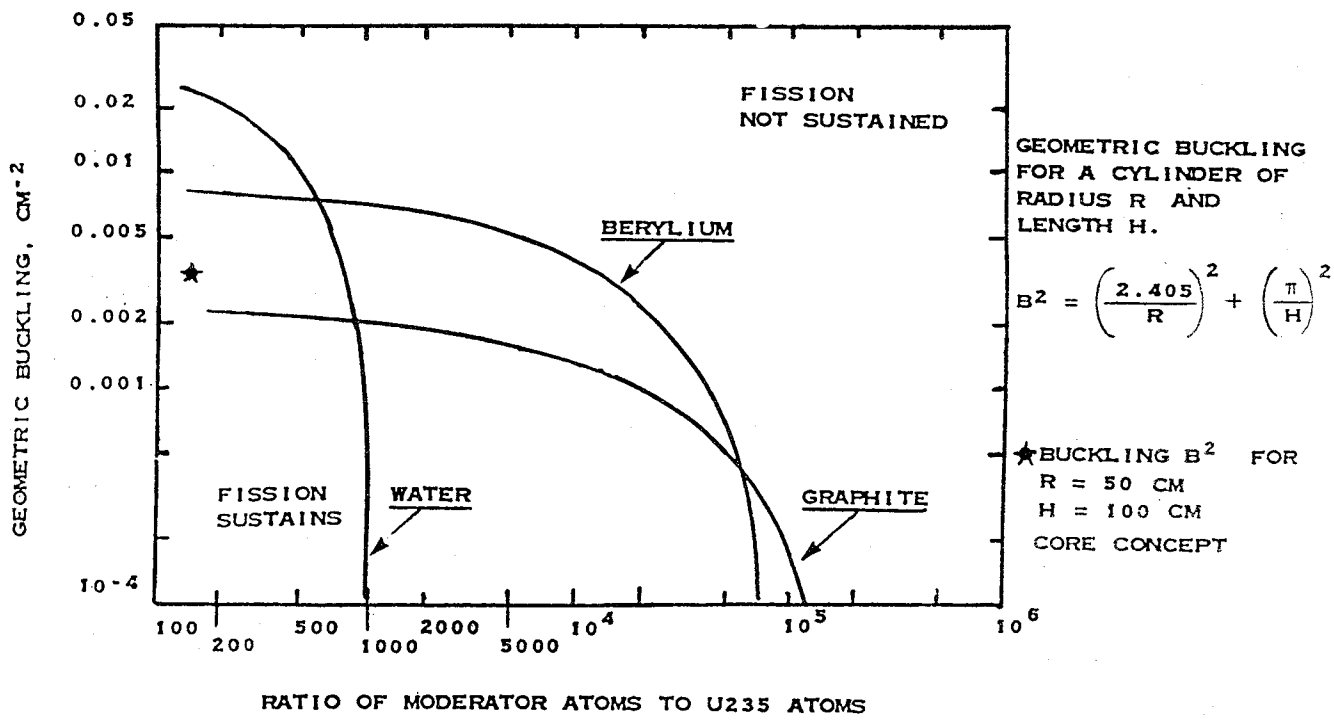

Figure 3.4-5 Geometrical Shape Parameters for Core Critical Mass Determination (from Reference 7)

B. Control Considerations

The curves in Figure 3.4-5 also suggest that a shape with $B^2 = 0.016$ cm^{-2} as two times the limit for Be would not go critical even as a sub-element of a core. A value of $B^2 = 0.016$ cm^{-2} yields a radius of 19 cm for a 1 m length and suggests control rod spacings equivalent to three or four fuel elements. A symmetric pattern on this basis yields 58 locations divided between control and safety rod configurations. Figure 3.4-3 also shows the concept for construction of the rods. In operation the active portion is within the core, and movement of a rod replaces active material with a moderator such that the core volume and flow passages do not change. The active portions of the rods contain an 80-20 mix of neutron absorber and BeO; the remainder of the rod contains just BeO.

The safety rods need to contain a strong absorber; in this case, $CdSiO_3$ was selected on the basis of temperature compatibility. Operating control rods contain an appropriate absorber selected from a range of materials of which U238 is a candidate and used here as the oxide for weight estimates. In operation, safety rods make a full-length travel and leave the active control rods to regulate neutron population by means of selective adjustments in position. Although other techniques for control exist and would be considered in an actual design, control by moving rods is a well established technique.

C. Core Coolant and Heat Transfer

Liquid sodium functions as the coolant for the core and represents a best-available option. The Na liquifies at 370 K ($670^{\circ}R$) and remains liquid to 1156 K ($2082^{\circ}R$). The Na has low absorption characteristics for neutrons; however, it does interact to generate MeV-range gamma

radiation. Therefore, the Na stream must be kept isolated from the NaK which powers the turbine. The Na coolant extracts heat from the core with a 27.5 K (50°R) temperature rise and delivers heat to NaK while maintaining a 55 K (100°R) temperature above the NaK flow; Na operates from 1103 K to 1131 K (1987° to 2037°R). The total flow rate is 97 kg/sec (213.88 lb/sec) and results in a maximum wall temperature of 1137 K (2049°R) and a maximum UO_2-BeO temperature of 1163 K (2096°R). Internal power generation is considered mid-range at 5.8 Watts/cm^3 as compared to 4 Watts/cm^3 for low power units and 7 Watts/cm^3 or more for higher power installations (Reference 3-9). The heat transfer characteristics for liquid metals permit use of small-volume heat exchangers. Figure 3.4-6 shows a concept for a counterflow unit using Na and NaK. Heat transfer requires 1.76 m^2 (19 ft^2) of area configured as 10 plates with a counterflow on each side. Spacing of the plates and the selection of velocities were tailored to match the heat transfer characteristics of the individual fluids. Table 3.4-1 summarizes the principal heat transfer-related parameters for the reactor system.

3.4.3 Shielding Considerations

A radiation shield for a fission reactor must attenuate high energy gamma rays and neutrons generated by the fission process. The degree of attenuation required to provide a man-rated shield is a function of the power density within the core as the underlying source for radiation from the surface of the core itself. The reactions are diagrammed in Figure 3.4-7 and show the results from fission within the core and the attenuating interactions within the shield material. The Compton effect is an elastic scattering that reduces the energy of an incident gamma

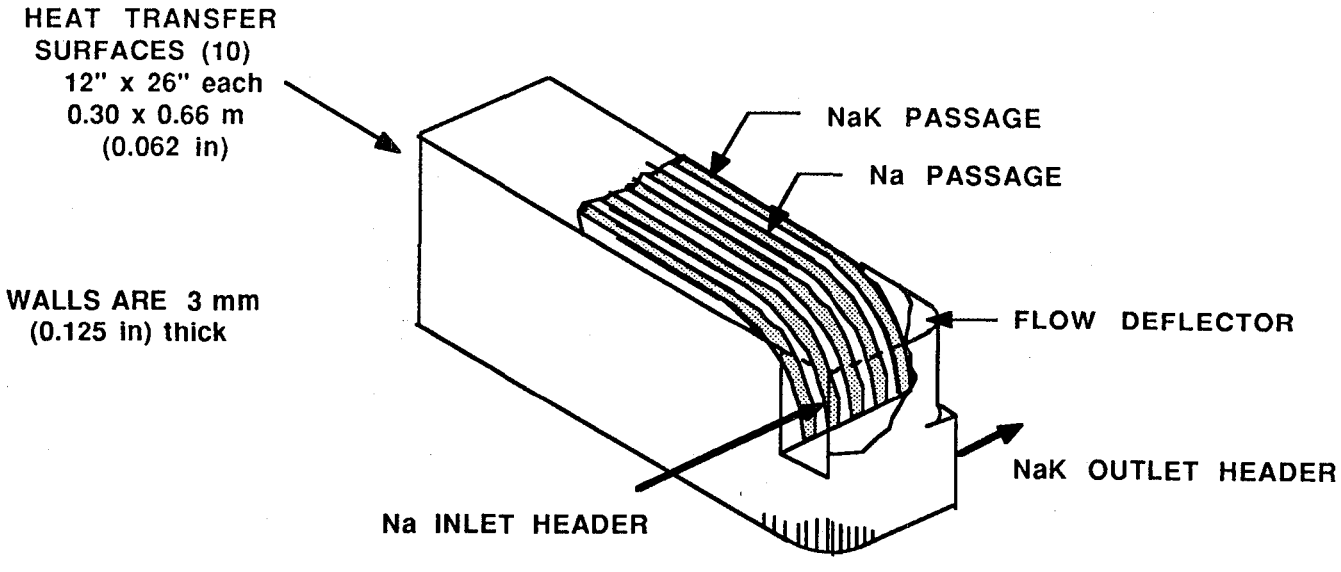

Figure 3.4-6 Concept for a Na-NaK Counterflow Heat Exchanger

TABLE 3.4-1 SUMMARY OF REACTOR PARAMETERS

Energy, Fuel, Moderator Requirements		
Total Energy	1.067×10^{15}kJ	(1.016×10^{15} Btu)
(10 yrs, 3375 kW)		
U235 Consumed	13 kg	(29 lb)
Fuel Inventory (130 kg U235)	141 kg	(312 lb)
Fuel Weight UO_2	161 kg	(354 lb)
BeO Moderator Weight	1461 kg	(3287 lb)
Power Control Rods	26	
Emergency Rods (Scram)	32	
Reflector, BeO (10 cm thick)	1315 kg	(2899 lb)
Core Thermal Parameters		
Energy Delivered	3375 kW	(3208 Btu/sec)
Energy Density	5797 kW/m	(156 Btu/sec-ft^3)
Heat Transfer Rate	251 kW/m^2	(22 Btu/sec-ft^2)
Maximum Wall Temperature	1137 K	(2049 ^oR)
Maximum Fuel Temperature	1163 K	(2096 ^oR)
Core Coolant Na In	1102 K	(1987 ^oR)
Core Coolant Na Out	1130 K	(2037 ^oR)
Core Coolant Na Flow	97 kg/sec	(215 lb/sec)
Heat Exchangers		
Heat Exchanged	1123 kW	(1069 Btu/sec)
Heat Transfer Area	1.76 m^2	(19.0 ft^2)
Na Velocity	0.95 m/sec	(3 ft/sec)
NaK Velocity	2.44 m/sec	(8 ft/sec)

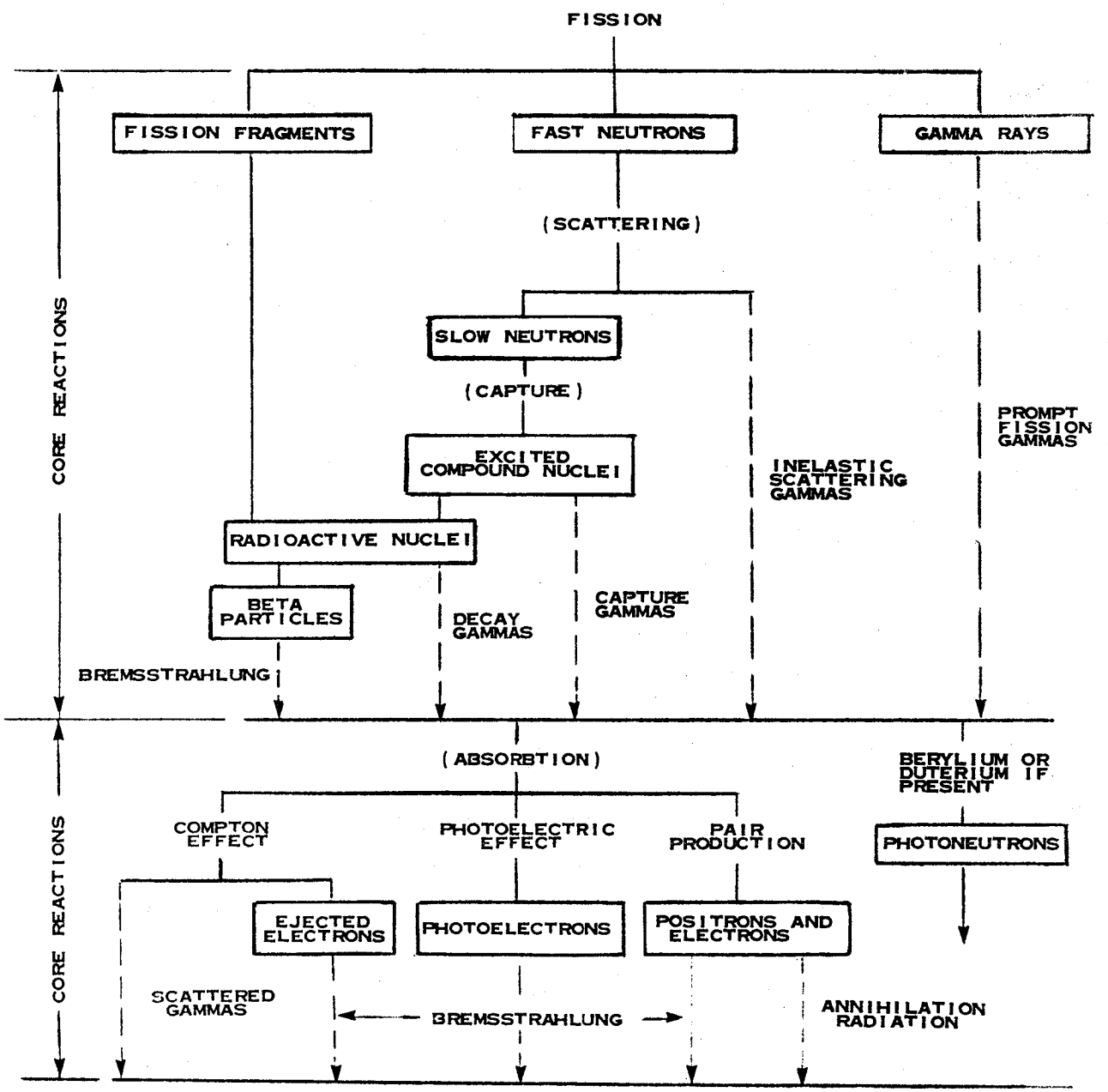

Figure 3.4-7 Radiation Shielding Considerations for Reactor Cores (from Reference 7)

ray by an exchange of energy with an electron. The photoelectric effect exchanges a gamma ray for an electron of the same energy. Pair production has an energy threshold equal to the rest mass of an electron-positron pair (1.05 MeV). Photoneutrons are absorbed into the nuclei of other atoms. All the effects are mass dependent; and the limiting parameter appears as attenuation of 4 MeV gamma radiation for an application to the ATSS.

A. Shield Thickness Predictions

The attenuation model considers gamma radiation energy per unit area (cm^2) at a distance from an emitting surface also defined in terms of energy per unit area. A conservative model assigns 20 MeV of gamma energy to each fission; therefore, the gamma energy generation rate is 20 MeV times the fissions/cm^3. The gamma energy released from the surface will represent the generation rate modified by a factor which accounts for the internal absorption of gamma energies within the materials of the core. The physical property which can be measured is an absorption coefficient with the dimensions of cm^{-1}. An inverse of the absorption coefficient is defined as a relaxation length, and is the thickness required for attenuation by a factor of "e" (2.71828). The relaxation length also becomes the multiplying factor which accounts for radiation released from subsurface atoms. For the cores in this comparison study, the gamma shield begins at the outer surface of the insulation layer. The reflector, the structure, and the ZrO_2 provide some attenuation, and the source terms become:

Gamma energy from fissions = 2.68×10^{11} MeV/cm^3sec (core internal)

Core surface activity emission = 3.14×10^{13} MeV/cm^2sec

Gamma energy into shield = 4.04×10^{12} MeV/cm^2sec

A conservative approximation for shield thickness (Reference 3-7) equates the input energy to the output energy in terms of shield thickness, relaxation lengths, and the area of the source. The equation takes the form:

$$\text{Energy Out } (\text{MeV/cm}^2\text{-sec}) = \frac{0.5[\text{Input Energy } (\text{MeV/cm}^2\text{-sec})]\, e^{-\left(\frac{\text{Thickness (cm)}}{\text{Relaxation Length (cm)}}\right)}}{0.5 + \frac{2[\text{Relaxation Length (cm)}]^2}{[\text{Source Diameter (cm)}]^2}\left(\frac{\text{Thickness (cm)}}{\text{Relaxation Length (cm)}} + 1\right)}$$

The allowable energy associated with a man-rated shield is subject to continuous review. The early data allowed 4000 MeV/cm^{2}sec for a 40 hour exposure. The calculations for this example used 2000 as an upper limit and considered thicknesses which were integer multiples of relaxation lengths.

B. Shield Configuration Model

The gamma radiation shield surrounds both cores and has a constant thickness in all directions perpendicular to the surface of the insulation layer. Figure 3.4-8 shows the geometric concept for the shield as a combination of six specific shapes defined in terms of the diameter of the cylinder (D) and the thickness of the shield (T). The volume of the shield becomes the sum of geometrical volumes which combine to generate the expression:

$$V = 11.112\ D^2T + 13.103\ DT^2 + 4.158T^3 \qquad \text{(D and T in meters)}$$

For the purposes of the shield calculations, the cores have a diameter "D" of 1.4 meters.

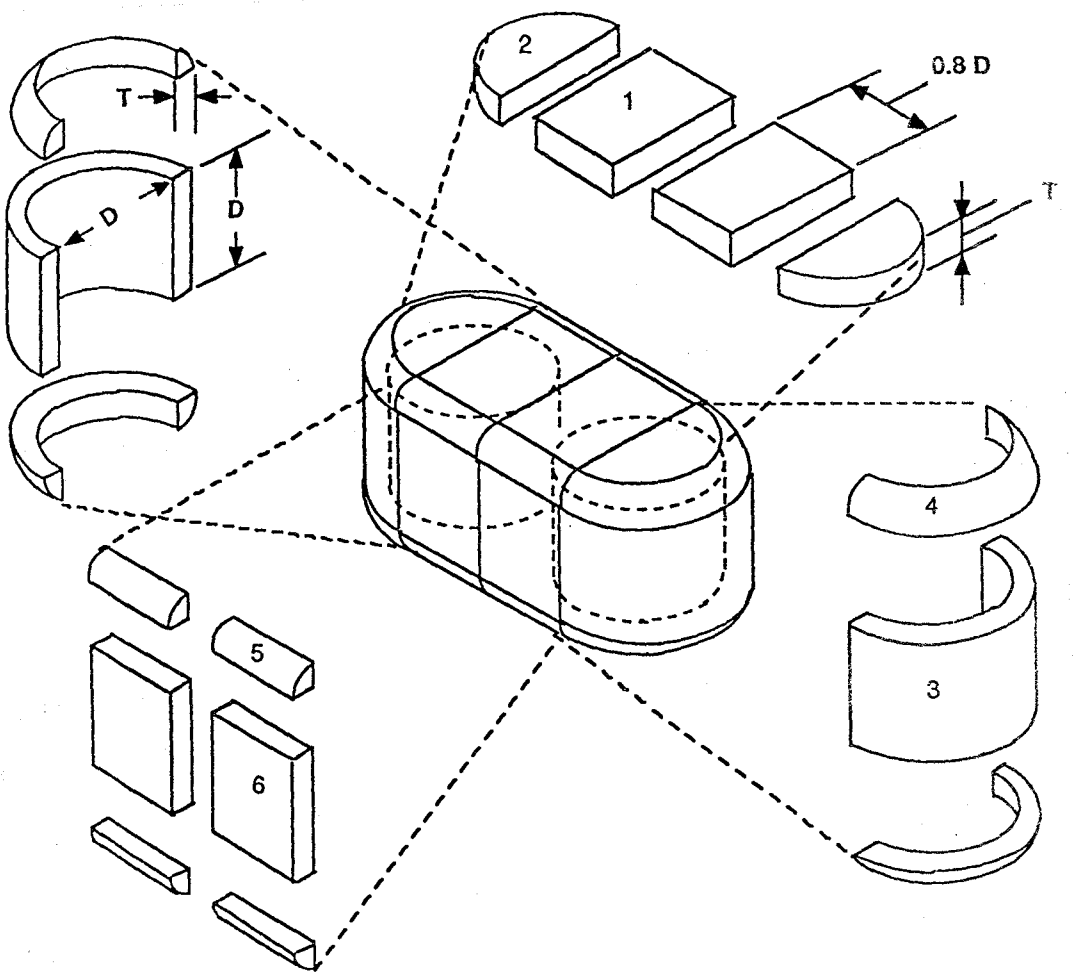

1, Top (Rectangle) 3, End (Cylinders) 5, Filler (Cylinder)
2, Cap (Cylinder) 4, Fairing (Toriod) 6, Side (Rectangle)

Figure 3.4-8 Shield Element Model

C. Shield Material Options

The transcendental equation to define thickness was solved for lead, steel, dense concrete, and water shields using published relaxation lengths (Reference 3-7), the calculated input energy, and the dimensions of the core. These results appear in Table 3.4-2. Thickness predictions and core diameter were then applied to the volume equation and weights were based upon density values. The results show the mass dependency for a radiation shield. More dense material with a corresponding shorter relaxation length enjoys a total shield mass advantage. These values provide the basis for summing the masses of a nuclear reactor based power system.

3.4.4 Summary of System Masses

The summary of masses for a nuclear reactor system considers the cores and the radiation shield together with the same converters and radiator sections as used in the solar dynamic system. In an overall mass assessment, the cores, converters, and radiator elements are independent of the shield mass. Table 3.4-3 summarizes the masses for each and shows the effect of the shield option on the total.

The core and heat exchangers present the smallest contribution to the total system mass. The core elements include fuel (160 kg each) and moderator, 1416 kg, plus BeO in the reflectors, 1314 kg, to account for more than 70 percent of the core mass. The balance of the mass is Ni alloy structure. Approximately 80 percent of the control and rod assessment is in the seal and actuation-related items. The ZrO_2 insulation at 50-percent open is used throughout. The heat transfer

TABLE 3.4-2 SUMMARY OF REACTOR RADIATION SHIELD OPTIONS

	Lead	Steel	Dense Concrete	Water
Relaxation Length, cm	2.5	3.7	10	30
Number of Lengths	21	21	21	20
Thickness	52.5	77.7	210	600
Volume, m^3	17.1	29.9	165.4	1695
Density, kg/m^3	11300	7800	3400	1000
Weights, kg (lbs)	193163 (425925)	233693 (515293)	562333 (1239944)	1695028 (3737537)

TABLE 3.4-3 SUMMARY OF REACTOR SYSTEM MASSES

	kg	(lb)
Reactor Elements		
Core, Reflector and Support	3957	(8725)
Control Rods and Actuators	1134	(2500)
Thermal Insulation (ZrO_2)	2384	(5256)
Heat Exchangers (3)	360	(794)
Pumps, Lines, Valves	907	(2000)
Liquid Metal	453	(1000)
Total Each Core	9195	(20275)
Total Installation	18390	(40550)
Shield Options (from model)		
Lead	193163	(425925)
Steel	233693	(515293)
Concrete	562333	(1239944)
Water	1695028	(3737537)
Common Items		
Converters (6 at 3863 each)	23016	(50750)
Radiator Structure 612 Panels and Lines	76494	(168669)
Lines and Radiator Fill (water)	87042	(191927)
System Mass Totals		
With a Lead Shield	398105	(877623)
With a Steel Shield	438638	(967197)
With a Concrete Shield	767275	(1691841)
With a Water Shield	1899970	(4189433)

elements as Ni alloy plate, together with pumps and lines, show a modest mass, and the liquid metal inventory corresponds to about 0.5 m^3.

The combined mass for the two reactors, the six converters, and the radiator panels (considered as three tiers of panels around the periphery of the platform) are combined with the shield masses for each of the alternates. A comparison of totals shows more than a factor of four in mass range from a lead shield to a water shield.

3.4.5 Summary of System Control Requirements

The nuclear reactor control complex consists of the previously described converter-radiator elements, adapted to work with the control elements particular to a nuclear reactor installation. The configuration requires locating all six converters adjacent to the reactors in order to limit heat losses in the liquid metal (NaK) loops. Reactor systems can adjust power to demand and thereby ease the response requirements associated with electrical load leveling. The control requirements pertinent to the nuclear reactors are summarized in Table 3.4-4. Power control and housekeeping functions follow conventional Earth power plant approaches; the difference is in the complexity of the overall system. Under ordinary operations, nuclear power plants make slow changes in power settings and are effectively steady state systems (the control response relates to the 0.7 percent of delayed neutrons). Response to an emergency, however, would be rapid. Earth operation uses stored energy (springs, hydraulic accumulators, etc.) to move the emergency (scram) rods, and reactions are measured in tenths of seconds. Shut-down of a reactor does not imply shut-down for all the system. Flow of coolant and

TABLE 3.4-4 SUMMARY OF REACTOR CONTROL REQUIREMENTS

CONTROL ELEMENT OR FUNCTION	OUTPUT OR ACTION	RANGE	PRECISION	FREQUENCY
Reactor Power Control Algorithm (Each Core)				
· Emergency Rod Position	Rod Position in Response to operate and Safety Signals	Motion 1.2 m (4 ft)	1 mm (0.04 in)	Stroke in 0.1 sec Shut Down
· Control Rod Position	Rod Position in Response to Signal	1.2 m (4 ft)	1 mm (0.04 in)	Stroke in 0.1 sec modulate at 10 cm/sec
· Neutron Flux	Input to Rod Position and Power Demand	0 to 10^{15}/sec cm^2	1%	Steady
· Coolant Temperatures	Input Signal	300 K-1200 K ($500^{o}R$-$2160^{o}R$)	2 K ($3^{o}R$)	Steady
· Coolant Flow	Input Signal	0 to 150 kg/sec (0 to 333 lb/sec)	0.1 kg (0.25 lb)	Steady
· Flow Control Valve Positions	Response to Demand	Open-Close	1% position	Steady
· Coolant Pump Operation	Current Modulated in Response to Power Demand	0 to 1000 A	2 A	Steady

TABLE 3.4-4 SUMMARY OF REACTOR CONTROL REQUIREMENTS (concluded)

CONTROL ELEMENT OR FUNCTION	OUTPUT OR ACTION	RANGE	PRECISION	FREQUENCY
System Operating Monitor and Safety Functions, Multiple				
• Structure Temperatures and Profiles	Input Signals to Safety	270-1380 K (460-2450°R)	2 K (3°R)	Steady
• Neutron Profiles	Input Signals to Safety	0 to 10^{15}/sec cm^2	1%	Steady
• Radiation Profiles	Input Signals to Safety	0 to 10^{15}/sec cm^2	1%	Steady
• Shield Coolant Flow	Input Signals to Safety	0 to 100 kg (0 to 220 lb/sec)	0.1 kg (0.25 lb)	Steady
• Shield Coolant Temperature	Input Signals to Safety	220-500 K (460-100°R)	2 K (3°R)	Steady
• Shield Coolant Flow Control Valves	Enable Signals to Safety	Open-Close	1%	Steady
• Radiation Safety Monitors	Input to Safety	0 to 10x man limit each type	1%	Steady

monitoring of temperatures must continue for indefinite periods after a core shut-down.

3.4.6 Special Considerations

The special considerations relate to radioactivity effects. All nuclear systems require a thorough radiation monitor capability to assure continuous man-safety. This capability is included in all power plants. Operation of nuclear-powered submarines provides a major source for information pertinent to reactor operations in a confined environment. A further consideration is the change-out of spent (or damaged) fuel elements, control rods, or exchange of other materials from within the radiation field of the core. Nuclear reactors must have a configuration which allows change-out by a remote operation technique plus the availability of equipment which can perform that change-out without violating radiation limits. The requirement involves both handling equipment and shielded casks for containment of radiation. The storage location for such items has not been addressed. Equipment masses will be significant, and the degree of on-board storage or capability for change-out represents an uncertain increment in a mass comparison.

3.4.7 Low-Power Limit Threshold for Space Nuclear Reactor Systems

The shielding model shown in Figure 3.4-8 offers a means to compare shield volumes and masses with reactor power in a manner which indicates a practical low-power limit for a reactor system. If the reactor power generation per unit volume is kept constant, then the thermal output of the reactor becomes a function of the core volume. For this evaluation, the reflector thickness and thermal layers remain the same (Figure

3.4-2), and the thermal power can be calculated for various fueled cores as ratios to the "example" fueled core which was a right circular cylinder 1 m in diameter and 1-m long. These thermal output values are shown as a function of the radiation input source diameter in Figure 3.4-9. The shield volumes and masses were calculated using the thicknesses and densities listed in Table 3.4-3, and these values also appear in Figure 3.4-9. The effect of size (radiation input source diameter) in the shield equation, (see paragraph 3.4.3A.) could introduce as much as two relaxation length differences for water; however, the effect does not change the general trend which shows that reactor power increases at a higher rate than does the mass of the shield. Increasing the size of the core increases the thermal power output and requires less shield mass for each kW produced by the reactor. A plot of electrical power delivered versus the specific mass (shield mass per kW delivered) is shown in Figure 3.4-10. The electrical power delivered follows the same profile as the thermal power (assumes the same conversion efficiency). The reduction in the specific mass of the shield shows an initial rapid fall-off which becomes more gradual. For this study, each of the 1.4-m cores delivers 1275 kW of electrical power from a thermal output of 3667 kW, and this power level brings the specific mass for some shield options below 100 kg/kW. This level is comparable to mass ratios for other power systems and suggests a threshold for nuclear power systems at or about that general level. Increasing the power density in a reactor core will increase the power delivered; a factor of 2 increase is practical. On the other hand, the inputs to the shield (surface activity) follow directly and thereby adds a relaxation length to the shield thickness. The specific mass would not necessarily improve by the

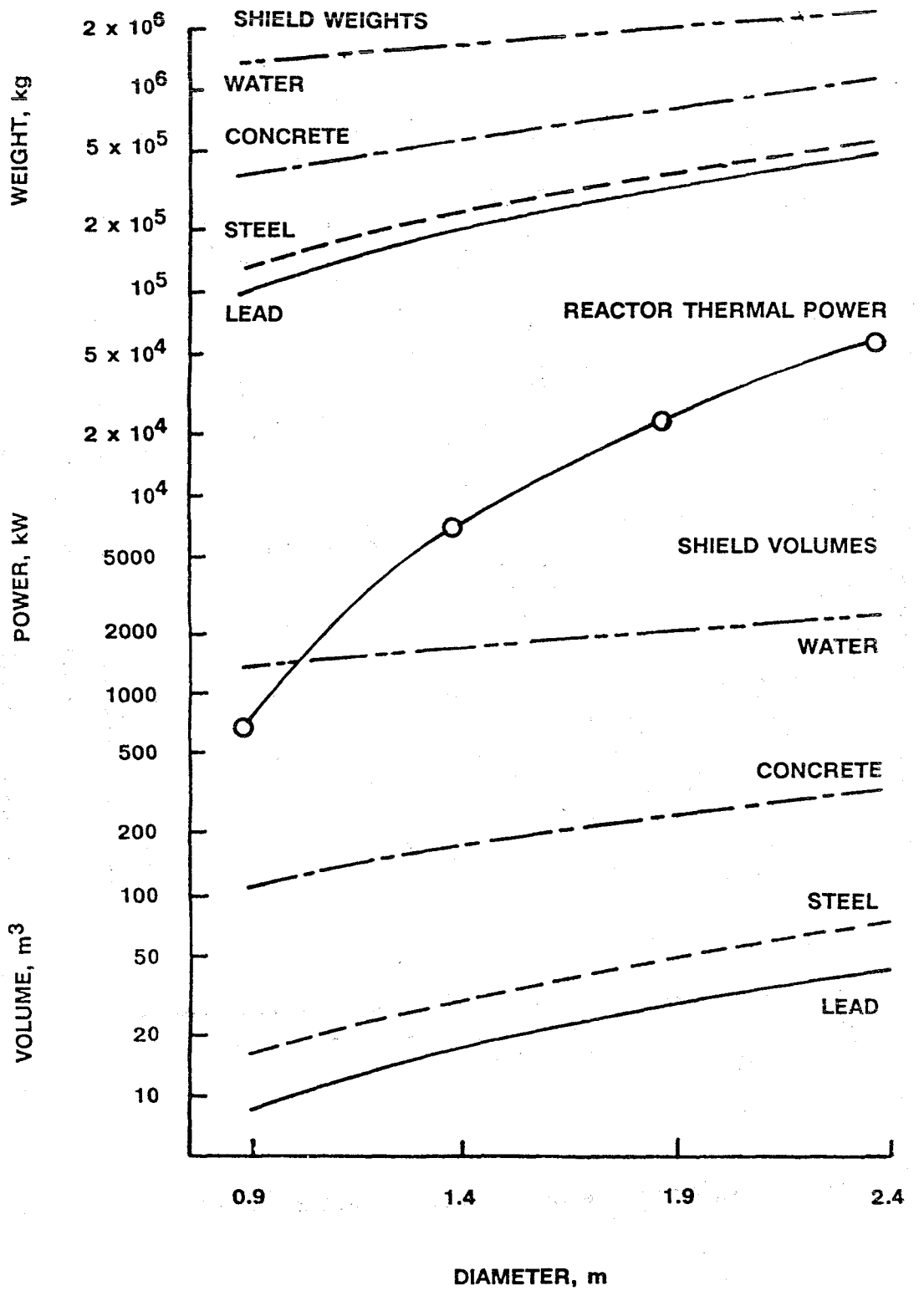

Figure 3.4-9 Shield Weights, Shield Volumes and Reactor System Thermal Power as a Function of Core Diameter

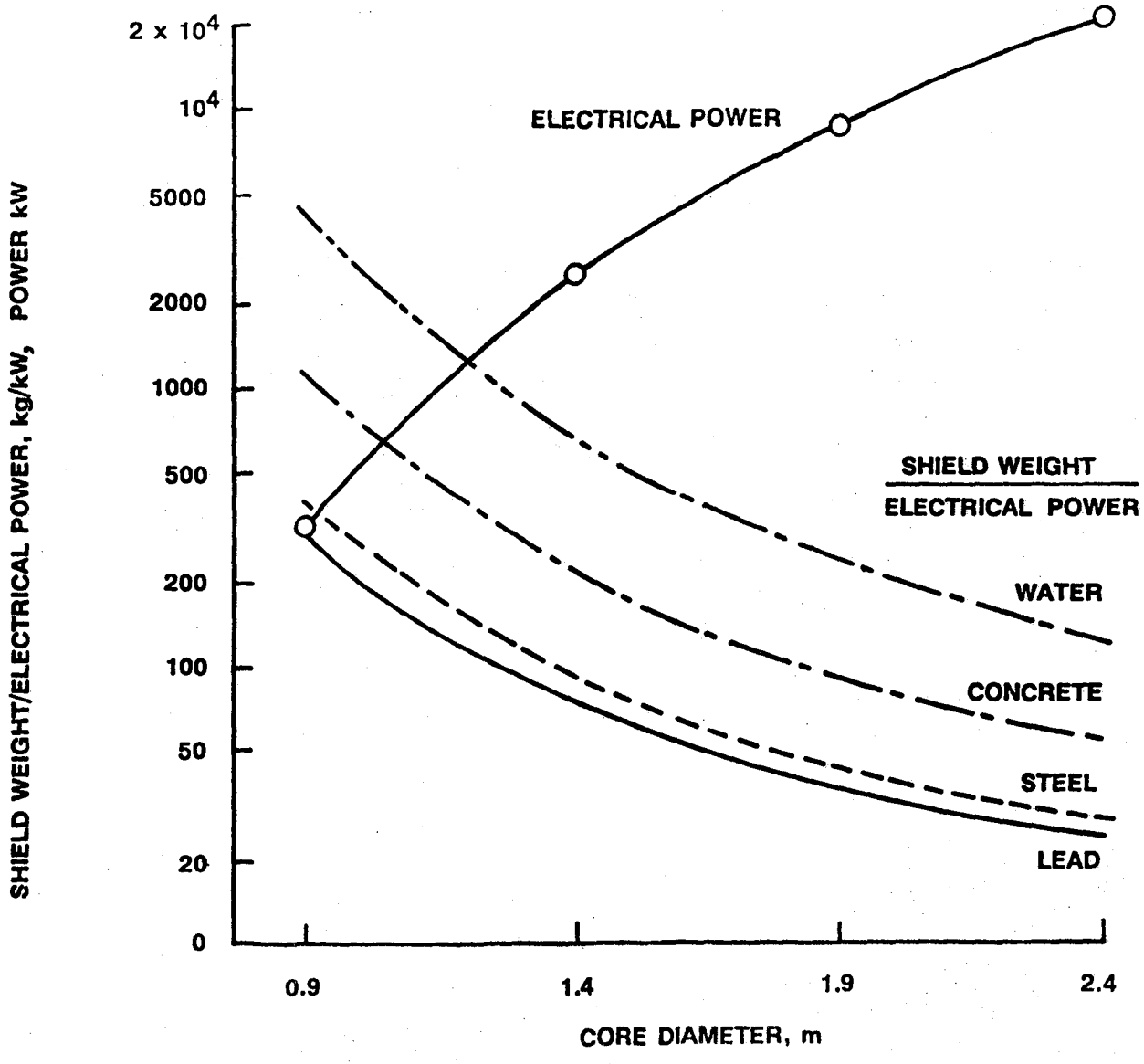

Figure 3.4-10 Reactor System Delivered Electrical Power and Shield Weight-to-Electrical Power Ratios as a Function of Core Diameter

same ratio as the power density. The study shows no sharp limit similar to that for a nuclear critical mass or Euler buckling of a column. On the other hand, at or near a thermal power output level of 3 MW for a reactor core, the shielding mass requirement begins to appear reasonable and potentially competitive with other power source options.

3.5 Comparisons and Conclusions

The comparisons between the solar dynamic and nuclear fission systems address mass, control, and the pertinent considerations as the basis for the assessments and conclusions included in the following discussions.

3.5.1 Comparison of System Masses

A summary and comparison of masses for the two systems appears in Table 3.5-1 and shows the total contribution from the common elements, the solar dynamic elements, and the reactor elements together with each of the shielding options. The values also include a specific mass assessment for electrical power delivered in terms of kg/kW. Specific masses are then compared with similar results from previous studies. It is recognized that no direct comparison exists either in power generated (previous studies addressed lower output powers) or in details of the configuration. In particular, many of the previous studies into reactor applications utilized shielding configurations which were man-rated only in the direction of the inhabited portion of the spacecraft; therefore, the comparisons reflect partial shields relative to total shields.

TABLE 3.5-1 COMPARISON OF SYSTEM WEIGHTS

	ESTIMATES		kg/kW	kg/kW (FROM REFERENCES 3-1 THROUGH 3-4)
COMMON ITEMS	kg	(lb)	DELIVERED	
CONVERTERS (6)	23016	(50750)	9.025	11.3
RADIATORS (6)	76494	(168669)	29.997	18, 65.7
RADIATOR FILL (6)	87042	(191927)	34.134	
SOLAR DYNAMIC ELEMENTS				
CONCENTRATORS (6)	135030	(297741)	52.952	39.81
COLLECTORS (6)	93876	(206996)	36.814	59.14
REACTOR ELEMENTS				
REACTORS (2)	18390	(40550)	7.211	3-10
SHIELDS- LEAD	193163	(425925)	75.750	80
STEEL	233693	(515293)	91.644	
CONCRETE	562333	(1239944)	220.522	
WATER	1695028	(3737537)	664.717	
TOTAL SYSTEMS				
SOLAR DYNAMIC	415458	(916084)	162.924	60-185: 186
NUCLEAR- LEAD	398105	(877623)	156.119	120-160
STEEL	438638	(967197)	172.015	
CONCRETE	767275	(1691841)	300.892	
WATER	1899970	(4189433)	745.086	

A. Common Elements; Converter and Radiator

Radiator requirements dominate the mass for these items. The need for radiating area is dictated by the radiator operating temperature. A higher operating temperature coupled with a coolant which operates with a wider temperature range can reduce the area by a modest margin; however, a flat surface radiator will carry a mass penalty as compared with some of the advanced technology units such as the liquid droplet types. The masses of aluminum and water show the need for development of mass-efficient radiator configurations.

B. Solar Dynamic Elements

The solar concentrators become large, complex structures with stringent accuracy and stability requirements. The need for large areas of reflectors and the need for local pointing translate into the developmental goals for the surface accuracy. Mass efficiency coupled with improved stiffness and stability appear as the critical parameters for development of materials. The mass of the collector appears driven by the quantity of phase change material required and the particular insulating materials utilized for temperature retention and thermal control. Materials for structure and the materials in contact with the coolants can benefit by development of a lower density alternative. Within the configuration evaluated, the mass of phase change material amounts to 8 kg/kW for electrical power delivered and leaves about 25 kg/kW subject to reduction by materials-related developments.

C. Reactor Elements

The reactor core and core-related elements make a small contribution to the overall mass and offer only a limited potential for improvement. The composition of fuels, moderators, and reflectors have

limited alternatives. Cladding, support structure, and auxiliary elements offer the only real potential for improvements. The mass associated with shielding dominates the nuclear reactor system. A detail design for an actual shield would utilize more than one material and show some overall improvement. Within the context of this study, mass values show the efficiency of dense material for shielding, and at the same time indicate the dependence upon mass to attenuate radiation. Innovative utilization of materials can reduce the total shield mass but not to the point where shield mass will not continue to dominate the nuclear reactor portion of the system.

D. System Comparison

The mass requirements to man-rate a reactor shield were anticipated, however, the comparison result which shows a cross-over between solar dynamic and reactors in terms of a shield option was not anticipated. A concerted effort to reduce the mass of solar dynamic items would probably match the minimum mass condition for a reactor shield. In such a context, selection of the heat source would not be decided upon mass criteria alone. Other mission effects or mission requirements will make the determination. In the context of "other conditions," mass comparisons become even more complex. The estimates show that concrete or water impose a severe mass penalty when used as a shield. If the ATSS were part of a lunar base support such that the raw materials for the concrete aggregate originated from lunar sources, then the mass would not have the same transport penalty as a more dense material of terrestrial origin. In the same context, a shield based upon a combination of steel, concrete, and water, would permit use of the water as a storage or recyclable item within the Space Station. Finally, the massive unit

represented by the reactor plus the shield and the converters would become an effective center of gravity "anchor" for the system. A substantial amount of mass could be moved elsewhere in the ATSS without shifting the center of gravity outside the envelope of the reactor-shield-converter package.

The location for the nuclear reactor installation within the ATSS will need a trade study. Location at the center of gravity has inertial benefits but would disrupt the present concept for transfer of materials into the torus. A convenient location would be in alignment with the platform which would ease connections to the radiator. Such a location would require water ballast retention in the berthing bay members or in portions of the volume presently reserved for the safe haven habitat. Ballast stored in, or adjacent to, the berthing bay would shift up the central tube to compensate for spacecraft dockings. A reactor location within the central tube would have some impact on the operational capabilities of the microgravity facility with the minimum effect being a reduction in volume available for processing.

3.5.2 Control Comparisons

The control comparisons show a significant requirement related to the operation of the converters with supplementary requirements for either the solar dynamic or reactor power sources.

A. Common Item Controls (Converters and Radiators)

The requirements for frequency and voltage dictate a precise control unit at each of the converters. These two effects then reflect into the requirement for temperature, pressure, and flow controls. Neither option for input heat relieves the requirement for external

electrical load leveling. The reactor system does have the capability to modulate the output power level as compared with the near-constant requirement for the solar dynamic unit; however, the changes must be gradual. In effect, the converter-radiator control requirements are effectively the same for both the solar dynamic and nuclear power inputs.

B. Comparisons Between Solar Dynamics and Nuclear Power Systems

The solar dynamic related controls must assure the cyclic throughput of the collected energy; system operation is continuous with little margin for compromise. The reactor operation can modulate in power output and does not have a cyclic energy input; however, once started, a reactor system cannot be brought to a zero heat generation condition. The two systems, while different in detail operation, show no difference in their operating implications. Control requirements show offsetting complexities and represent near equality in comparison.

3.5.3 Other Considerations

The pertinent comparisons between the systems relate to installation operations, the start up sequence, and the shutdown requirements of the solar dynamic unit compared with handling high level radioactive materials. The large scale solar dynamic units have an identified complexity associated with on-orbit assembly and alignment processes. The long-reach, precisely controlled handling booms and manipulators that install the solar dynamic units move to the berthing bay and continue to support the ATSS. In such a context, solar dynamic units show an advantage by synergistic usage of major equipment items. The alignment of the concentrator reflecting elements and the start-up process will consume time as some form of EVA, and these operations are

more than offset by assembly and start-up of the reactor system which would proceed indoors. The shutdown and dismantling of a reactor does involve major equipment items which would be essentially single purpose (e.g., radiation shielded casks and containers). The dismantling and recovery technology exists for Earth-based reactors and could be adapted to space applications. A concern for inadvertent exposure to radioactive materials is real and cannot be discounted. Handling and control of radioactive materials in a space environment together with requirements for special purpose equipment become the principal negative considerations relative to the use of nuclear fission power sources in manned space stations.

3.5.4 Technology Implications

The comparisons and assessments discussed above identify technology areas pertinent to attainment of the ATSS. Most areas have active development projects underway which could lead to a configuration for the ATSS. The following comments serve to focus, emphasize, or further justify such present activities in their role as precursor steps to the ATSS.

A. Converter Elements

While rotating machinery itself makes the smallest contribution to the system mass, the thermal efficiency has a significant impact, and AC generation does make a major contribution to the control requirements. A set of alternators operating at 400 Hz and delivering 440 V imposes very stringent requirements on rotation speeds and magnetic fields. Fortunately, AC systems tend to hold themselves in-phase. However, the requirement for load control by pressure regulation involves the

transfer of heat through the walls of pressure vessels, which is an inherently slow process.

The thermal performance of closed-cycle gas turbines stems from the efficiencies of the heat transfer elements and justifies a continuing effort to improve the performance of heat exchangers. The needs for improvements place a particular emphasis upon the cycle-critical regenerator. Within any cycle defined by temperature limits and a pressure range, the heat transfer and pressure losses in the regenerator will dictate the achievable thermal efficiency. For any heat cycle, high thermal efficiency demands recovery of waste heat, and for space operations, thermal efficiency represents the effective countermeasure to system mass. The heat rejection radiator makes a major contribution to the mass of the converter system, and the surface operating temperature becomes the defining parameter. The fourth-power relationship for radiation heat transfer implies a multiplied reduction in surface area for each incremental increase in operating temperature. For example, an increase in radiator temperature from 320 to 380 K (576 to 684^{o}R) would double the heat rejection and reduce radiator area (and mass) by a factor of 2. On the other hand, a 60 K (108^{o}R) increase in the low temperature for the cycle requires a 120 K (216^{o}R) increase in the high temperature in order to retain the same cycle efficiency. Therefore, the physics of high-efficiency thermal cycles justify (and almost dictate) a continuing development effort to accommodate higher operating temperatures for heat transfer media, for heat transfer surfaces, and for rotating machinery.

B. Solar Dynamic Elements

The technology requirements for large area solar concentrators have been addressed in present development efforts as mass efficient

materials, rigidized structures, and improved reflecting surfaces. These efforts need to continue. The considerations for solar collectors have also received significant attention, therefore, a number of configurations have been proposed, constructured, and evaluated (References 3-2 and 3-3). Size introduces a feature which appears unique to the ATSS. Motion to track the Sun for pointing represents a universal requirement for all solar concentrators. However, the ability to interrupt power by moving off-Sun may not exist for a 450 kW unit. For example, the concentrator for a 75 kW unit would have a diameter of about 20 m (65 ft) and permit a mounting that could be rotated completely off-Sun (e.g., a trunnion located 10 m (33 ft) above a platform). On the other hand, a concentrator of twice that diameter may not permit trunnion mounting or offer that much clearance for movement. Consequently, 425 kW solar dynamic units become continuous operations in the same context as oil refineries, paper mills, fiber spinning lines, etc. Techniques for assuring continuous operations exist, and development for space station applications appears prudent.

C. Reactor Elements

The comparison study anticipated radiation shielding as 90 percent of the total reactor system mass. Reactor systems and solar dynamic systems of essentially equal mass were not anticipated. This result leaves selection of the heat source for electric power dependent upon mission content and mission operating requirements, since masses and complexities show no singular preference. The critical reactor technology requirements appear as the development of materials compatible with the operating temperatures for the operating life. Long-life nuclear systems are well established for ship-board propulsion and

central-station power generation. In both cases they are presently based upon high-pressure water configurations. Long-life liquid-metal systems have been addressed but not brought to full development.

REFERENCES

3-1 Roschke, E. John; and Wen, L.: Preliminary Systems Definition Study for Solar Thermal Dynamic Space Power Systems. Jet Propulsion Laboratory, 1984.

3-2 Roschke, E. John: Solar Dynamic Systems for Power Applications. AIAA 24th Aerospace Sciences Meeting, January 6-9, 1986.

3-3 Nainiger, Joseph J.; and McKessock, David B.: Mass Area, and Propellant Requirement Comparisons of Several Potential Growth Space Station Power Systems. Space Station System Directorate, Lewis Research Center, PIR No. 71, October 1984.

3-4 Queijo, M.J. et al.: An Advanced-Technology Space Station for the Year 2025, Study and Concepts. NASA CR 178208 March 1987.

3-5 Norman, C.A. and Zimmerman, R.H.: Introduction to Gas-Turbine and Jet-Propulsion Design. Harper Brothers, 1948.

3-6 Brandt, Donald E: Heavy Duty Turbo Power: The MS7001F. Mechanical Engineering, July 1987.

3-7 Glasstone, Samuel; Principles of Nuclear Reactor Engineering. D. Van Nostrand, 1955.

3-8 Queijo, M.J. et al.: Analyses of a Rotating Advanced-Technology Space Station for the Year 2025. NASA CR 178345, January 1988.

3-9 Kastem, Paul R.; Cleveland, John C.; and Bowers, Howard I.: New Approaches for High Temperature Gas Cooled Reactors, Paper 849554. 19th Intersociety Energy Conversion Engineering Conference, San Francisco, California, August 19-24, 1984.

4.0 ENVIRONMENTAL FORCES AND TORQUES ACTING ON THE ATSS

The attitude control and pointing requirements for the Advanced-Technology Space Station (ATSS) are derived from the angular deviation limits for the solar dynamic power units. The individual unit mountings and pointing elements can accept up to 1 degree off-Sun. (See paragraph 3.3.) These tolerances are superimposed upon the solar-facing one revolution per year orbit constraints in analyses to predict attitude control and pointing forces, orbital decay forces, and reboost requirements. This section examines the disturbing forces and torques on the station, mentions some means of counteracting these disturbances, and discusses orbital decay and reboost requirements.

4.1 Computational Methods

The computational methods used in the analyses are those of the I-DEAS^2 (I-DEAS Squared) programs of Reference 4-1. The integrated capability of I-DEAS^2 is indicated in Figure 4.1-1, and some background information on the I-DEAS^2 programs is given in References 4-2 through 4-4.

The computational process begins with the specification for the dimensions, weight, and position of each component of the spacecraft. The Geometric Modeling (GEOMOD) program uses that information to produce computer-generated drawings of the spacecraft and to compute moments of inertia, total weight, center of mass, and center of pressure locations. The model generator (MODGEN) program converts the data into a form usable by other programs. This information, along with specified orbit parameters, becomes part of the data base which can be used as required in other programs, such as Articulated Rigid-body Control Dynamics

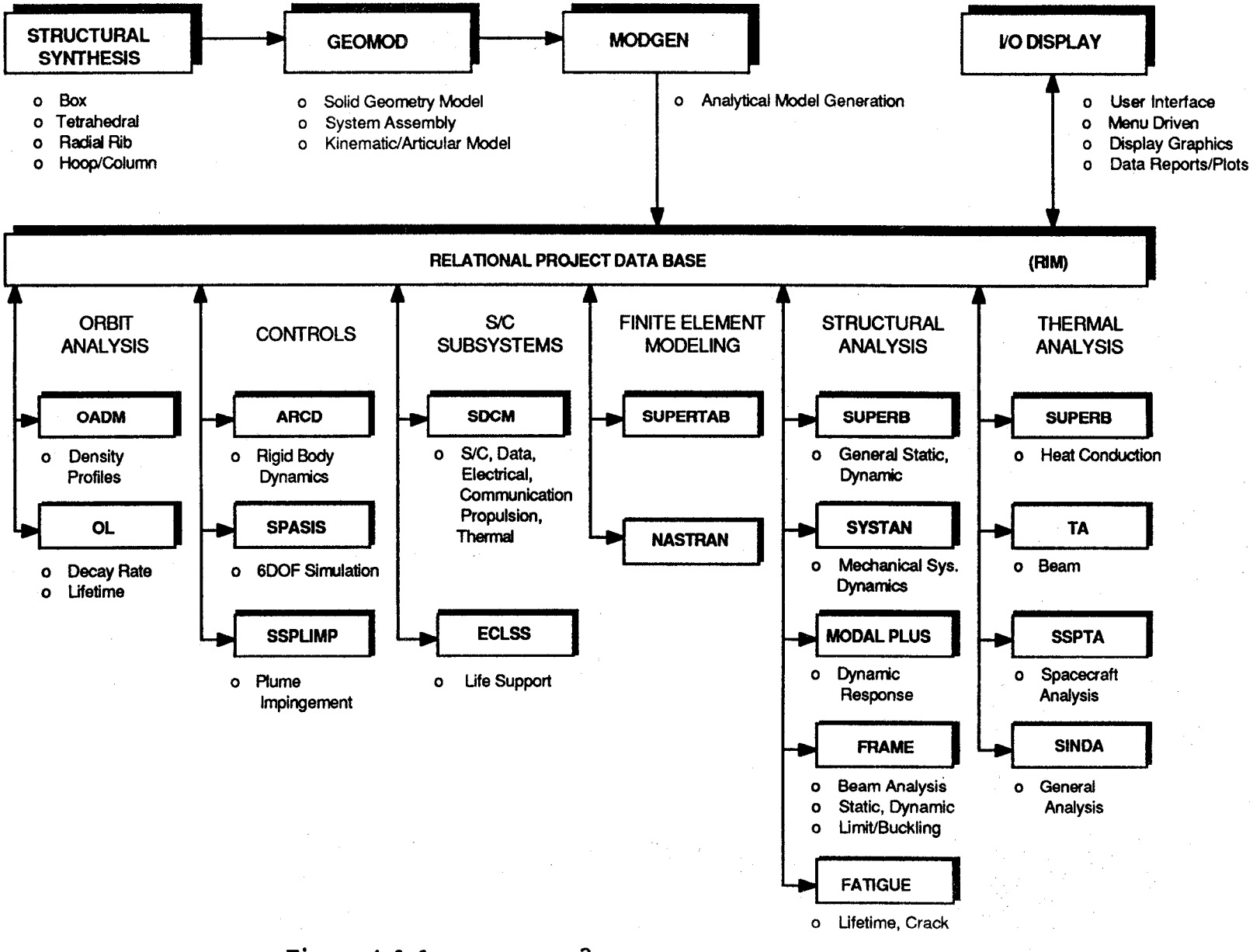

Figure 4.1-1 NASA I-DEAS^2 Integrated Program Capability

(ARCD), Attitude Prediction (ATTPRED), and Orbital Lifetime (OL). References 4-5 through 4-9 are examples of uses of I-DEAS^2.

4.2 Math Model of the ATSS

The dimensions and component weights of the ATSS were generated in the studies of References 4-10 and 4-11, and are repeated herein as Figures 2.0-1 and 2.0-2, respectively. The geometry and dimensions were used in the I-DEAS GEOMOD program to produce a computer-generated geometrical representation of the conceptual model (Figure 4.2-1). This type of representation is useful in that it provides a visual check of the configuration that has been modeled. The dimensions and weights of the various ATSS components were then used in the GEOMOD and MODGEN programs of I-DEAS^2 to determine total mass, moments of inertia, center of mass, and center of pressure locations for the ATSS. The axis system selected for the computation has the origin at the center of mass which is 0.856 m (2.81 ft) above the plane of the torus. The axes are oriented as shown in Figure 4.2-2.

Results from the GEOMOD calculations are shown in Table 4.2-1. These values are directed through MODGEN and put into a form that makes them applicable as part of the data base for other IDEAS^2 programs.

TABLE 4.2-1 ADVANCED-TECHNOLOGY SPACE STATION
MASS AND INERTIA PARAMETERS

Total Mass (kg)	Moments of Inertia (kg-m^2)
8.2865×10^6	$I_{xx} = 2.5422 \times 10^{10}$
	$I_{yy} = 2.2452 \times 10^{10}$
	$I_{zz} = 4.4142 \times 10^{10}$
	$I_{xy} = -4.6256 \times 10^6$
	$I_{xz} = 28.706$
	$I_{yz} = -15.960$

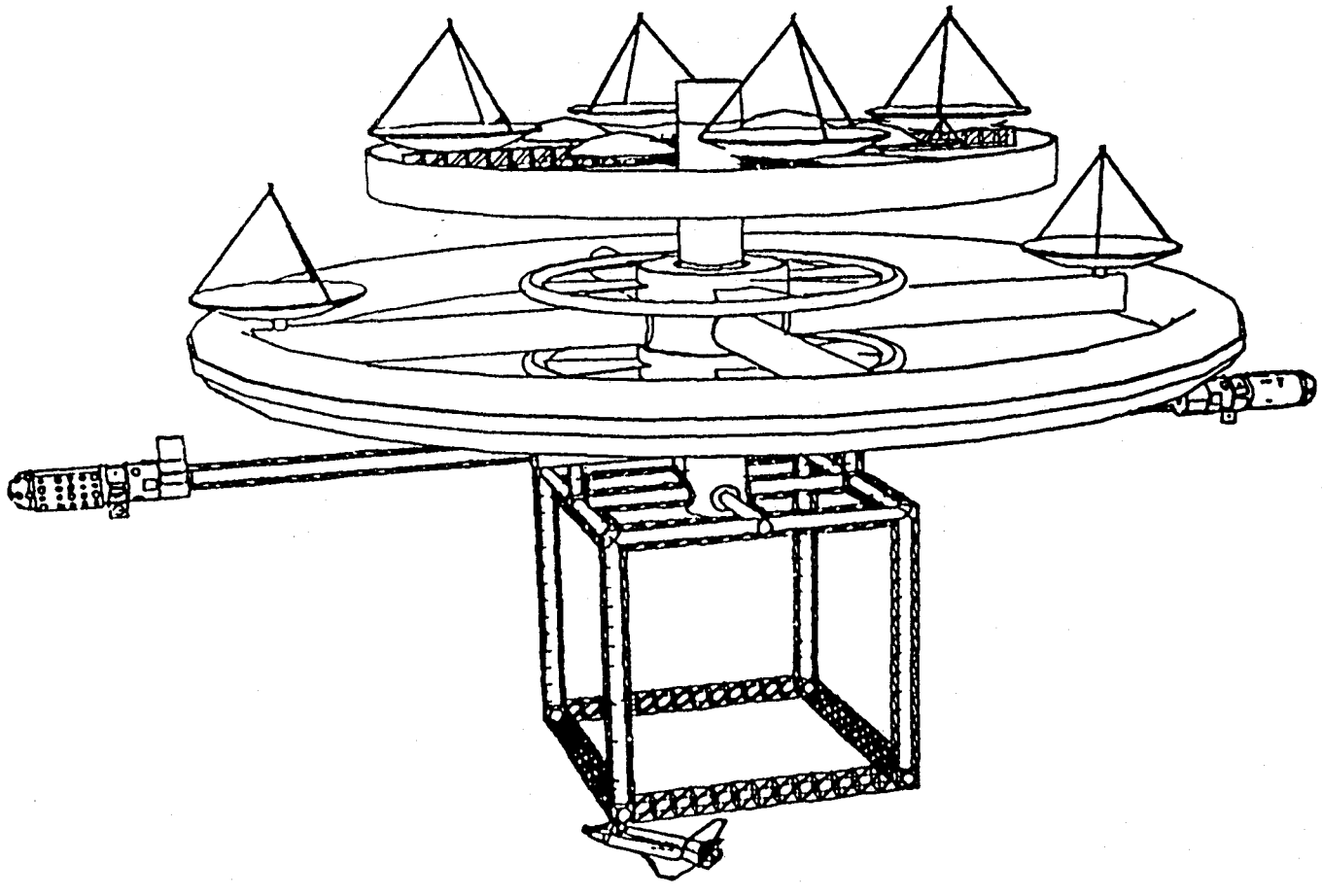

Figure 4.2-1 Computer-Generated Drawing of the Advanced-Technology Space Station

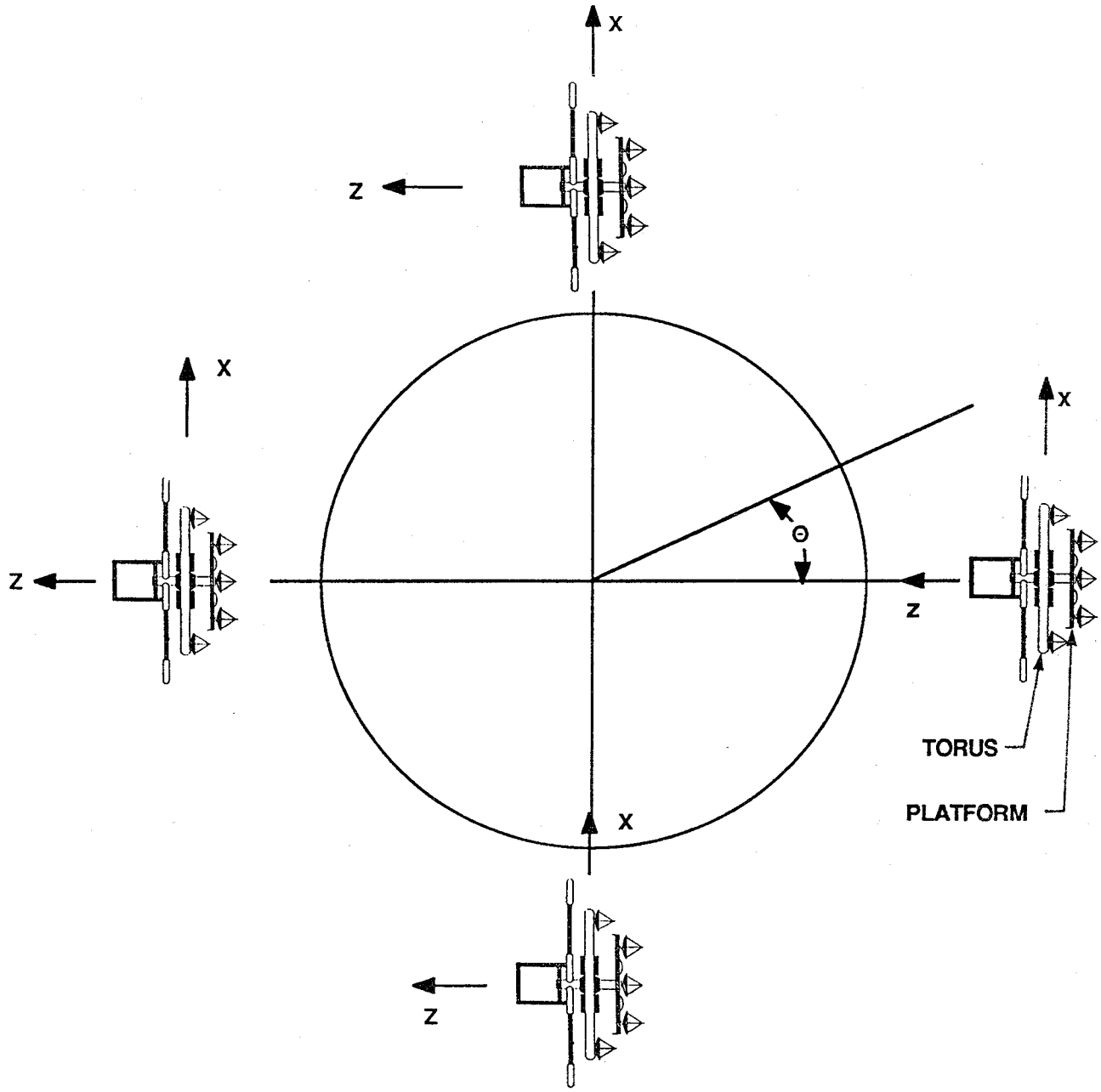

Notes for a Solar Facing Orbit

1. θ is the Orbit Angle measured from Solar Zenith
2. y Axis is positive away from the plane of view
3. The origin for the Axis system is 0.856 m (2.8 ft) toward the platform from the plane of rotation for the Torus

Figure 4.2-2 Orientation of the Advanced-Technology Space Station in Orbit

4.3 External Forces and Torques Acting on the ATSS

The external forces and torques depend on the specified orientation of the ATSS as it orbits the Earth and the desired orbit characteristics. As mentioned previously, it is assumed that the ATSS will be kept Sun-pointing; therefore, for the time required for a single orbit, it can be considered to be fixed inertially. Forces and torques acting on the ATSS are those associated with gravity, aerodynamics, and solar radiation pressure. These forces and torques were computed and used in determining attitude control requirements.

The nominal orbit parameters are:

Attitude (km)	500.0
Orbit Inclination (deg)	28.5
Orbit ascending mode (deg)	0
Day of year	80.0

Calculations pertinent to attitude control analysis were made by use of the ARCD program of IDEAS[2].

4.3.1 Aerodynamic Drag and Torque

The atmospheric drag is dependent on the Space Station orientation relative to its velocity vector, its velocity, and the density of the atmosphere. In this study, the orbit velocity is 7.613 km per second. The spacecraft projected area in a plane perpendicular to the flight direction is determined by the ARCD program. The variation of atmospheric density with position in orbit is shown in Figure 4.3-1 and is based on the atmospheric models discussed in References 4-12 through 4-14.

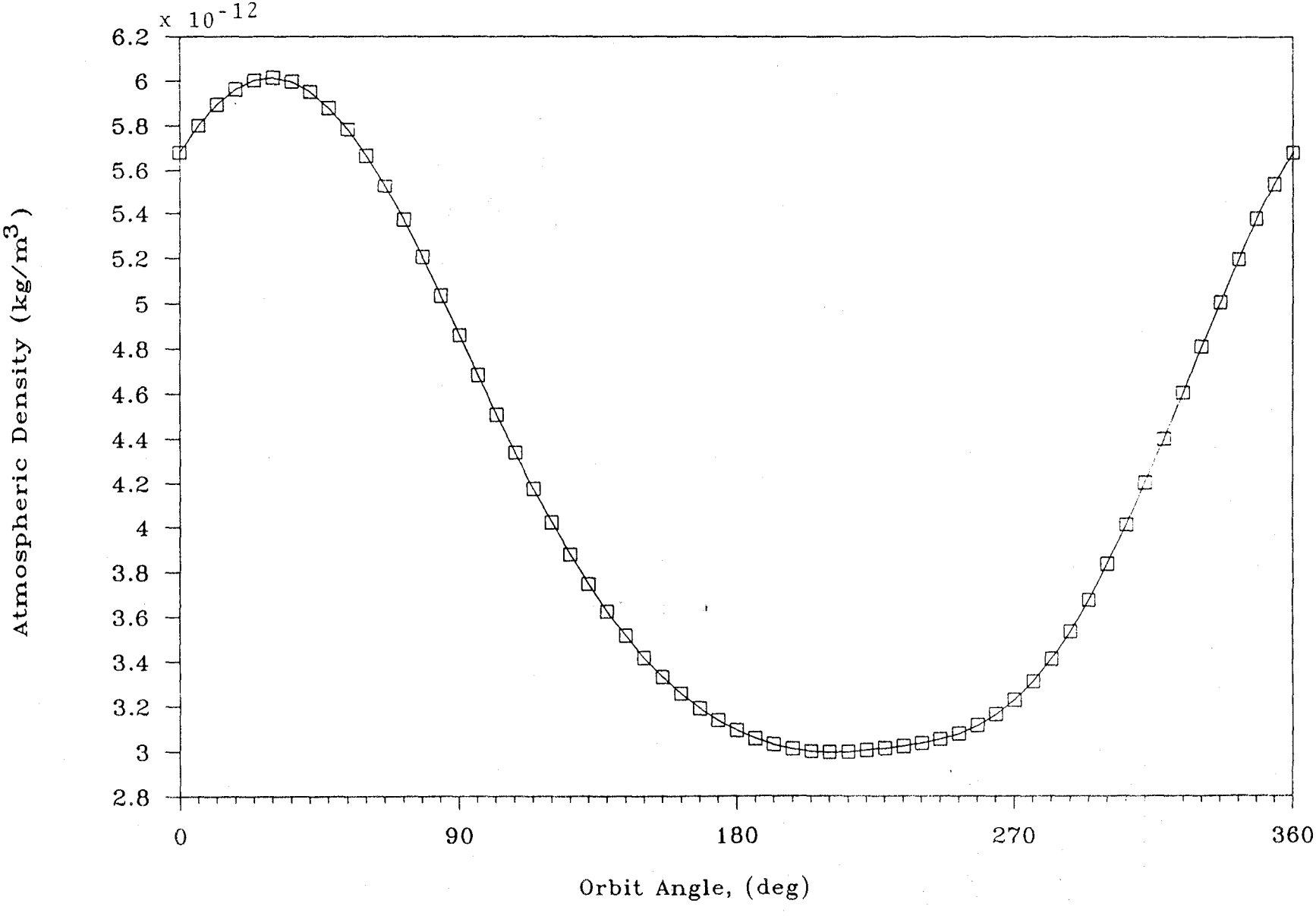

Figure 4.3-1 Atmospheric Density as a Function of Orbit Angle

The variation of aerodynamic force with orbital position is shown in Figure 4.3-2. As expected, the forces are very small, primarily because of the extremely low atmospheric density. The resulting aerodynamic torques are also very small (Figure 4.3-3).

4.3.2 Solar Radiation Force, Torque and Momentum

The solar radiation force is shown in Figure 4.3-4 as a function of orbit angle. Because the ATSS has its z-axis pointed at the Sun, the solar radiation force is along the ATSS z-axis. The force is small when the ATSS is in sunlight and drops to zero when the ATSS is out of the sunlight. There is no torque because of the symmetry of the ATSS about the z-axis.

4.3.3 Gravity Gradient Torque

The variation of gravity gradient torque acting on the ATSS, as a function of orbit angle, is shown in Figure 4.3-5. The variation is cyclical, with a frequency of two cycles per orbit. The gravitational torque is quite high, peaking at about $\pm$ 35000 N-m (25,863 lb-ft). Because of the orientation of the ATSS, the gravity gradient torque is about the ATSS y-axis.

4.3.4 Control Requirements

As mentioned previously, the ATSS is to remain pointed toward the Sun. Since there are environmental torques (aerodynamic and gravity gradient) acting on the Space Station, these must be nulled by a control system. The capability requirements of the control system, therefore,

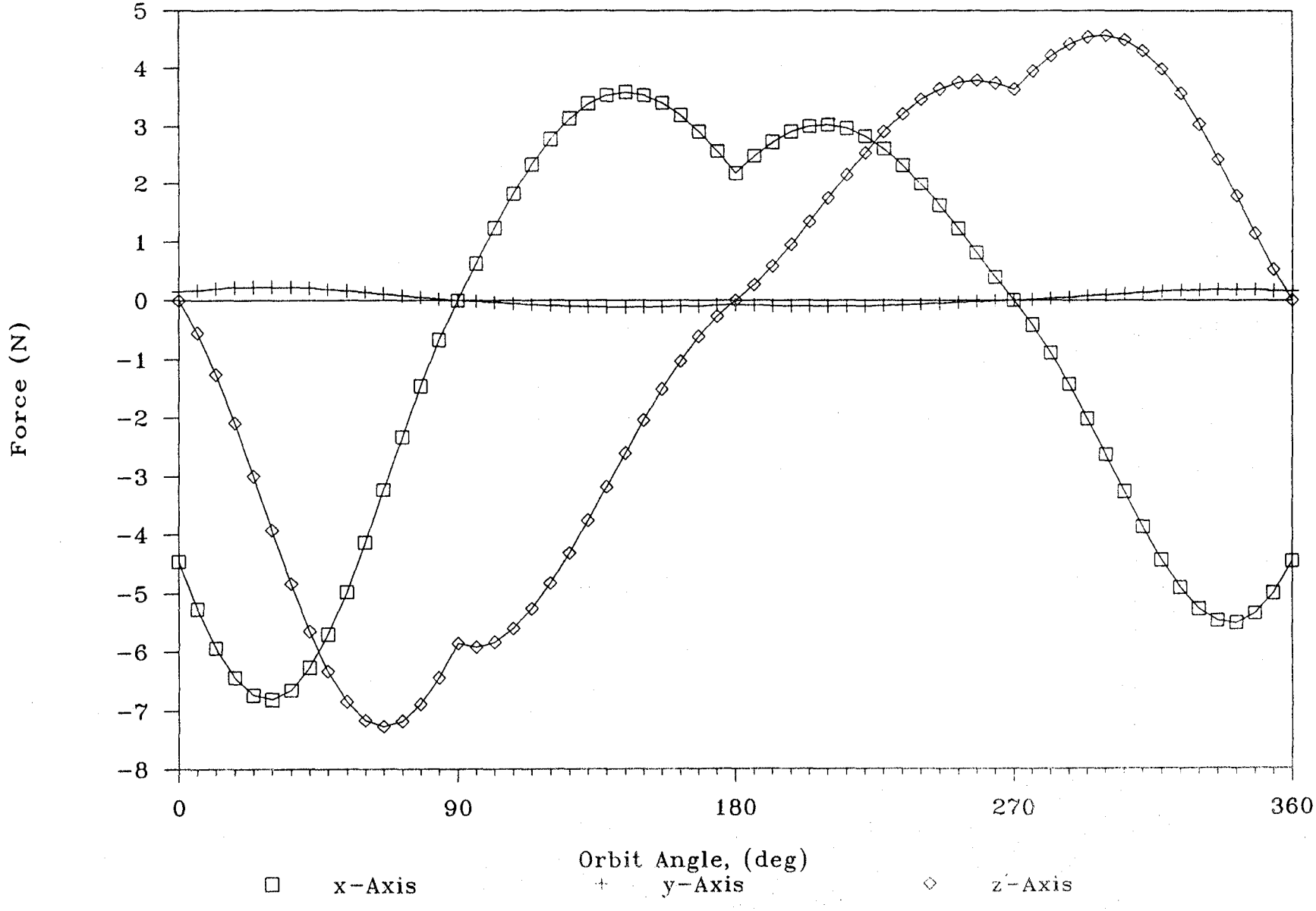

Figure 4.3-2 Aerodynamic Force on the ATSS as a Function of Orbit Angle

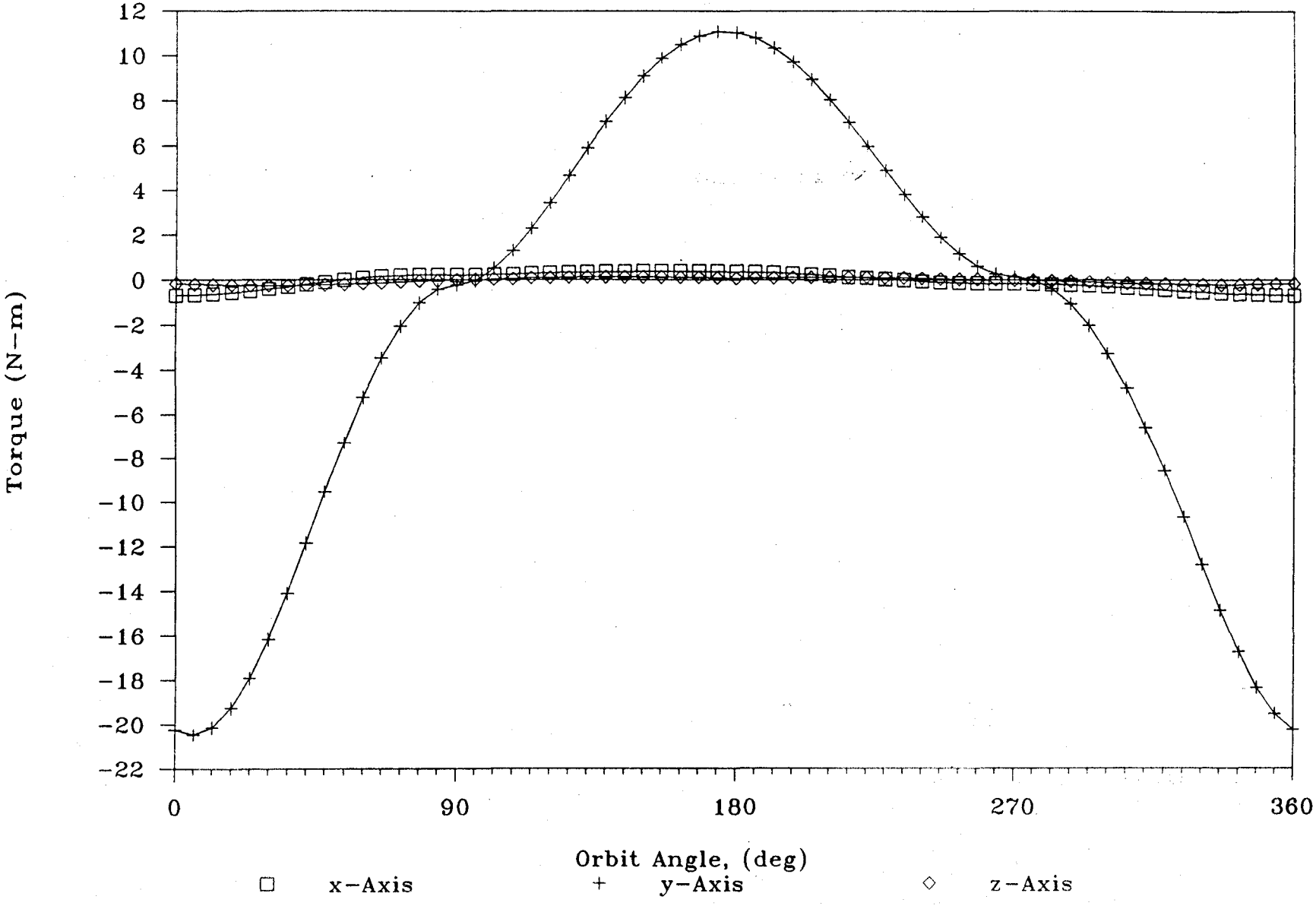

Figure 4.3-3 Aerodynamic Torque on the ATSS as a Function of Orbit Angle

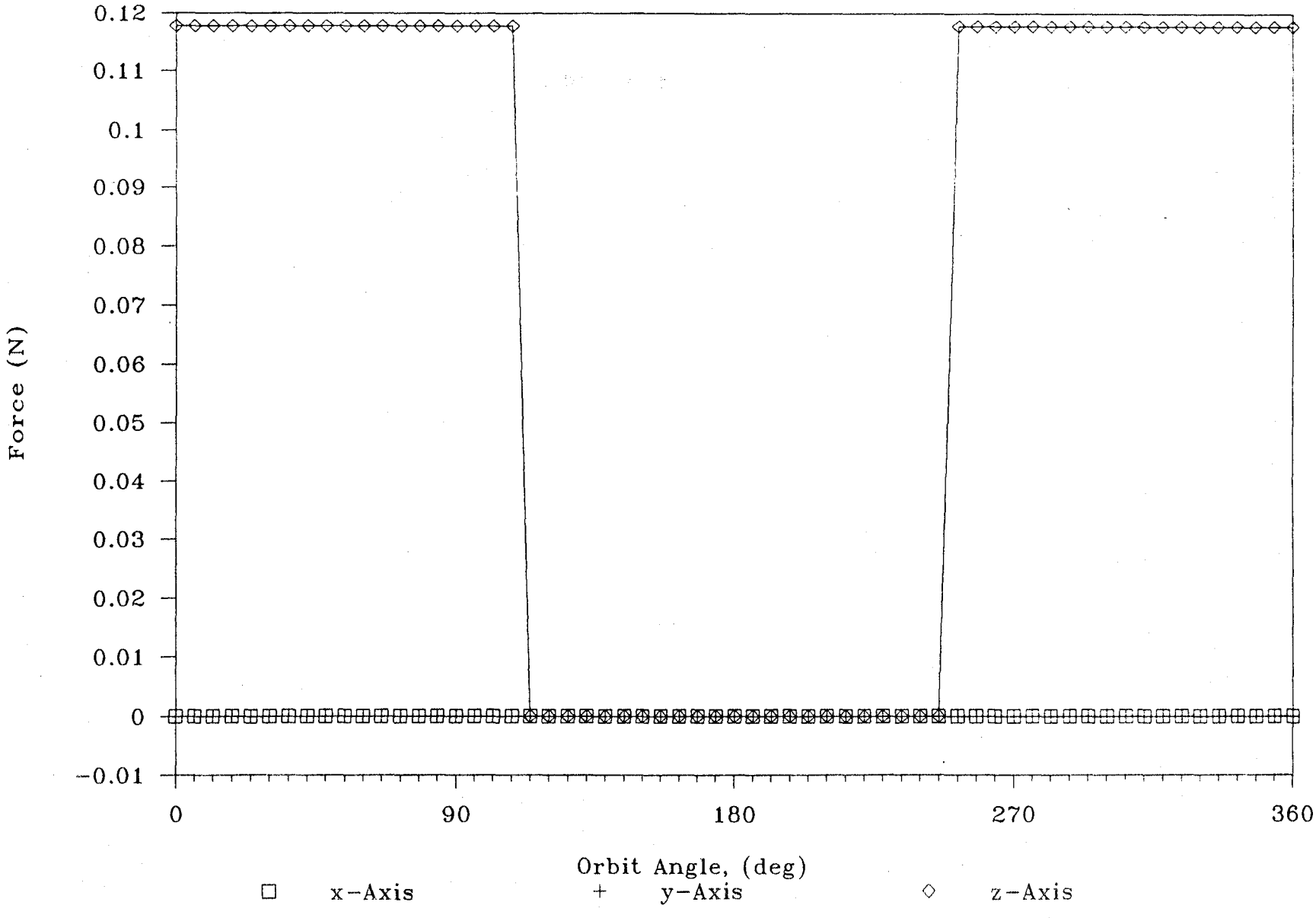

Figure 4.3-4 Solar Radiation Force on the ATSS as a Function of Orbit Angle

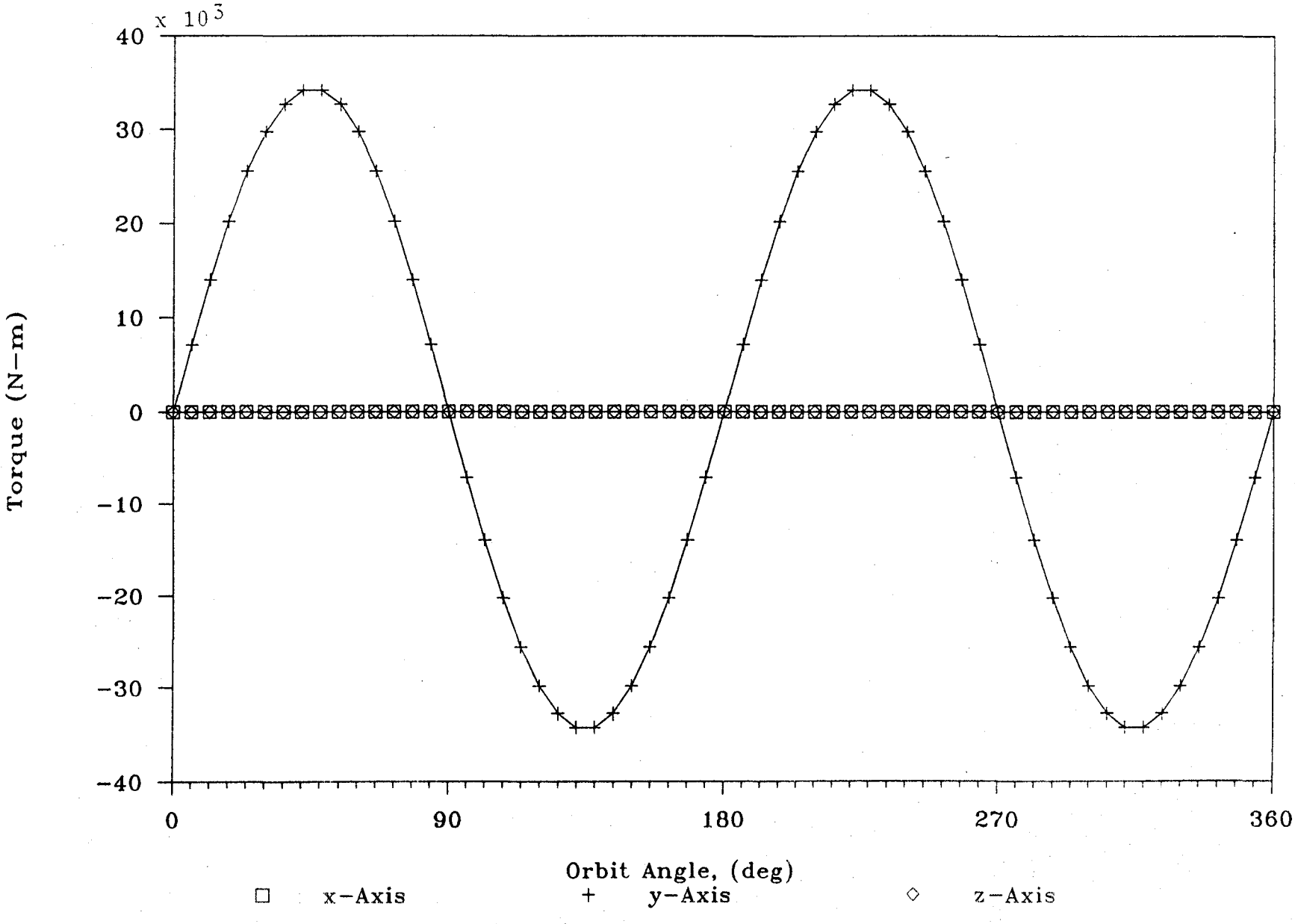

Figure 4.3-5 Gravity Gradient Torque on the ATSS as a Function of Orbit Angle

depend on the maximum values and the variation with time of the environmental torques.

4.3.4.1 Attitude Control

Integration of environmental torques versus time is a measure of the required control system capability. In the present case, the gravity gradient torque (Figure 4.3-5) far exceeds that caused by aerodynamic forces and is the only one that needs to be considered in a preliminary study. Various classes of controllers are available for attitude control, including reaction jets, control-moment gyros (cmg), dual counterrotating wheels, or combinations of these. Selection of a system depends on many factors such as weight, power required, and maintenance. This area is suitable for future study.

4.3.4.2 Orbitkeeping Requirements

The aerodynamic force acting on the ATSS reduces its velocity and causes it to lose altitude. For the ATSS the atmospheric drag imparts a linear impulse of 2945 N-m along the velocity vector per orbit. If the orbitkeeping jets thrust at a level and direction to counter the drag, about 6.8 kg (15 lb) of H_2-O_2 fuel will be used per orbit.

REFERENCES

4-1 "I-DEAS^2 Users Manual," Structural Dynamics Research Corporation, December 1985, San Diego, CA.

4-2 "I-DEAS Level 3.0 GEOMOD Users Guide," Structural Dynamics Research Corporation, 1986.

4-3 "I-DEAS Level 3.0 GEOMOD Reference Manual,: Structural Dynamics Research Corporation, 1986.

4-4 Leondis, A. "Large Advanced Space Systems Computer-Aided Design and Analysis Program," NASA CR 159191-1, July, 1980.

4-5 Heck, M. L., "Users Guide for Articulated Rigid Body Control Dynamics (ARCD)," AMA Report No. 85-2, NASA Contract No. NAS1-17511, March 18, 1985.

4-6 Heck, M. L., Orr, Lynne H., DeRyder, L. J., "Articulated Space Station Controllability Assessment," AIAA Paper No. 85-0024, January, 1985, Reno, Nevada.

4-7 Robertson, B. P., Heck, M. L., "Spacecraft Attitude Control Momentum Requirements Analysis," NASA CR 178219, January, 1987.

4-8 Troutman, P., "ARCD Update: Articular Part Feathering and Turbine Modeling-User's Guide & Test Cases Verification Results," AMA IOM 139, May 31, 1985.

4-9 Ferebee, M. J., "Advanced-Technology Space Station Systems Studies at Langley Research Center," AAS Paper No. 87-525, August 1987, Kalispell, MO.

4-10 Queijo, M. J. et al.: An Advanced-Technology Space Station for the Year 2025, Study and Concepts: NASA Contractor Report 178208, March 1987.

4-11 Queijo, M. J., et al.: Analysis of a Rotating Advanced-Technology Space Station, NASA CR-178345, January 1988.

4-12 Jacchia, L. G., "New Static Models of the Thermosphere and Exosphere with Empirical Temperature Profiles." Smithsonian Astrophysical Observatory Special Report No. 313, 1970.

4-13 Jacchia, L. G., "Revised Static Models of the Thermosphere and Exosphere with Empirical Temperature Profiles." Smithsonian Astrophysical Observatory Special Report No. 332, 1971.

4-14 Anon., "Models of Earth's Atmosphere (90 to 2500 km)." NASA SP-8021, 1973.

5.0 EFFECTS ON HUMAN SUBJECTS AND MATERIALS IN THE ARTIFICIAL GRAVITY OF THE ROTATING ADVANCED-TECHNOLOGY SPACE STATION

5.1 Human Factors Considerations in Artificial Gravity

Artificial gravity has one specific purpose: to maintain a satisfactory physiological condition of the crew members. This is elucidated in Reference 5-1, which also identifies effects associated with the rotation necessary for artificial gravity to which crew members must adapt. Other examinations of human performance in a rotating or a simulated artificial gravity environment are included in References 5-2 to 5-19.

This section discusses the effects of artificial gravity on materials as well as human subjects. It begins by delineating the artificial gravity environment at various locations in the rotating Advanced-Technology Space Station (ATSS) and describes both static and dynamic conditions. These conditions are listed in Table 5.1-1. Figure 5.1-1 depicts the areas of the ATSS within the spokes and torus where crew members will live and work. These range from the smallest radius of rotation, 16.76 m (55 ft), to the outer deck with a radius of 119.63 m (392.5 ft). For these areas, angular motions and material handling effects within the rotating environment are described. Finally, cognitive and psychomotor testing within the rotating environment, observations of astronaut performance, and physiological aspects of the ATSS are discussed.

5.2 Some Static Characteristics of Artificial Gravity for the ATSS

Table 5.1-1 (Reference 5-2) lists the various characteristics that exist in artificial gravity when people or objects are stationary

TABLE 5.1-1 EXPRESSIONS OF THE CHARACTERISTICS OF ARTIFICIAL GRAVITY

STATIC CHARACTERISTICS

g LEVEL, $a = r\,\omega_V^2$

g GRADIENT, $da/dr = \omega_V^2$

g RATIOS, $a_1/a_2 = r_1/r_2$

ARTIFICIAL WEIGHT CHANGE, $\Delta W/W = (r_1 - r_2)/r_2$

HYDROSTATIC PRESSURE VARIATIONS, $\Delta P_{Hs} = \rho/2\,(r_2^2 - r_1^2)\omega_V^2$

DYNAMIC CHARACTERISTICS

RADIAL CORIOLIS ACCELERATION

$$\ddot{x} = \ddot{r} - r\,(\omega_V^2 + 2\omega_V\omega_W + \omega_W^2)$$

TANGENTIAL CORIOLIS ACCELERATON

$$\ddot{y} = 2\dot{r}(\omega_V + \omega_W) + r\dot{\omega}_W$$

DISTANCE OBJECTS FALL FROM EXPECTED POSITION

$$d = r_F\left(\frac{\sqrt{r_F^2 - r_1^2}}{r_1} - \tan^{-1}\frac{\sqrt{r_F^2 - r_1^2}}{r_1}\right)$$

ANGULAR CROSS COUPLING

$$\dot{\omega}_{hX} = \dot{\omega}_{h\phi} - \omega_V(\omega_{h\theta}\sin\theta + \omega_{h\psi}\cos\theta\sin\psi)$$

$$\dot{\omega}_{hY} = \dot{\omega}_{h\theta} - \omega_V(\omega_{h\psi}\cos\theta\cos\psi - \omega_{h\phi}\sin\theta)$$

$$\dot{\omega}_{hZ} = \dot{\omega}_{h\psi} + \omega_V(\omega_{h\theta}\cos\theta\cos\psi + \omega_{h\phi}\cos\theta\sin\psi)$$

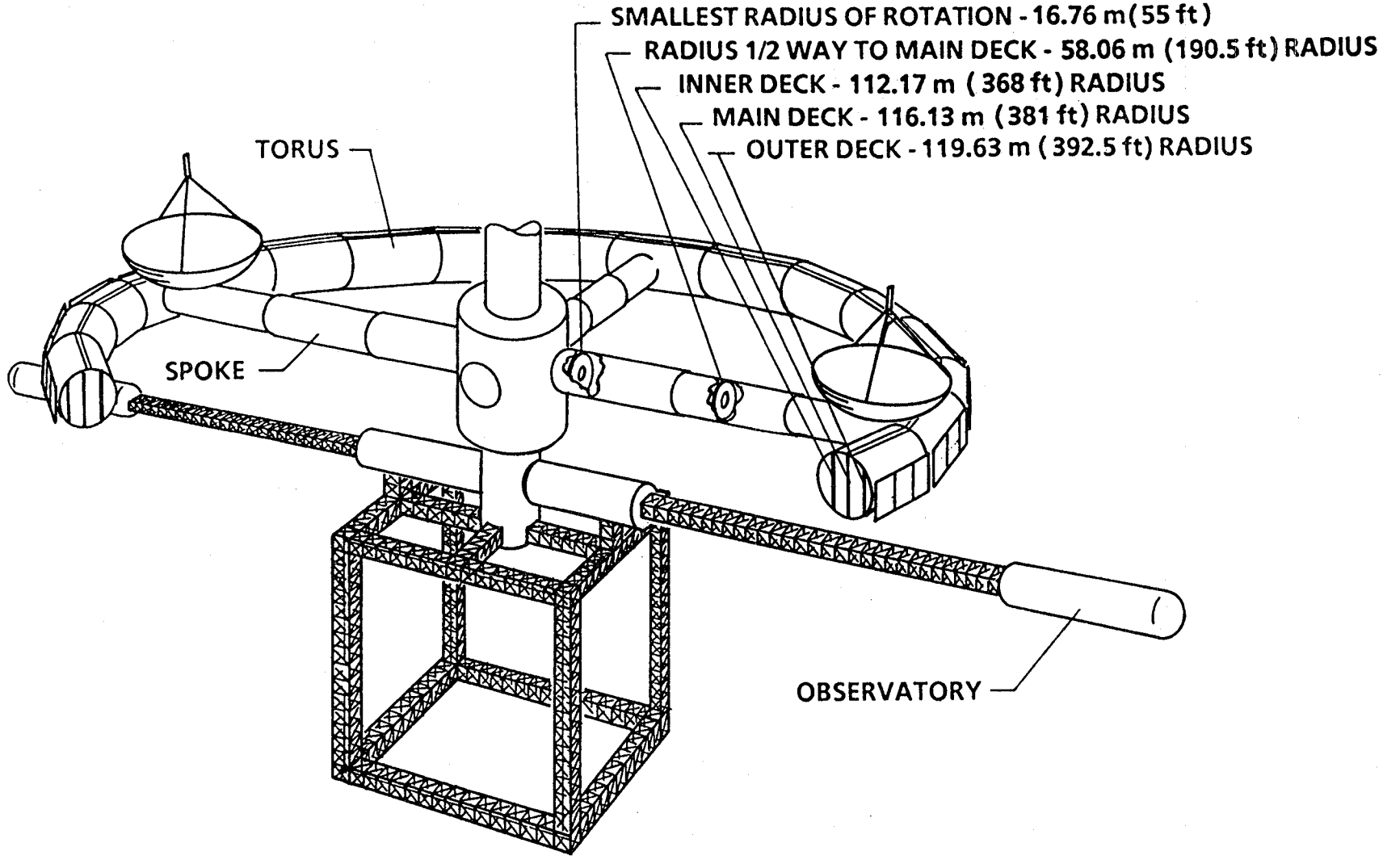

Figure 5.1-1 Areas of Space Station with Rotation where Crew Members Function

relative to the spacecraft frame of reference. These include variation in the artificial gravity level, its gradient as change in the artificial weight of objects, gravity variation along the body, and hydrostatic pressure variations in fluid systems.

Table 5.1-1 also shows the various characteristics that exist in artificial gravity when people or objects are in motion relative to the vehicle frame of reference. These include the tangential and radial Coriolis accelerations that exist when radial and tangential motions occur, respectively, within the vehicle. Included are the angular cross couplings that exist when people or objects are rotated within the vehicle and the phenomenon of dropped or thrown objects not falling into expected positions.

5.2.1 Variations of Artificial Gravity Level

The variation of artificial gravity level with radius is shown in Figure 5.2-1. The concept of having 1 g at the main deck floor, (Reference 5-1) requires a torus rotation of 0.291 rps (2.776 rpm). The value of 1 g in the main occupied area has been selected for physiological reasons where one artificial g should most adequately replace one Earth g to maintain the crew's well-being.

No data exist on the effects of partial gravity levels on human physiology, and the rather serious effects of long-term weightlessness are evident (Reference 5-1). In the torus area, the outer deck has about 3 percent larger g level and at the inner deck about 3 percent lesser g level than the 1 g at the main deck. This difference is not expected to have any significant influence on human physiology and performance.

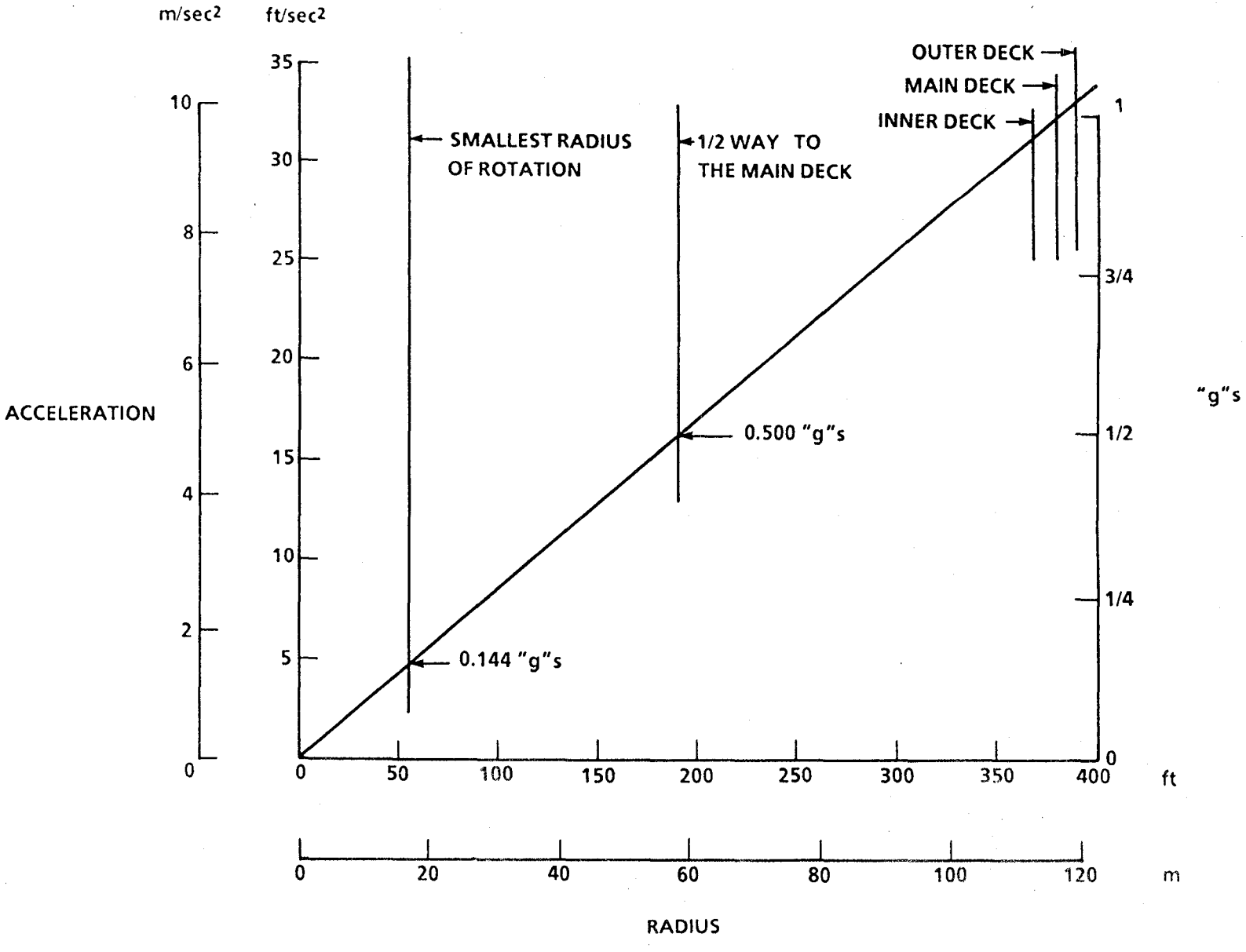

Figure 5.2-1 Artificial Gravity Level

The spokes of the ATSS are 9.14 m (30 ft) in diameter and provide adequate space for living facilities and work stations with any g level from about 0.14 g at the smallest radius of rotation to the 1 g of the main deck. The ATSS therefore, provides a considerable opportunity to study man and his performance, other biological systems, and special manufacturing processes through a range of g levels.

The gravity gradient along the radius is a constant and equal to ω^2 because the rate of rotation is constant and the g ratios are equal to the ratio of the radii involved.

5.2.2 Weight of Objects

The artificial weight of an object or person, of course, varies with radius in accordance with the distance the object is raised or lowered. These variations for heights of 0.91 m (3 ft) and 1.83 m (6 ft) are shown in Figure 5.2-2. The weight variations are less than 1.5 percent at the main deck and nearly 12 percent at the smallest radius of rotation. The reduction of weight when lifting an object and the increase in weight when lowering an object may have some influence on materials handling. Materials handling will be discussed in a later section.

5.2.3 Hydrostatic Pressure

The hydrostatic pressure of a column of fluid at a given height will vary markedly with radius in artificial gravity. The hydrostatic pressure has a very special effect on the cardiovascular system of man as was discussed in Reference 5-1. The reduction of the hydrostatic pressure of the blood system to zero, as in weightlessness causes a

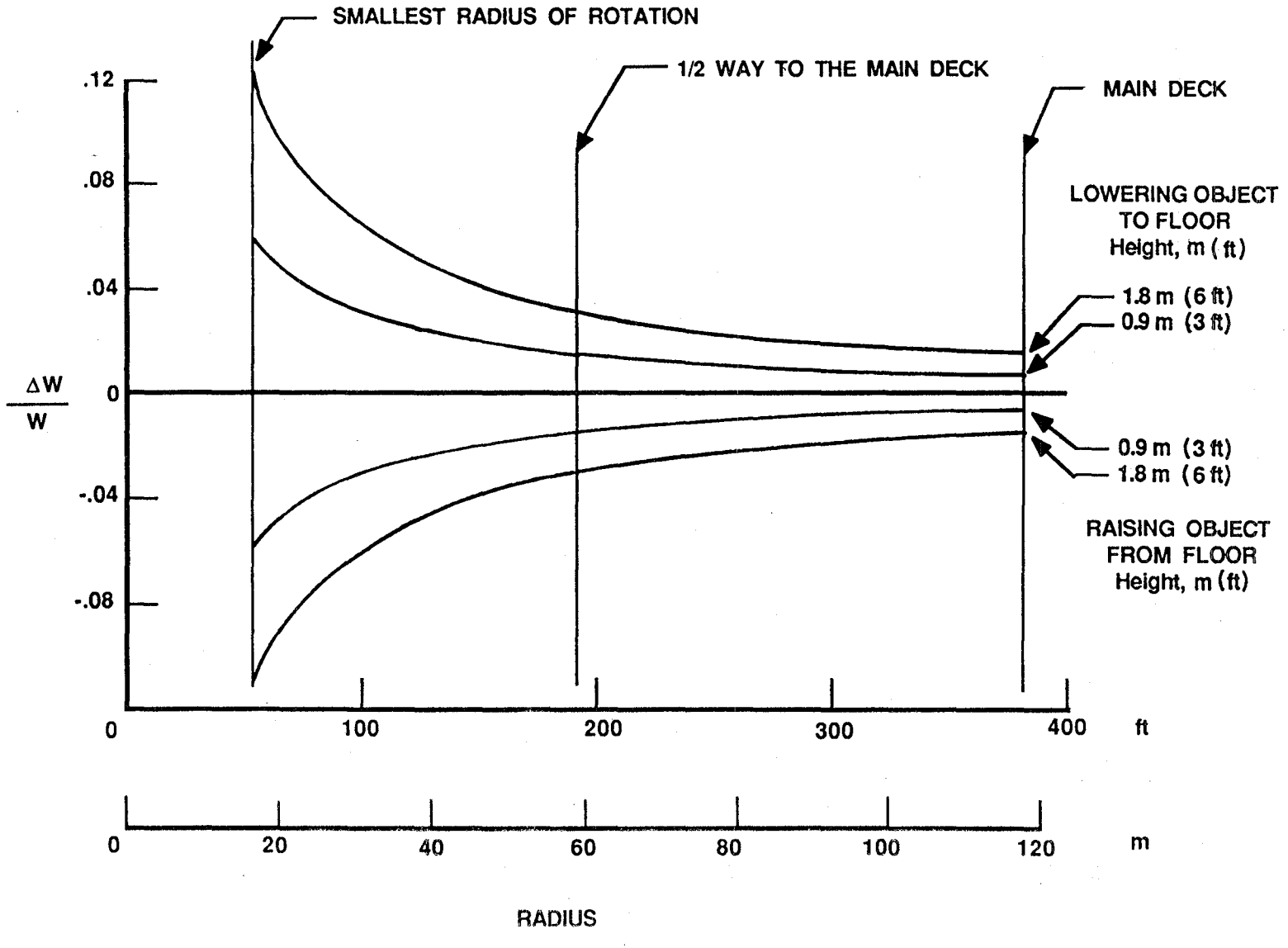

Figure 5.2-2 Object Weight Change with Height above the Floor

significant degeneration of the cardiovascular process with dramatic effects on returning to Earth. It is not known if there is a level of hydrostatic pressure above which no harmful effects occur. The ATSS provides the most reasonable process for studying this phenomenon. The variation of the hydrostatic pressure along the total spoke length may have significant effects on the operation of hydraulic systems and must be considered in their design. The variations of hydrostatic pressure with column height and radial position are shown in Figure 5.2-3. From this figure, the hydrostatic pressure at the main deck is equivalent to that in Earth's gravity, and the cardiovascular system probably will respond as it does on Earth.

5.3 Some Dynamic Characteristics of Artificial Gravity on the ATSS

Table 5.1-1 lists the various characteristics that exist in artificial gravity when people are moving or objects are moved in the vehicle frame of reference. Figure 5.3-1 also depicts some of these characteristics. The effects of tangential, radial, and axial motion are shown.

Tangential motions, either in a pro-spin or anti-spin direction, cause radial Coriolis forces to increase or decrease the artificial weight of man or objects. The magnitude of these Coriolis forces are shown in Figure 5.3-2 for walking speeds of 0.914 m/sec (3 ft/sec) and 1.829 m/sec (6 ft/sec) in both directions. The acceleration experienced, i.e., the change in weight, varies only a little with radius being near 0.125 g at the larger walking speed. At the smallest radius, 16.76 m (55 ft), the gravity level decreases to 0.095 and 0.056 g while walking at 0.914 m/sec (3 ft/sec) and 1.829 m/sec (6 ft/sec) at which

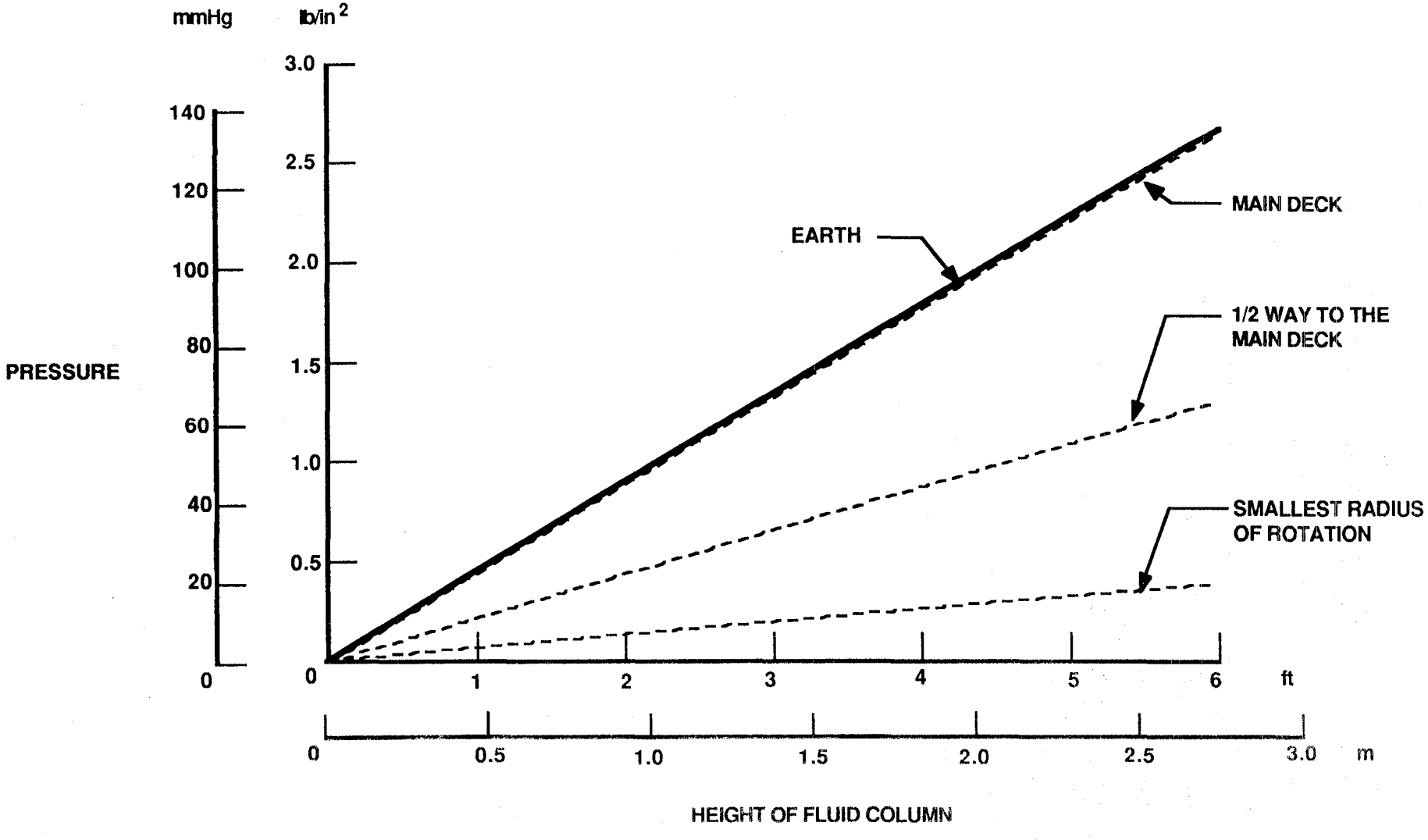

Figure 5.2-3 Hydrostatic Pressure of a Column of Water

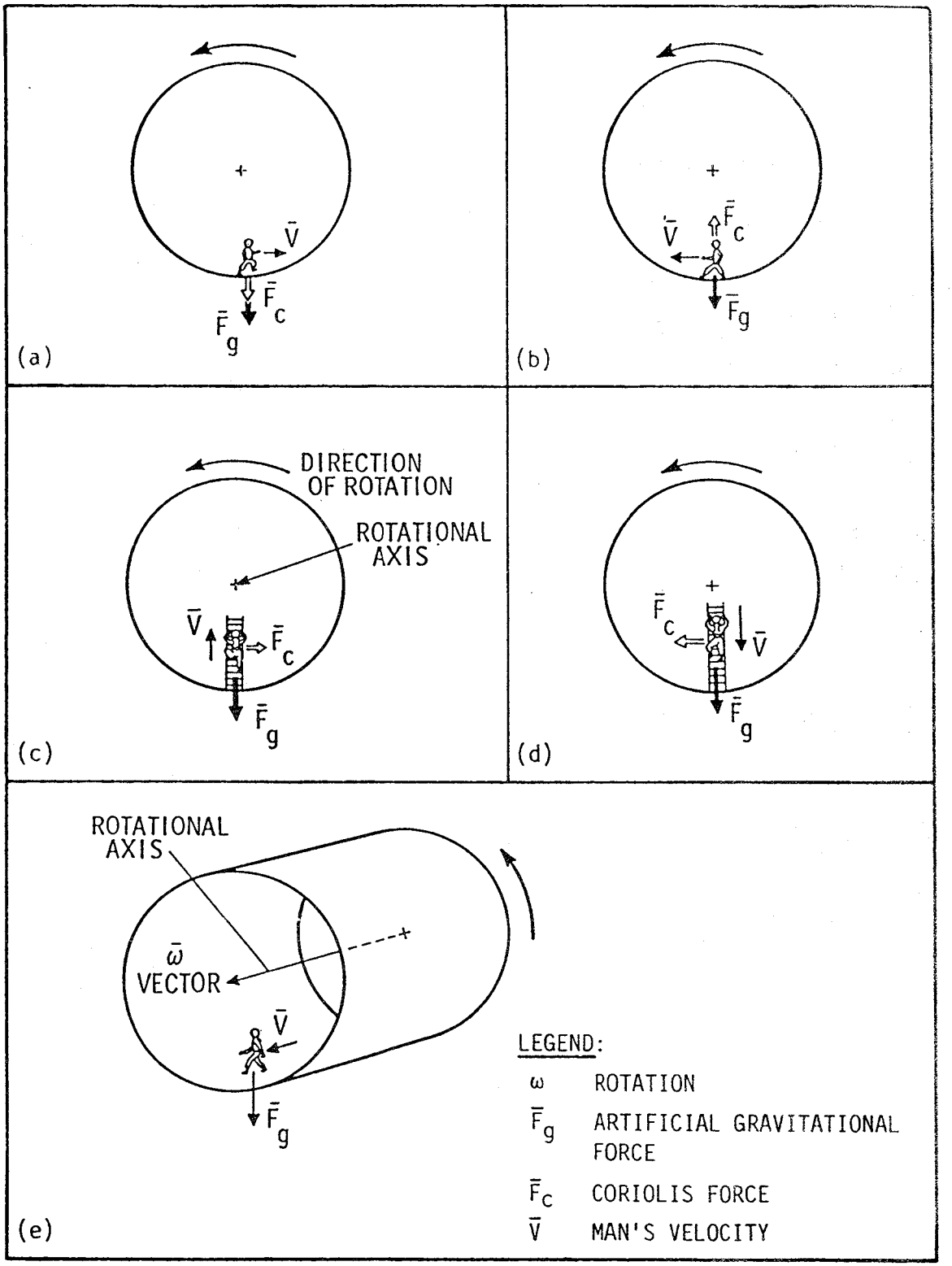

Figure 5.3-1 The Coriolis Forces Experienced when Moving in a Rotating Environment

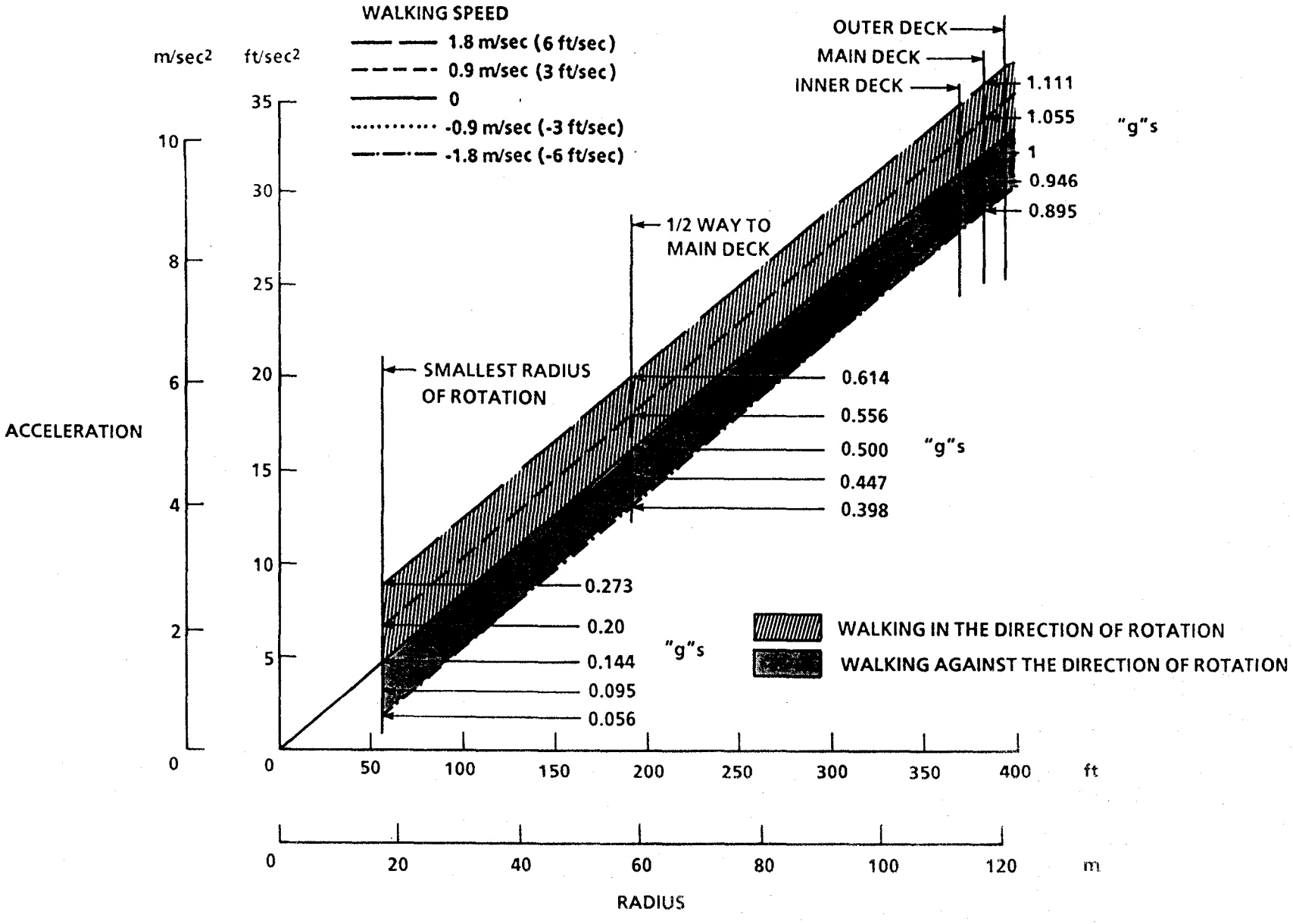

Figure 5.3-2 Effects of Walking Tangentially

values traction would be reduced and walking probably would not be possible as noted by the traction limits shown in Reference 5-2. Reasonable walking, however, seems quite feasible in all other areas of the station. A walking speed of 0.914 m/sec (3 ft/sec) is normal from measurements of walking in working areas, although walking at twice this speed would be readily possible in many areas of the ATSS. Walking and running speeds and step rates as measured in Earth's gravity are shown in Figure 5.3-3 (References 5-10 and 5-19).

Leg heaviness as noted in Reference 5-2 and reported in Reference 5-20 is a phenomenon that occurs because of the nature of walking. The speed of the leg while walking is cyclic and varies from no relative speed while the foot is on the floor, to about twice the walking speed as the leg is moved forward. The Coriolis accelerations acting on the legs and feet are, therefore, different than those on the body and are quite variable. Early simulations (References 5-8 and 5-20) indicated that leg heaviness caused by this factor was readily recognized and was sometimes objectionable. The level of artificial gravity and relative artificial leg weight probably have a significant effect. The studies of this reported phenomenon had maximum radii of 6.1 m (20 ft) and artificial gravity levels of 0.05 to 0.75 g. It is not expected that the phenomenon will be objectionable on the ATSS with radii of 16.76 m (55 ft) to 119.63 m (392.5 ft). The phenomenon is shown in Figure 5.3-4, indicating the leg weight to be about 0.1 g heavier or lighter at the main deck when walking 1.829 m (6 ft/sec), whereas the leg at the smallest radius of rotation would be about 0.3 g heavier or 0.125 g lighter at 1.829 m (6 ft/sec).

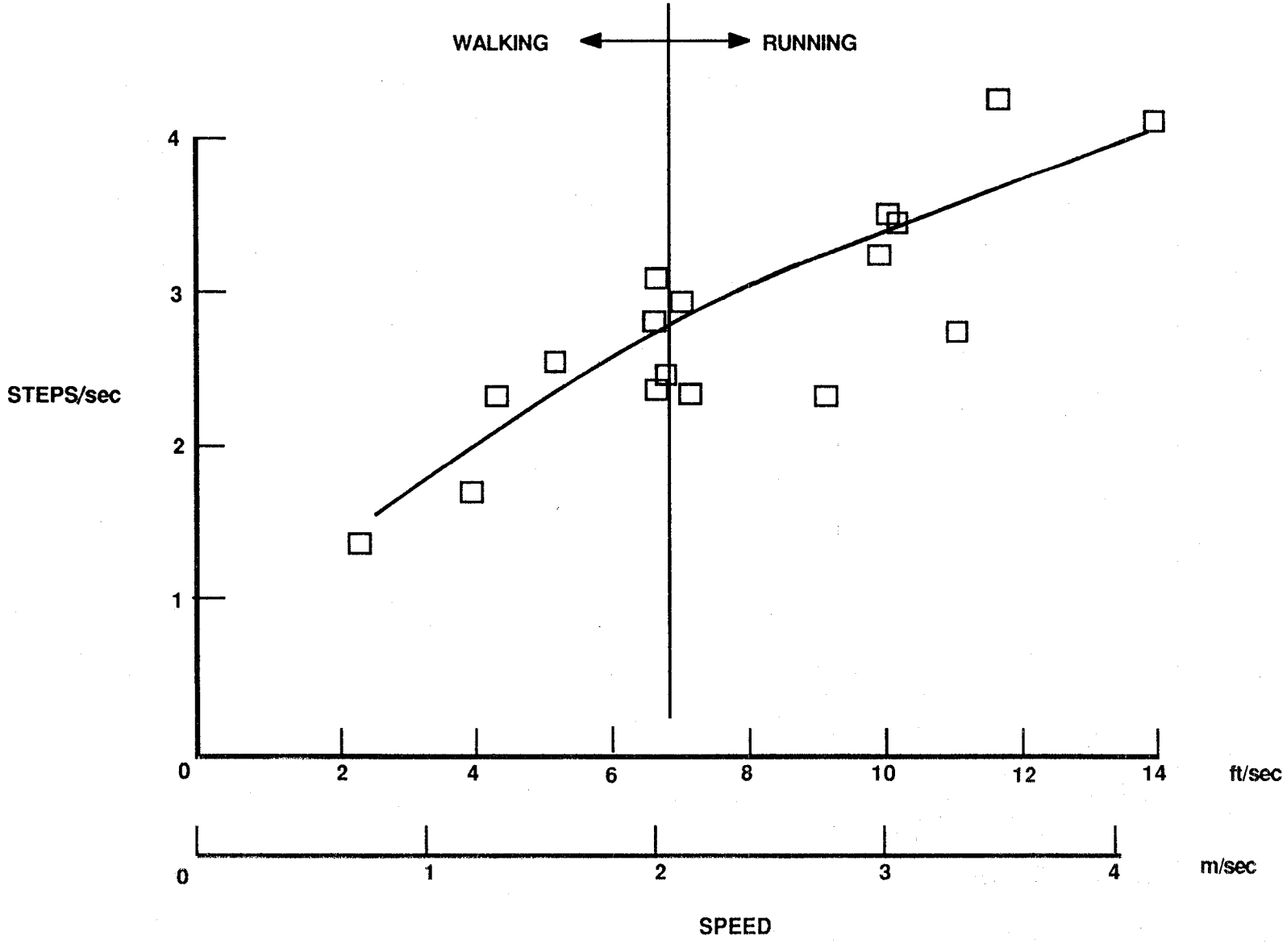

Figure 5.3-3 Comparison of Stepping Frequency in Earth Gravity

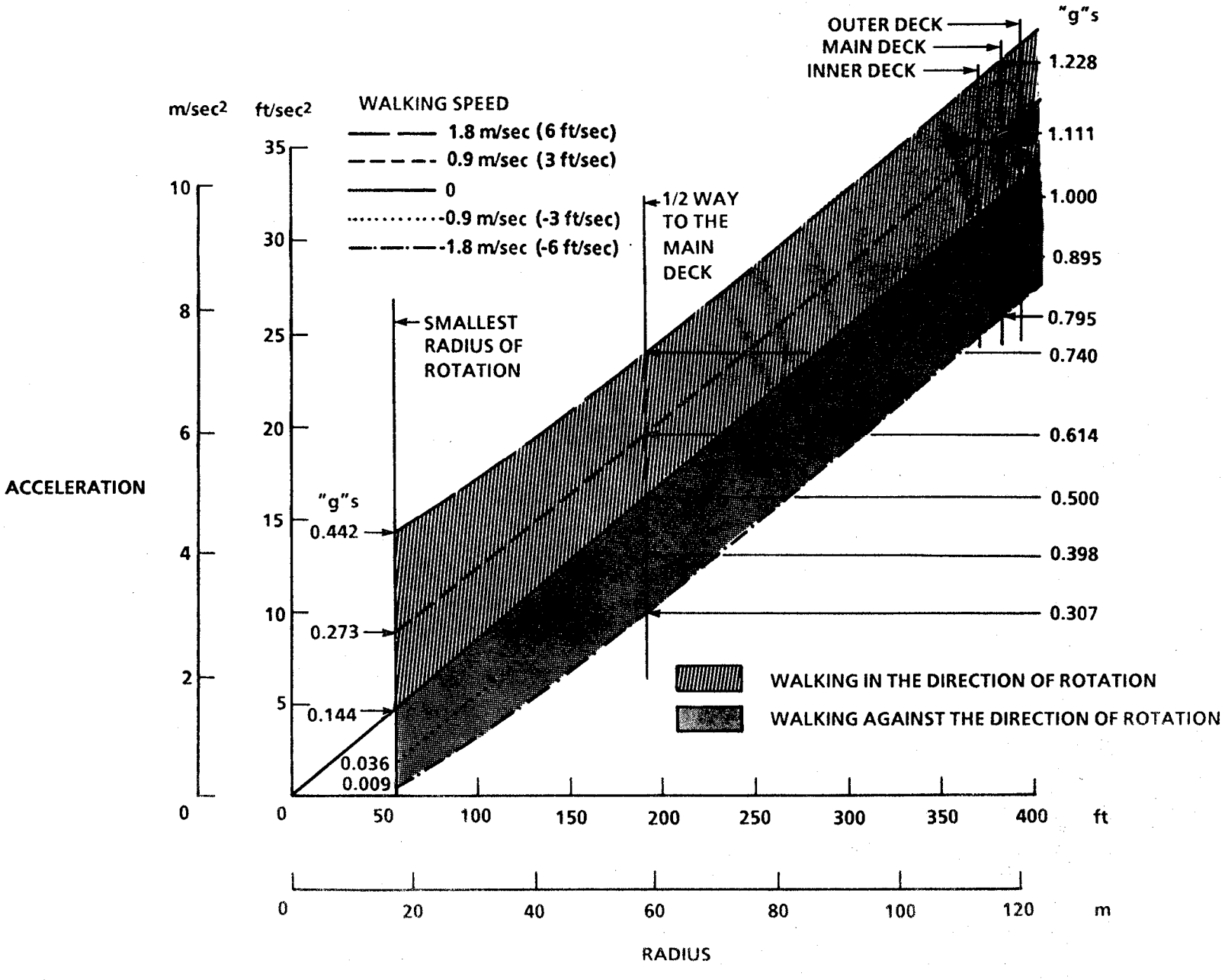

Figure 5.3-4 Leg Heaviness

When moving radially, Coriolis forces acting tangentially are experienced (Figure 5.3-1). This is shown more dramatically in Figure 5.3-5, where climbing a ladder, which is a straight path in the ATSS frame of reference, is (in inertial space) a curved path from whence the tangential Coriolis forces occur. The magnitude of the tangential Coriolis accelerations in the ATSS are plotted in Figure 5.3-6. Radial speeds up to 3.048 m (10 ft/sec) are shown. The tangential acceleration of somewhat less than 0.2 g would be experienced. Forces required to restrain the body in a radial path would act in an anti-spin direction when ascending (moving to smaller radii) and in a pro-spin direction when descending. This phenomenon is described in References 5-11, 5-12, 5-14, 5-15, and 5-16. These references recommended that restraints should be used in elevators if the tangential Coriolis accelerations exceed 3 m/sec^2 (19.84 ft/sec^2) on the ATSS. A radial velocity of 5.15 m/sec (16.896 ft/sec) or greater would be required to exceed this recommendation. At 3.048 m/sec (10 ft/sec) the time required to go from the main deck to the smallest radius of rotation would be 32.6 seconds which may be adequate. At the radial speed of 5.15 m/sec (16.896 ft/sec), for which restraints would be required, a person could move from the main deck to the smallest radius in about 20 seconds.

In Reference 5-1, stairways are proposed for the torus deck areas. Stair climbing can involve both tangential and radial motions resulting in a combination of the phenomenon previously discussed. Therefore, changes in tangential and radial accelerations will be experienced. Assuming a stair riser of 20.3 cm (8 in) and a tread of 30.5 cm (12 in), the radial speed would be 0.66 the tangential speed. The radial and tangential accelerations have been calculated for radial speeds up to

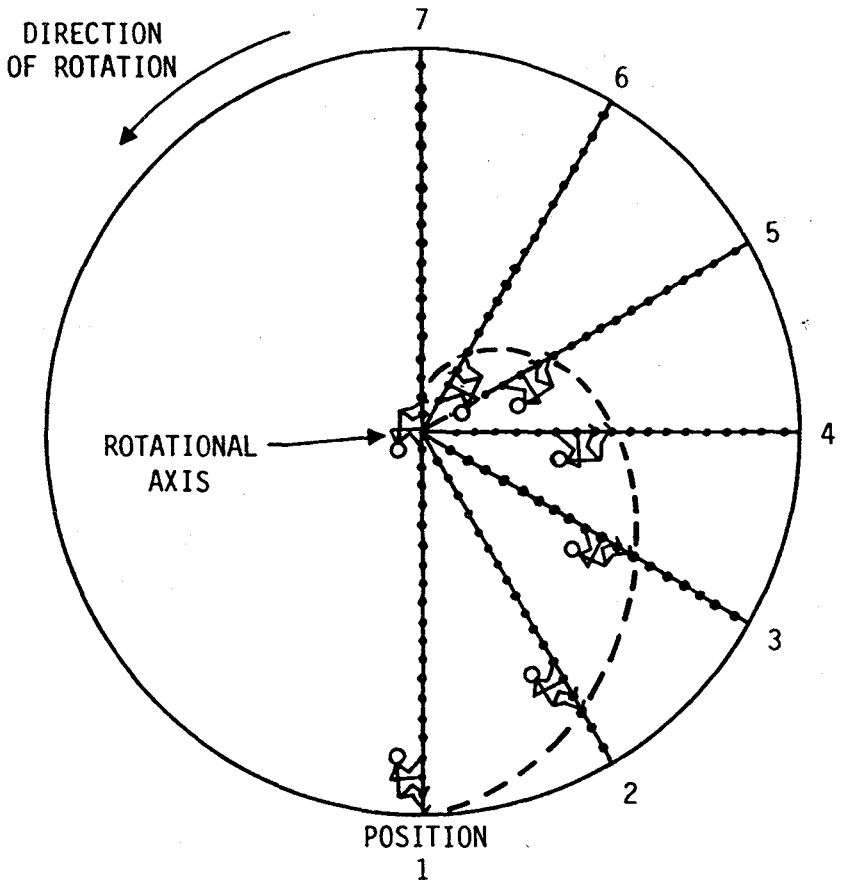

Figure 5.3-5 A Straight Line in a Rotating Environment

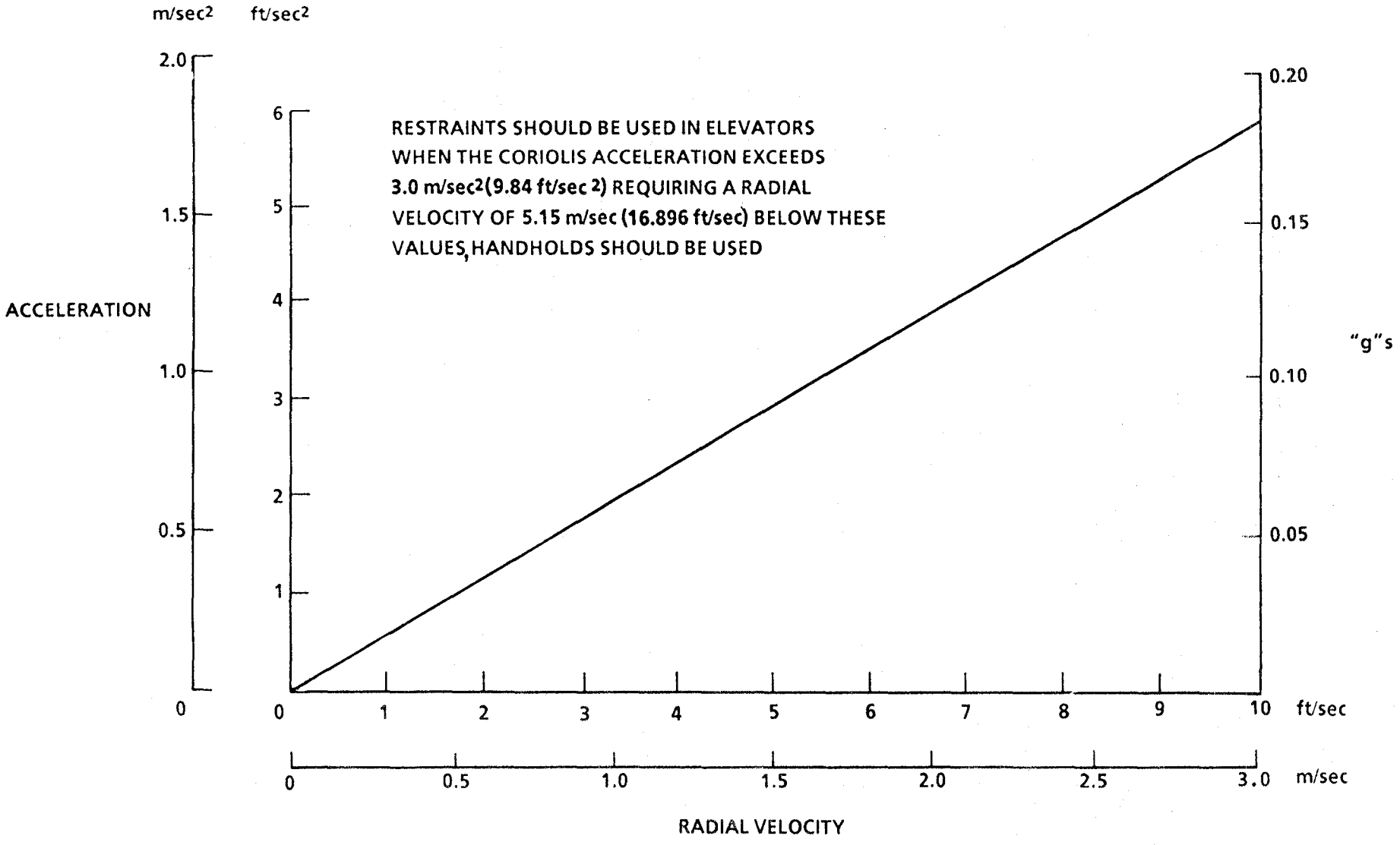

Figure 5.3-6 Tangential Coriolis Acceleration in Radial Ladder Climbing or Elevator Riding

1.52 m/sec (5 ft/sec) while climbing in the direction of rotation, Figure 5.3-7, and against the direction of rotation, Figure 5.3-8. The combination of these forces implies that one must learn to cope with the tangential Coriolis force, either by leaning or by holding handrails. When climbing in the direction of rotation, one would have to lean backwards while ascending the stairs, a potentially dangerous and frightening situation. When descending in the direction of rotation, one would have to lean forward over the descending stairs, also not desirable. When climbing against the direction of rotation, one would lean forward over the ascending stairs, probably the better situation. When descending against the direction of rotation, one would lean backward over the stair, perhaps the better descending situation. The lean angles for these combined accelerations are shown in Figure 5.3-9 for climbing in the direction of rotation, and in Figure 5.3-10, for climbing against the direction of rotation. For the main deck, these angles are 5 degrees or less. At the halfway position, lean angles of 10 degrees or less are possible. For the smallest radius, angles in excess of 20 degrees are possible. For a likely climbing speed of 0.61 to 0.91 m/sec (2 to 3 ft/sec) the angles are significantly less. It is probable that crew members will adapt to these conditions.

Another alternative is that of climbing stairs axially where only the tangential Coriolis acceleration occurs and where one leans sideways on the stairs. Lean angles for axial stair-climbing are shown on Figure 5.3-11. These results show that one leans away from the direction of rotation when ascending and into the direction of rotation when descending. These angles are somewhat less than 5 degrees at the main deck and are 30 degrees at the smallest radius of rotation. Leaning

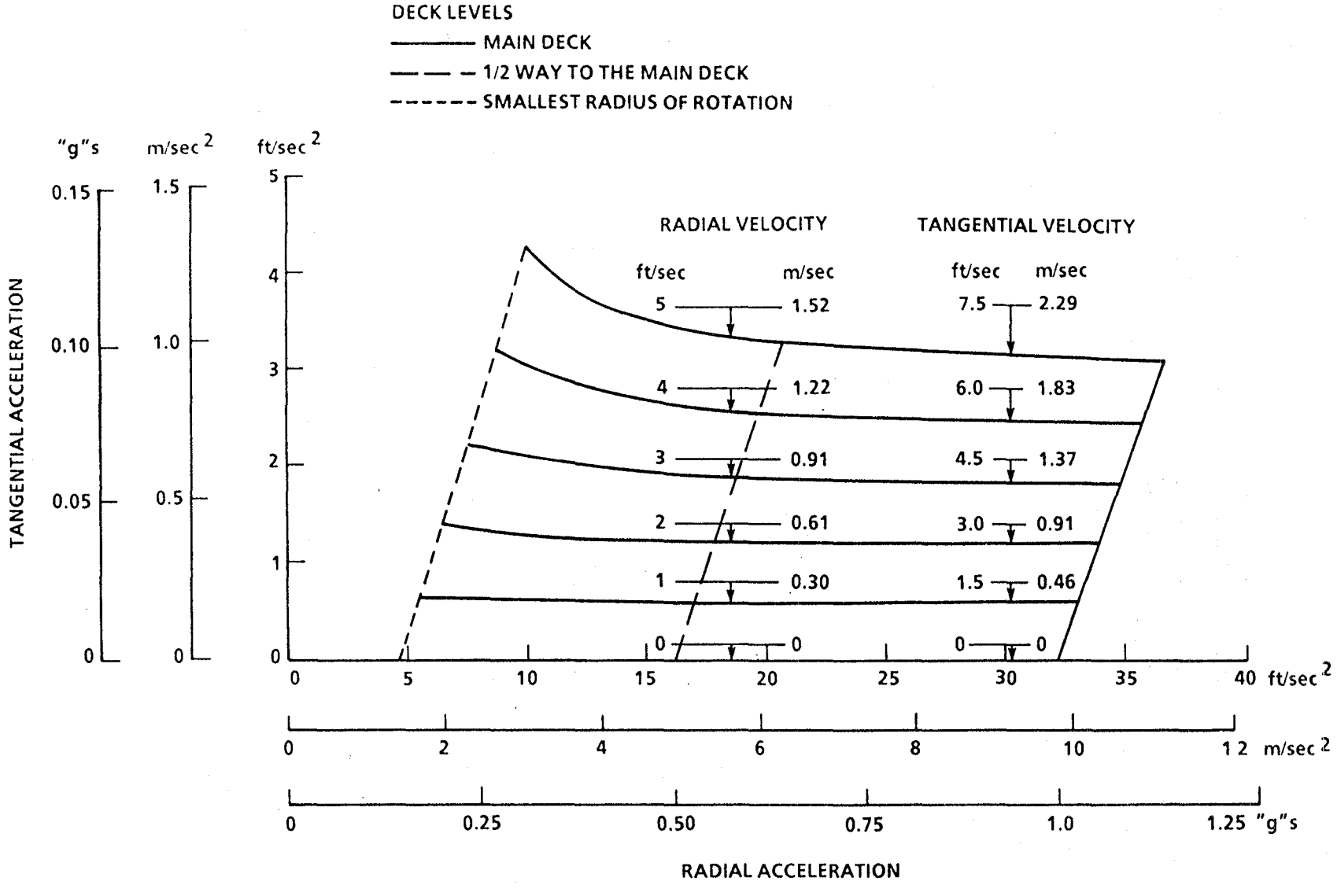

Figure 5.3-7 The Effects of Stair-Climbing in the Direction of Rotation

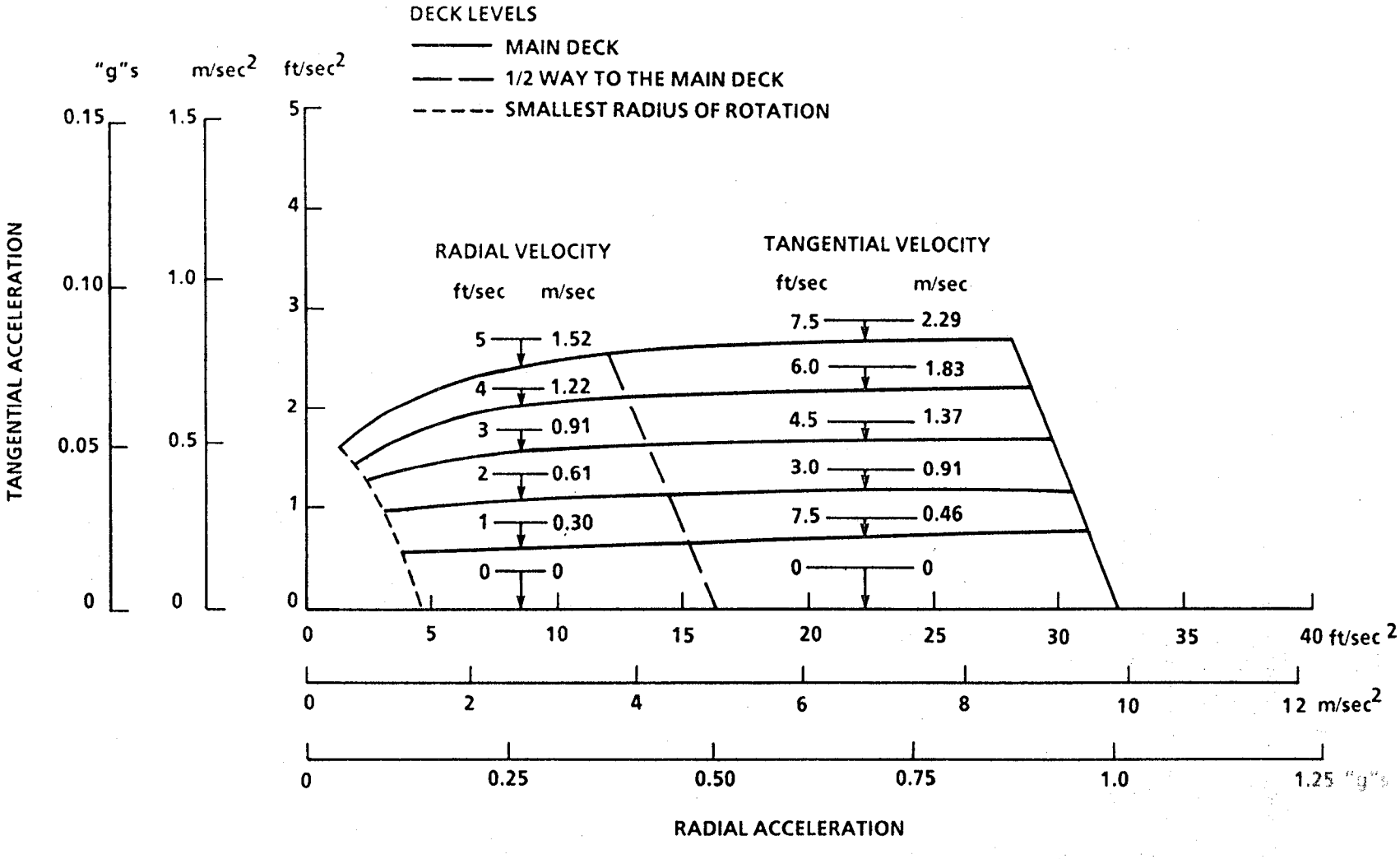

Figure 5.3-8 The Effects of Stair-Climbing Against the Direction of Rotation

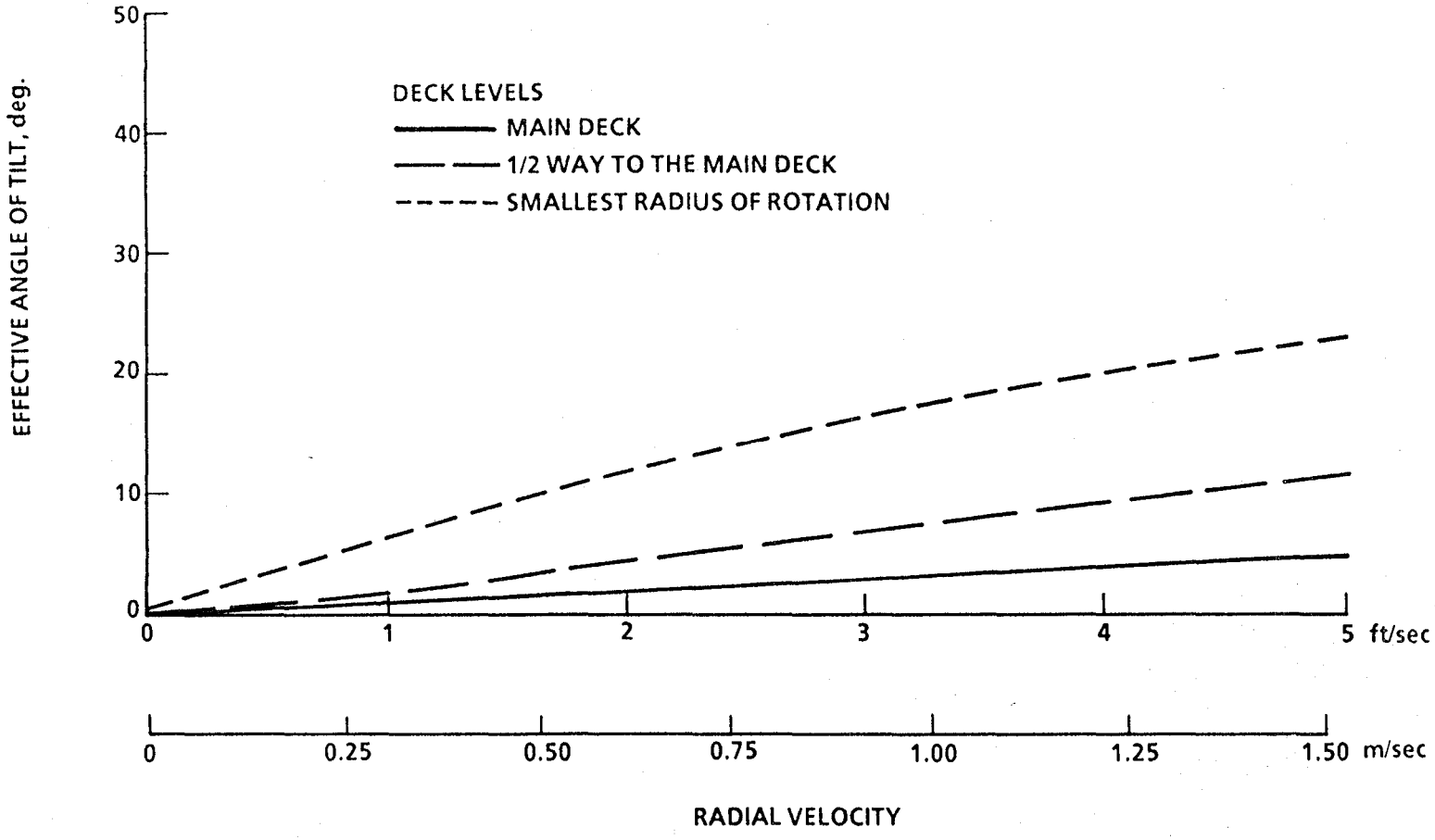

Figure 5.3-9 Effective Angles of Tilt when Climbing Stairs
(Climbing in the Direction of Rotation)

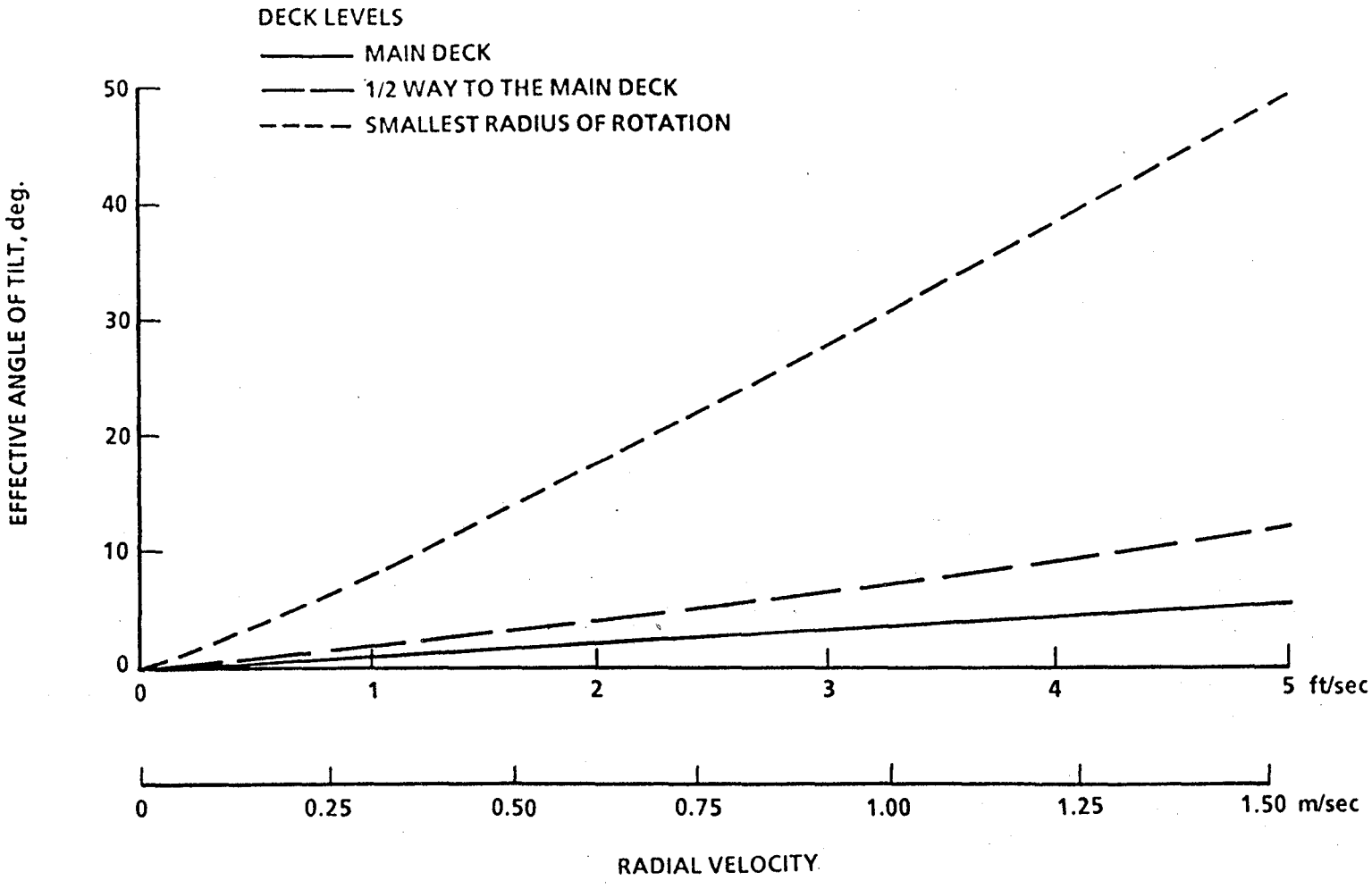

Figure 5.3-10 Effective Angles of Tilt when Climbing Stairs (Climbing Against the Direction of Rotation)

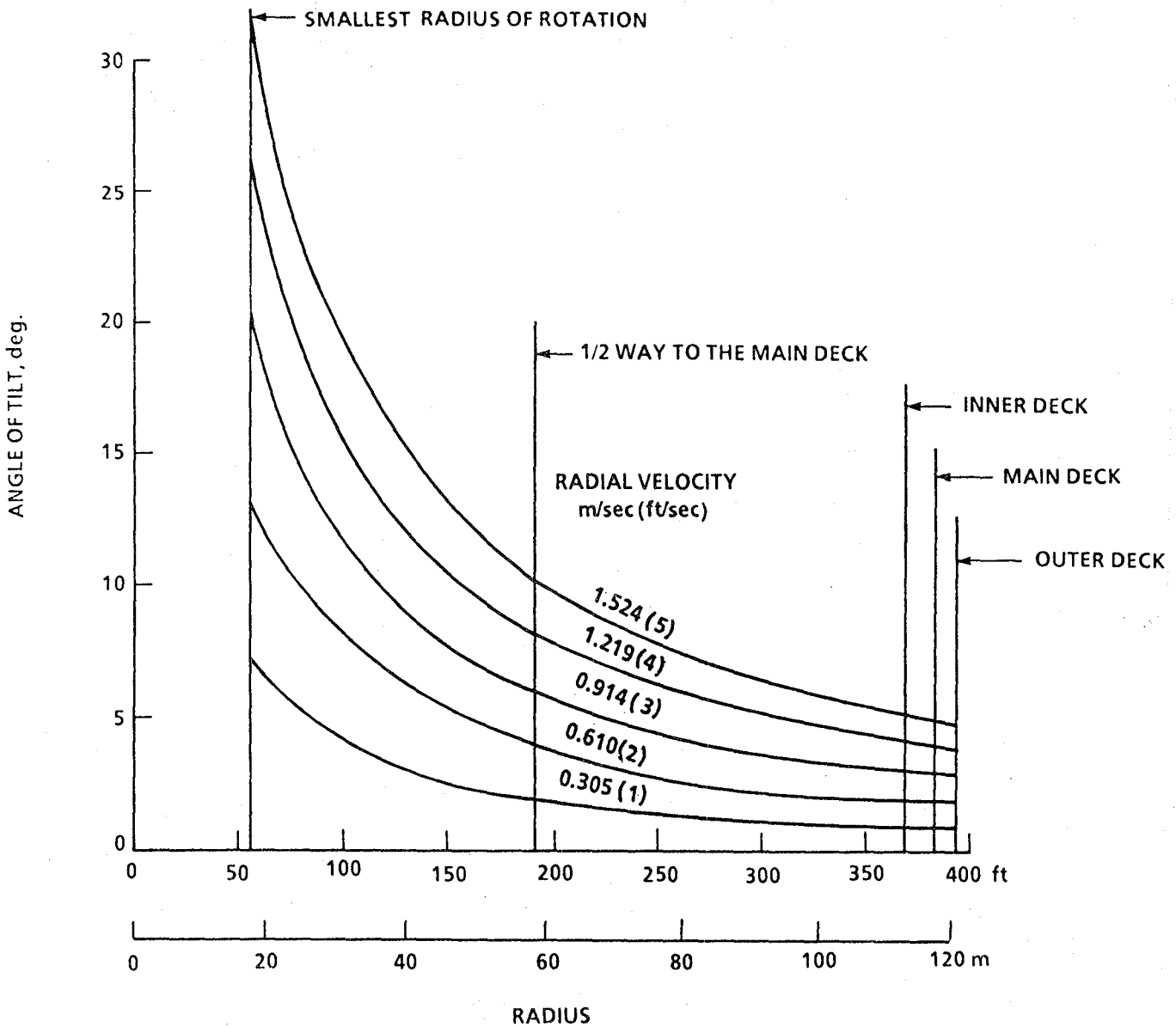

Figure 5.3-11 Angle of Tilt when Climbing Stairs Axially

sideways on the stairs seems more desirable than leaning down the stairs and maybe even up the stairs.

Another phenomenon that may have some annoyance is that objects dropped in artificial gravity will not fall where expected. Unless given a radial or tangential velocity relative to the vehicle frame of reference, objects will always strike the floor opposed to the direction of rotation from the spot over which it was dropped. The circumferencial displacement of such objects are shown on Figures 5.3-12 and 5.3-13. On the main deck, something dropped from 1.83 m (6 ft) will strike the floor less than 0.75 ft (0.23 m) from the expected position, whereas at the smallest radius, this distance will exceed 0.61 m (2 ft), Figure 5.3-12. Fluids may be poured from shorter distances (Figure 5.3-13). Since fluids will fall within fractions of an inch from where planned, coffee can be poured into a cup.

5.4 Some Effects of Angular Motions within the Rotating Environment of the Advanced-Technology Space Station

Table 5.1-1 lists angular cross couplings that will exist and lead to sensory responses that can be disorienting and even cause motion sickness (Reference 5-1). Figure 5.4-1 is a vectorial representation of head orientation and angular motion in the rotating environment. Here the orientation angles of the head relative to the rotating Space Station are zero when facing axially. Reference 5-4 gives a complete development of the equations relating head orientation and motion and Space Station rotation to the experienced sensory responses of crew members in the spacecraft. These angular cross-coupled equations also relate to moments required to rotate objects within the artificial gravity environment.

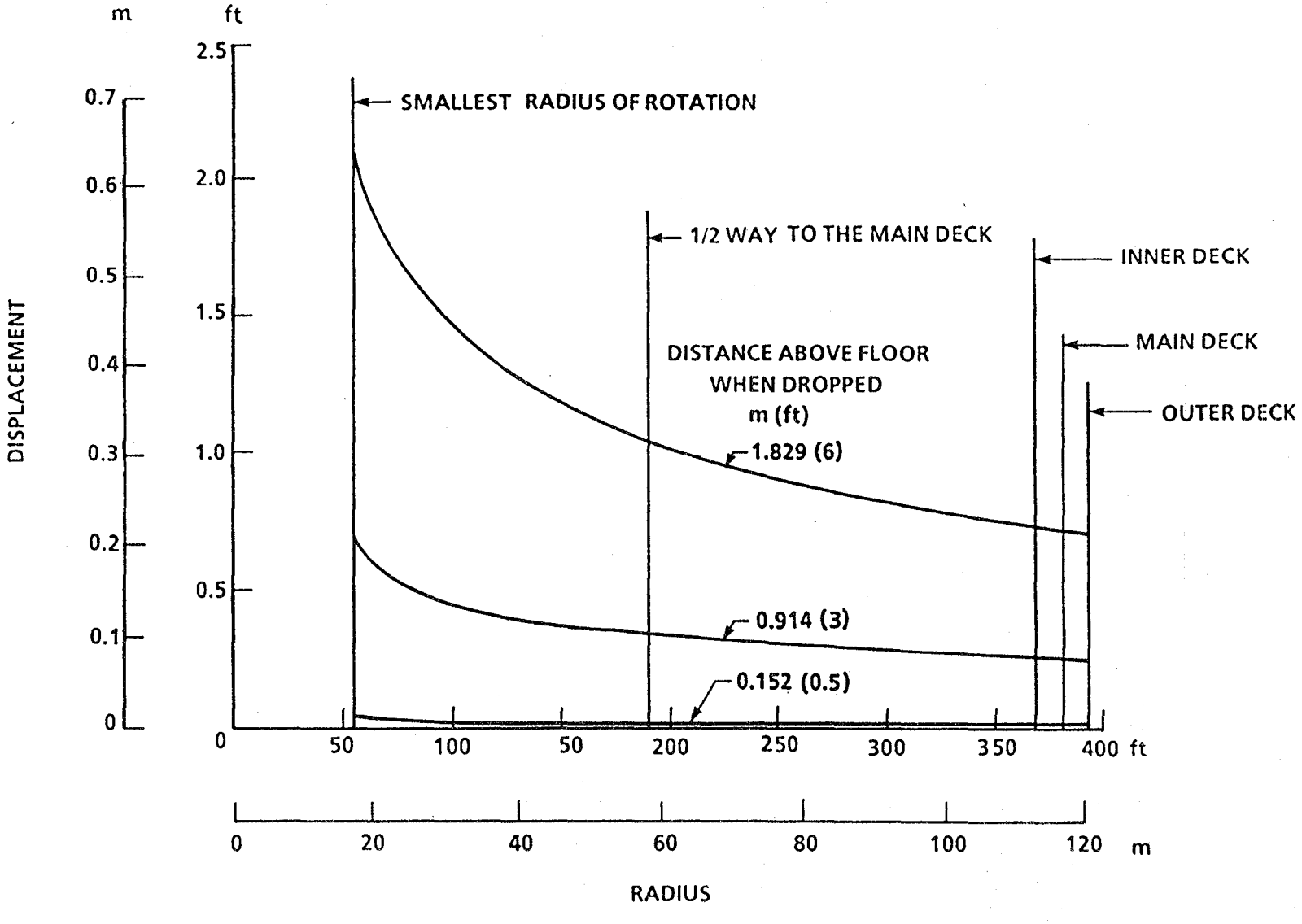

Figure 5.3-12 Displacement of Dropped Objects from Expected Locations

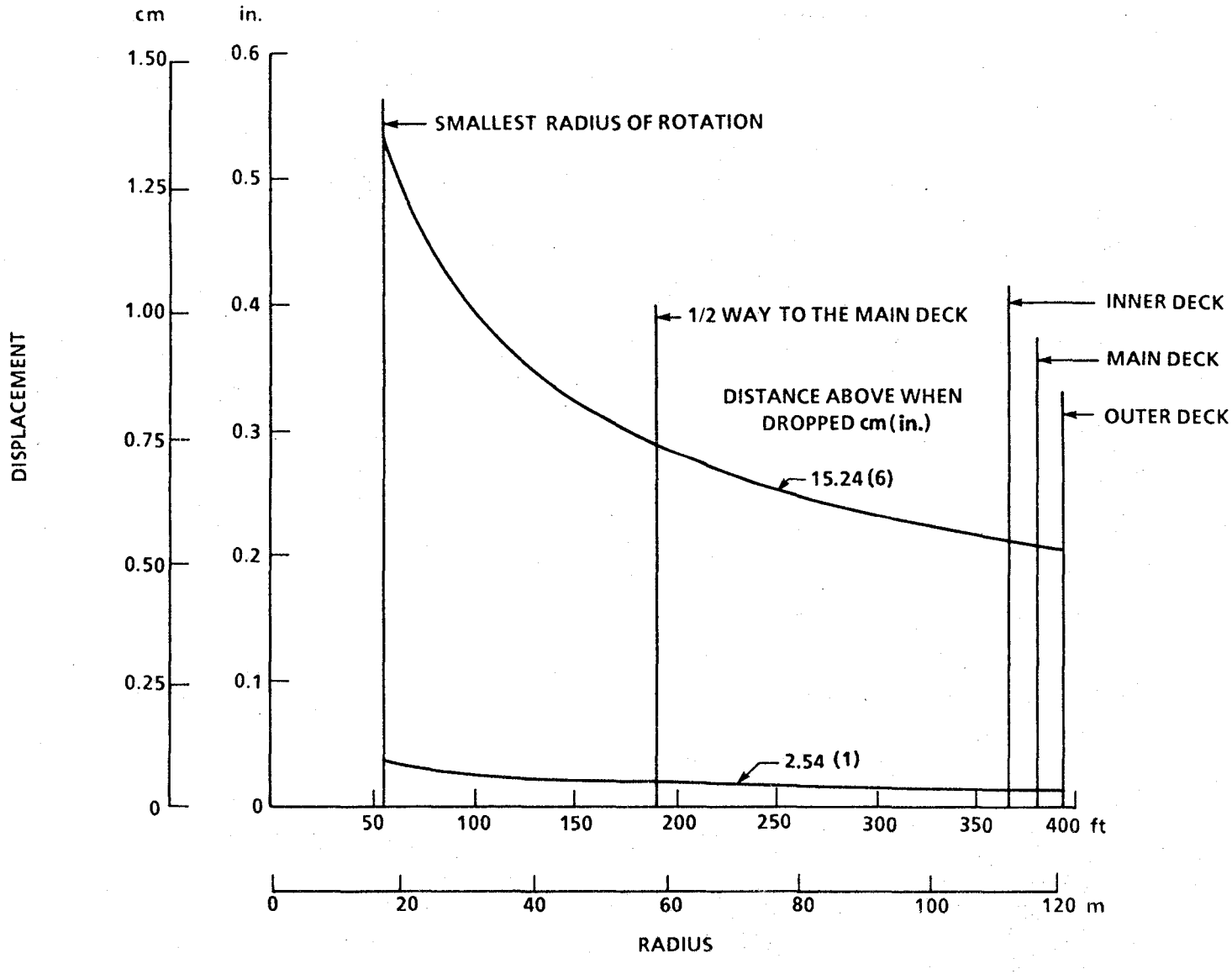

Figure 5.3-13 Displacement of Dropped Objects or Poured Fluids from Expected Locations

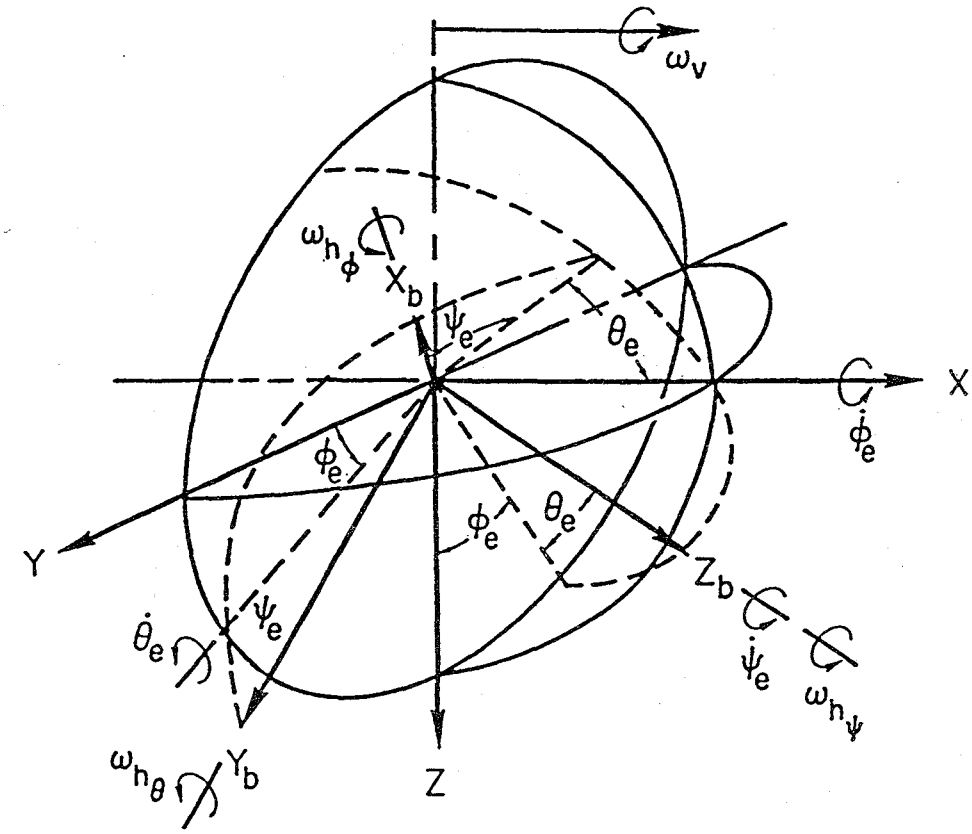

Figure 5.4-1 Vectorial Representation of Head Orientation and Angular Motions in a Rotating Space Vehicle

The angular accelerations experienced as developed in Reference 5-4 are:

$$\dot{\omega}_{h_x} = \dot{\omega}_{h_\phi} - \omega_v(\omega_{h_\theta}\sin\theta_e + \omega_{h_\psi}\cos\theta_e\sin\psi_e) \quad (1)$$

$$\dot{\omega}_{h_y} = \dot{\omega}_{h_\theta} - \omega_v(\omega_{h_\psi}\cos\theta_e\cos\psi_e - \omega_{h_\theta}\sin\theta_e) \quad (2)$$

$$\dot{\omega}_{h_z} = \dot{\omega}_{h_\psi} + \omega_v(\omega_h \cos\theta_e\cos\psi_e + \omega_{h_\theta}\cos\theta_e\sin\psi_e) \quad (3)$$

where the second terms of these equations are the cross-coupled angular accelerations, which are sensed by the semicircular canals, and are the cause of the disquieting effects experienced in rotating vehicles, especially when vision is limited to the interior of the vehicle.

Consider a situation where a crew member is seated in an axial direction where:

$$\Phi e = \theta e = \omega h_\phi = \omega h_\theta = \dot{\omega} h_\phi = \dot{\omega} h_\theta = 0$$

and the head is moved from about 45^o to the left to about 45^o to the right and back with $\dot{\omega}_{h_\psi}$ and ω_{h_ψ} not zero. Equations (1), (2), and (3) then become:

$$\dot{\omega}_{h_x} = -\omega_v(\omega_{h_\psi}\sin\psi_e) \quad (4)$$

$$\dot{\omega}_{h_y} = -\omega_v(\omega_{h_\psi}\cos\psi_e) \quad (5)$$

$$\dot{\omega}_{h_z} = \dot{\omega}_{h_\psi} \quad (6)$$

The expressions (4) and (5) are the cross coupled motions and (6) is the expected motion. Figure 5.4-2 shows a turning motion measured in a rotating Space Station simulator representing the conditions expressed above. Also shown is an apparent nodding motion as expressed by equation (5). Although not shown, there exists an apparent head rolling motion expressed by equation (4).

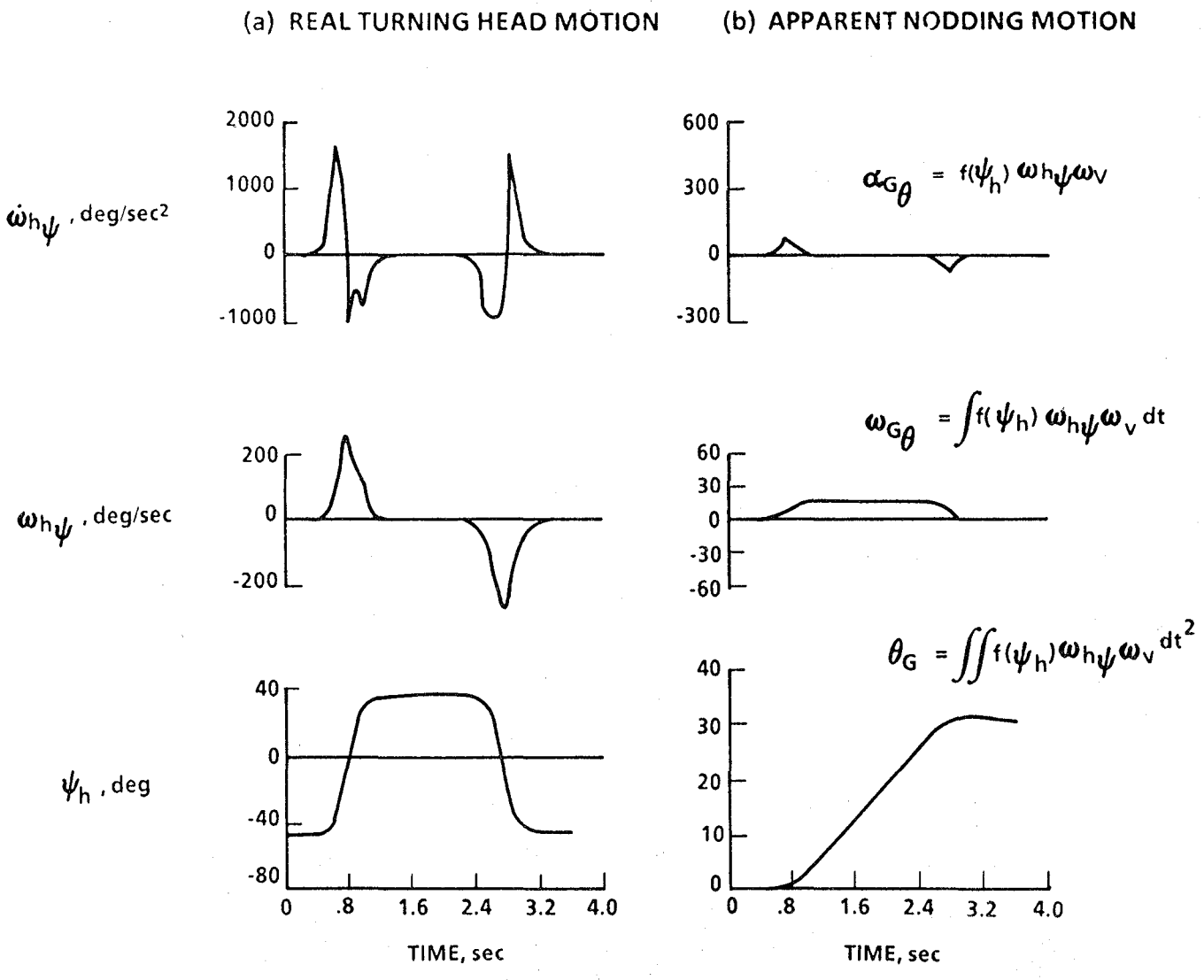

Figure 5.4-2 Typical Head Turning Motion and Resulting Apparent Nodding Motion (Simulator Rate: ω_V - 3 rpm)

Consider also the same orientation noted previously where

$$\Phi_e = \Psi_e = \omega_{h_\Phi} = \omega_{h_\Psi} = \dot{\omega}_{h_\Phi} = \dot{\omega}_{h_\Psi} = 0$$

and the head is moved in a nodding motion looking up then down and up again with $\dot{\omega}_{h_\Theta}$ and ω_{h_Θ} having finite values. Equations (1), (2), and (3) then become:

$$\dot{\omega}_{h_x} = -\omega_v(\omega_{h_\Theta} \sin\Theta_e) \quad (7)$$

$$\dot{\omega}_{h_y} = \dot{\omega}_{h_\Psi} \quad (8)$$

$$\dot{\omega}_{h_z} = \omega_v(\omega_{h_\Theta} \cos\Theta_e) \quad (9)$$

Equation (8) represents the expected motion and equation (7) and (9) are the cross-coupled motions. Figure 5.4-3 represents a measured nodding motion as expressed previously and a calculated turning motion expressed by equation (9). A head rolling motion (equation 7) although not shown will also exist.

The apparent motions shown in Figures 5.4-2 and 5.4-3 are for a rotation of 3 rpm (0.314 rad/sec), the maximum cross coupled accelerations are about 100 deg/sec^2 (1.745 rad/sec^2) for the apparent turning motion and about 85 deg/sec^2 (1.484 rad/sec^2) for the apparent nodding motion. As noted in Reference 5-1 and reported in References 5-4, 5-12, and 5-13, 3 rpm is a rotational velocity to which man can adapt, whereas values of 6 rpm and 10 rpm can cause serious problems and adaptation becomes problematic. A value somewhat less than 3 rpm has been selected for the ATSS with an artificial gravity of 1 g at the main deck. The major stimulant is, of course, the cross-coupled accelerations, and the implications are that 100 deg/sec^2 (1.745 rad/sec^2) are amenable. Values of 170 deg/sec^2 (2.967 rad/sec^2) and greater may not be. Other head orientations and head motions in the

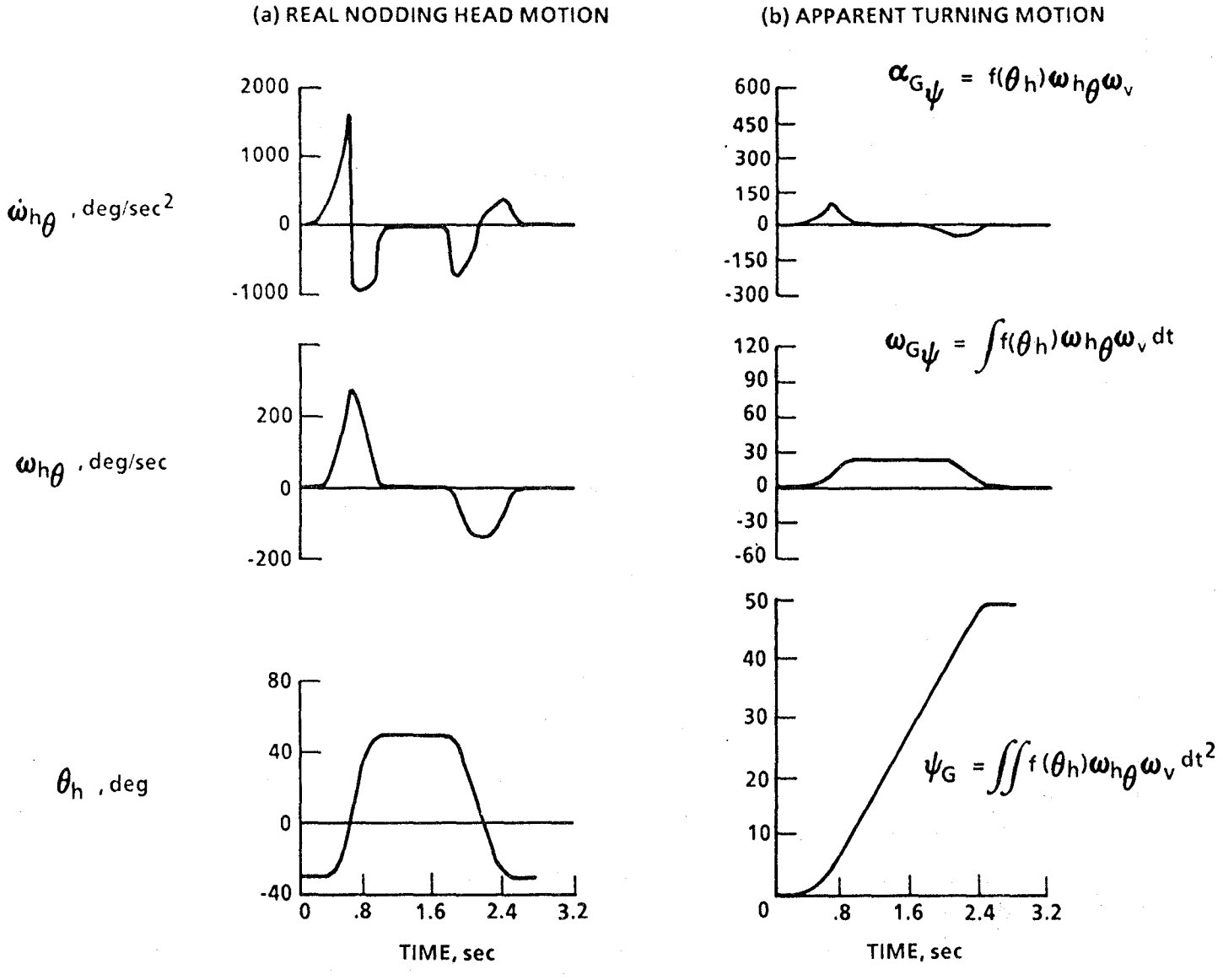

Figure 5.4-3 Typical Head Nodding Motion and Resulting Apparent Turning Motion (Simulator Rate: ω_v = 3 rpm)

ATSS will cause different cross-couplings than those specifically discussed; the conclusions, however, remain.

The orientations within the rotating environment that are most comfortable and favor performance of both fine and gross motor tasks are pure tangential or axial directions, (Reference 5-16). Facing axially or tangentially against the direction of rotation seemed more comfortable and efficient than facing tangentially in the direction of rotation, (Reference 5-16). Arranging controls, displays and work areas to minimize the requirement for excessive head and limb movements is desirable, (References 5-21 and 5-22).

5.5 Materials Handling within the Rotating Environment of the Advanced-Technology Space Station

A part of the research reported in References 5-11, 5-14, 5-15, and 5-16 was devoted to the handling and manipulation of material in the rotating environment. There are major problems that may effect material handling. The first is the mere ability to carry objects in the tangential direction where the artificial weight of objects will increase or decrease depending on the tangential direction one moves. The second is the changing artificial weight previously mentioned, as things are raised and lowered and the ensuing tangential Coriolis accelerations occur which are associated with radial motions. The last problem is associated with angular cross-coupling where rotating an object in the rotating environment of the Space Station requires moments to be supplied to maintain the object in its desired orientation. This relates directly to the phenomenon that happens to the vestibular organs during head motions.

As described in Reference 5-14, a 0.028 m^3 (1 ft^3) object weighing 14.52 kg (32 lb) was moved in both tangential directions. The Earth weight was sling-supported and the artificial weight, due to simulator rotation, was supported by the experiment subjects. Various radii up to 21.3 m (70 ft) with rates of rotation of 3, 4, and 5 rpm were studied. The artificial weight of the object varied from about 0.91 kg (2 lb) to about 8.16 kg (18 lb). The results in Figure 5.5-1 for walking with and without cargo show little effect of the cargo. The walking distance for these tests was 4.57 m (15 ft) on flat floors. Starting and stopping, caused by the lean angles of the flat floors, strongly affected the walking speed performance, reaching only a maximum of about 0.91 m/sec (3 ft/sec). Heavier artificial weights may have some effect on performance.

The results of References 5-11, 5-14, and 5-16 indicate no apparent effect of radial motion on cargo handling. Handling cargo with specific linear and rotary motions was included in these studies. The cargo consisted of 0.3 m (1 ft) cubes weighing 2.27 kg (5 lb). The cross-coupled angular accelerations were readily felt. The effects were of little concern for cargo of this size and were used by some to help in the task performance. Heavier cargoes or those with larger moments of inertia, however, may present handling problems. The results from these studies indicated an adaptation to the phenomenon since performance improved with experience.

5.6 Cognitive and Psychomotor Testing within the Rotating Environment of the Advanced-Technology Space Station

Reference 5-16 presents a number of experiments performed in a rotating environment to test cognitive and psychomotor performance. Mental functions and short-term memory are affected primarily with

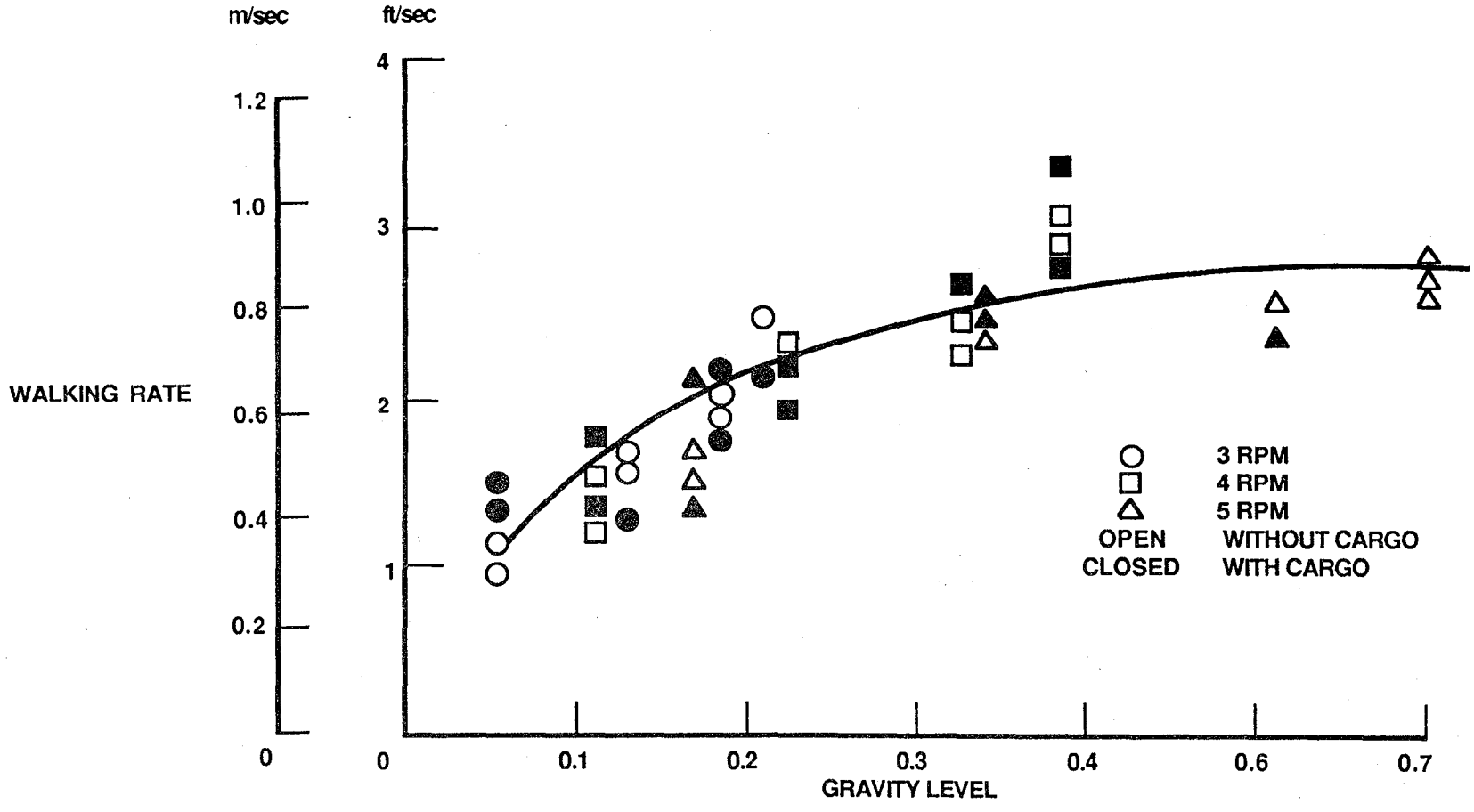

Figure 5.5-1 Variations in Tangential Walking Rate Relative to Artificial-g Level, with and without Cargo

increasing rate of rotation at the onset of testing but significantly decreased or disappeared through adaptation or accommodation with increasing experience. Task performance requiring extensive arm and head motions were degraded by 8 to 11 percent with increasing rotational rates up to 6 rpm. The greatest degradation occurs while facing tangentially in the pro-spin direction, suggesting again that these tasks be performed facing axially or in the anti-spin direction. Head motion lowered psychomotor performance at the onset of rotational experience but nearly disappeared in two days. Programmed head motions hasten the adaptation process.

5.7 Some Further Observations of Astronaut Performance on the Advanced-Technology Space Station

The ATSS has a relatively large radius, 116.13 m (381 ft) at the main deck, and a relatively low angular velocity, 0.291 rad/sec (2.776 rpm). These factors result in an artificial gravity of 1 g at the main deck. As noted in Reference 5-1, 1 g is expected to maintain acceptable physiological conditions, in regard to the cardiovascular system, the musculoskeletal systems, and space sickness caused by weightlessness.

As noted, artificial gravity does have its side effects. These effects have been reviewed herewith and cited in numerous documents. The specific tests of References 5-11 through 5-16 examined areas where these side effects could be critical to human performance in a rotating environment as would be experienced on the ATSS. For these experiments, radii of 8.4 m (27.5 ft), 15.2 m (50 ft), and 21.3 m (70 ft) and rates of rotation of 0.314 rad/sec (3 rpm), 0.419 rad/sec (4 rpm), and 0.524 rad/sec (5 rpm) were generally used. The problems reported in these various references occurred primarily at the 8.38 m (27.5 ft) and 15.24 m

(50 ft) radii and 0.524 rad/sec (5 rpm) and sometimes 0.419 rad/sec (4 rpm). The proposed ATSS, with a primary radius over five times that of the maximum experimental radius and with a rotational rate somewhat less than the minimum rate 0.314 rad/sec (3 rpm) of the experiments, will probably avoid most of the performance problems of the experiments. It is probable that ground-based experiments, similar to those in References 5-11 and 5-16, will be performed for cases where the radii and rate of rotation are equal to the proposed ATSS.

REFERENCES

5-1 Queijo, M.J. et al: Analysis of a Rotating Advanced Technology Space station, NASA CR 178345 January 1988.

5-2 Stone, R.W.: An Overview of Artificial Gravity pp 23-33 Fifth Symposium of the Role of the Vestibular Organs in Space Exploration, NASA SP-314, 1973.

5-3 White, W.J.: Space-based Centrifuge, pp. 209-213, The Role of the Vestibular Organs in the Exploration of Space, NASA SP-77, 1965.

5-4 Stone, R.W. & Letko, W.: Some Observations on the Stimulation of the Vestibular System of Man in a Rotating Environment, pp. 263-278, NASA SP-77 as above.

5-4 Newsan, B.D. and Brady, J.F.: Observations on Subjects Exposed to Prolonged Rotation in a Space Station Simulator, pp. 279-292 NASA SP-77 as above.

5-5 Faget, M.A. & Olling E.H.: Orbital Space Stations with Artificial Gravity, pp. 7-16 Third Symposium on the Role of the Vestibular Organs in Space Exploration, NASA SP-152, 1968.

5-6 Newsom, B.D. & Brady, J.F.: Display Monitoring in a Rotating Environment, pp. 37-47, SP-152 as above.

5-7 Letko, W. & Stone, R.W.: The Effects of the Plane of Vestibular Stimulation on Task Performance and Involuntary Eye Motion, pp. 49-55, SP-152 as above.

5-8 Stone, R.W., Piland, W.M. & Letko, W.: Certain Aspects of On-board Centrifuges and Artificial Gravity, pp. 331-345, Fourth Symposium on the Role of the Vestibular Organs in Space Exploration, NASA SP-187, 1970.

5-9 Piland, W.M. et al.: Design of Experimental Studies of Human Performance Under Influence of Simulated Artificial Gravity, pp. 55-65, Fifth Symposium, as in Reference 5-2.

5-10 Letko, W. Locomotion in a Rotating Environment, pp. 67-72, SP-314 as above.

5-11 Green, J. A., et al.: Some Aspects of Locomotion and Cargo Handling in Simulated Artificial Gravity, AIAA Paper No. 71-886, AIAA/ASMA Weightlessness and Artificial Gravity Meeting, August 9-11, 1971.

5-12 Peacock, J.J. & Green, J.A., Initial Assessment of Various Human Behavior Capabilities in a Rotating Environment, AIAA Paper No. 71-890, as above.

5-14 Green, J. A., et al: Locomotion and Cargo Handling in Simulated Artificial Gravity, pp. 535-539, Journal of Spacecraft & Rockets, Volume 9, Number 7, July 1972.

5-15 Green, J.A., Peacock, J.L. & Holm, A.P.: A Study of Human Performance in a Rotating Environment, NASA CR 111866.

5-16 Green, J. A. & Peacock J.L.: Effects of Simulated Artificial Gravity on Human Performance, NASA CR-2129, November 1972.

5-17 Stone, R.W. & Letko, W.: The Effects of Angular Motion of Rotating Space Vehicles on the Ability of an Astronaut to Perform Simple Tasks presented at the Annual Meeting of the Institute of Environmental Sciences, Chicago, IL, April 10-13, 1962.

5-18 Stone, R.W. & Letko, W.: Tolerance to Vehicle Rotation of Subjects Using Turning and Nodding Motion of the Head While Performing Simple Tasks, pp. 437-442, Journal of Spacecraft & Rockets, Vol 2, No. 3, May-June 1965 (also NASA PP-583).

5-19 Stone, R.W.: Man's Motor Performance Including Acquisition of Adaptation Effects in Reduced Gravity Environments, presented at the Fourth International Symposium on Basic Environmental Problems of Man in Space, Yerevan, USSR October 1-5, 1971.

5-20 Hewes, D.E. & Spady, A.A., Jr.: Status Report on Recent Langley Studies of Lunar and Space Station Self-locomotion. Presented at the AGARD 24th Aerospace Medical Panel Meeting, Brussels, Belgium October 24-27, 1967.

5-21 Loret, B.J.: Optimization of Manned Orbital Satellite Vehicle Design with Respect to Artificial Gravity, ASD-TR-61-668. Wright-Patterson Air Force Base, Ohio, (1961) page 46.

5-22 Stone, R.W. and Piland, W.M.: Potential Problems Related to Weightlessness and Artificial Gravity, NASA TND-4980, January 1969.

6.0 RIGID-BODY DYNAMICS CONSIDERATIONS RELATIVE TO THE ADVANCED-TECHNOLOGY SPACE STATION

Two possible configurations for an Advanced-Technology Space Station (ATSS) were considered briefly in References 6-1 and 6-2. The difference between the two was that one had counterrotating elements to counteract the angular momentum of the large rotating torus, which is the primary feature of the station. It was pointed out in Reference 6-2 that the use of counterrotators was beneficial in reducing the torquing requirements to precess the ATSS to maintain Sun-orientation. Basically, the counterrotators reduce or eliminate the gyroscopic properties of the rotating torus and make turning the ATSS easier. At the same time, the loss of inertial stability from the gyroscopic effect makes the ATSS respond more readily to gravitational and aerodynamic torques, which is undesirable.

Because of the conflicting benefits and possible detrimental effects of the counterrotators, it was deemed advisable to examine some space station dynamics related to rotation. Since the configuration of the ATSS is conceptual and still evolving, it is premature to make a detailed analytical motion study. Instead, an initial examination of its rigid-body dynamics was made by reviewing some of the results from published studies which were judged to apply qualitatively to the rotating ATSS without counterrotators. Specific results discussed in this section are the effects of short-duration torques applied to a space station, and effects of asymmetric mass transfer within an initially symmetric space station.

6.1 Brief Review of Some Studies of Rotating Space Stations

During the 1960's, much attention was given to space stations as the next possible space program following Project Apollo. Space stations were considered to be longtime habitats for crews. Since it was recognized that the long-term effects of zero-gravity environment were not well-known, and that there were some undesirable effects (References 1-4 and 1-5, for example), several of the space station configurations studied were rotating, rigid bodies. The rotation created an artificial gravity field through centrifugal force. References 6-3 through 6-15 are indicative of studies made in the 1960-1968 time period.

The reports of particular interest are those concerned with the dynamic behavior of rotating space stations following the application of external torques, impacts, and transfer of weight within the space station. References 6-4, 6-11, and 6-13 treat such disturbances, and also examine methods of damping disturbances. There are some differences in the approaches and approximations made in each of the three papers, and it is informative to review the differences.

Reference 6-11 begins with general linearized equations of motion, including time-variable moments and products of inertia, and remains general throughout the analyses. The three moment equations were coupled and solved using a digital computer. Reference 6-13 starts with the same equations as Reference 6-11, then makes certain simplifying assumptions which permit reducing the equations to the point where closed-form, approximate solutions can be obtained.

Reference 6-4 begins with simpler linearized equations of motion, in which moments and products of inertia are all assumed to be constant.

However, this reference includes terms to account for rotating machinery, such as turbines, within the space station.

It should be noted that References 6-4, 6-11, and 6-13 treat space stations that are totally rotating: i.e., there are no inertially-fixed sections, or any counterrotating elements. Reference 6-14 briefly discusses the stability of a rotating space station with a nonrotating hub. It also discusses qualitatively the effects of friction between the rotating and nonrotating elements, and some effects of flexibility in the rotor.

References 6-4, 6-11, and 6-13 present motion studies for their particular configuration following a disturbance or a modification from an axially symmetric configuration. The starting configuration of Reference 6-4 is a circular cylinder spinning about a transverse axis. The results of these motion studies are not readily applicable to the configuration of the ATSS (Figure 1.0-2). The configuration used in References 6-11 and 6-13 (Figure 6.1-1) has the human habitat as a rotating torus. However, the configuration of References 6-11 and 6-13 does not have a non-rotating central section or counterrotating elements.

6.2 Qualitative Effects of Some Disturbances and Asymmetries on Space Station Motions

The equilibrium condition for the ATSS is a rotation about the axis of symmetry, which in this case is also the axis having the largest moment of inertia. The basic station is symmetric in weight distribution as well as in geometry. In examining the dynamic response of the space station to various disturbances, several items should be kept in mind relative to the ATSS and its operation:

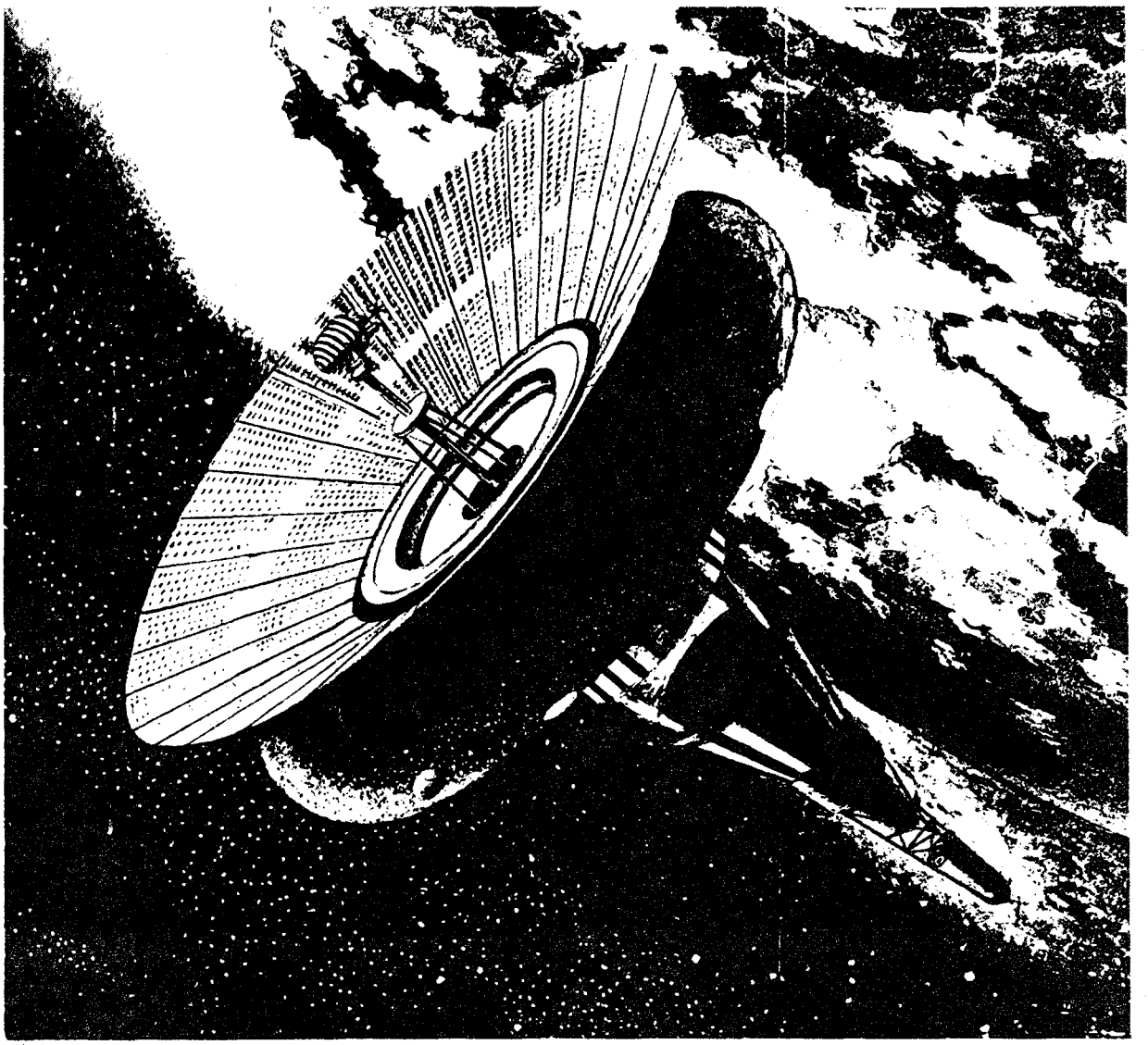

Figure 6.1-1 Sketch of Representative Space Station Configuration (from Reference 6-11)

1. The ATSS is Sun-oriented. Its axis of symmetry (the z-axis) points toward the Sun.

2. The ATSS precesses at the rate of once per year to remain Sun-oriented.

3. In examining the dynamic response over short periods of time, only the angular motion needs to be studied.

The disturbances to be discussed have been examined in several previous studies of rotating space stations. Some of the general observations apply qualitatively to the current configuration without counterrotating tanks, and are reviewed below.

6.2.1 Effects of Applying Short-Duration Torques

Short-duration torques could be the result of the docking of a spacecraft with the ATSS, the ejection of mass from the station, or the deliberate application of control thrusts. The results of a moment applied along an axis perpendicular to the spin axis were studied in Reference 6-11 for the configuration of Figure 6.1-1, having the relevant characteristics given in Table 6.2-1. The resulting motions show disturbances which start on application of the moment and cause residual oscillation in body angular rates (except for ω_z) and space orientation after the disturbance is removed (Figure 6.2-1). The spin axis is displaced from its original orientation and precesses around a tilted axis. The resulting motion appears as a wobbling of the Space Station that the crew would interpret as a rolling motion. Such a motion, coupled with the basic ATSS spin, could lead to disorientation and nausea of the crew (Reference 6-11). Of course, the magnitude of the effects

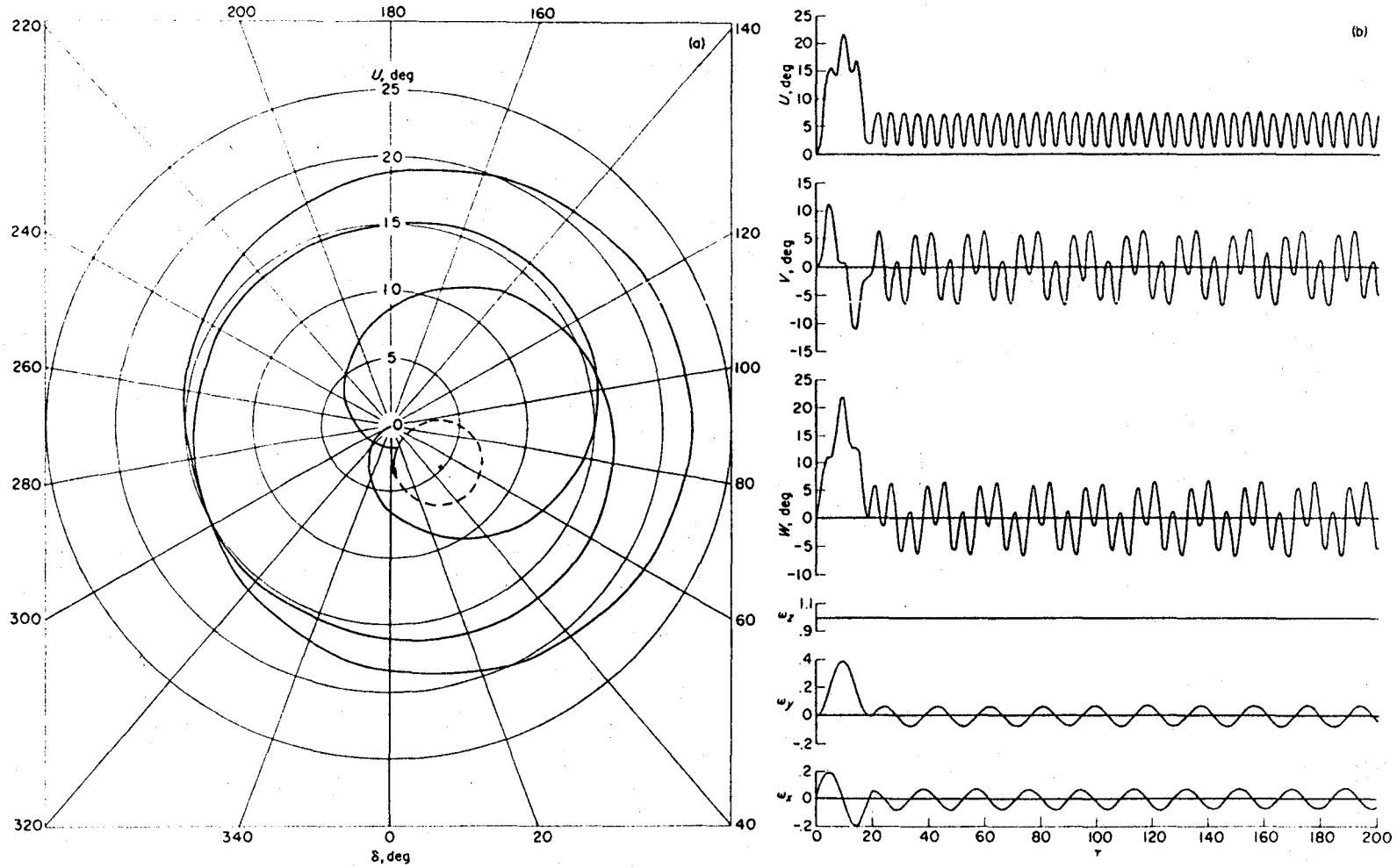

(a) Symmetry-axis trace.

(b) Time history.

Figure 6.2-1 Motion of Example Station for an Applied Moment (from Reference 6-11)

depends on the magnitude and duration of the applied moment, the mass, inertia, and initial angular momentum of the ATSS.

TABLE 6.2-1 MASS AND INERTIA PARAMETERS OF THE CONFIGURATION OF FIGURE 6.1-1

Mass = 3,670 kg	(8,100 lb)
I_x = 10,200 kg-m^2	(7,500 slug-ft^2)
I_y = 10,200 kg-m^2	(7,500 slug-ft^2)
I_z = 13,600 kg-m^2	(10,000 slug-ft^2)
Diameter = 9.14 m	(30 ft)
Spin Rate = 0.5 radians/sec	

Reference 6-11 examined the application of a gyroscopic stability system, (Figure 6.2-2) and a jet stability system (Figure 6.2-3) for damping out the residual oscillations shown in Figure 6.2-1, and found that the body angular rates could be removed, and that the precessing could also be reduced to zero. However, the spin axis remained tilted to about the average value which would have existed with no damping (Figures 6.2-4 and 6.2-5). The damping of the motions might alleviate the potential crew disorientation or nausea, but leaves a residual problem if inertial orientation is required. In such a case, sensors and a control system are necessary to return the station to its required orientation.

6.2.2 Effects of Asymmetric Mass Transfer

An unsymmetrical mass transfer within an initially symmetric rotating body can result in a dynamic unbalance. This could be caused by shifting cargo or by crew movements. Analytically, this effect manifests itself through the appearance of nonzero products of inertia in

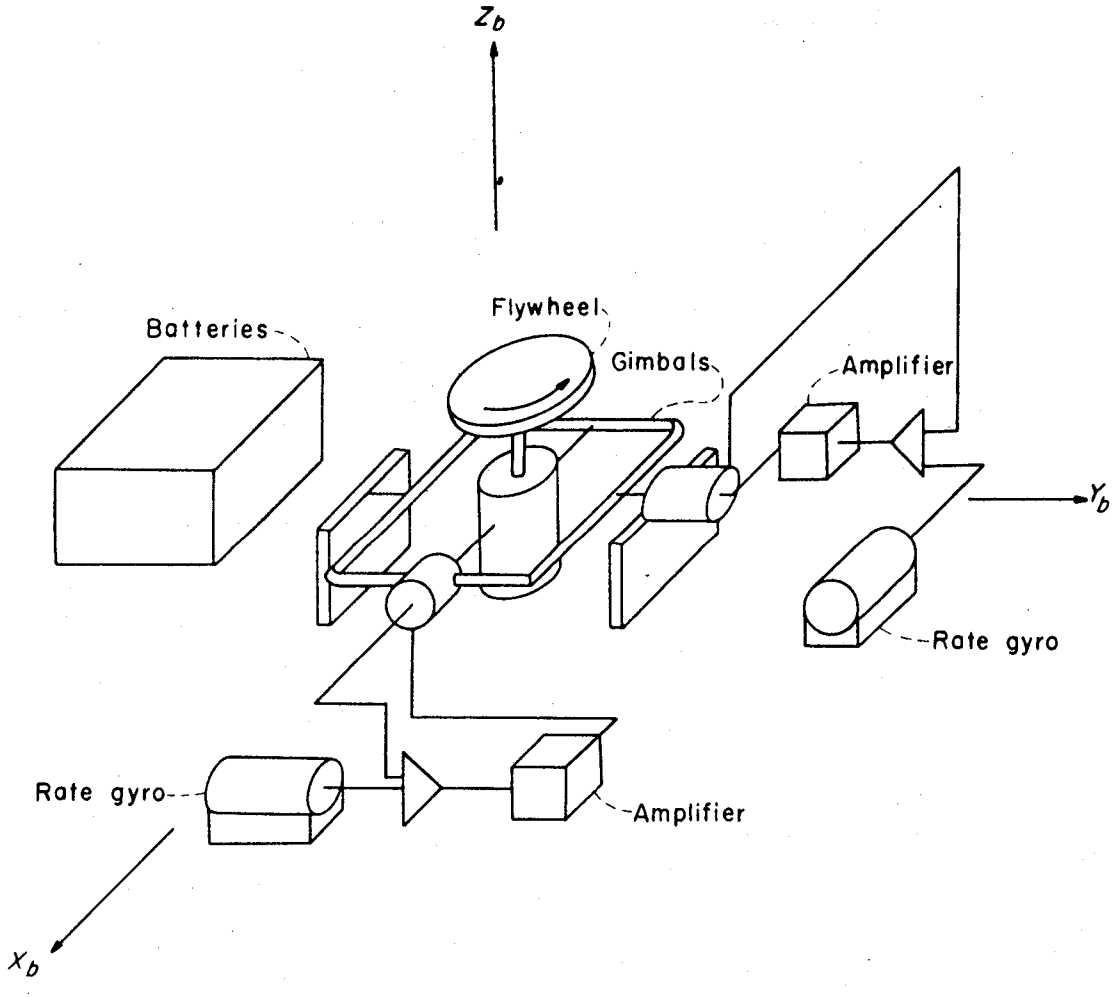

Figure 6.2-2 Schematic of Gyroscopic Wobble-Damper System for Space Station (from Reference 6-11)

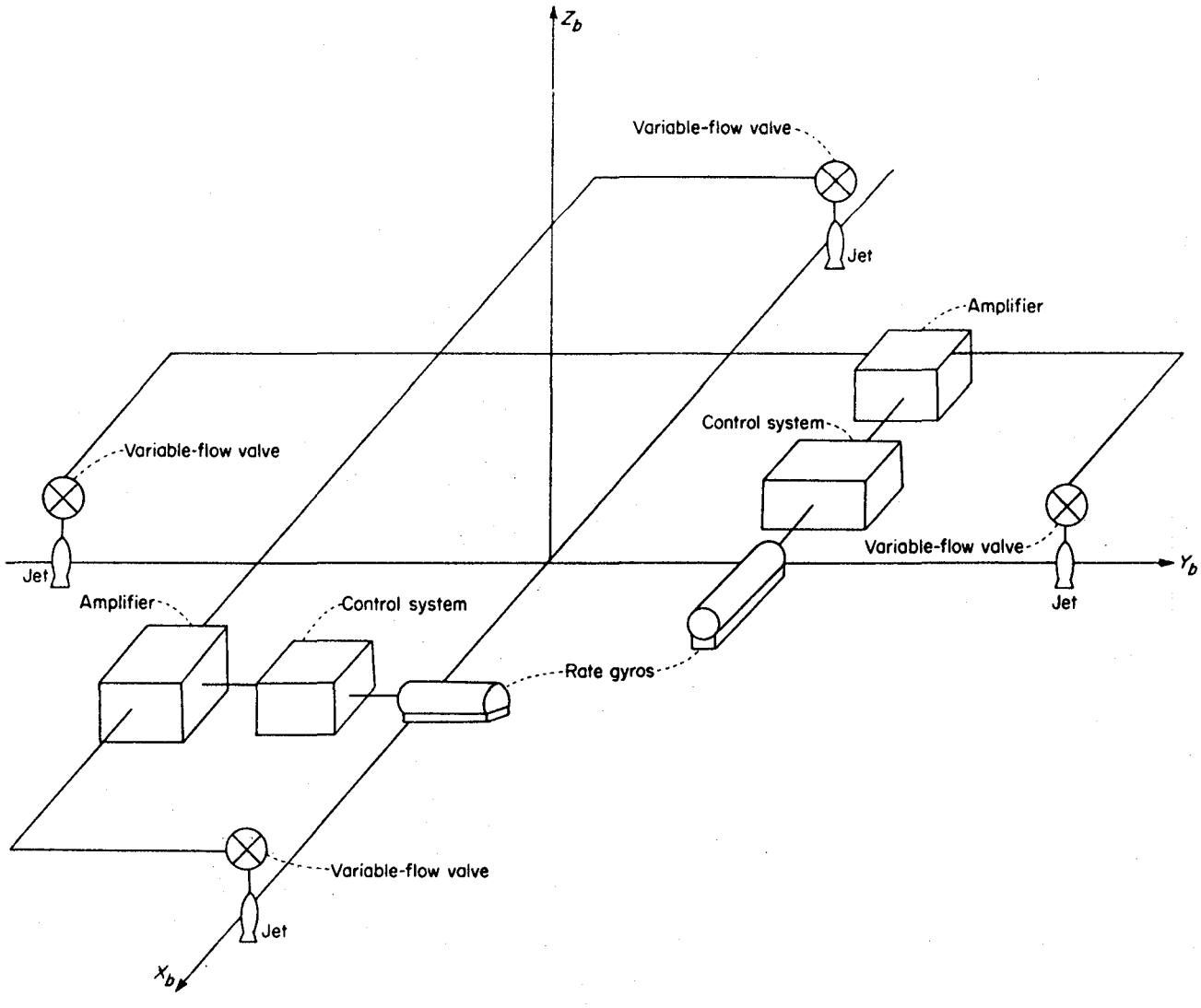

Figure 6.2-3 Schematic of Proportional Jet Damping System for Space Station (from Reference 6-11)

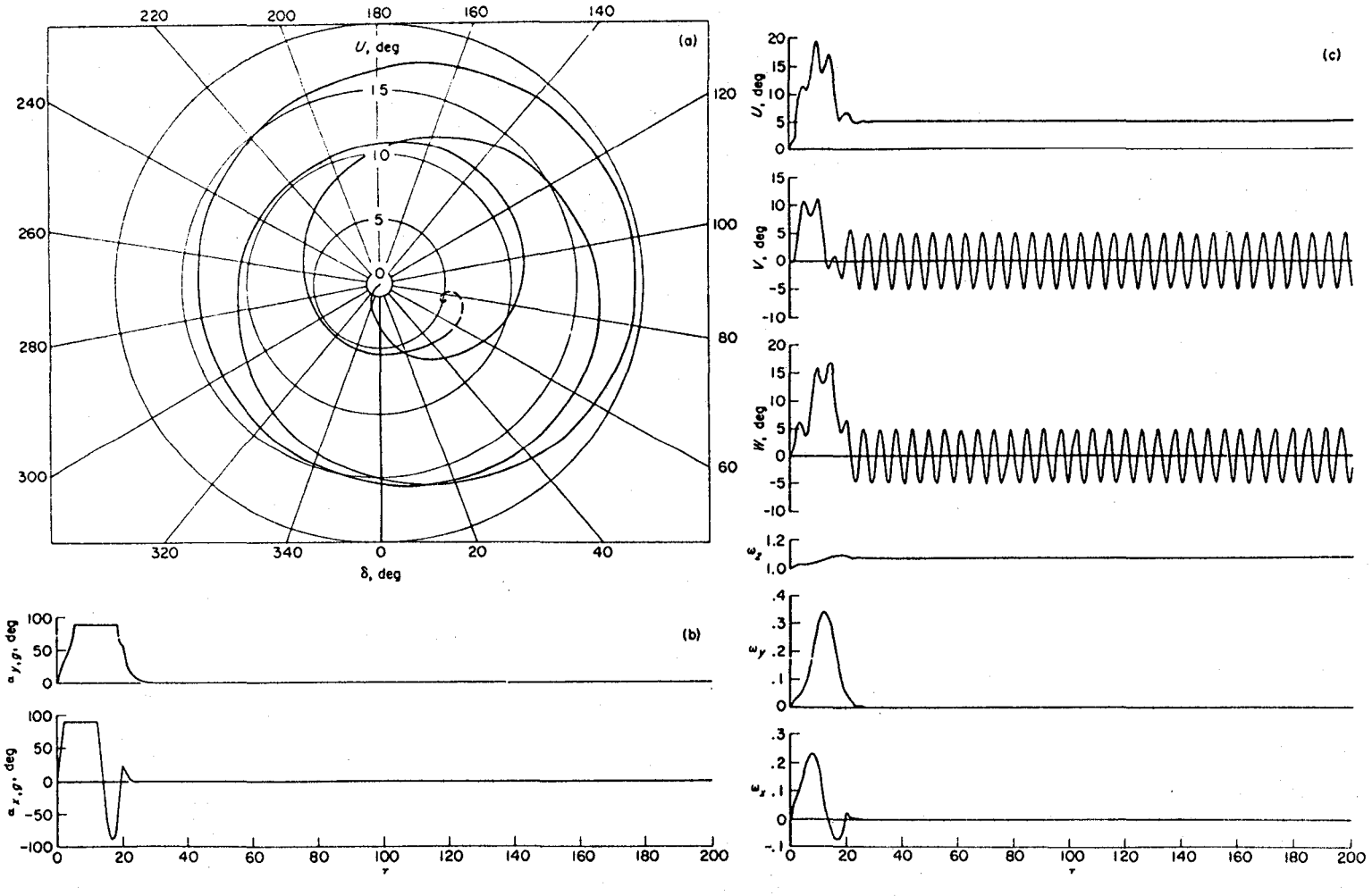

(a) Symmetry-axis trace.

(b) Gimbal angles.

(c) Time history.

Figure 6.2-4 Motion of Example Station for an Applied Moment with a Gyroscopic Stability System (from Reference 6-11)

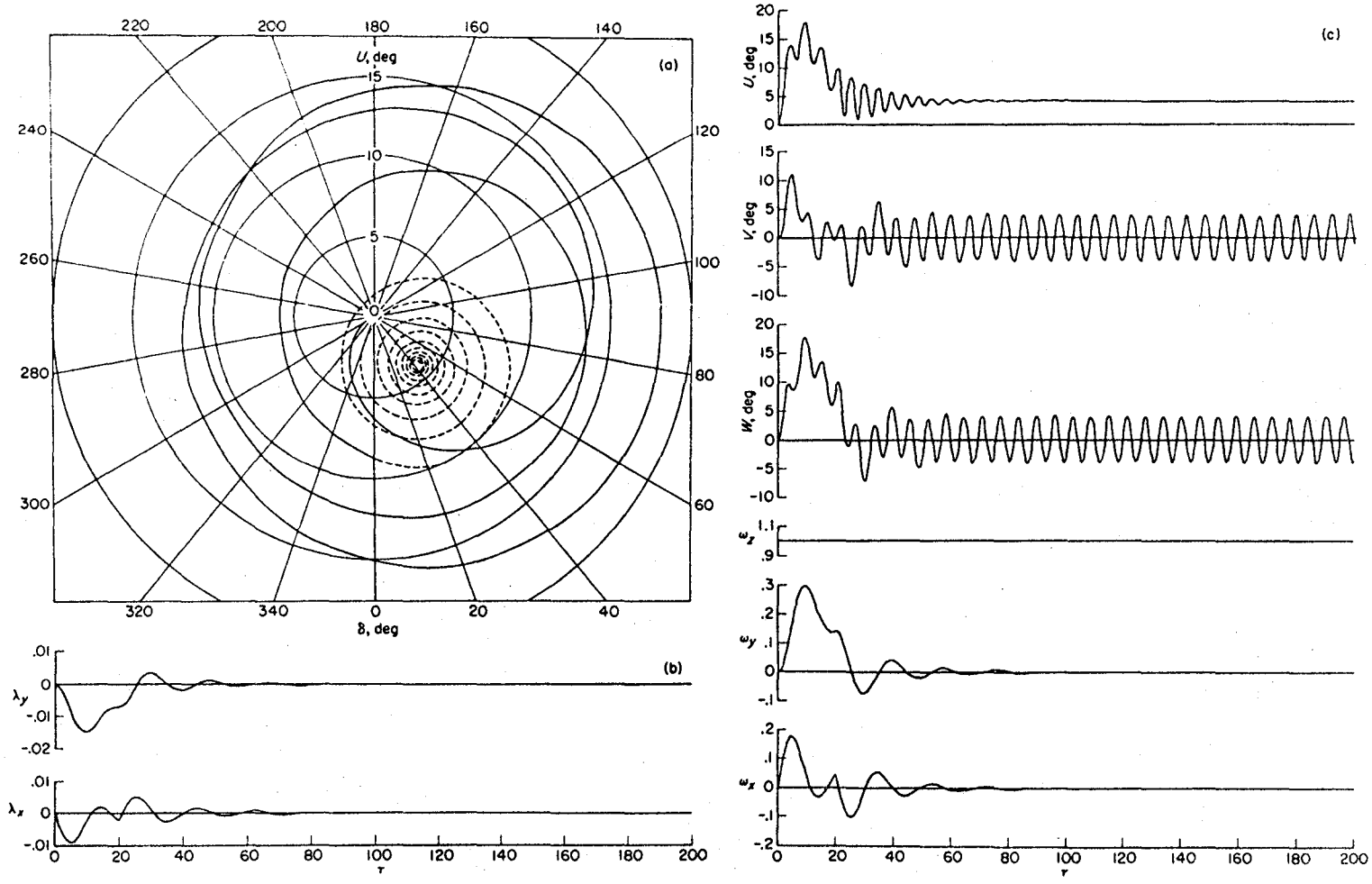

(a) Symmetry-axis trace.

(b) Damping moments.

(c) Time history.

Figure 6.2-5 Motion of Example Station for an Applied Moment with a Jet Stability System (from Reference 6-11)

the equations of motion. This particular effect was studied in some detail in References 6-4 and 6-11. The study of Reference 6-11 is by far the more exhaustive and, as stated previously, its configuration is a spinning torus and, therefore, has some semblance to the ATSS. The variations in mass transfer effects examined in Reference 6-11 were the following:

1. Instantaneous inclusion of product of inertia term Ixz which is maintained for approximately 400 seconds. The motions were studied for a wide range of the ratios I_x/I_z, I_y/I_z, and I_{xz}/I_z, and are presented as maximum inclination of the body axis relative to an inertial reference.

2. Temporary product-of-inertia disturbances. One case was examined in which a product of inertia was maintained for about 40 seconds and reduced to zero.

3. Instantaneous inclusion of equal products of inertia I_{xy}, I_{xz}, I_{yz}, which are maintained over approximately 400 seconds.

4. Transient radial product of inertia disturbance, in which a mass with an initial velocity experiences deceleration to arrive at a final position with zero velocity. Three velocities were used in this phase of the study.

5. Transient tangential product of inertia disturbance, in which a mass is moved tangentially (at a constant radius). Here again, three velocities were used, as for the radial case.

6. Transient combination of tangential motion and motion parallel to the spin axis. In this case the mass was essentially moved one time around the inside of the torus while being displaced (like going down a spiral staircase).

The effects of a gyroscopic damping system and of a jet damping system were studied for most of the above situations.

Results of the study for the six variations listed above are given in Reference 6-11. The results apply specifically to the configurations studied, and generally do not apply directly to the ATSS. However, the trends are of interest, therefore, the conclusions reached in Reference 6-11 are repeated herein for information and convenience.

a. Docking moments and mass transfer disturbances resulted in undamped station wobbling, which to the crew would appear as a rolling motion of the station floor. This rolling motion, when coupled with the station rotation, could possibly lead to nausea and disorientation of the crew.

b. Transient mass transfer from the center of the station to the rim of the station or parallel to the spin axis of the station produced smaller wobble angles than those produced by instantaneous mass transfer.

c. Transient mass transfer around the rim of the station in the direction of rotation resulted in maximum wobble angles five to seven times as large as those for the static mass transfer. Motion in a direction opposite to the direction of rotation, however, did not produce any amplification of the static results.

d. A gyroscopic damping system was capable of transforming the station wobble produced by docking moments and temporary mass unbalances into a spin about the final angular-momentum vector of the station. Since some of these damped disturbances resulted in attitude errors, the Station must be provided with an additional system capable of maintaining the orientation in space, if such orientation is required by the mission. For a continuously applied dynamic mass unbalance, the

gyroscopic system reduced the resultant wobbling motion to a smaller wobble or a spin about the maximum principal axis of inertia.

e. A proportional jet damping system reduced the station wobble for all disturbances to a steady spinning motion about an axis defined by the principal inertial axes of the station. For temporary disturbances, the spin vector for this motion coincided with the station symmetry axis, while for continuously applied disturbances, this vector was aligned with the principal axis of inertia. The effects of the continuously applied disturbances and the resultant wobble were thus reduced to a rotation of gravity vector or a small apparent tilt of the station floor.

f. The gyroscopic damping system produced faster damping than the proportional jet system for small wobble angles, but the jet system produced faster damping than the gyroscopic system at the larger wobble angles.

6.3 Overview of Space Station Dynamics

As noted previously, the ATSS configuration is conceptual and still evolving at this stage. It is premature to make detailed calculations relative to dynamic behavior following disturbances. However, this review of past studies does point out areas of research for this configuration or other rotating configurations, should they appear feasible and desirable for the future.

It was noted that past studies of rotating stations did not involve counterrotating elements to reduce or eliminate the gyroscopic stability of the space station. It would be informative to use the ATSS configuration to study motion following disturbances, control

requirements, microgravity envelope, materials transfer, general mechanization, etc., with and without counterrotators.

REFERENCES

6-1 Queijo, M. J. et al.: An Advanced-Technology Space Station for the Year 2025, Study and Concepts. NASA CR-178208, March 1987.

6-2 Queijo, M. J. et al.: Analyses of a Rotating Advanced-Technology Space Station for the Year 2025. NASA CR-178345, January 1987.

6-3 Martz, William: Methods of Approximating the Vacuum Motions of Spinning Symmetrical Bodies with Nonconstant Spin Rates. NASA TR-115, 1961.

6-4 Grantham, William D.: Effects of Mass-Loading Variations and Applied Moments on Motion and Control of a Manned Rotating Space Vehicle. NASA TN D-803, May 1961.

6-5 Beauchamp, G.T.: Adverse Effects Due to Space Vehicle Rotation. Astronautical Sciences Review. October-December 1961.

6-6 Hill, Paul R. and Schnitzer, Emanuel: Rotating Manned Space Stations. September/Astronautics 1962.

6-6 Lally, Eugene F.: To Spin or Not to Spin. Astronautics, September 1962.

6-8 Berglund, Rene A.: AEMT Space Station Design. Astronautics, September 1962.

6-9 Langley Research Center Staff: A Report on the Research and Technology Problems of Manned Rotating Spacecraft. NASA TN D-1504, August 1962.

6-10 Kurzhals, Peter R. and Adams, James J.: Dynamics and Stabilization of the Rotating Space Station. Astronautics, September 1962.

6-11 Kurzhals, Peter R. and Keckler, Claude R.: Spin Dynamics of Manned Space Station. NASA TR R-155, December 1963.

6-12 Anon.: Study of a Rotating Manned Orbital Space Station. Spacecraft Organization. Lockheed-California Company. Burbank. March 1964.

6-13 Piland, William M.: An Analytical and Experimental Investigation of the Motion of a Rotating Space Station. NASA TND-2981, September 1965.

6-14 Austin, Fred: Stability Criteria for a Rotating Space Station with a Nonrotating Hub. AIAA Journal, Vol. 6, No. 11. November 1968.

6-15 Suddath, Jerald H.: A Theoretical Study of the Angular Motions of Spinning Bodies in Space. NASA TR-83, 1961.

7.0 FEASIBILITY OF MANUFACTURING SPACECRAFT COMPONENTS ON-BOARD THE ADVANCED-TECHNOLOGY SPACE STATION

The Advanced-Technology Space Station (ATSS) proposed for the year 2025 will have provisions for on-board manufacture and processing of materials for fabrication and assembly of spacecraft components. The feasibility of on-board manufacture of components must be evaluated against the feasibility of both terrestrial and extraterrestrial manufacture of spacecraft components. The space-based manufacture of spacecraft components is divided into four categories based on the manufacturing sites as shown in Figure 7.0-1. The four categories are: the manufacturing on Earth of ATSS structures and subassemblies, manufacturing aboard the ATSS, manufacturing at a lunar base and manufacturing from materials supplied from the Martian moons and asteroids. All of these will be reviewed briefly in Sections 7.2 through 7.5.

7.1 Launch Concept for the ATSS

The ATSS components and subsystems will be designed, developed, manufactured, and assembled on Earth from Earth-supplied materials. Each subsystem would be thoroughly tested prior to disassembly and launch into space for reassembly in low Earth orbit (LEO). The following assumptions relate to the projected space transportation architecture for the 2025 time frame and the rotating ATSS structural configuration (Reference 7-1):

- The ATSS will be manufactured on Earth comprised of structural elements and subassemblies compatible with the size and weight limitation of the space transportation architecture available in the 2025 time frame.

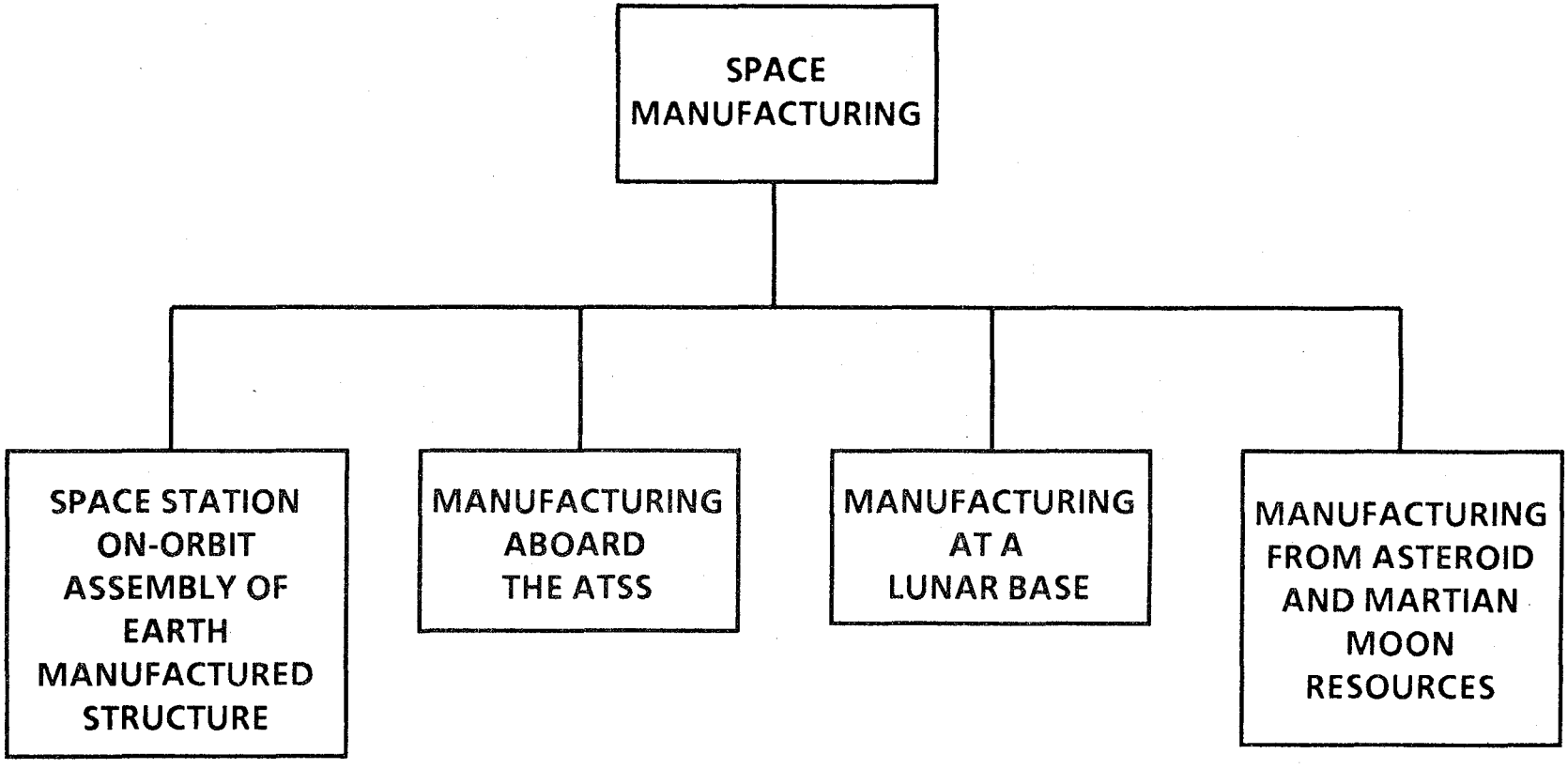

Figure 7.0-1 Space Manufacturing

- o The ATSS would be disassembled into structural elements, components and subassemblies and manifested for launch to LEO to maximize the space transportation system's capabilities.
- o The space transportation system architecture will require heavy lift launch vehicles (HLLV) capable of lifting greater than 2.72×10^5 kg (6×10^5 lb) per launch to LEO (250 - 270 nautical miles altitude at an inclination of 28.5 degrees).
- o The assembly and checkout of the ATSS would occur on orbit in an essentially weightless condition.

Several HLLV concepts have been proposed over recent years ranging from 2.27×10^5 kg (5×10^5 lb) to 9.07×10^5 kg (2×10^6 lb) payload launch capability to LEO. Payload diameters are limited in size from 15.24 m (50 ft) up to 25.9 m (85 ft) for the larger of the proposed vehicles as shown in Figure 7.1-1 (Reference 7-2) and Figure 7.1-2, (Reference 7-3).

7.2 On Earth Manufacture of ATSS Structure Elements and Subassemblies

Successful assembly on orbit of the ATSS structure and subassemblies depends heavily on practical packaging for transport and the assembly and use of expandable and modular structures. Expandable and modular structures provide a means of achieving high density payload packaging at a minimum volume. Much work was done on expandable structures in the early to mid 1960's because of limitations of payload weight and volume of the launch systems then available. On Earth manufactured expandable and modular structures will be reviewed in the functional categories of nonrigid, semirigid and rigid structures as referred to in Figure 7.2-1.

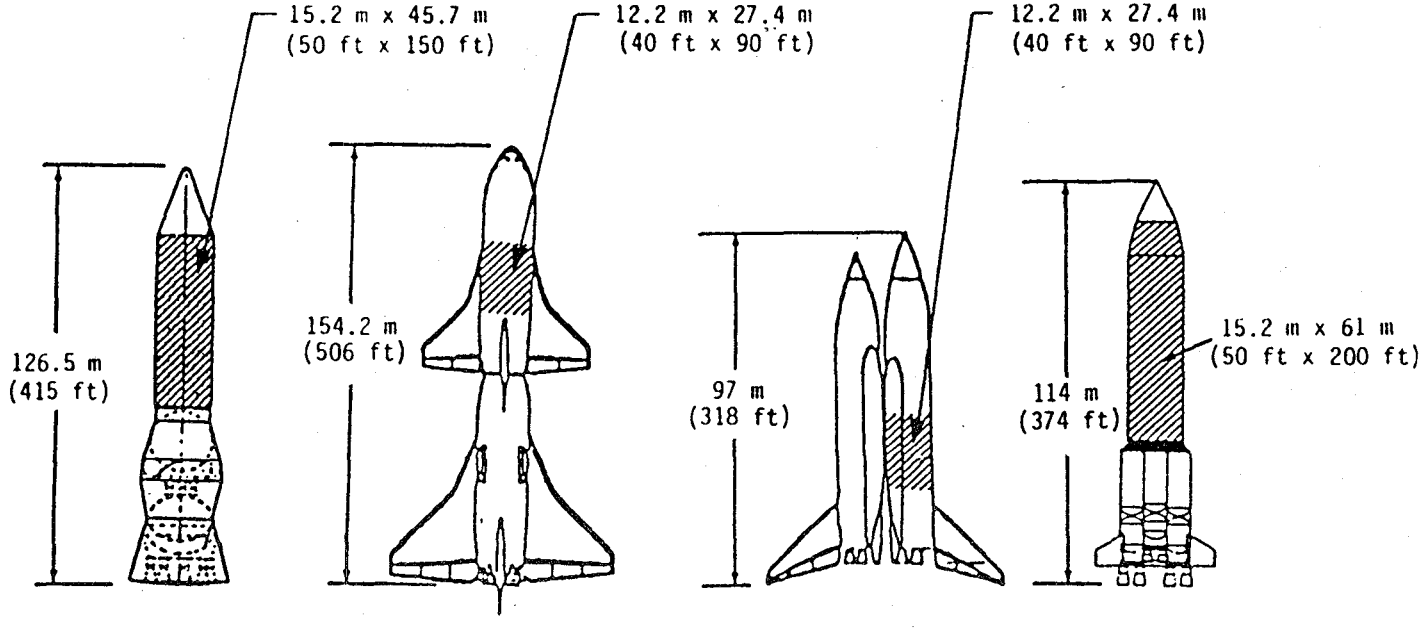

Figure 7.1-1 Heavy Lift Launch Vehicle Concepts (2.27×10^5 kg or 5×10^5 lb payload class) (Reference 7-2)

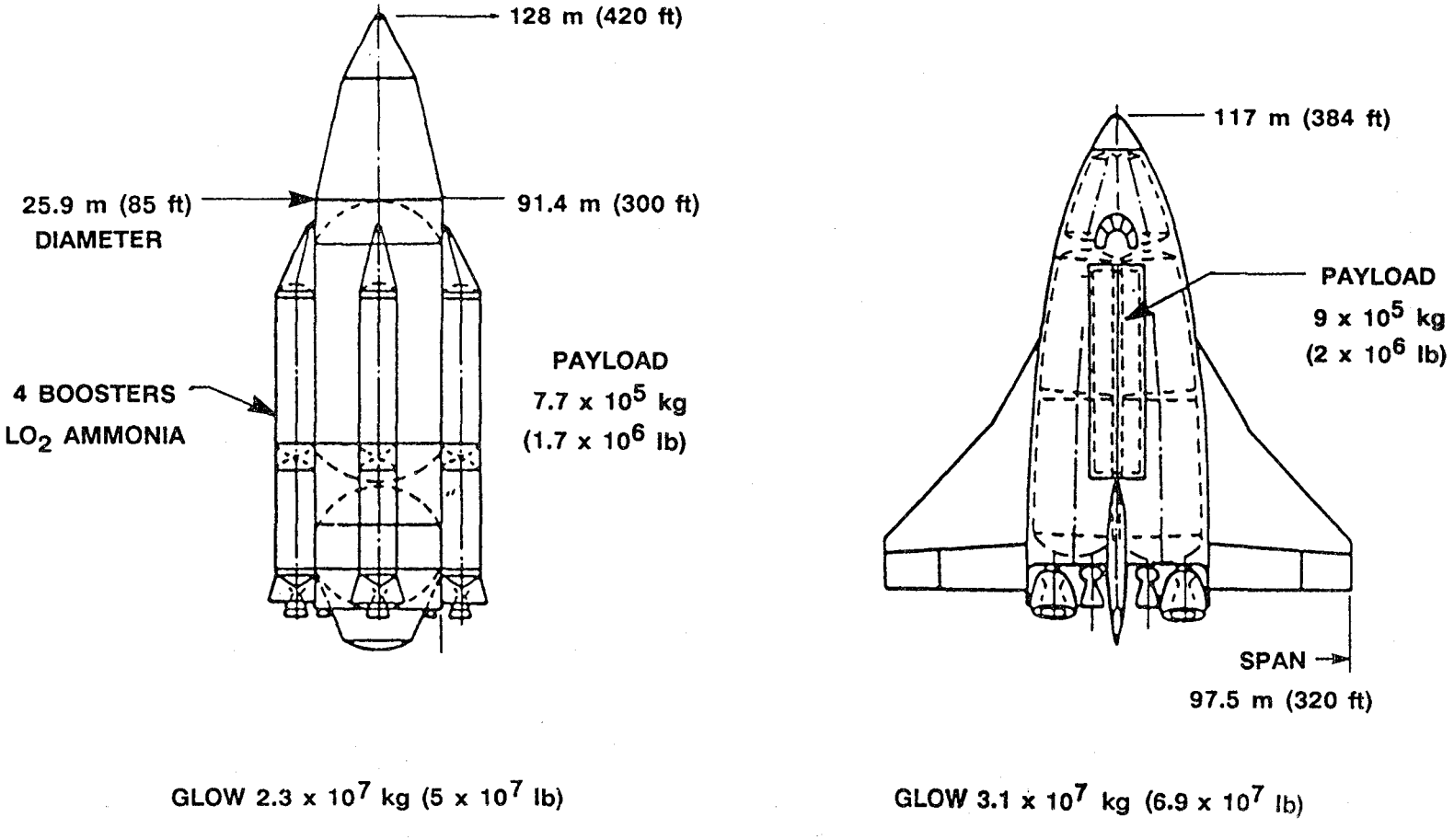

Figure 7.1-2 Launch Vehicle Concepts (adapted from Reference 7-3)

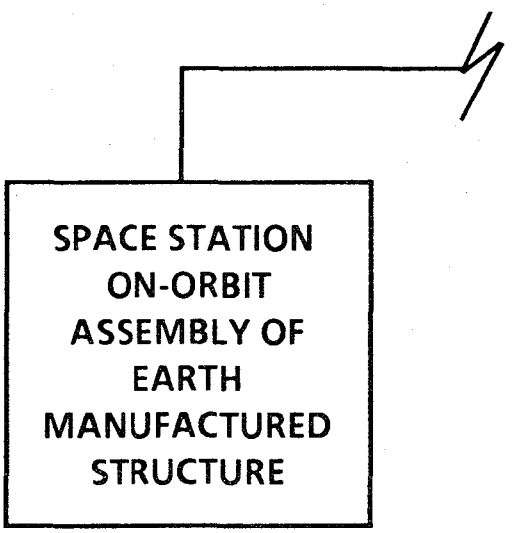

NON RIGID

- **FLEXIBLE**
- **RIGIDIZE IN SPACE**
  (UMBRELLA, ELASTIC RECOVERY, CHEMICAL HARDENING)

SEMI RIGID

- **RIGID PANELS, SECTIONS OR MODULES**
- **CHANGE SHAPE OR VOLUME**
  (SELF-DEPLOYED, UNFURLABLE, TELESCOPIC)
- **METALLIC OR NON METALLIC**

RIGID

- **ASSEMBLE IN SPACE**
- **PRETESTED COMPONENTS AND SUBSYSTEMS**
- **FIXED VOLUME AND WEIGHT**
  (MODULES, STRUTS)
- **SPENT TANKAGE UTILIZATION**

Figure 7.2-1 On Earth Manufactured Expandable and Modular Structures

7.2.1 Nonrigid Expandable Structures

Examples of nonrigid expandable structures would include fully assembled components such as an umbrella construction which could be folded for payload packaging and opened remotely upon achieving LEO. The combination of a flexible membrane and semirigid structural elements was investigated for structure such as antenna dishes.

Another example of nonrigid expandable structure consisted of a flexible foam core sandwich encased between flexible skins. Structures fabricated of flexible sandwiches could be compression-packaged in a small volume for payload installation, and upon release, the sandwich structure would assume its prepackaged shape due to the release of residual stress confined within the sandwich's core of flexible foam. The concept and examples of elastic recovery structures are shown in Figures 7.2.1-1 and 7.2.1-2 (References 7-4 and 7-5).

Passive communication satellites, Echo I, II, and Pageos, were fabricated as spherical-shaped balloons using thin gage polyester film as a gas tight membrane. The Pageos Satellite is shown as inflated in Figure 7.2.1-3. The membrane construction of Echo I and Pageos consisted of polyester film vacuum metalized with aluminum. Echo II used a composite membrane laminate of aluminum foil and polyester film. The inflatable satellites were evacuated, folded, and compactly enveloped within a payload canister. The balloon's inflation gas was provided by sublimable solids to inflate and maintain shape of the spheres in orbit (Reference 7-6).

Inflatable structures have been developed whereby the aluminum foil of the membrane composite hardens due to strain when inflated by an internal gas pressure sufficient to exceed the elastic limit of the foil.

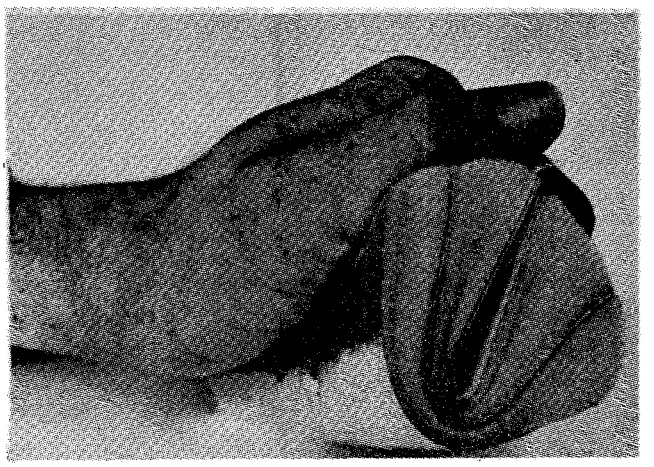

Compressed

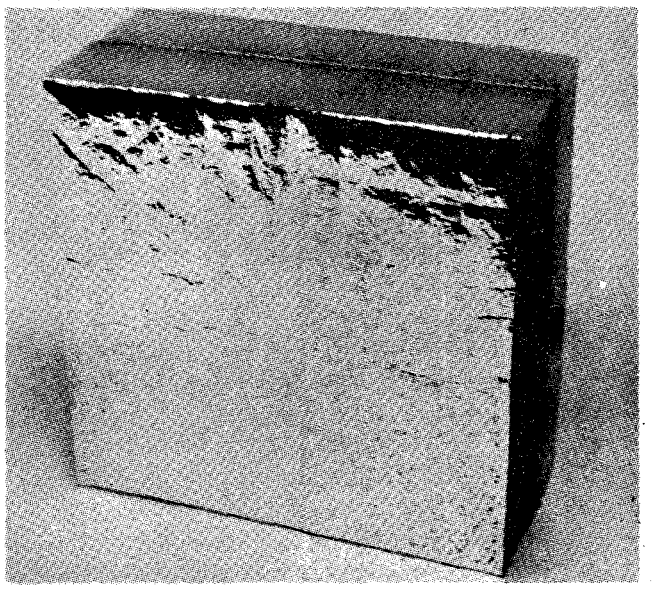

Expanded

Figure 7.2.1-1 Elastic Recovery Foam Sample (Reference 7-4)

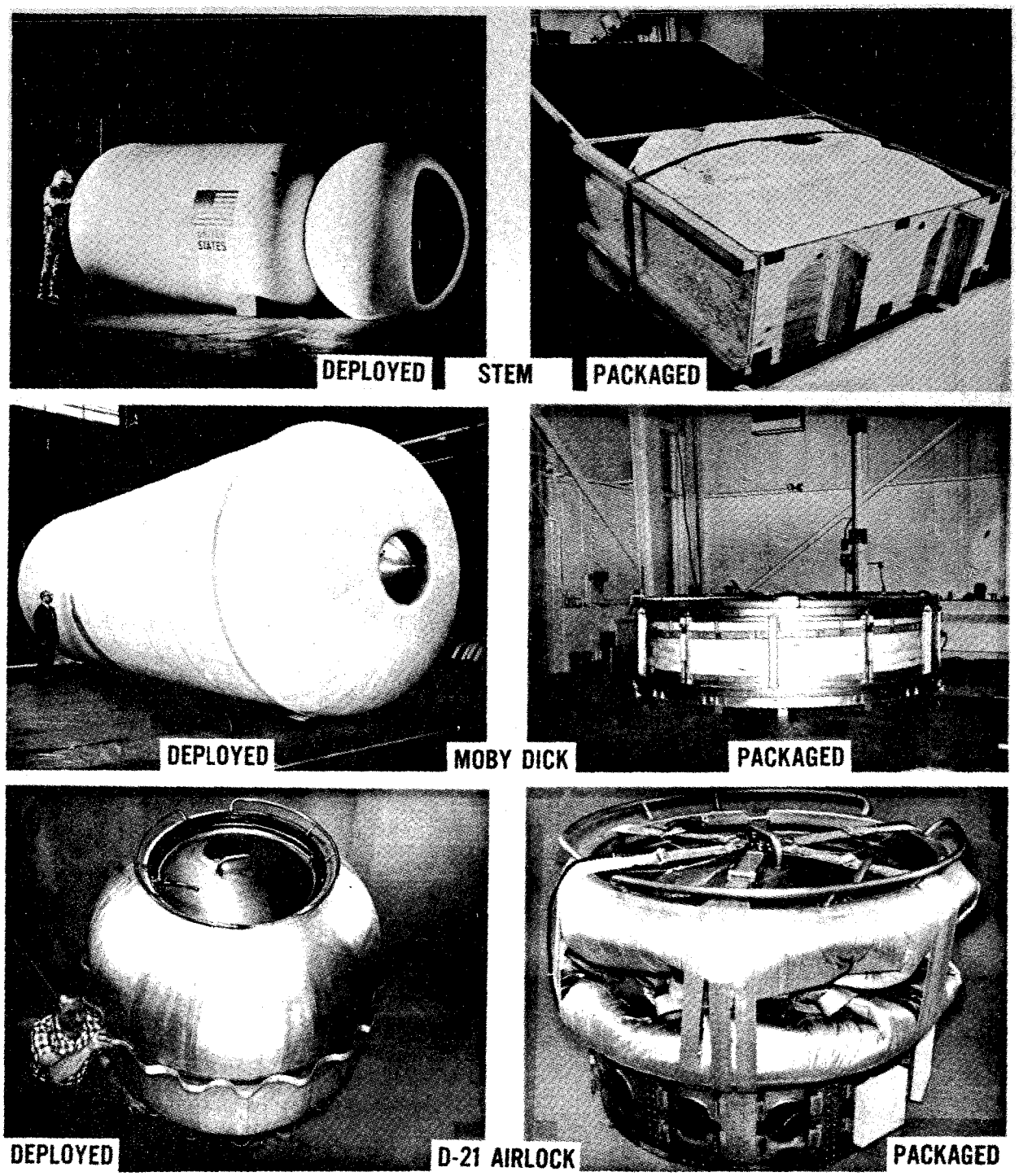

Figure 7.2.1-2 Existing Technology of Elastic Recovery Composite Structures (Reference 7-5)

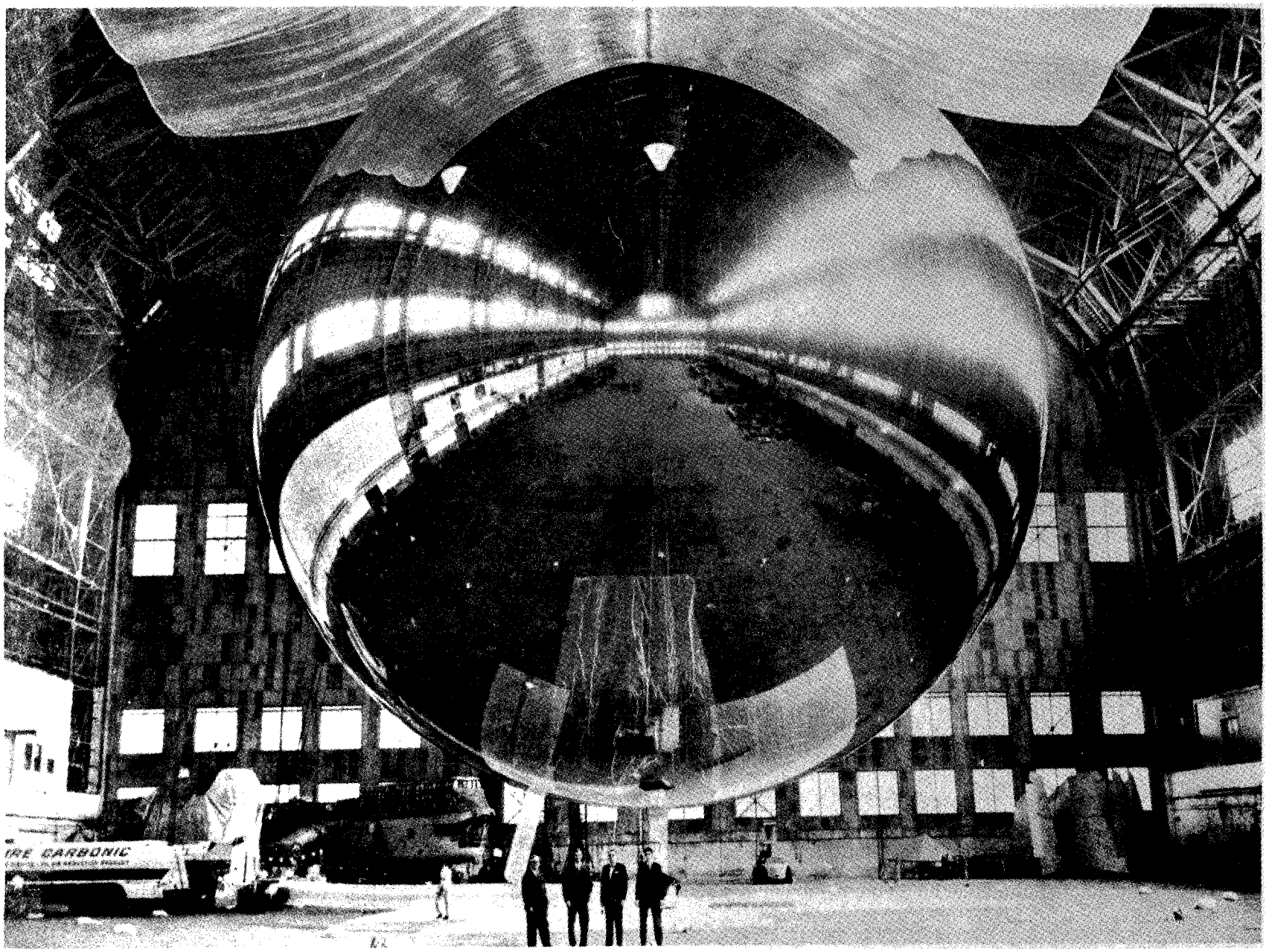

Figure 7.2.1-3 Pageos Static Inflation (Reference 7-6)

The strain hardened composite laminate is free of fold lines and wrinkles and will retain its inflated shape in the weightless rarefied gas environment of LEO. The polyester film has a percent elongation to failure greater than that of the aluminum foil, thus assuring the gas tight integrity of the composite membrane. The passive communication satellite Echo A-12 used this strain hardening concept for shape control (Reference 7-7).

Flexible fabric reinforced synthetic resin can be rigidized in space on command. These structural concepts may be used for spacecraft construction using bidirectionally woven fabrics preimpregnated on Earth with an uncured synthetic resin. The tacky matrix resin laminate is clad on both sides with a thin plastic film to assure a gas tight membrane and prevent the tacky impregnated fabric layers from adhering to one another when compacted as a payload. An internal inflation gas can erect the structure on-orbit. The selection of pressurant gas and the degree of gas permeability of the plastic films can provide matrix hardening by mechanisms such as loss of water from a gelatin matrix, vapor catalysis of the matrix resin by the pressurant gas, or by laminate exposure to ultraviolet or infrared solar radiation. Examples of rigidized in-space structures are shown in Figure 7.2.1-4 (Reference 7-8) and Figure 7.2.1-5 (Reference 7-9).

Pre-sewn fabric sandwich reinforcements can be preimpregnated with an uncured synthetic matrix resin on Earth. Examples of presewn structures are shown in Figure 7.2.1-6 (Reference 7-10). Plastic film can be applied to both sides of the uncured sandwich laminates to prevent blocking or adherence of the tacky layers in their compacted state when enveloped in the payload canister. On-orbit gas inflation of the

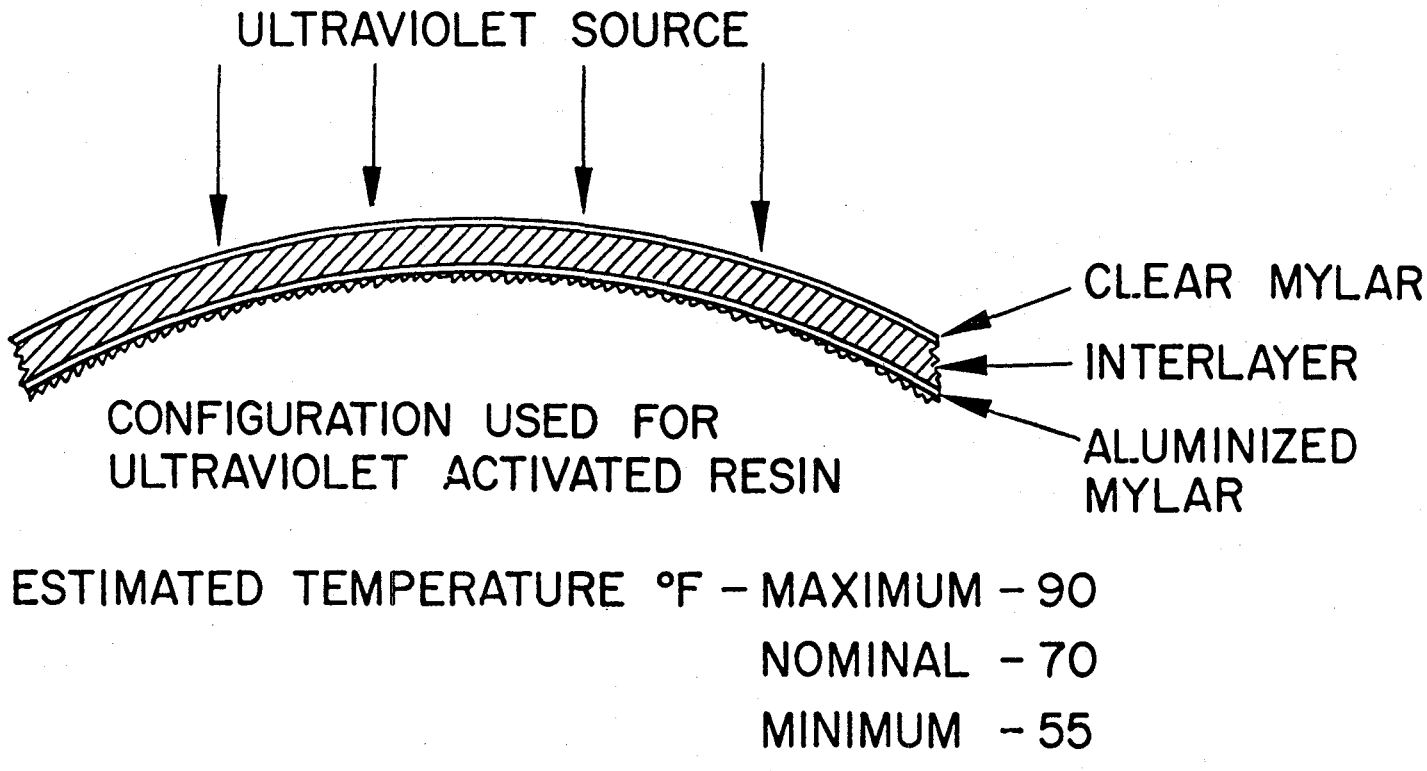

Figure 7.2.1-4 Configuration used for Ultraviolet Activated Resin (Reference 7-8)

Contraves Develops Space-Rigidizing Concept

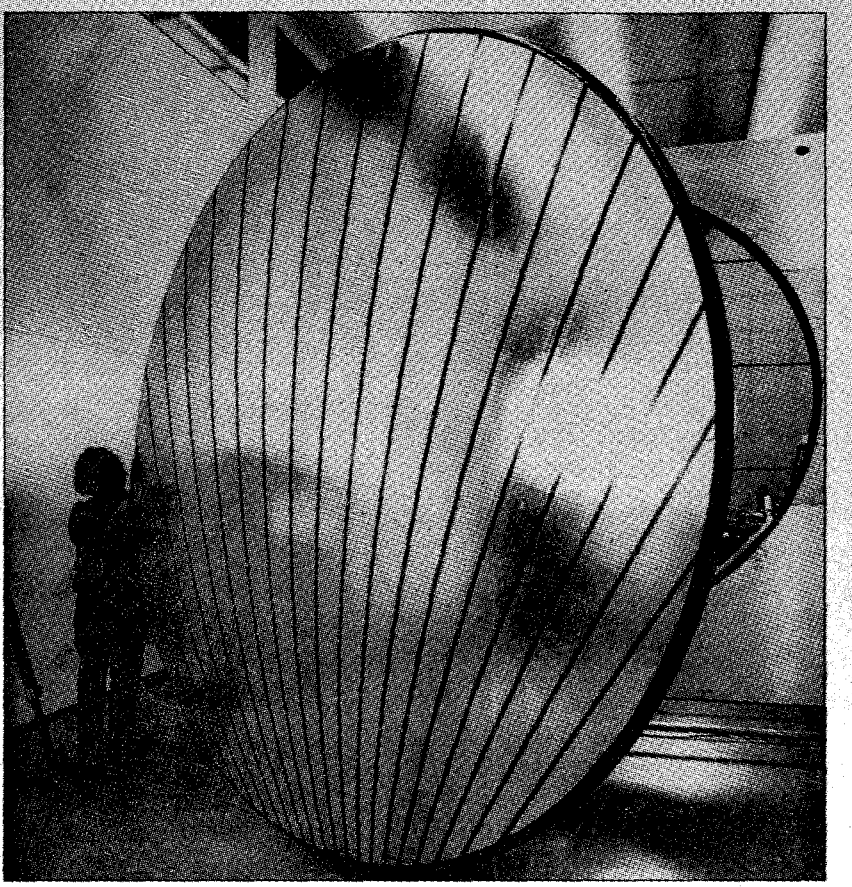

Switzerland's Contraves has developed an inflatable space-rigidizing structure concept for use in large antennas, thermal shields, space enclosures, truss structures, solar sails and thermal propulsion systems. After being inflated in space, the structure would become rigid when cured by its exposure to solar radiation. Contraves has manufactured three models of a 3.2-meter-dia. (10.5 ft.) offset reflector (shown here) weighing less than 3 kg. (6.6 lb.) under contract to the European Space Agency. Company officials said ground-based vacuum tests of the reflector cured under infrared radiation have shown promising results in terms of its geometrical accuracy and electrical performance.

Figure 7.2.1-5 Contraves Developed Space-Rigidizing Concept (Reference 7-9)

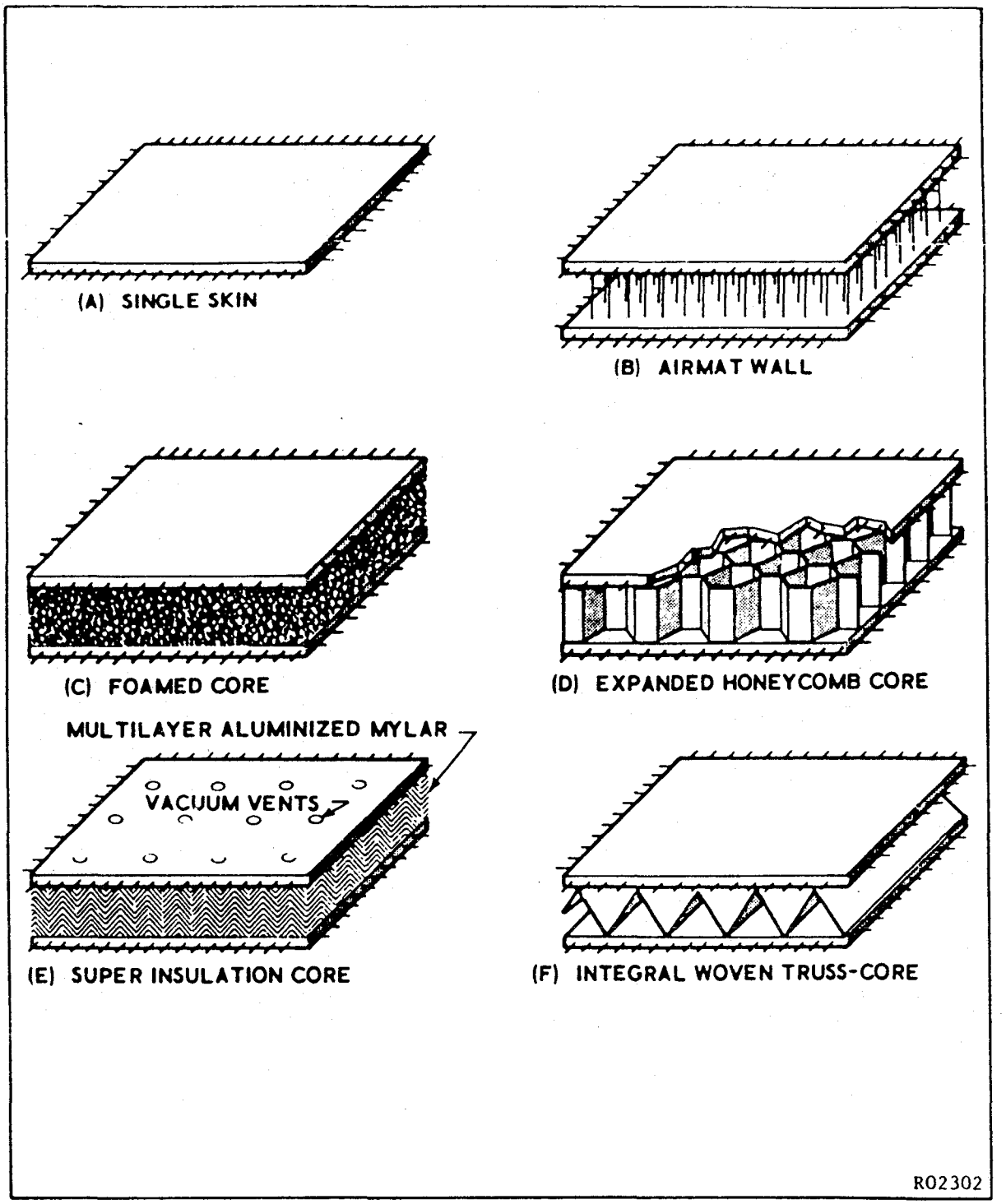

Figure 7.2.1-6 Flexible Wall Concepts (Reference 7-10)

sandwich structure and the injection of a liquid foam-in-place resin between the sandwich skins to form a low density core will provide a strong rigid lightweight structure. Solar radiation will cause the sandwich skins matrix resin to harden after the core foam has cured (Figure 7.2.1-7) (Reference 7-11).

7.2.2 Semirigid Expandable Structures

Semirigid expandable structures can utilize cylinders, panels, struts, sheets, and other rigid configurations that permit high density payload packaging and can be deployed mechanically on orbit to form a larger size assembly or structure than as delivered to orbit. The following examples of semirigid structure are briefly described.

A hexagonal rotating space station design was evaluated whereby six cylinders would be assembled to form a hexagon with three spokes attached from the hexagon to a central hub. The assembly was to have retracted mechanically to fit within the payload weight and volume constraints of a Saturn V booster payload shroud. The Space Station was designed to self deploy on command in space as shown in Figures 7.2.2-1 and 7.2.2-2 (Reference 7-12). The flexible joints interconnecting the rigid station elements were designed to be gas tight thus permitting space station atmospheric pressurization immediately after assembly.

Solar panels that can be furled permit storage of a large solar panel boom assembly in a small volume for launch configuration. The boom panels are mechanically unfurled on orbit to their functional configuration (Figure 7.2.2-3) (Reference 7-13).

A parabolic-shaped dish solar concentrator has been designed consisting of rigid petals that are nested for launch configuration and

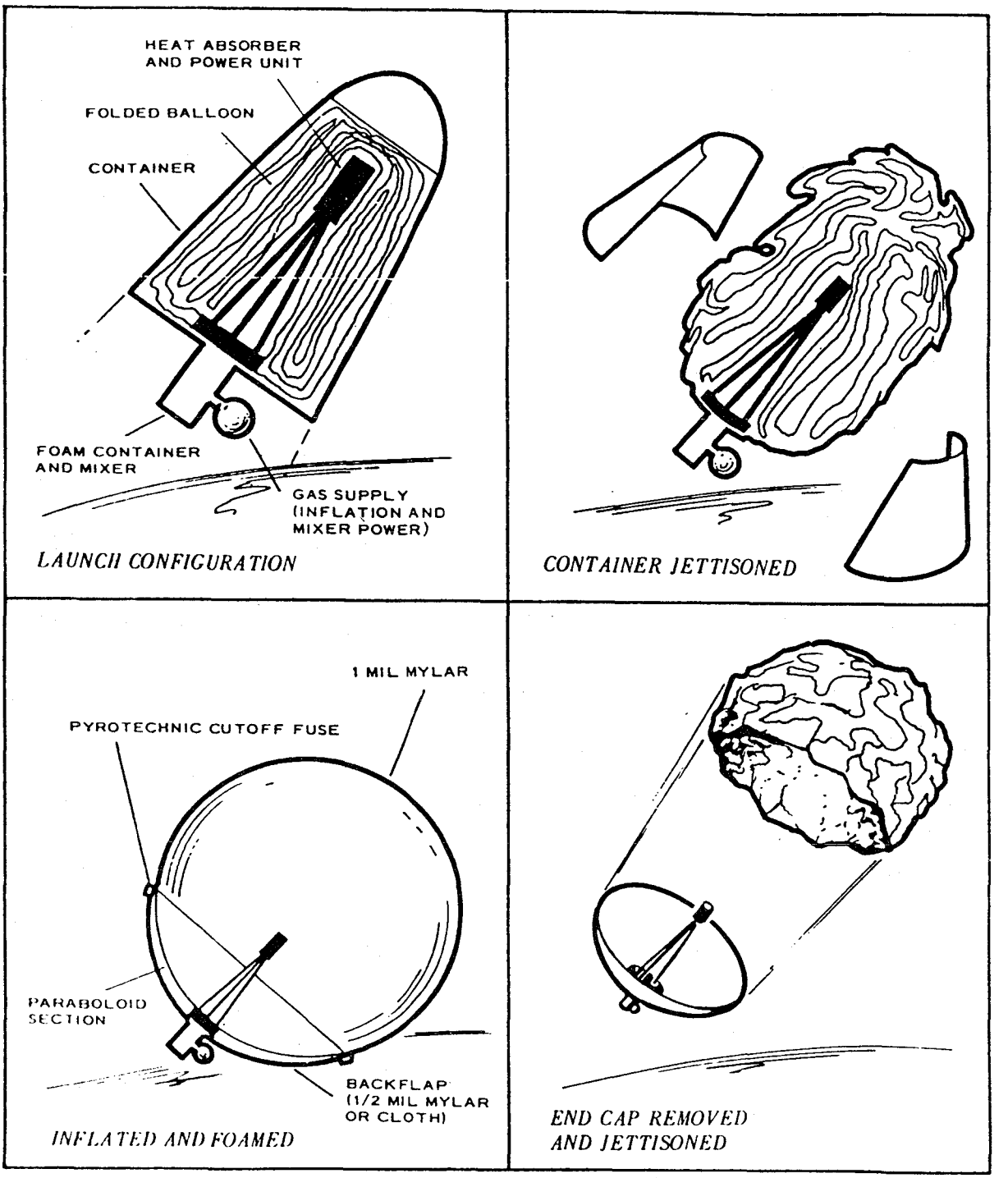

Figure 7.2.1-7 Deployment and Rigidization of Solar Concentrator (Reference 7-11)

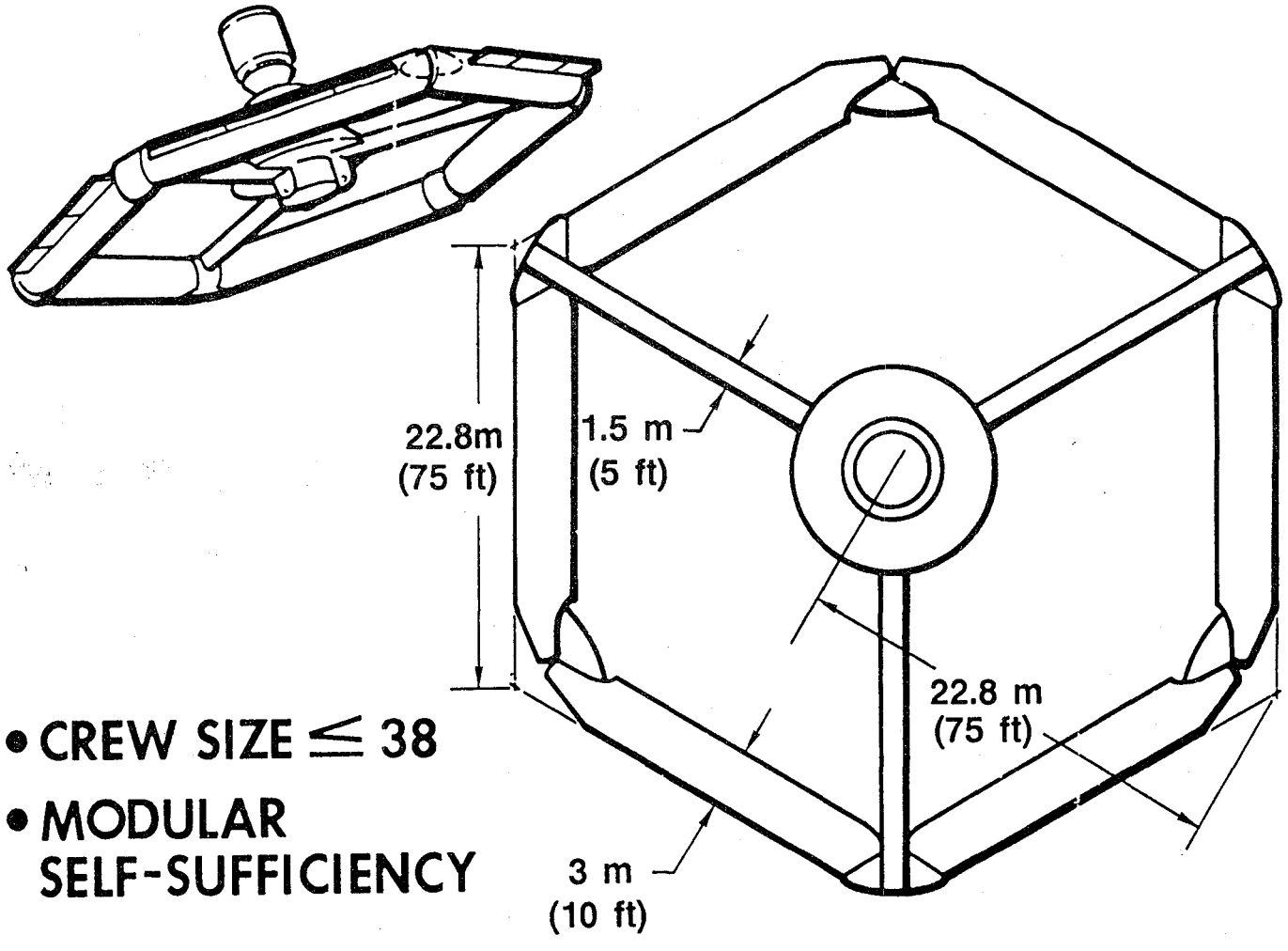

Figure 7.2.2-1 Self Deployed Space Station (SDSS) (adapted from Reference 7-12)

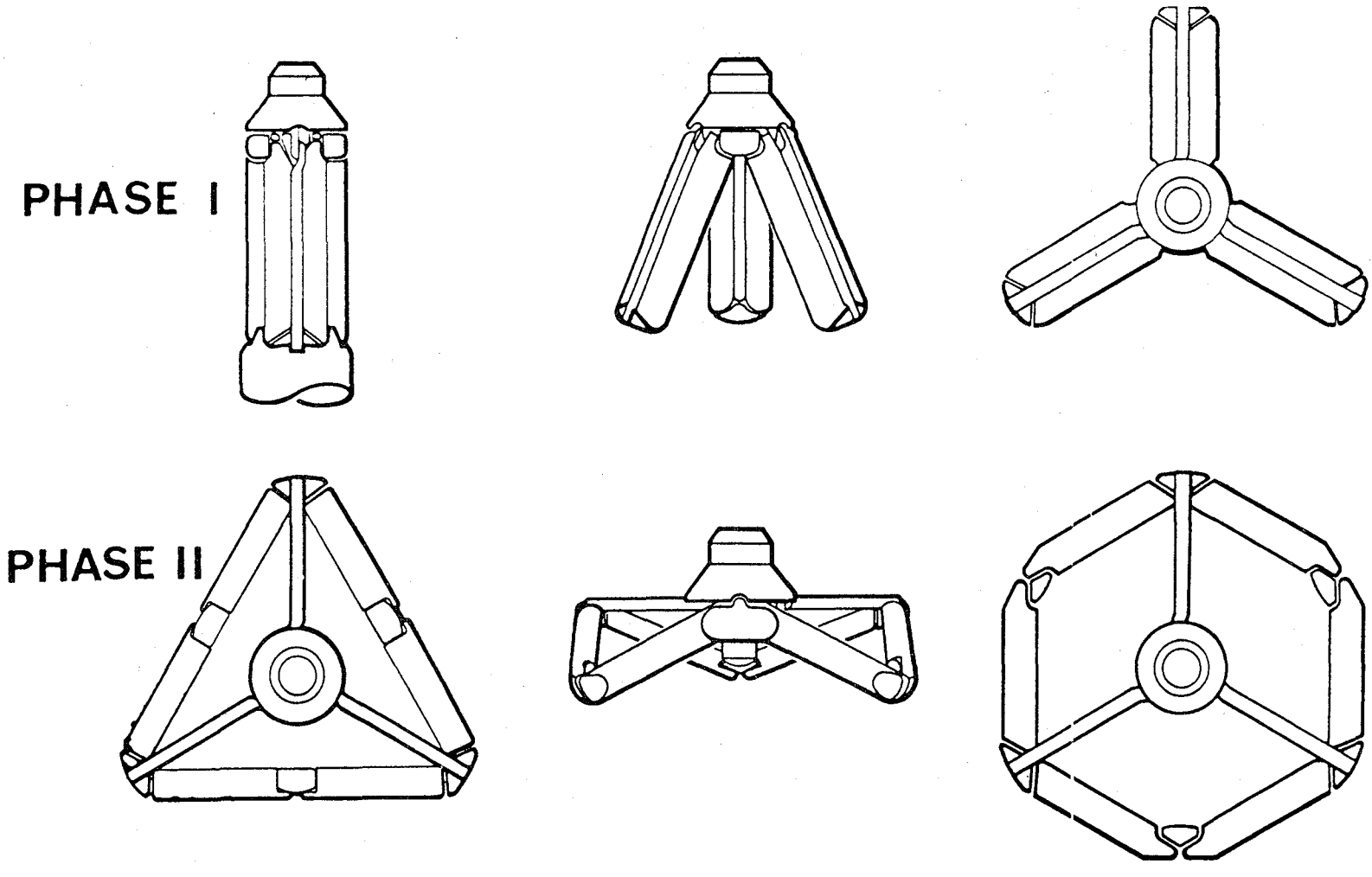

Figure 7.2.2-2 SDSS Deployment Concept (Reference 7-12)

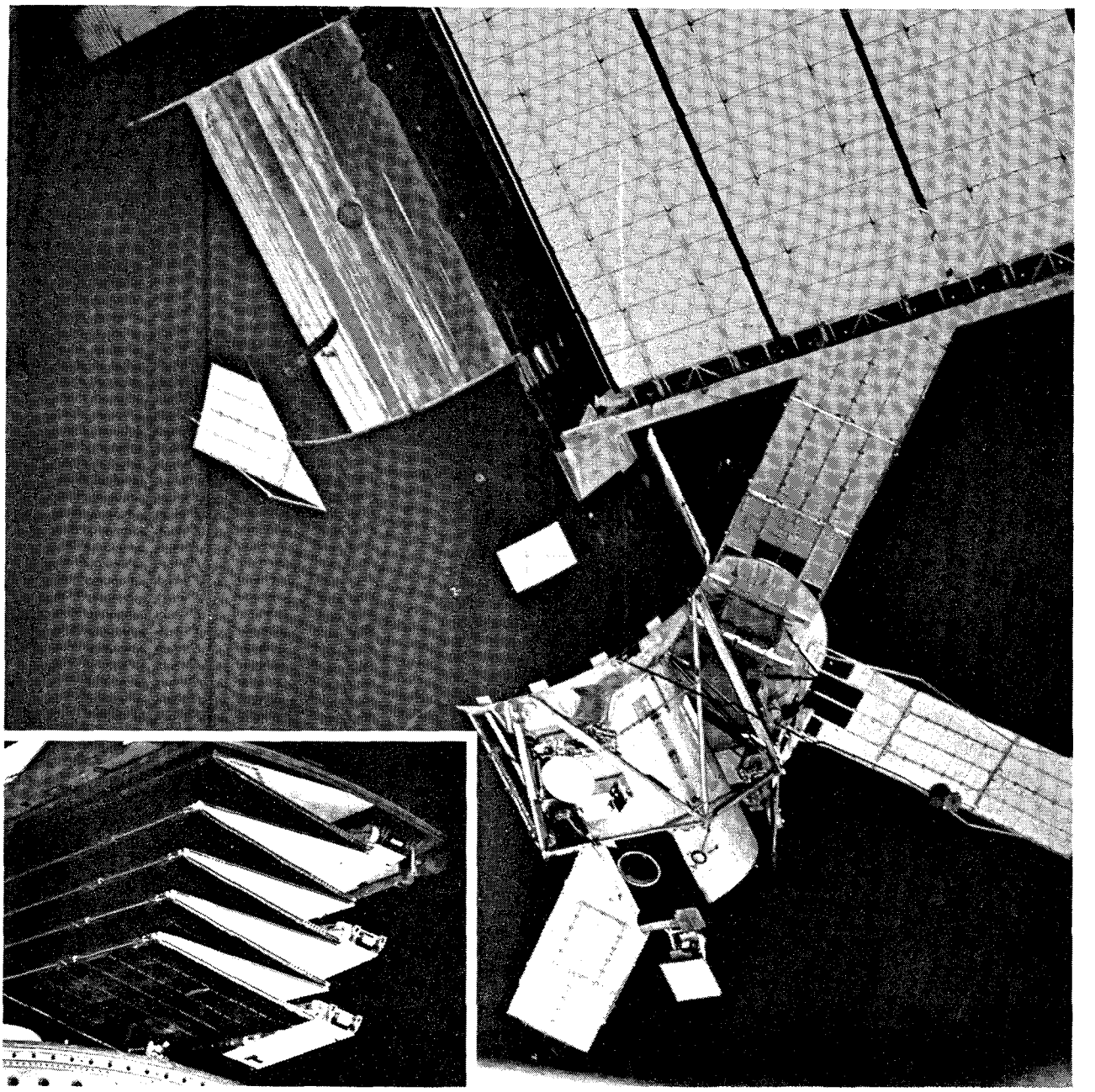

Figure 7.2.2-3 Furlable Solar Array Wing of the Skylab Workshop (Reference 7-13)

mechanically deployed to interlock at the proper circular configuration and contour (Figure 7.2.2-4) (Reference 7-7). Also rigid parabolic dish shaped petals have been designed for assembly and interlock by inflating a flexible gastight annulus used as a backup deployment structure for the dish.

A helical wrapped band tube assembly is a method of rolling a sheet metal strip into a cylinder whereby the strip is wound in a helical path. The wound cylinder can be telescoped by restraining one end of the helix while winding the opposite end of the metal strip into a smaller radius and telescoping the cylindrical column to the height of the metal strip's width. The telescoped cylinder can be secured and transported to orbit where the cylinder can be released to resume its as-rolled length, due to residual stress confined within the sheet metal. The edges of the metal strip could be prepared on Earth for a suitable space joining method such as mechanical cold welding, pipe lock seam with elastomeric seal or electron beam fusion welding to provide a gastight structural cylinder (Figure 7.2.2-5).

The ATSS may utilize counterrotating tori filled with water to nullify the gyroscopic effects of the rotating habitat torus. Each counterrotator torus could be attached to the central hub bearing assembly using cables placed in tension and arrayed like spokes of a bicycle wheel. The cables could be tension-tuned for uniform load distribution and translation. The coiled cables provide high density payload packaging and simplified assembly of the counterrotator tori in LEO.

The present design concept for the spokes of the ATSS torus are to be fabricated as telescopic cylinders. The spoke length in its extended

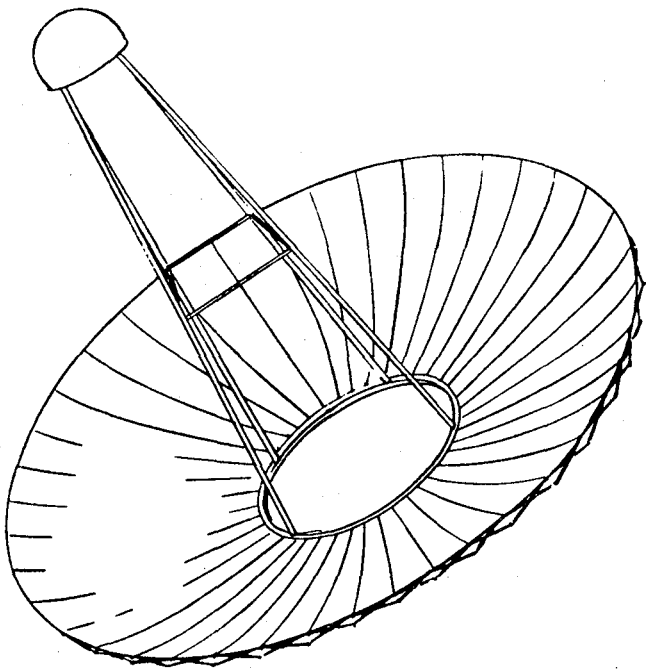

Figure 7.2.2-4 Deployable Solar Concentrator (Reference 7-7)

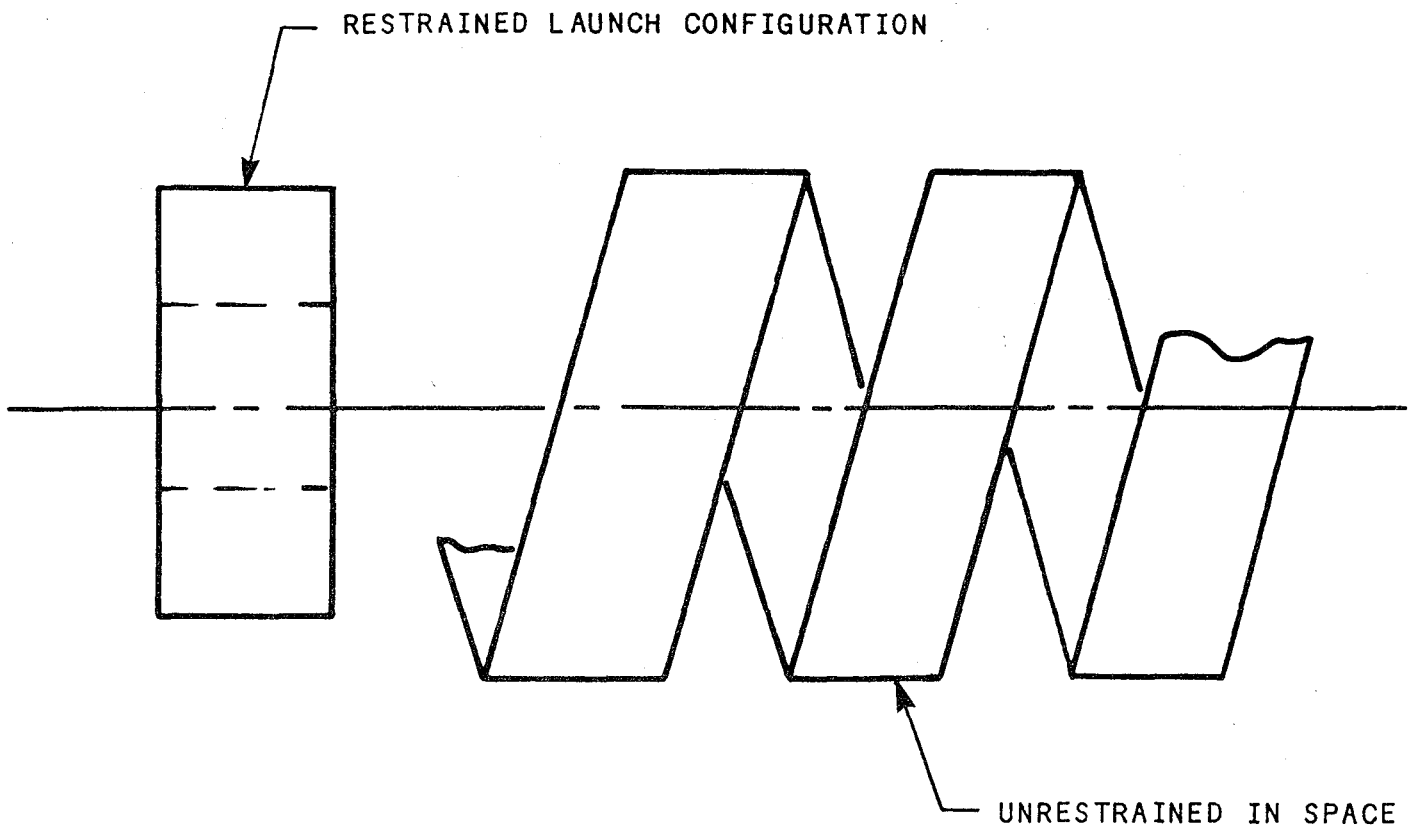

Figure 7.2.2-5 Helical Seam Tube

form would be approximately 89.9 m (295 ft). By making each spoke of three telescoping cylinders, the packaged spoke would be to 30 m (100 ft) in length, permitting two spokes to be manifested for each launch of a HLLV. Upon delivery to orbit, each spoke could be extended to its full length and structural flanges would serve as extension stops to provide a metal-to-metal load bearing contact complete with elastomeric seals to provide a gastight spoke assembly. An example telescopic cylinder design from the early 1960's is shown in Figure 7.2.2-6 (Reference 7-14).

The ATSS is presently planned to be inertially oriented and precessed to provide Sun-pointing, thus, providing near continuous sunlight for operation of the solar dynamic electric power units. Another possible source of electrical power for the ATSS would be to employ a nuclear powered generator system. If this concept is used, then the ATSS could be gravity gradient stabilized since sun-orientation would not be required.

Tethers from a gravity gradient stabilized station could be employed to position fuel depots or maintenance facilities for refurbishing orbital transfer vehicle (OTV) spacecraft. The tethers would be prefabricated of high specific strength fibers and small enough in diameter so that the tether could be coiled for stowage aboard the launch vehicle. The tether would be released in space from a drum or coil from the station to the length required (Figure 7.2.2-7) (Reference 7-15).

A variable geometry structure offers the advantage of fully assembled structural elements which are hinged and compactly folded for launch. The structure can be self-assembled on orbit, such as a truss structure boom. An example of the variable geometry structure is shown

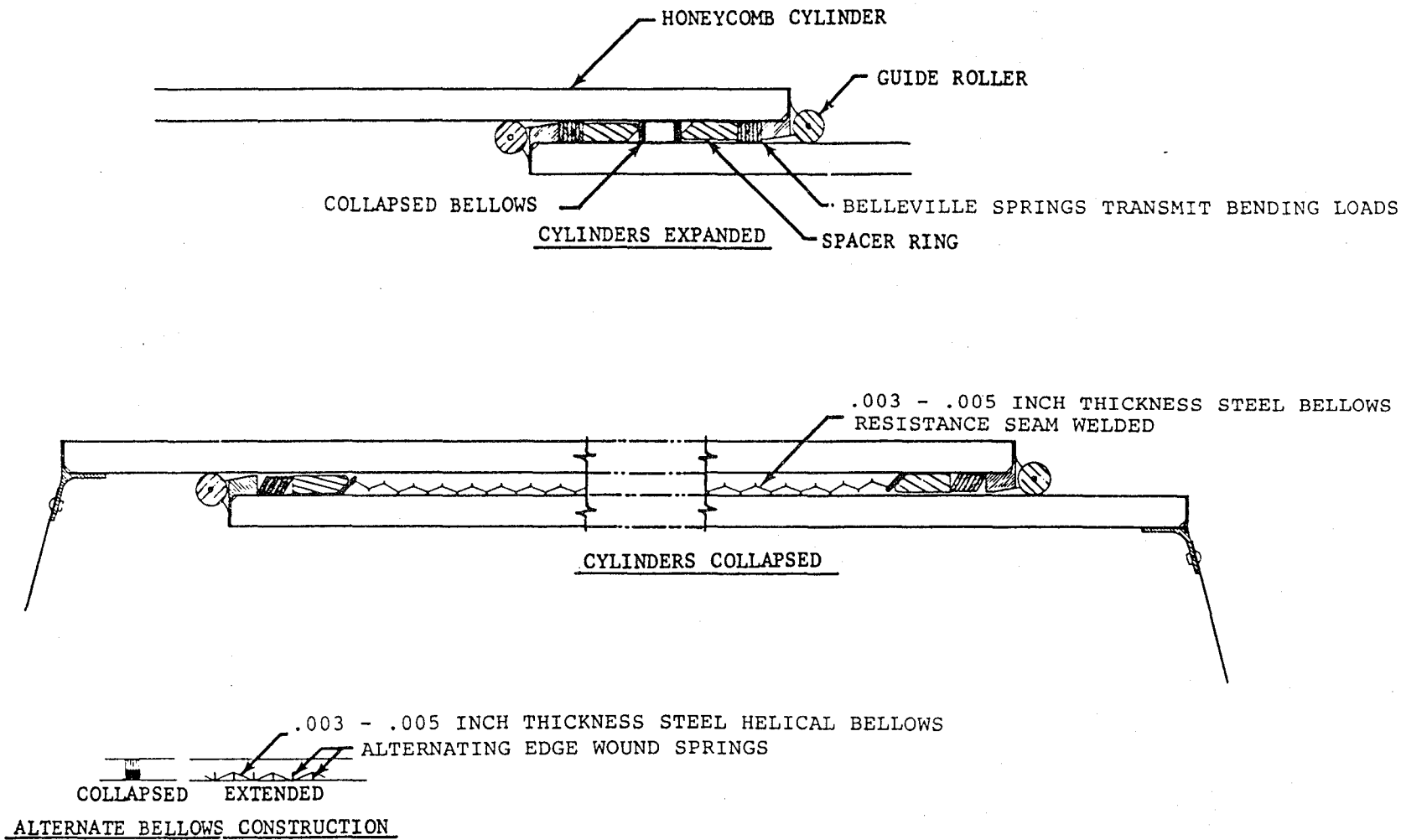

Figure 7.2.2-6 Telescopic Design Concept Utilizing Belleville Spring and Bellows (adapted from Reference 7-14)

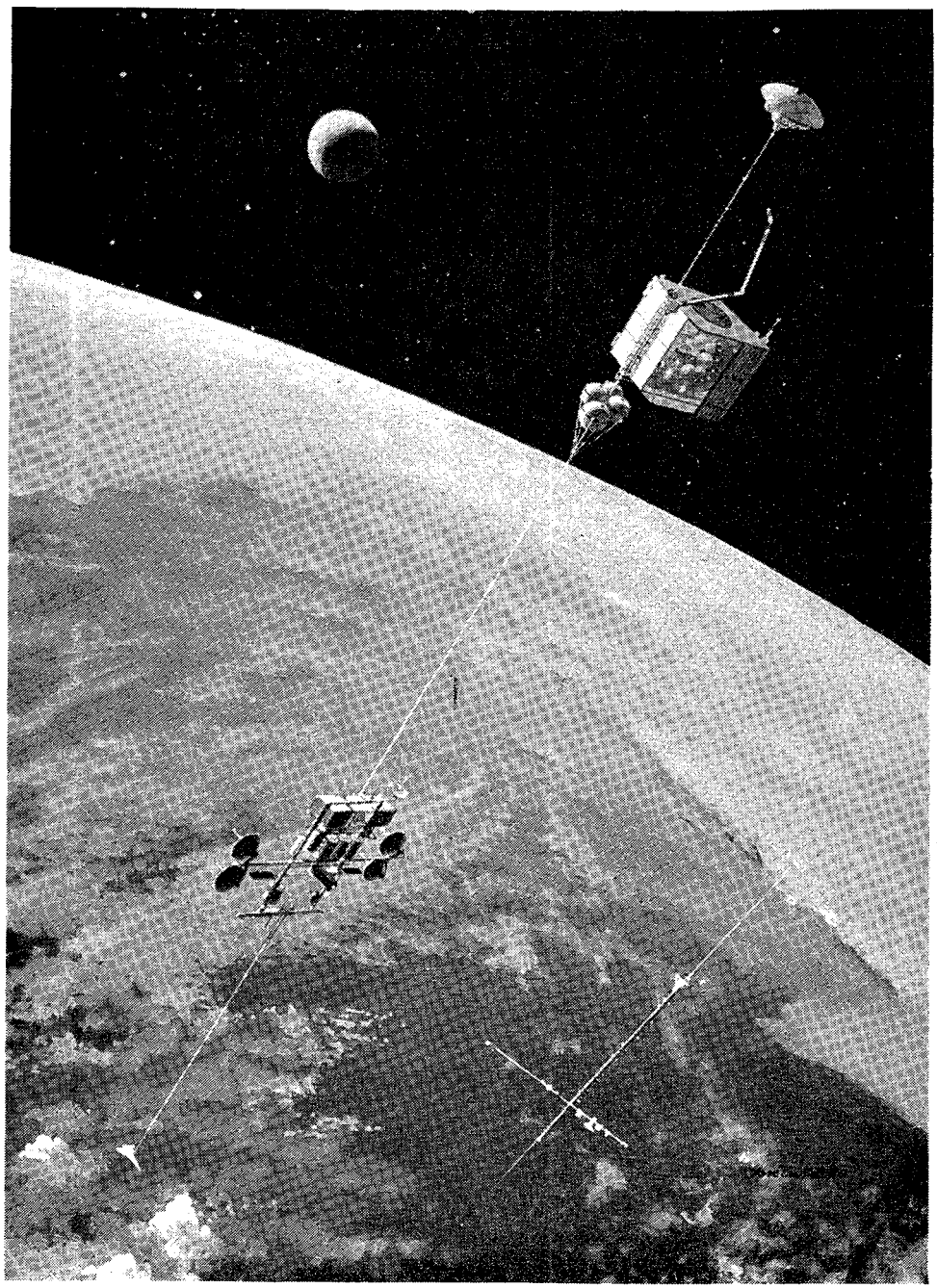

Figure 7.2.2-7 Tethered Earth Spaceport for Spacecraft Maintenance and Fuel Depot (Reference 7-15)

in Figure 7.2.2-8, and is presently under study at the NASA Langley Research Center (Reference 7-16).

7.2.3 Rigid Expandable and Modular Structures

A modular concept is presently planned for the IOC Space Station and is considered a logical approach for assembly of the torus of the ATSS. The torus modules offer the advantage of being sized for transport to LEO on-board a HLLV. The modules would be completely outfitted with all electrical, plumbing, ventilation, and electronic hardware, as required. The modules may be fabricated gastight and operate as independent modules until joined with their contiguous spacecraft structure during assembly. The modular construction offers the convenience of Earth manufacture, assembly, and checkout, prior to disassembly and insertion in LEO, thereby, minimizing extravehicular activity (EVA) and intravehicular activity (IVA) required to place the modules in service as shown during the assembly phase in Figure 7.2.3-1.

Spacecraft docking nodes can be linked to modules and IVA tubes to offer the advantage of an air lock and serve as pressure chambers for depressurization purposes during EVA.

An erectable truss structure offers the advantage of compactly stowing individual truss tubular elements in the launch vehicle. Upon delivery to LEO, the truss elements and associated connector nodes may be assembled into an orthogonal tetrahedral truss structure to construct the observatory boom, solar dynamic platform and the berthing and assembly bay truss structure of the ATSS (Figure 7.2.3-2) (Reference 7-16). Experiments can be attached to these truss structures, and with

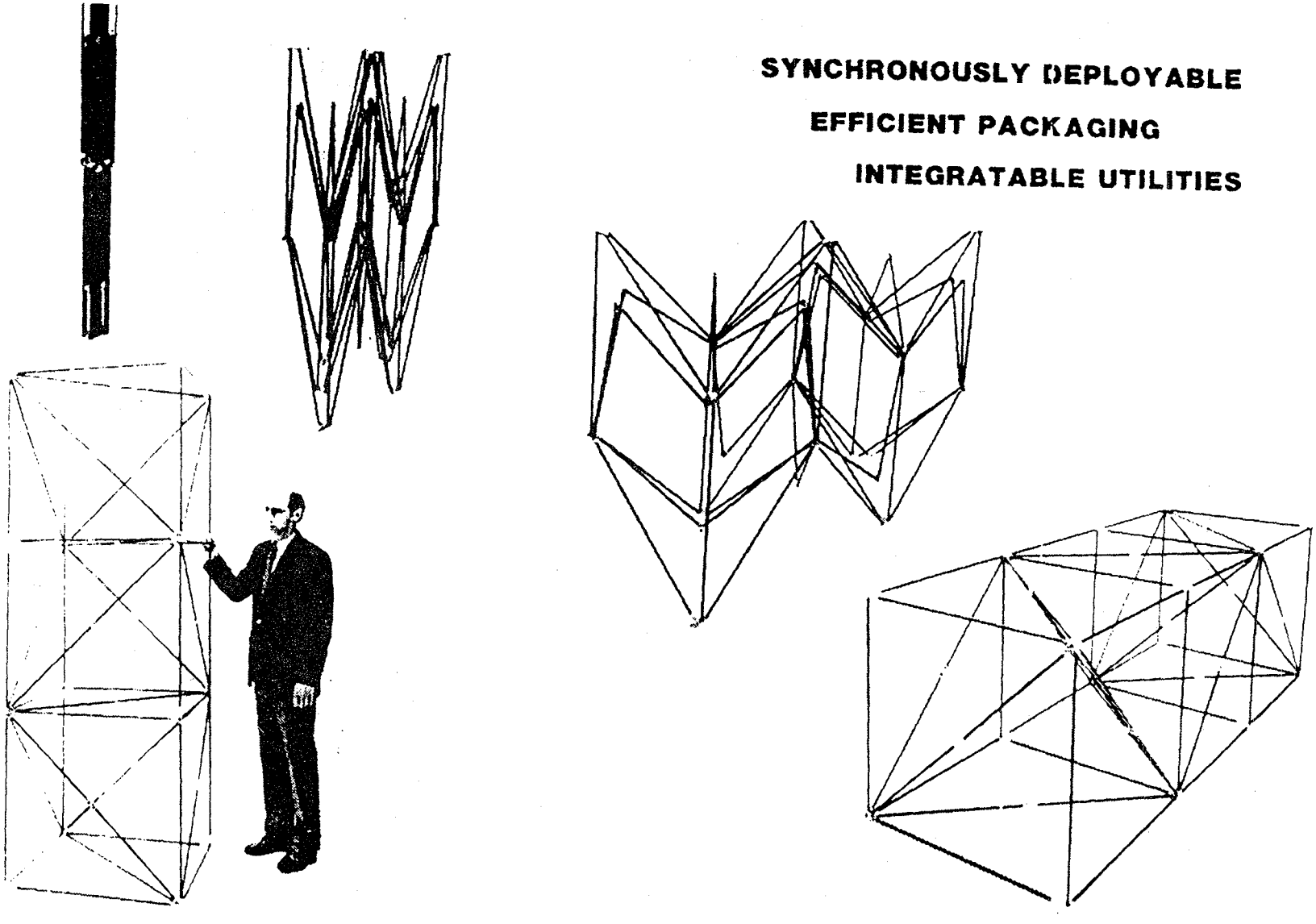

Figure 7.2.2-8 Deployable Pactruss Model (Reference 7-16)

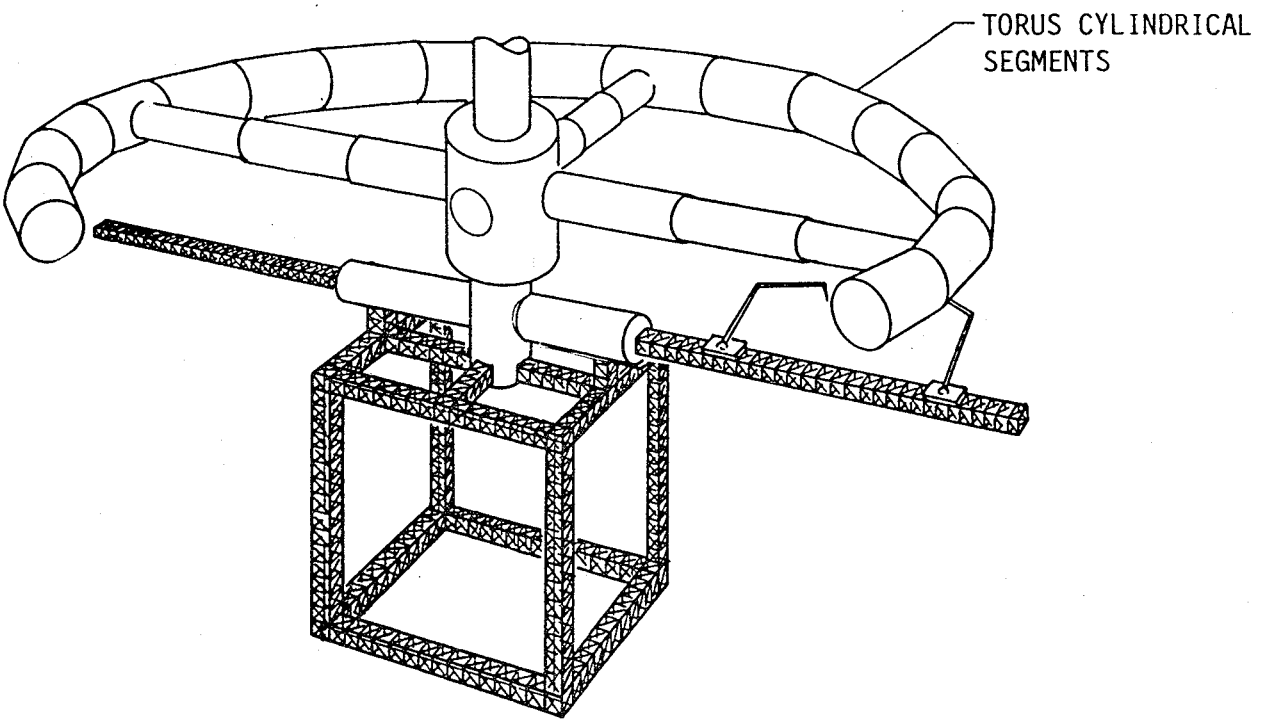

Figure 7.2.3-1 Joining Cylinders to Form a Torus

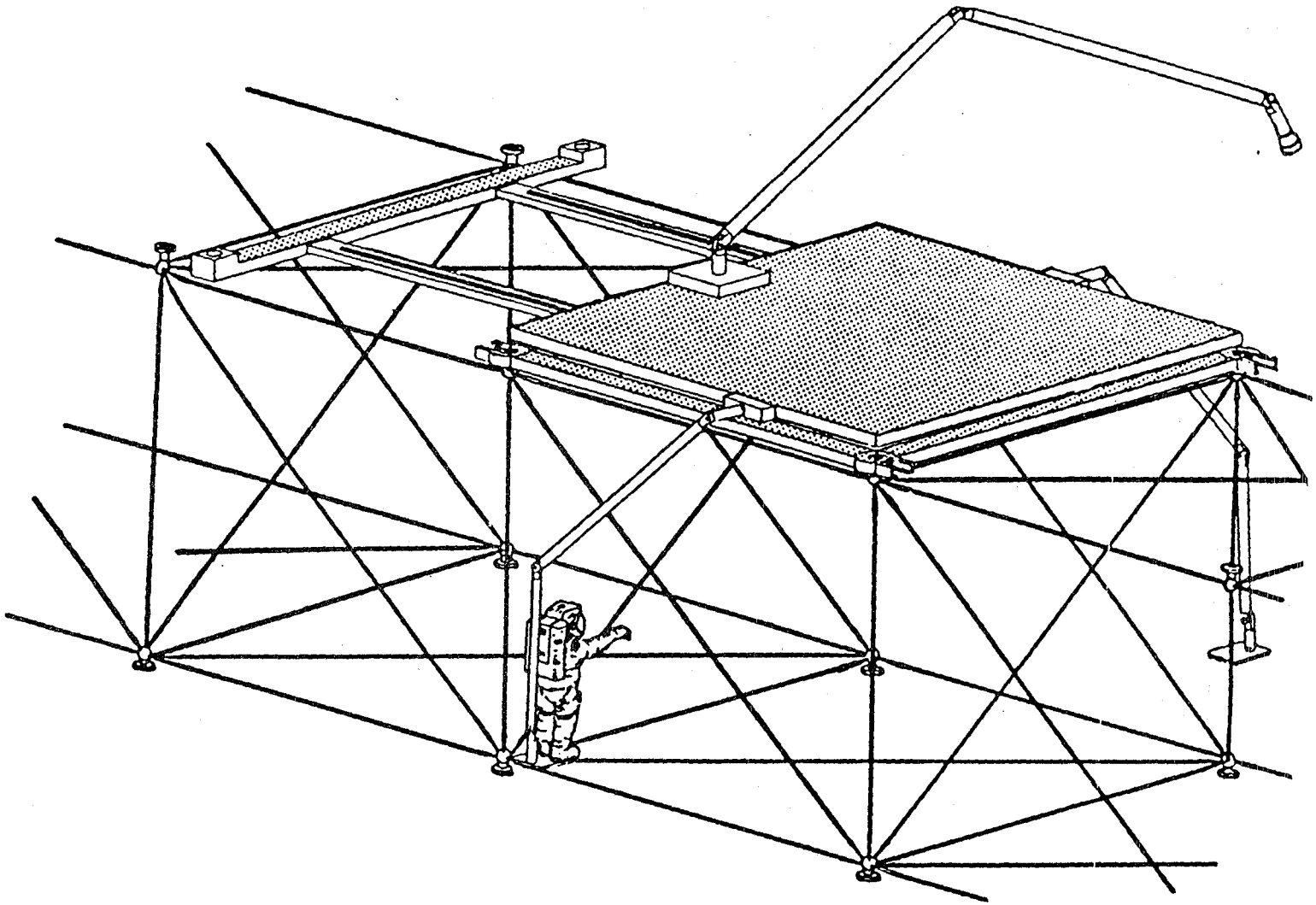

Figure 7.2.3-2 Mobile Remote Manipulator System (Reference 7-15)

the use of IVA tubing, the astronauts can move about the truss structure in a shirtsleeve work environment.

Mobile cranes will be utilized to aid the astronauts for the reassembly of the ATSS on orbit. These cranes are mobile remote manipulator systems that can be stowed for launch configuration and extended for service use on orbit. The cranes will be used for the assembly of the solar dynamic units, positioning and joining torus cylindrical sections to form the habitat torus, positioning of spokes to connect the central hub with the torus, and positioning the solar and celestial observatories (Figure 7.2.3-3).

Research scientific instruments ideally will be supplied to the ATSS as modules to be used inside the ATSS at prepared locations or in some instances, attached to the exterior of the ATSS. The nodes of the truss structure are convenient points for attachment of research instruments and experiments on the ATSS exterior (Figure 7.2.3-4) (Reference 7-16).

The orbital maneuvering vehicles (OMV) may be sized so that they can be transported within the cargo bay of either Shuttle I or II.

The OTVs will utilize large diameter aerobraking heat shields and thus may have to be delivered in sections to the ATSS and assembled in the berthing and assembly bay using the mobile remote manipulator systems. The OTV shown in Figure 7.2.3-5 is indicative of the size of the ceramic heat shield as compared to the six propellant tanks and the cylindrical module containing several astronauts (Reference 7-15).

Expended National Space Transportation System (NSTS) external tanks appear attractive for use as cryogenic fuel storage vessels. The weights and volumes of an external tank is shown in Figure 7.2.3-6

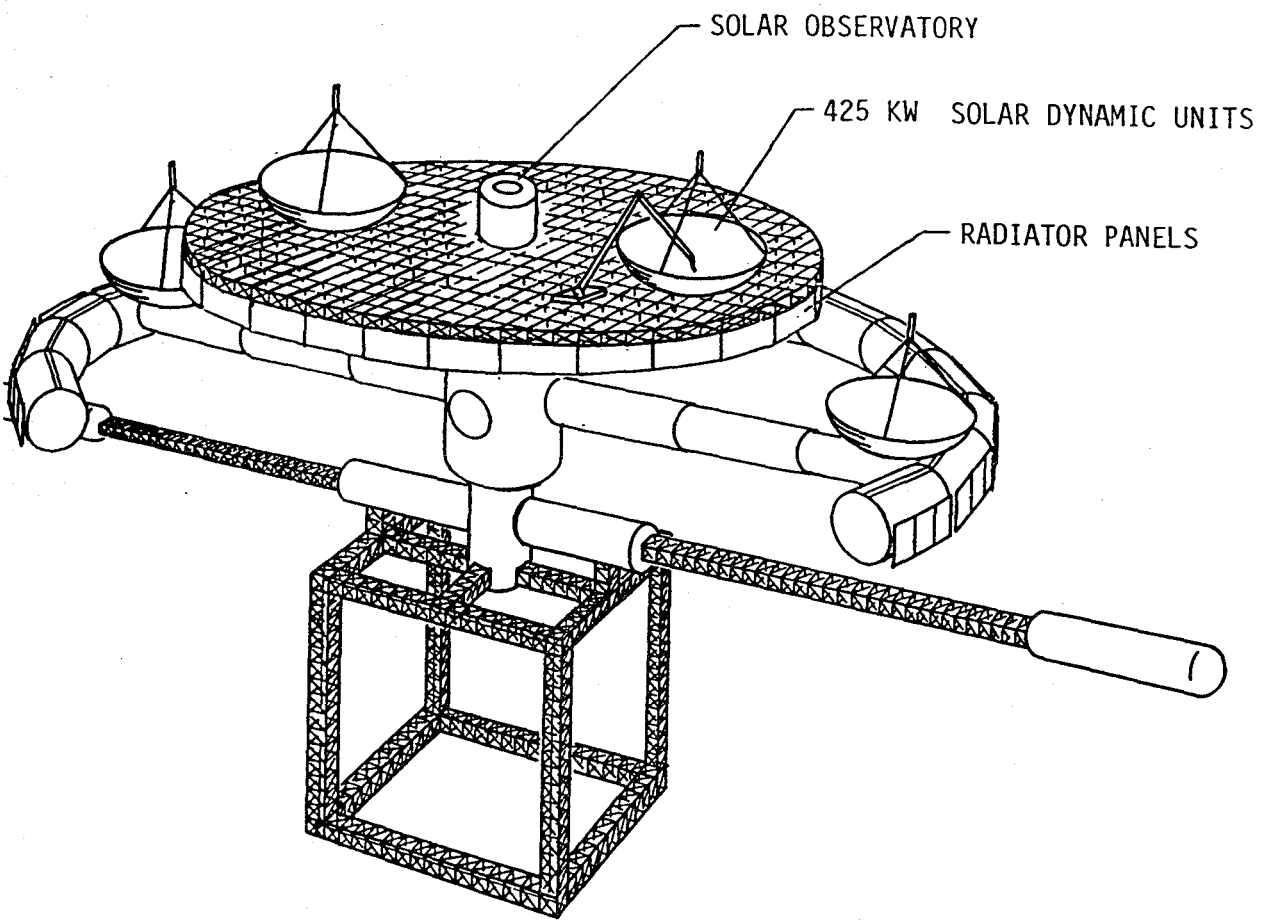

Figure 7.2.3-3 Four Solar Dynamic Units and Solar Observatory Installed Using Mobile Remote Manipulator System

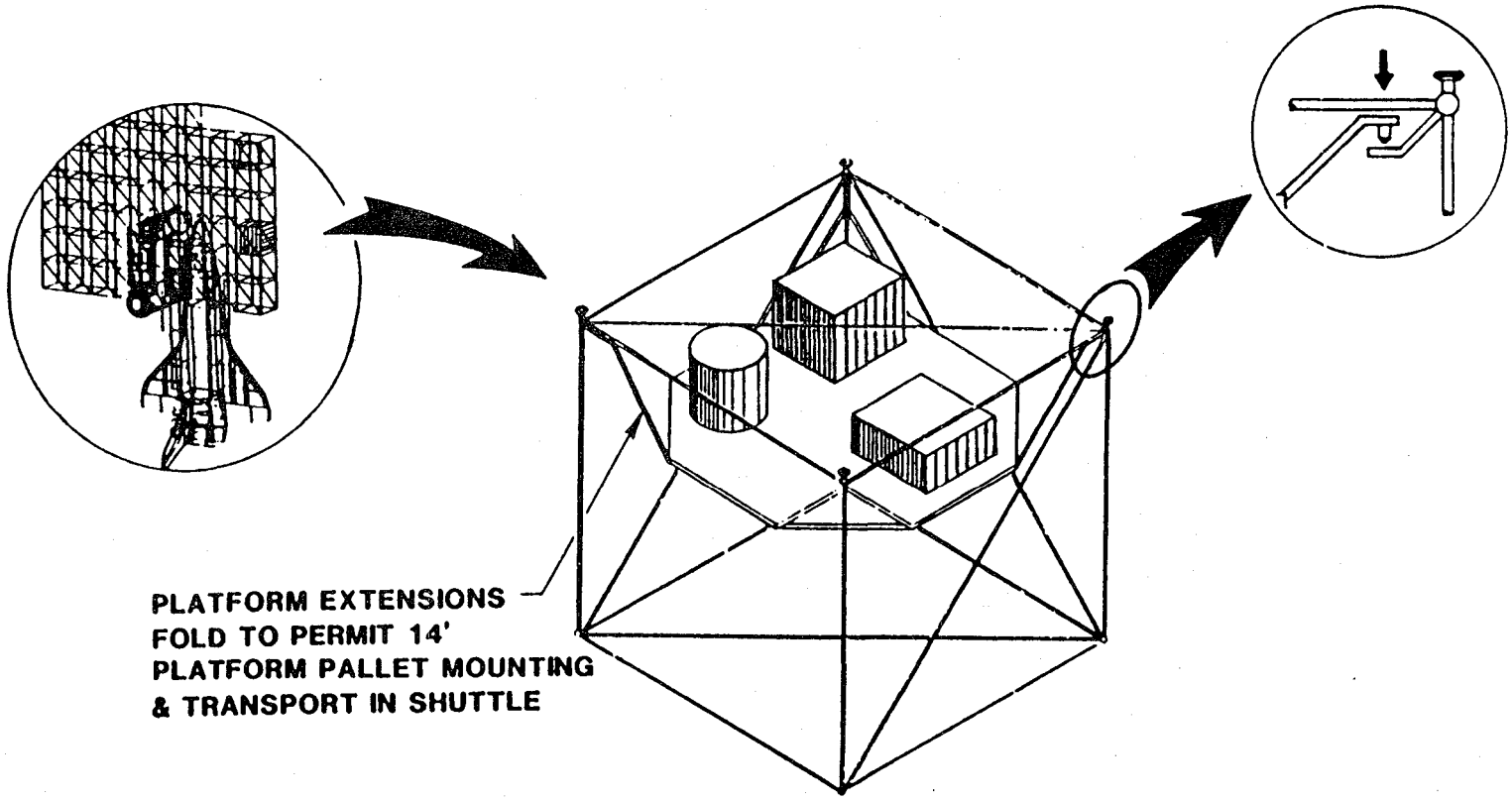

Figure 7.2.3-4 Schematic of a Shuttle/Station Pallet with Instruments of Small Experiments Attached (Reference 7-16)

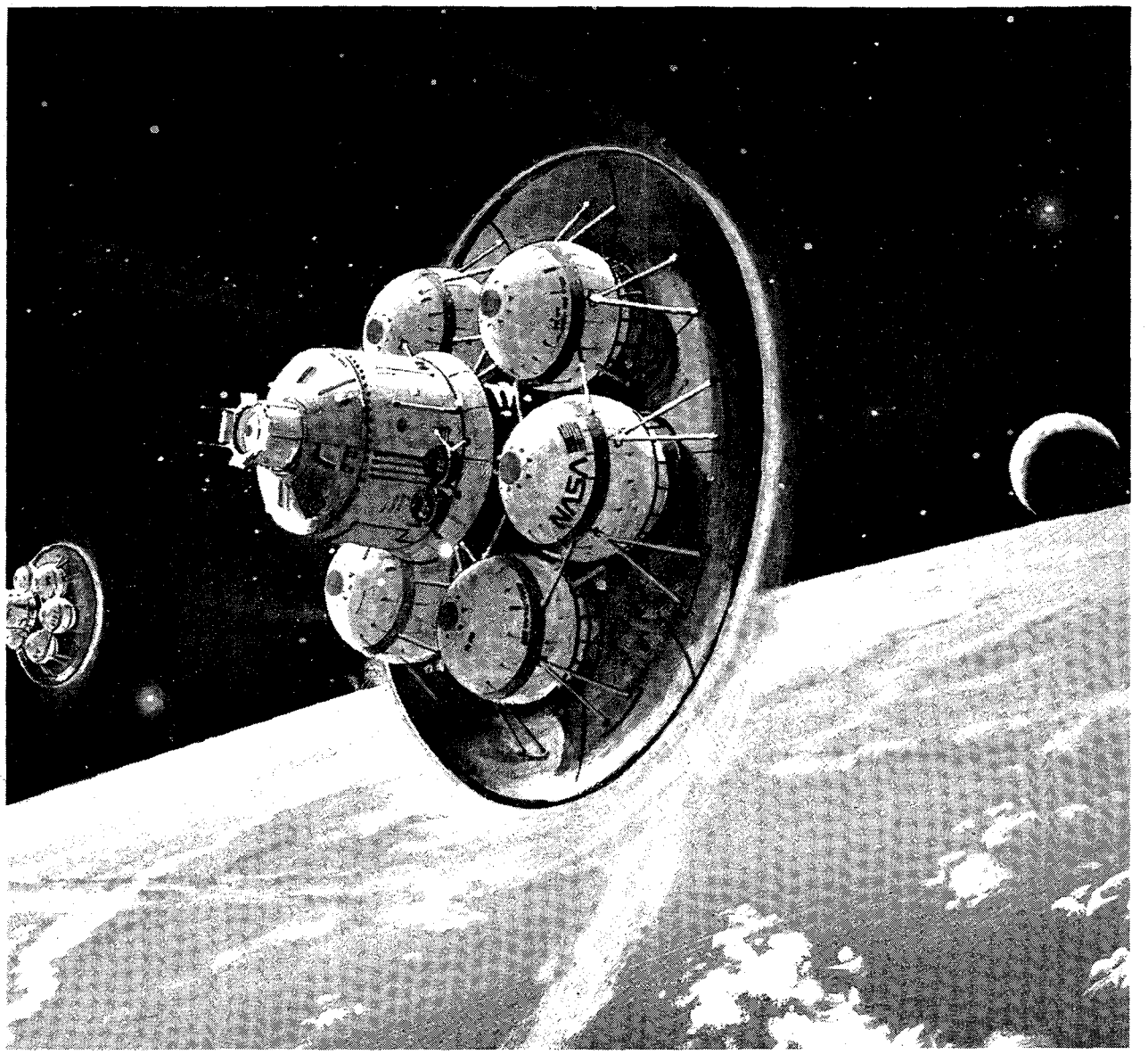

Figure 7.2.3-5 Orbital Transfer Vehicles Reentering the Earth's Atmosphere (Reference 7-15)

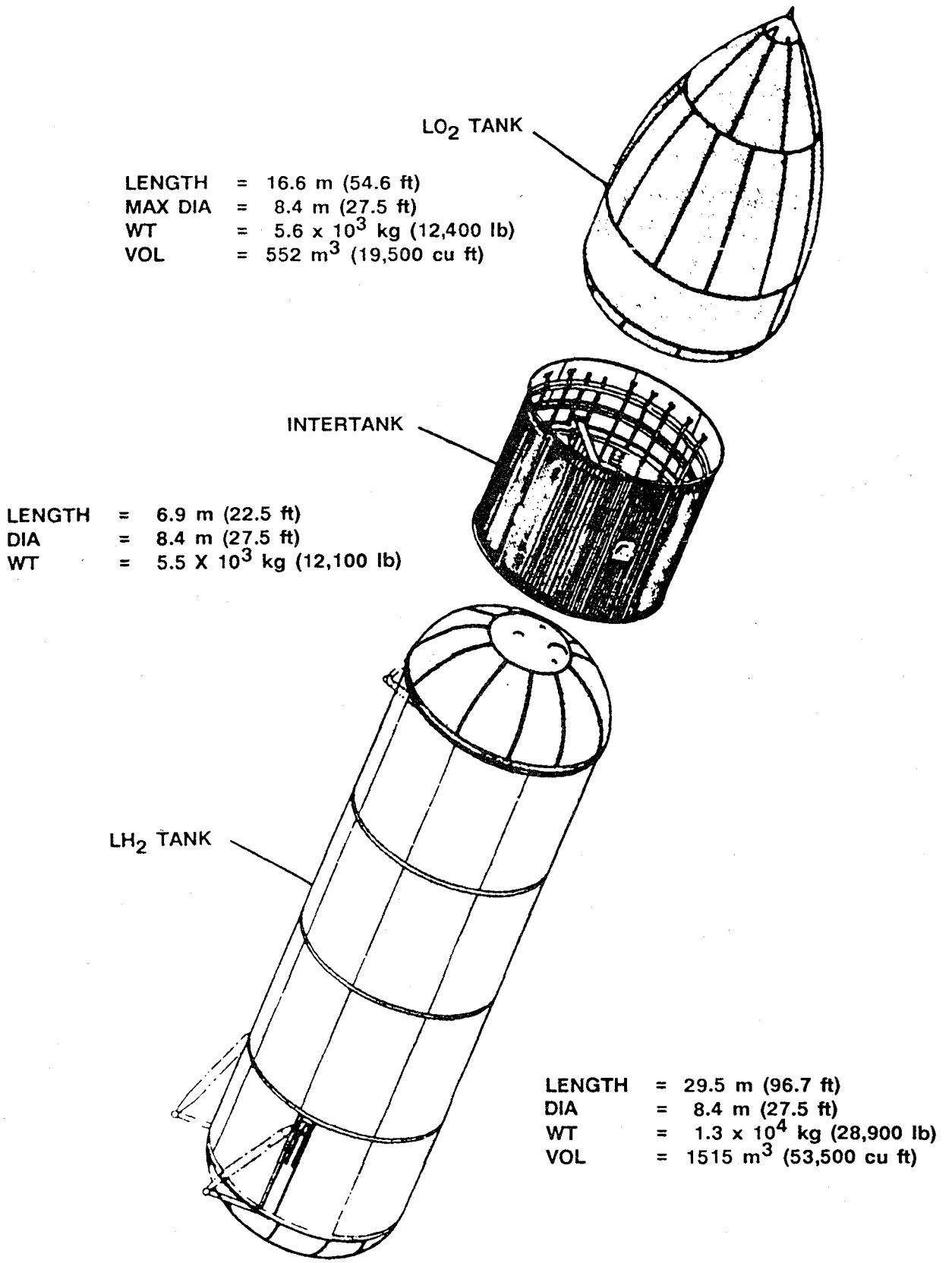

Figure 7.2.3-6 External Tank Structure (adapted from Reference 7-17)

(Reference 7-17). Studies have been made for use of the Shuttle external tank in LEO. One of the Mars reference missions will use about 10^6 kg (2.2 x 10^6 lb) of H_2 and O_2 as fuel/oxidizer for a round-trip to Mars as discussed in Section 9 of this report. One NSTS external tank is capable of containing 6.8 x 10^5 kg (1.5 x 10^6 lb) of fuel. The external tank is coated with a spray-on foam insulation of polyurethane resin. This material is known to outgas in space and is an undesirable cryogenic insulation for use in the vicinity of the ATSS. The tanks may well serve as efficient fuel storage depots if a low outgas insulation were substituted for the polyurethane foam and additional multilayer polyester film cryogenic insulation blankets were added to the tank's exterior on orbit.

The NSTS Shuttle has a cargo bay size of 4.57 m (15 ft) diameter by 18.29 m (60 ft) in length, thus limiting the size of payload that can be transported to LEO. The Shuttle maximum cargo weight per launch is limited to 2.95 x 10^4 kg (65,000 lb) ascent to LEO and 1.45 x 10^4 (32,000 lb) for descent to the Earth's surface. The Shuttle payload volume is normally the launch constraint rather than payload weight, thereby permitting the NSTS to have reserve payload lift capability along with contingency fuel for orbital insertion of the external tank attached to the Shuttle.

An add-on module has been evaluated that could be attached to the existing external tank design. The module has been named aft cargo carrier (ACC) and has a cargo size capacity of 8.38 m (27.5 ft) in diameter by 6.1 m (20 ft) in length. Several uses of the ACC are shown in Figure 7.2.3-7 (Reference 7-17). The ACC could be used to transport cryogenic tankage multilayer insulative blankets which could be placed

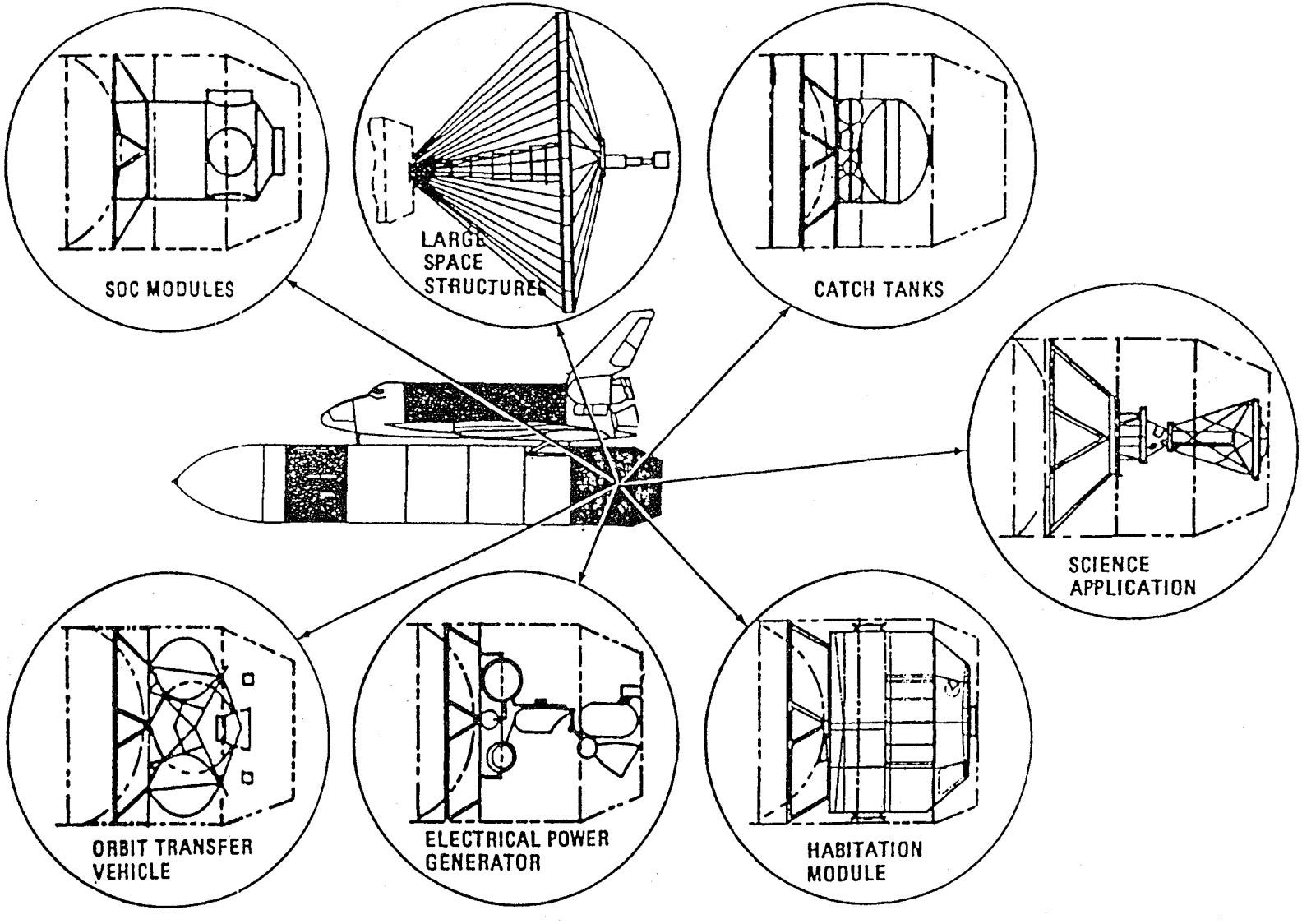

Figure 7.2.3-7 Potential ET Applications in Space Using an Aft Cargo Carrier (Reference 7-17)

about the external tank on-orbit using EVA to reduce cryogenic fuel boiloff. The boiloff rates of oxygen and hydrogen are indicated in Figure 7.2.3-8 (Reference 7-17). An effective conservation concept of liquid oxygen and hydrogen would utilize cryopumping to reconvert the cryogenic fuel vapors back to liquid form.

7.3 Manufacturing Aboard the ATSS

The ATSS will provide laboratory and pilot plant materials processing capabilities within the station's central tube. The effects of gravity can be studied in an environment ranging from weightlessness in the central tube to a pseudogravity equivalent of one Earth gravity in the torus. Experiment temperatures may range from cryogenic to high temperature and ambient pressure may range from hard vacuum to multiple atmospheres. Manufacturing and repair facilities will also be provided at two diametrically opposite locations within the torus. These manufacturing locations will have facilities and equipment to permit experiment modifications, checkout, and installation as well as on-board facilities for limited spacecraft repair. The life support system of the ATSS can provide propulsion fuel for use by the OMV, OTV, Lunar, and Mars mission spacecraft (Figure 7.3-1).

7.3.1 Materials Processing (Microgravity)

The central tube of the ATSS will have a microgravity materials processing facility located at the center of gravity of the Space Station. Experiments may be conducted within a canister which will free-float within the central tube during the critical experimental procedures. Station keeping, control dynamics, and crew motion should

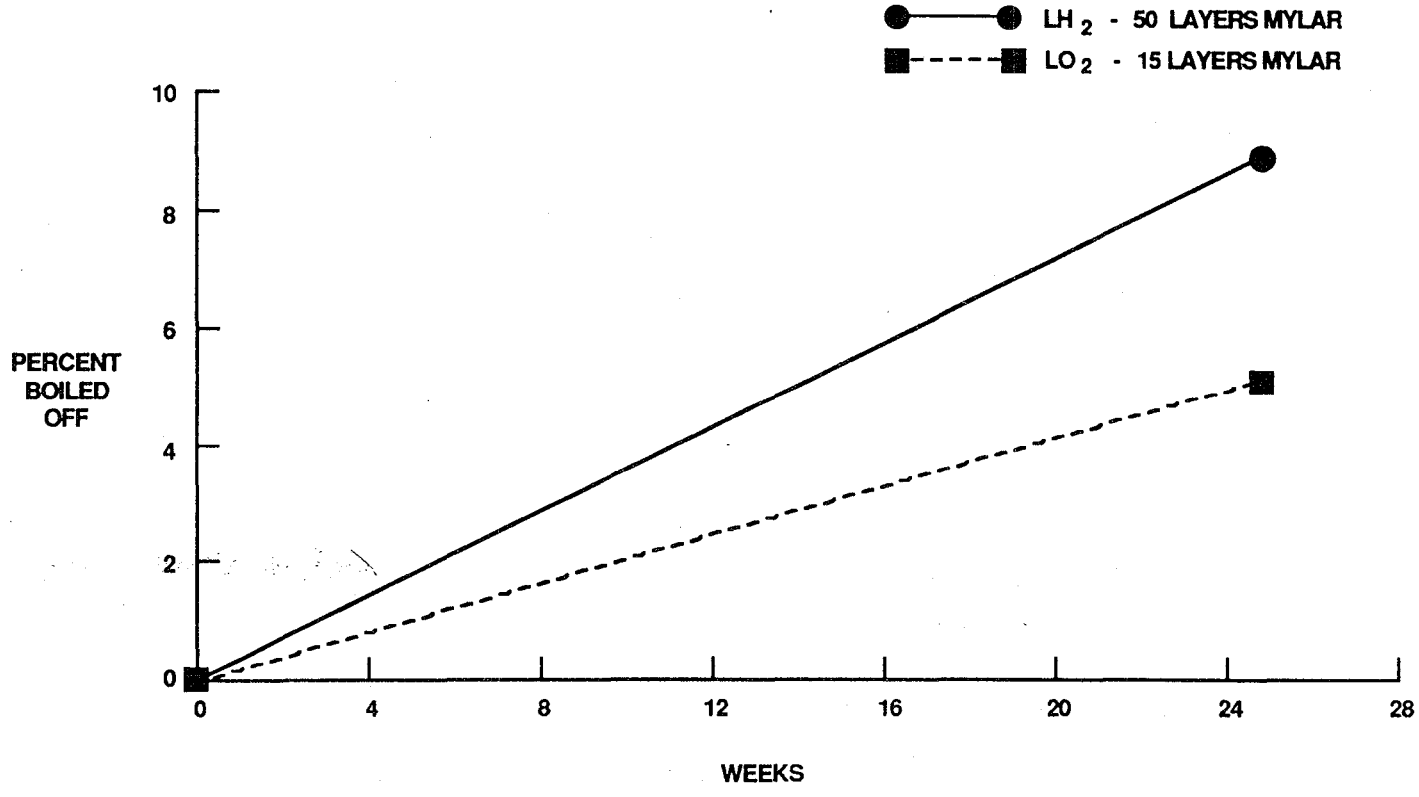

Figure 7.2.3-8 Cryogenic Boiloff Rates for LH_2 and LO_2
(adapted from Reference 7-17)

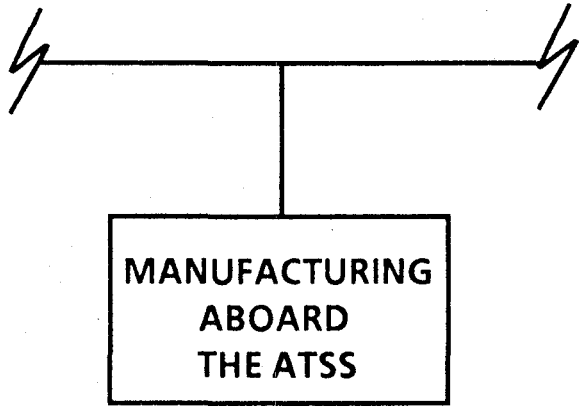

- **MATERIALS PROCESSING**
  (GRAVITY AND AMBIENT PRESSURE OPTIONS)
- **DAMAGE REPAIR**
- **EXPERIMENT MODIFICATIONS**
- **SPACECRAFT ASSEMBLY AND MAINTENANCE**
  - -- OTV
  - -- OMV
  - -- LUNAR MISSION
  - -- MARS MISSION
- **ON-BOARD FUEL MANUFACTURE**
  (10,000 LBS/DAY AT 1.25 MWe)

Figure 7.3-1 Manufacturing Aboard the Advanced-Technology Space Station

not influence the microgravity environment of the experiment within the canister. The experiment's control parameters will be monitored and recorded for interaction by the principal investigator. The materials processing facility should serve as a pilot plant for determining experiment parameters. Successful experiment results would encourage scaling up the materials processes for installing aboard a free-flying platform to achieve the highest product processing efficiency resulting from the pilot plant studies.

7.3.2 Manufacturing Facilities

The ATSS torus will have two manufacturing locations. One location will provide a plastics and composites fabrication facility adjacent to torus Spoke 2. A metals fabrication facility will be located diametrically opposite at Spoke 4. These two facilities will be provided to perform several functions aboard the ATSS (Figures 7.3.2-1, 7.3.2-2 and 7.3.2-3).

Typical functions are as follows:

- Preparation of experiments for positioning in the interior or onto the exterior of the ATSS.
- Repair of disabled experiments where simple functions such as solder repair or electronic circuit card change out may be accomplished.
- Basic maintenance of the Space Station components and hardware.
- Basic manufacturing and fabrication capabilities such as welding, flanging, riveting, and shaping of metals and nonmetals.
- Composites fabrication using autoclaves and ovens for thermal processing of fiber reinforced synthetic resins.

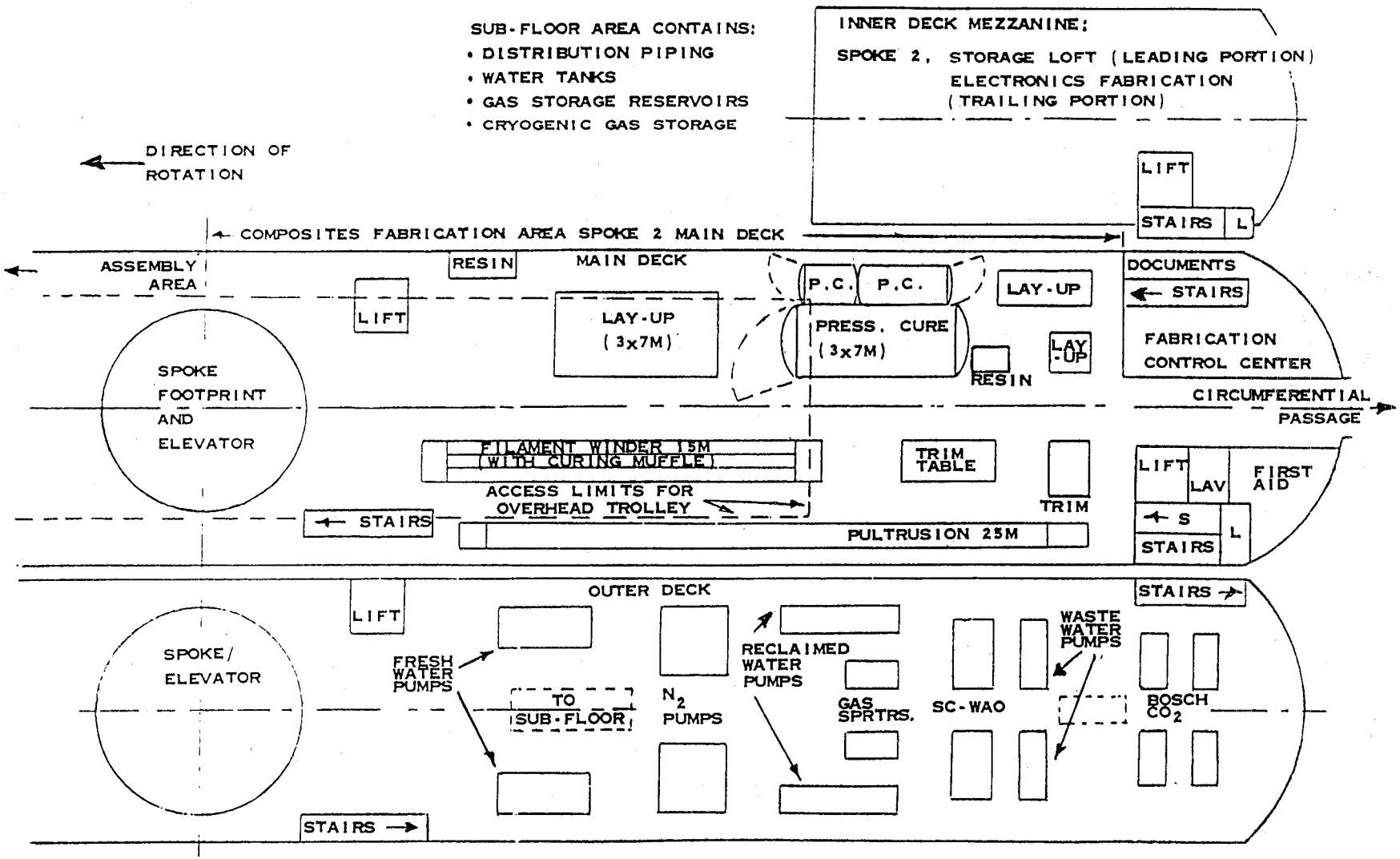

Figure 7.3.2-1 Functional Layout for the Areas at Spoke 2, Showing Composites Fabrication and Life Support (Reference 7-1)

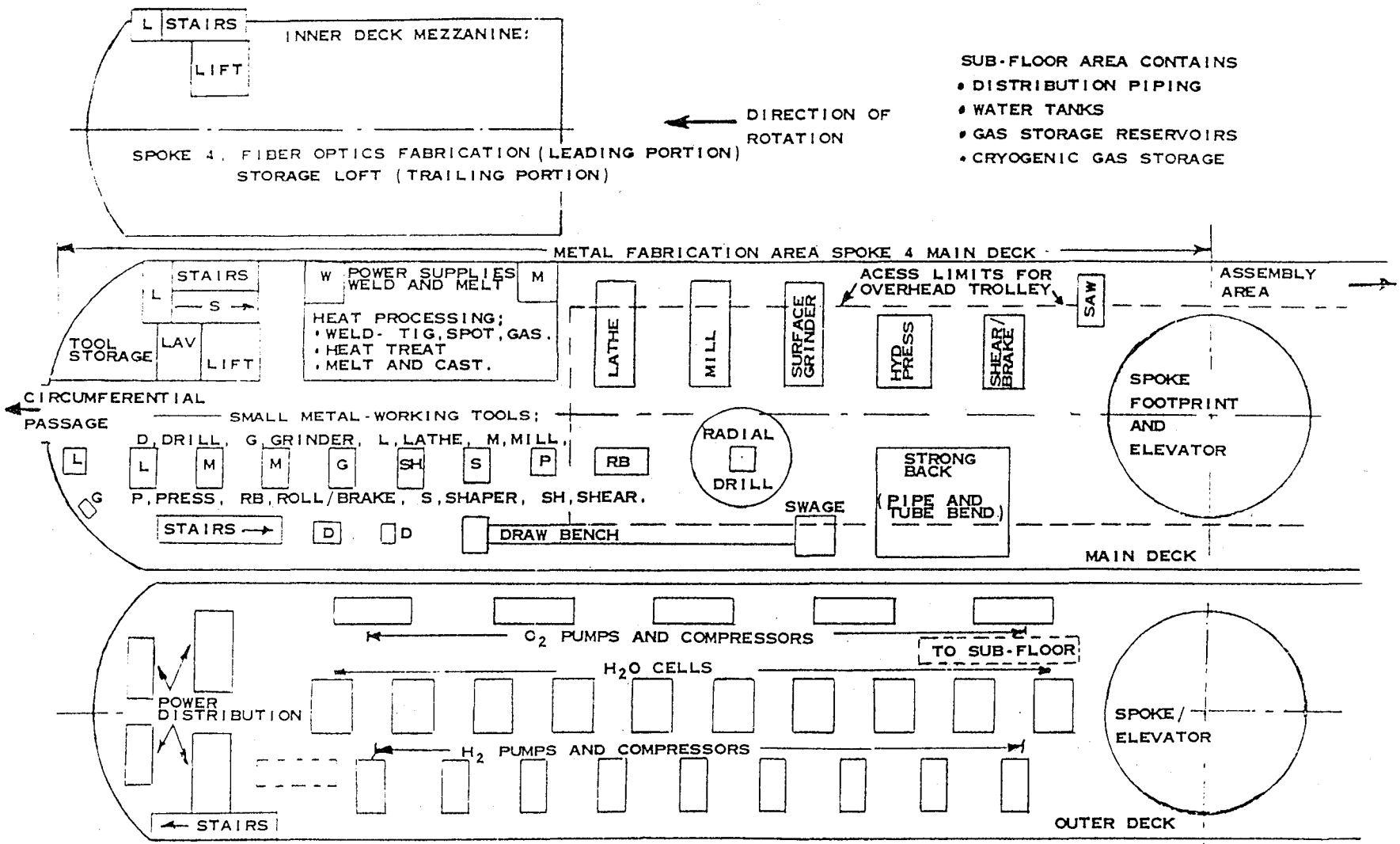

Figure 7.3.2-2 Functional Layout for the Areas at Spoke 4, Showing Metal Fabrication and Life Support (Reference 7-1)

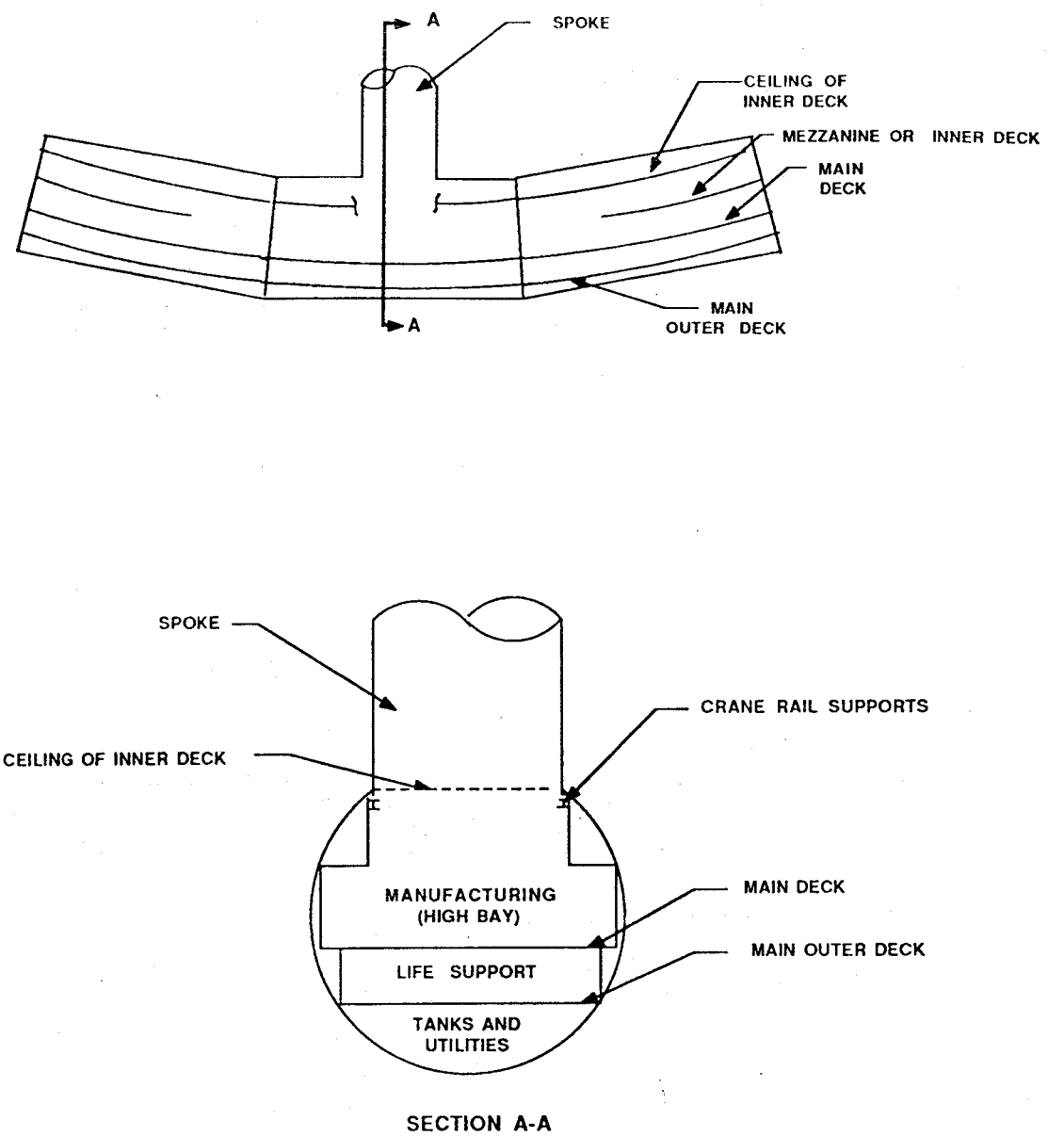

Figure 7.3.2-3 Cross Section of Torus near Spoke Locations 2 and 4

- o Adhesive bonding of metals and nonmetals.
- o Material shaping using such equipment as a drill press, shaper, milling machine and other metal removal methods.

The ATSS crew is sized for sixty people of which designated personnel are essential for continuous operation of the station and for monitoring its electrical power generation capabilities and distribution. The remaining personnel would consist of scientists, engineers and technicians with a skill mix to meet the needs of the current ATSS research and development activities. Normally, a limited number of manufacturing technicians may be aboard the ATSS at any particular time. Therefore, large manufacturing and fabrication undertakings may not be practical aboard the ATSS. Station equipment repair, maintenance, research experiment preparation, and experiment modification appear to be the logical uses of these facilities. Both of the torus manufacturing locations have redundant life support equipment for processing water into oxygen and hydrogen by electrolysis for generation of the cabin oxygen atmosphere and for hydrogen and oxygen fuel manufacture.

7.3.3 Experiment Modifications

It is anticipated that experiments will be supplied from Earth to the ATSS complete with spare parts to maintain a reliable functioning experiment. The principal investigator for the experiment and trained experiment technicians will be available to service the experiment module as required, utilizing the manufacturing facilities aboard the torus. It is planned that the torus will have a pseudogravity equivalent to approximately one Earth gravity; therefore, the more conventional

manufacturing processes may be conducted in this environment without modification.

7.3.4 Spacecraft Assembly and Maintenance

The utility of the ATSS will be greatly enhanced by the transportation architecture associated with transporting materials, personnel, and structures from Earth to LEO. Shuttles I and II, the aerospace plane, and HLLVs are contemplated for those purposes.

OMV will be transported from Earth to LEO aboard Shuttle I or II with the size restriction imposed by the diameter and length of the shuttle's cargo bays. Another option would be to transport the OMV in an ACC attached to an external tank as discussed in paragraph 7.2.3, whereby a structure up to 8.38 m (27.5 ft) in diameter by 6.1 m (20 ft) in length may be accommodated. The OMV (space tug) would be used during the collection and assembly of the various Space Station components in LEO and also used for a variety of applications in regards to maintenance and inspection activities during the life of the Space Station.

An OTV will have the capability to transport spacecraft from LEO to geosynchronous equatorial orbit (GEO) and return. The OTV will utilize aerobraking techniques when returning from higher orbits to LEO to minimize fuel usage. The aerobraking concept will utilize heat resistant ceramic heat shields which are large in diameter and may require on-orbit construction and refurbishment. The OTV will require refueling with hydrogen and oxygen at the ATSS. Personnel and spacecraft can be transferred from LEO to GEO and returned as required, thereby permitting retrieval of spacecraft for repair and modification at the ATSS for later return to GEO.

Lunar bases are anticipated as sites for manufacture of oxygen to support missions such as the Mars mission. The transport of personnel, equipment, and supplies from LEO to the surface of the Moon will be discussed in more detail in paragraph 7.4. The assembly of Earth supplied components of the lunar mission spacecraft will take place in the berthing and assembly bay of the ATSS utilizing remote manipulator systems as required. The manufacture of hydrogen and oxygen fuel for the lunar mission could be accomplished aboard the ATSS. Spacecraft returning from the Moon would employ aerobraking to conserve fuel.

The manned Mars mission will require construction of a large spacecraft in LEO using the berthing and assembly bay of the ATSS for the erection site. Complete functional checkout of the Mars spacecraft would occur while captive with the ATSS utilizing both on-board electronic checkout equipment as well as Earth based support capabilities. Fueling of the spacecraft could occur from on-board manufactured hydrogen and oxygen stored in a fuel storage depot for the Mars mission.

7.3.5 Fuel Manufacture

The ATSS will employ on-board fuel manufacturing capability, whereby, water transported from Earth to the ATSS will be electrolyzed to form hydrogen and oxygen. These gases will be liquified and stored as cryogenic fuel. For mission support, such as OTV flights or a Mars mission, the fuel will be manufactured in the torus of the spacecraft utilizing the life support machinery, pumps, and compressors to manufacture and liquify the gases. Storage of the liquified gases may utilize a fuel storage depot which will co-orbit with the ATSS or be tethered to it, as discussed in paragraph 7.2.2. The ATSS is capable of

manufacturing 4535 kg (10,000 lb) of fuel per 24 hour day, using 1.25 MW of electrical energy. The total power generation capability planned for the ATSS is 2.5 MW and there should be adequate reserve energy for ATSS operation, fuel manufacture, as well as the conduction of experiments in the central tube and torus. The fuel storage depot tankage would be insulated to minimize the boiloff of the cryogenic gases. A free-flying, co-orbiting fuel depot would require station keeping to maintain an orbital path similar to that of the ATSS. A direct fluid connection from the tank farm to the ATSS may be accomplished if the tank farm is tethered to the station, thereby, permitting reliquification of the hydrogen and oxygen boiloff gases.

7.4 Manufacturing at a Lunar Base Site

Lunar surface material samples were returned to Earth during the Apollo program and were representative of six Apollo lunar landing sites. The results of the laboratory analyses of these samples indicated that several elements could be separated from the lunar regolith. Oxygen, iron, aluminum, silicon, magnesium, titanium, and calcium are the seven most abundant lunar elements, and they vary in percentage depending on the sample retrieval sites. Nitrogen, water, and carbon sources were not identified. Researchers have hypothesized that permafrost several meters in depth may exist at the north and south poles of the Moon in deep, permanently shadowed craters along with clathrates of water that contain carbon dioxide, methane, argon, and other substances. It is anticipated that water ice at a surface temperature of 120 K (-244 ^{o}F) or below would be stable over the probable age of the Moon. A lunar polar orbiting prospector satellite equipped with a gamma-ray spectrometer and

electromagnetic sounder could determine if water ice exists in the crater depths of the lunar poles (Reference 7-18). Lunar ice would provide a valuable resource for O_2-H_2 rocket fuel, life support, and for chemical processing applications.

7.4.1 Transportation Energy Comparisons

There is interest in the use of materials available on the Moon's surface for the manufacture of liquid chemical propulsion fuels, lunar concrete for structures, glasses for structural composites, ionizing radiation shielding, and metals beneficiated from the lunar regolith as listed in Figure 7.4.1-1. The utilization of these materials will depend on the ability to efficiently process them at a lunar site or at a space manufacturing facility and to transport them to their end use location. The ATSS will be placed in LEO and the question must be addressed: Is it more efficient to manufacture products on Earth and transport them to LEO, or to manufacture products on the Moon and transport them to LEO? One study indicates that it takes seven times more energy to transport 1 kg (2.2 lb) from the Earth's surface to LEO than it does to transport 1 kg (2.2 lb) from the lunar surface to LEO (assuming that aerobraking is used to slow down the spacecraft returning from the Moon) (Reference 7-19).

The lunar regolith is comprised of over 40 percent of oxygen by mass. It appears logical that oxygen could be manufactured on the surface of the Moon at a suitable processing plant. The oxygen in liquified form could be placed in cryogenic canisters, each having a capacity of approximately 500 kg (1100 lb) of LO_2. A mass driver located on the Moon's surface could use electromagnetic acceleration to launch

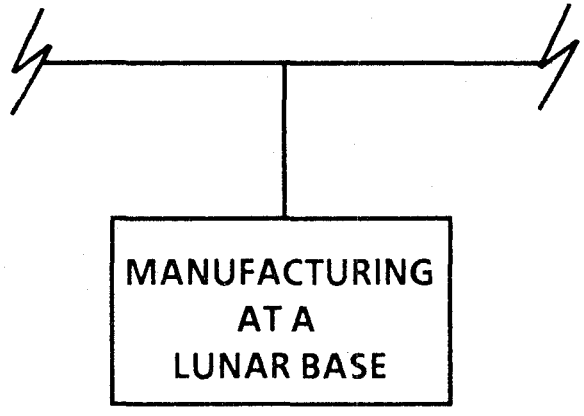

- **SHELTER** (LUNARCRETE OR CONCRETE)
- **MASS DRIVER**
- **500 kg O_2 CANNISTERS**
- **OXYGEN MANUFACTURE**
- **PERMAFROST HYPOTHESIZED AT LUNAR POLES**
- **GLASS FIBER REINFORCED GLASS MATRIX COMPOSITES**
- **METAL BENEFICIATION FROM LUNAR REGOLITH**
  - -- **IRON**
  - -- **ALUMINUM**
  - -- **SILICON**
  - -- **MAGNESIUM**
  - -- **TITANIUM**
  - -- **CALCIUM**
- **N2, H_2O AND C SOURCES ARE NOT VERIFIED**

Figure 7.4.1-1 Manufacturing at a Lunar Base

the canisters into space as shown in Figure 7.4.1-2. An orbiting spacecraft would capture and collect the canisters for transfer of LO_2 to a Earth-Moon transport tanker (Figure 7.4.1-3). The tanker would utilize aerobraking to deliver the LO_2 to LEO for use as the oxidizer of a hydrogen-oxygen fuel system (Figure 7.4.1-4). The hydrogen fuel required would comprise approximately 18 percent of the propellent mass and be supplied from Earth or manufactured aboard the ATSS (Reference 7-21). The economics of manufacturing and transporting oxygen from the Moon to LEO, versus oxygen and hydrogen electrolyzed from water transported from Earth to LEO requires further study.

7.4.2 Applications for Lunar Regolith Beneficiated Materials

A lunar base will require a shelter for use by personnel assigned for assembly of the mass driver and the robotic facilities to automate the manufacture of oxygen, the loading of canisters, and placing of canisters on the launcher. The astronaut's shelter could be made of concrete, since 95 percent of the mass of constituents required to formulate Portland cement are in plentiful supply on the Moon's surface. A 3-percent to 5-percent mass of cement additive (hydrated $CaSO_4$) must be supplied from Earth to control the setting properties of the concrete. Solar wind hydrogen that has been deposited in the lunar fines could be extracted and reacted with oxygen derived from the regolith to yield water. The Portland cement combined with aggregate and water would harden in place due to hydration reactions for the contained cement compounds (Reference 7-22). Another structural material "Lunarcrete", would require the regolith fines be compacted and fused using concentrated solar energy (Reference 7-23).

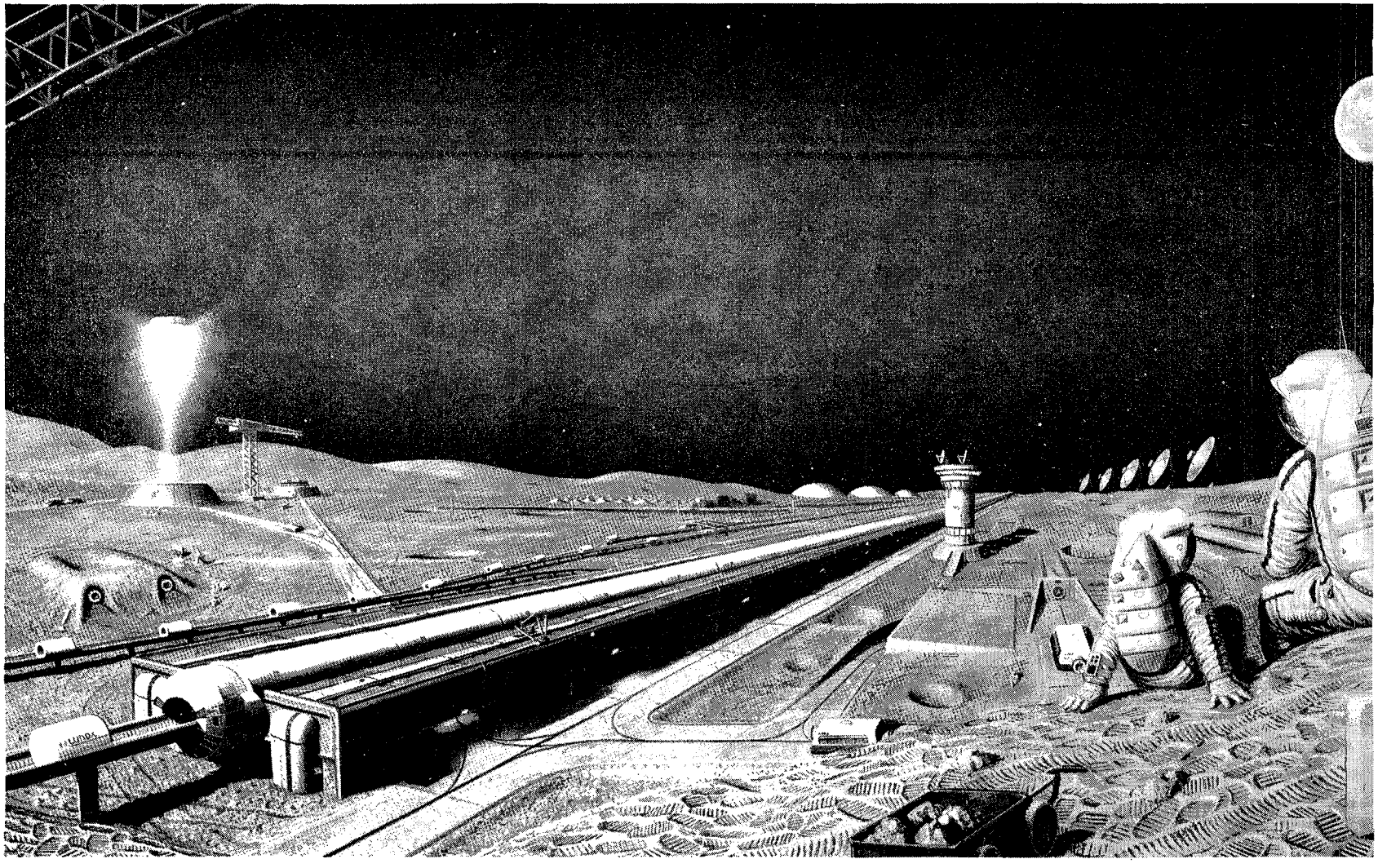

Figure 7.4.1-2 Mass Driver Lunar Launcher (MDLL) (Reference 7-20)

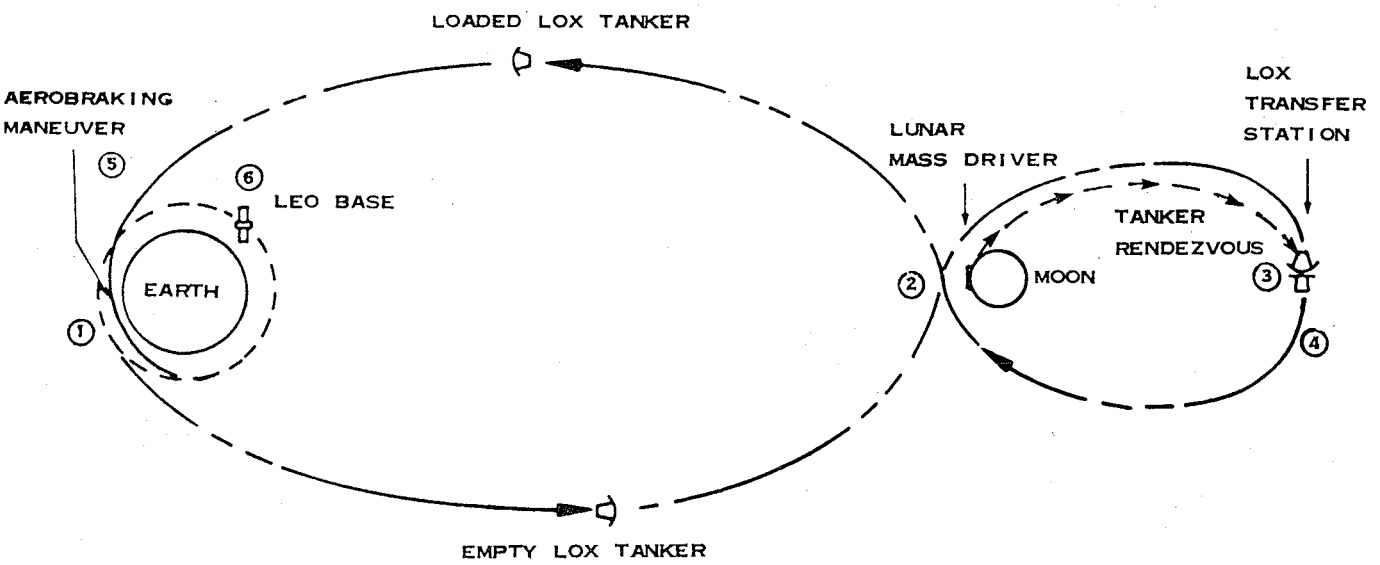

Figure 7.4.1-3 Lunar Oxygen Transportation Scenario
(adapted from Reference 7-21)

BURNOUT MASS = 4000 kg (8.8×10^3 lb)
OXYGEN CAPACITY = 40,000 kg (8.8×10^4 lb)
HYDROGEN CAPACITY = 1,500 kg (3.3×10^3 lb)
(4 TANKS)

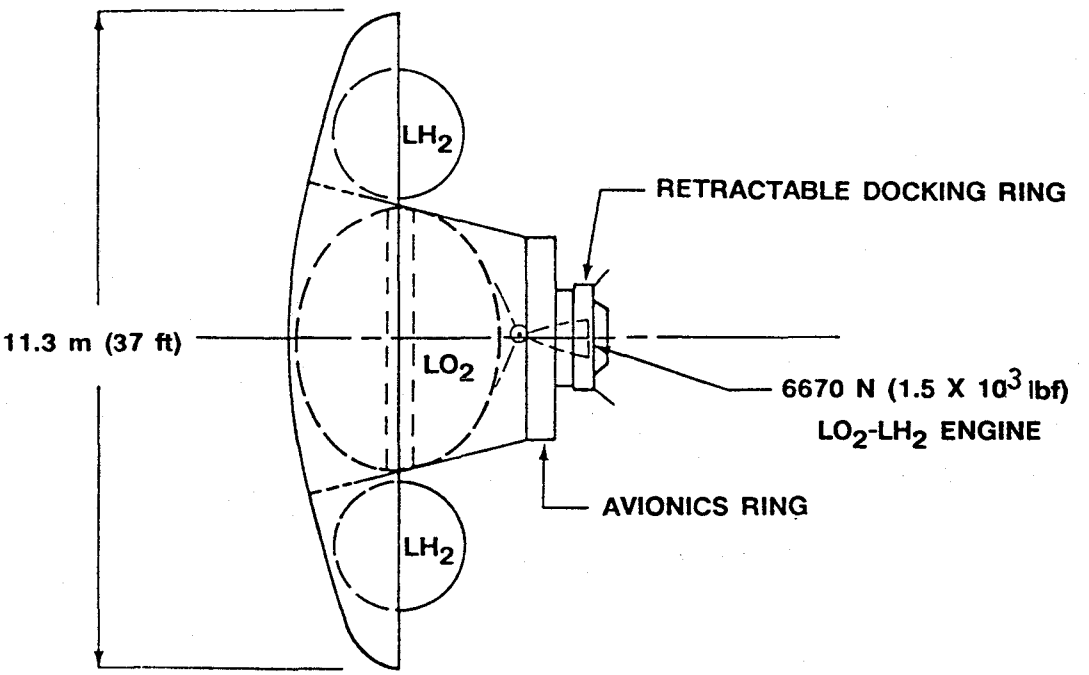

Figure 7.4.1-4 Aerobraked Oxygen Tanker (adapted from Reference 7-21)

Oxygen can be obtained from the lunar regolith using vapor phase pyrolysis at 2000 to 5000°C (3632 to 9032°F), hydrogen reduction, or by wet chemical processing as example processes. Iron meteorite fragments may be magnetically separated from the lunar regolith. Since manganese and carbon are not available on the Moon's surface, the iron cannot be made into a heat treatable, hardenable alloy. Carbon and manganese must be provided from sources other than the Moon (Reference 7-19).

The lunar regolith contains fiber producing feldspar and basalt and enriched blends of these materials could provide an equivalent of Earth's high strength S-glass fiber. A low fusing glass matrix could also be formulated so that glass fiber reinforced glass matrix composite laminates could be manufactured from lunar materials. The all glass structural composite offers a material of high strength, vacuum tight structure with a minimal offgas rate for much less energy expenditure than required for beneficiating, refining, and processing metals (Reference 7-24).

7.4.3 Mass Driver Lunar Launcher

The mass driver lunar launcher (MDLL) will be used to propel the canisters containing 500 kg (1100 lb) of liquid oxygen into space. The MDLL will be assembled on Earth, tested and then dismantled for transport to the Moon's surface for reassembly. The electrical energy to operate the MDLL will be derived from photovoltaic sources which receive direct sunlight for half of the Moon's rotation period of 28 days (Reference 7-21). Orbiting lunar mirrors have been proposed to provide reflected sunlight for continuous electrical power generation at the mass driver site. Locating the photovoltaic arrays at the lunar poles would provide

continuous sunlight for power generation. An alternate power source for a lunar base would use nuclear reactors.

7.4.4 500 kg Liquid Oxygen Canisters

Canisters containing 500 kg (1100 lb) of liquified oxygen would be transported from the lunar surface to an orbiting LO_2 transfer station spacecraft by the MDLL. The smart canisters would be guided by the orbiting spacecraft and the canister's path auto-corrected to allow being caught and stowed out of direct sunlight to minimize oxygen boiloff (Reference 7-21).

7.5 Manufacturing from Resources Obtained from Asteroids and Martian Moons

Earth-crossing asteroids and the Moons of Mars, Phobos and Deimos, are believed to contain various combinations of compounds of iron, carbon, water, nitrogen, nickel, cobalt, and precious metals as identified using reflectance spectroscopy. The reflectance spectra of the Martian moons and well over 100 asteroids have been measured (Figure 7.5-1) (Reference 7-25).

7.5.1 Asteroids in Earth Orbit about the Sun

Scientists have hypothesized that asteroids might revolve about the Sun in the Earth's orbital path but none have been detected to date. It has been proposed that a remote sensing satellite be placed in a smaller diameter orbit than the Earth's orbit about the Sun. The satellite's sensors would look away from the Sun and survey the entire orbital path of the Earth for detection of asteroids. The retrieval of asteroids in the Earth's orbital path could be accomplished at a minimum of energy

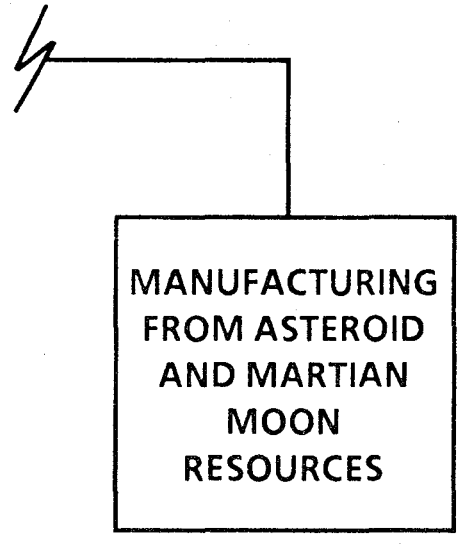

- ASTEROIDS MAY EXIST IN EARTH ORBIT ABOUT THE SUN
- PHOBOS AND DEIMOS MARTIAN MOONS
- ASTEROIDS AND MARTIAN MOONS CAN PROVIDE
  - -- CARBON
  - -- WATER
  - -- NITROGEN
  - -- NICKEL
  - -- COBALT
  - -- PRECIOUS METALS

Figure 7.5-1 Manufacturing from Asteroid and Martian Moon Resources

expenditure and would be a very attractive source for carbon, water, and other elements that might be available (Reference 7-15).

7.5.2 Earth-Crossing Asteroids

A number of asteroids have been detected whose orbital paths come near the Earth. Several of these asteroids have been selected based on their reflectance spectra as candidate sources of materials to be placed in high Earth orbit. The method proposed to capture a substantial mass of material from an asteroid in the Earth's gravitational field would be accomplished by diverting the material's orbital path using a propulsive method. Several orbits may be necessary for the asteroid material to be diverted to swing around Mars or Venus, the Earth-Moon system, and eventually orbit about the Earth (Reference 7-26). Robotic mining of asteroidal material in high Earth orbit could provide materials for in-space manufacture that are unavailable or impractical to process on the Moon.

7.5.3 Martian Moons

The moons of Mars, Phobos and Deimos, are believed to be rich in carbon compounds, nitrogen and water. Since water can be electrolyzed to form hydrogen and oxygen, and carbon can be combined with hydrogen to form a family of hydrocarbon products, many useful materials could be synthesized. A round-trip travel time from LEO to the moons of Mars may take up to two years but the energy expended to accomplish the mission is less than a lunar mission. Phobos orbits Mars at approximately 9.7×10^3 km (6,000 miles) altitude. Phobos could serve as a refueling depot for

Mars missions for topping off the spacecraft's fuel reserves for the return to LEO (Reference 7-27).

Initially, landed automated prospecting spacecraft could determine the availability of compounds of interest. Later, automated mining and processing facilities could be landed and utilized to manufacture propulsion fuels and beneficiate the ores of Phobos.

7.5.4 Processing Materials Predicted to Exist on Asteroids and the Martian Moons

Reflectance spectroscopic analysis has been employed to determine that carbon, nitrogen, water, nickel, cobalt, precious metals, and other materials may exist on Earth-crossing asteroids and Martian moons. The lunar surface samples returned by the Apollo astronauts provided us the opportunity to analyze the elements that existed on the Moon. Although we did not discover elements that were new to us, we have not developed Earth manufacturing processes to efficiently separate the elements from the compound forms discovered. More likely, this will be the case for materials to be processed from the asteroids and Martian moons. Therefore, new processing technologies will be required to efficiently provide a yield from these sources.

REFERENCES

7-1 Queijo, M. J. et al.: Analyses of a Rotating Advanced-Technology Space Station for the Year 2025. NASA CR178345, January 1988.

7-2 Marshall, William R.; and Shelton, Billy W.: Advanced Launch Vehicles. Space Systems Technology: Proceedings of the Aerospace Congress and Exposition (SAE SP-593), Long Beach, California, October 15-18, 1984.

7-3 Davis, Hubert P.: Earth-To-Orbit Transportation for Advanced Space Facilities. Space Manufacturing Facilities (Space Colonies): Proceedings of the Princeton/AIAA/NASA Conference, May 7-9, 1975.

7-4 Duft, B.L.: An Elastic Recovery Concept for Expandable Space Structures, Narmco Research and Development - A Division of Telecomputing Corporation. Aerospace Expandable Structures Conference Transaction, AF Aero Propulsion Laboratory, October 1963.

7-5 Cordier, Kenneth L.; and Cross, William B.: Materials Technology Advancement Program for Expandable Manned Space Structures, Goodyear Aerospace Corporation, Akron, Ohio, NASA CR66949, August 1970.

7-6 Stenlund, S.J.: PAGEOS Fabrication Accuracy and Reliability. Third Aerospace Expandable and Modular Structures Conference. AF Aero Propulsion Laboratory - TR 68-17, May 1967.

7-7 Design Criteria and Structural Parameters, Section 3. Expandable Structures Design Handbook. AF Materials Laboratory, ASD-TDR-63-4275, Part II, June 1965.

7-8 Schwartz, S.; Jones, R.W.; and Keller, L.B.: Ultraviolet and Heat Rigidization of Inflatable Space Structures, Hughes Aircraft Company. Aerospace Expandable Structures Conference Transaction, AF Aero Propulsion Laboratory, October 1963.

7-9 Contraves Develops Space - Rigidizing Concept. Aviation and Space Technology Week, October 6, 1986.

7-10 Younger, D.G.: The Shape of Things to Come in Expandable Spacecraft. Aerospace Expandable Structures Conference Transaction, AF Aero Propulsion Laboratory, October 1963.

7-11 Manning, L.: Mechanically Mixed Polyurethane Foam - Rigidized Solar Collectors, Goodyear Aerospace Corporation. Aerospace Expandable Structures Conference Transaction, AF Aero Propulsion Laboratory, October 1963.

7-12 Weber, E.A.: Self-Deploying Space Station. Aerospace Expandable Structures Conference Transaction, AF Aero Propulsion Laboratory, October 1963.

7-13 Belew, L.F., Editor: Skylab, Our First Space Station. NASA SP-400, 1977.

7-14 Bandaruk, W.; Younger, D.G.; and Quackenbush, N.E.: Telescoping Pressurized Structures and Seals. Aerospace Expandable Structures Conference Transaction, AF Aero Propulsion Laboratory, October 1963.

7-15 Pioneering the Space Frontier. The Report of the National Commission on Space, Bantam Books, May 1986.

7-16 Deployable/Erectable Trade Study for Space Station Truss Structures. NASA Technical Memorandum 87573. Langley Research Center, July 1985.

7-17 Gimarc, J. Alex: Report on Space Shuttle External Tank Applications. Space Studies Institute, December 1, 1985.

7-18 Staehle, Robert L.: Finding "Paydirt" on the Moon and Asteroids. Jet Propulsion Laboratory, NASA Grant NAS7-918, 1983.

7-19 Carroll, W.F.; Steurer, W.H.; Frisbee, R.H.; and Jones, R.M.: Should We Make Products on the Moon? Jet Propulsion Laboratory. Reprint from Astronautics and Aeronautics, June 1983.

7-20 Mendell, W.W., Editor: Lunar Bases and Space Activities of the 21st Century. Book Cover.

7-21 Andrews, D.G.; and Snow, W.R.: The Supply of Lunar Oxygen to Low Earth Orbit. Proceedings of the Fifth Princeton/AIAA Conference, Space Manufacturing 4, May 18-21, 1981.

7-22 Agosto, William N; and Gadalla, Ahmed M.M.: Lunar Cement Formulations for Space Systems Shielding and Construction. Proceedings of the Seventh Princeton/AIAA/SSI Conference, Space Manufacturing 5. Engineering with Lunar and Asteroidal Materials, May 8-11, 1987.

7-23 Beyer, Larry A.: Lunarcrete, A Novel Approach to Extraterrestrial Construction. Proceedings of the Seventh Princeton/AIAA/SSI Conference, Space Manufacturing 5 Engineering with Lunar and Asteroidal Materials, May 8-11, 1987.

7-24 Goldsworthy, W. Brandt: Composites, Fibers and Matrices from Lunar Regolith. Proceedings of the Seventh Princeton/AIAA/SSI Conference, Space Manufacturing 5 Engineering with Lunar and Asteroidal Materials, May 8-11, 1987.

7-25 Gaffey, Michael J.; and McCord, Thomas B.: Mining Outer Space. Space World, March 1979.

7-26 Bender, David F.: The Lunar Capture Phase of the Transfer of Asteroidal Material to Earth Orbit by Means of Gravity Assist Trajectories. British Interplanetary Society Journal, Volume 41, March 1987, pages 129-132.

7-27 O'Leary, Brian: Phobos and Deimos (PhD): Concept for an Early Human Mission for Resources and Science. Proceedings of the Seventh Princeton/AIAA/SSI Conference, Space Manufacturing 5. Engineering with Lunar and Asteroidal Materials, May 8-11, 1985.

8.0 SOME EFFECTS OF INTERNAL PRESSURE AND OXYGEN-NITROGEN RATIO

Scientists have expressed a desire that the atmosphere of the IOC Space Station be a standard Earth atmosphere of 101.3 kPa (14.7 psia) to allow comparison of results of space conducted scientific experiments with results of experiments conducted on Earth. A standard Earth atmospheric pressure is being considered for the habitable areas of the Advanced-Technology Space Station (ATSS). The internal atmospheric pressure within the torus habitats, spokes, and central tube of the ATSS is being studied for effects on personnel, prebreathing requirements for EVA, ignition and flammability characteristics of materials, and the influence of internal pressure on the weight of the pressure confining shell structure. A report indicating the results of the study to date is presented below.

8.1 Physiological Effects Caused by Varying the Partial Pressure of Oxygen

A normal Earth atmospheric composition at sea level consists of 78 percent nitrogen, 21 percent oxygen and approximately 1 percent of other gases. The partial pressure of oxygen at sea level is 21.2 kPa (3.1 psia). When atmospheric air enters the lungs, it saturates with water vapor and exchanges some of its oxygen for carbon dioxide before expiration. Therefore, the partial pressure PO_2 of oxygen within the lung is reduced to 13.7 kPa (1.9 psia). The difference in the partial pressure of oxygen in the air and in the lung are shown in Figure 8.1-1 (Reference 8-1).

The National Space Transportation System (NSTS) Shuttle Orbiter space suit is designed to operate with an internal atmosphere of pure oxygen. The suit pressure is maintained at 29.6 kPa (4.3 psia) during

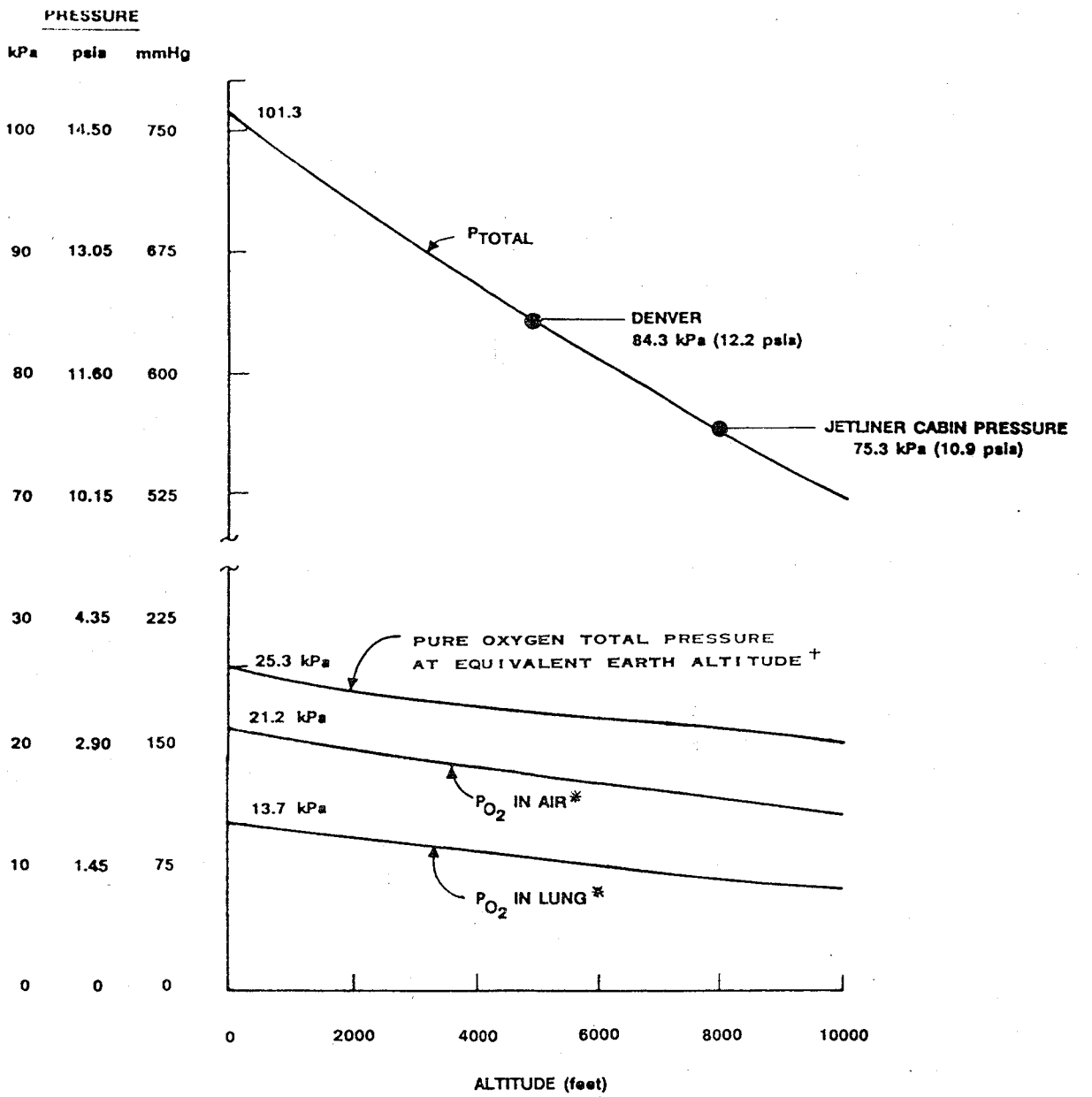

Figure 8.1-1 Partial Pressure of Oxygen in Air and Lung versus Altitude (Reference 8-1* and 8-2+)

EVA. This pressure assures that the sum of the partial pressures of oxygen, water vapor, and carbon dioxide in the astronaut's lungs are balanced by the suit's atmosphere and exceed the minimum pressure of oxygen for sea level air equivalent, as indicated in Figure 8.1-2 (Reference 8-2).

The total pressure of pure oxygen in the space suit can be correlated with an equivalent Earth altitude as shown in Figure 8.1-1. The curve represents the addition of the partial pressures of water vapor and carbon dioxide to the partial pressure of oxygen in the lung. The astronaut will experience the effects of working at altitude when the suit oxygen pressure is reduced to less than 25.3 kPa (3.7 psia) (Reference 8-2).

If the Orbiter cabin pressure is reduced, the partial pressure of oxygen will also be proportionately reduced causing the astronaut to tire more easily when performing tasks. An example of reduced cabin pressure would be flying aboard a jet liner whereby the ambient pressure is reduced to the equivalent of an 8,000 ft altitude and the partial pressure of oxygen in the lung would be reduced from 13.7 to 9.2 kPa (1.9 to 1.3 psia). This reduction in the partial pressure of oxygen would effect the astronaut in the same manner as if he were performing tasks atop an 8,000 ft mountain. Ideally, the astronaut should not be subjected to a partial pressure of oxygen in the lung less than 11.4 kPa (1.7 psia) which is an Earth altitude equivalent of 4,000 ft.

In preparation for EVA from the Shuttle Orbiter, the prebreathing protocols maintain or exceed the minimum partial pressure of oxygen within the lungs of the astronaut. During the initial depressurization period to 70.3 kPa (10.2 psi) in the cabin of the Orbiter, the entire

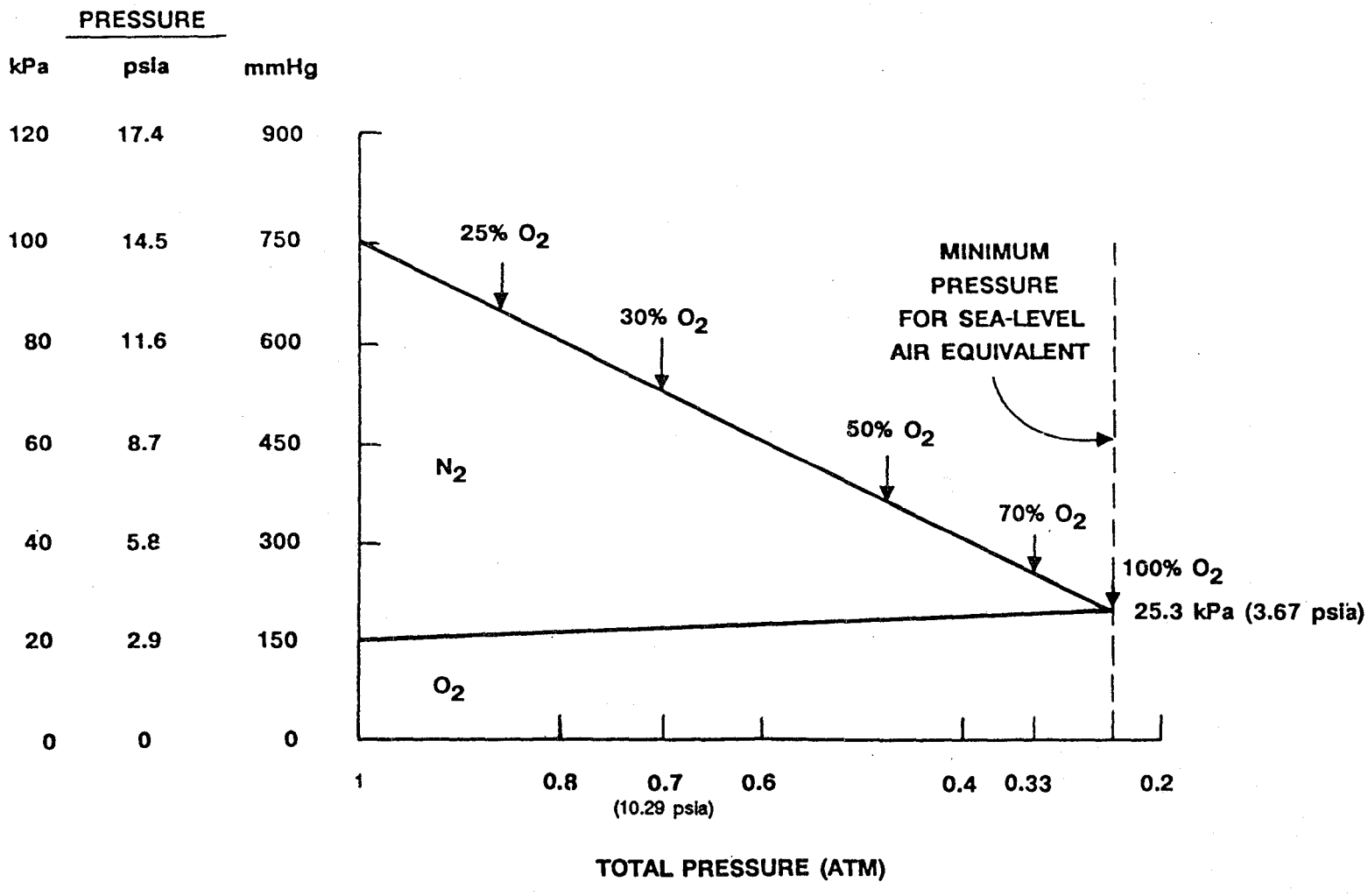

Figure 8.1-2 Composition of Oxygen-Nitrogen Mixtures Equivalent to Sea-Level Atmosphere as a Function of Total Pressure (Reference 8-2)

crew experiences an oxygen enriched atmosphere with the oxygen partial pressure equivalent to a 4,000 ft Earth altitude. These conditions have been determined adequate for normal healthy people to perform their duties quite efficiently.

The underlying concepts for protecting astronauts from altitude decompression sickness when varying the total ambient pressure in the spacecraft or space suit is achieved by the following methods (Reference 8-3):

- The partial pressure of oxygen in the lungs would ideally be maintained in the range of pressures from sea level air equivalent to a 4,000 ft altitude.
- The nitrogen pressure in the tissue/ambient pressure ratio would not exceed 1.65 during denitrogenation procedures for planned Orbiter operations and existing space suit working pressures.

8.2 Spacecraft Atmospheric Composition and Prebreathe Protocols for EVA

Early manned space flight used an approximate one-third Earth atmosphere pressure of 34.5 kPa (5 psia) pure oxygen as the internal atmosphere within the space capsules of projects Mercury, Gemini, and Apollo. Note in Figure 8.1-2 that the minimum pressure for sea level air equivalent for 100 percent oxygen is 25.3 kPa (3.7 psia) or about one-fourth Earth atmosphere. The Skylab workshop also contained an internal pressure of one-third of an Earth atmosphere but with a composition of 70 percent oxygen and 30 percent nitrogen. The Skylab atmospheric pressure of 0.33 standard atmosphere is indicated for reference purposes. Voice communications aboard Skylab were very difficult since atmospheric sound transmission was limited to approximately 5 m (16 ft) (Reference 8-2).

The NSTS Shuttle Orbiter has used a standard atmosphere of 101.3 kPa (14.7 psia) within the cabin for atmospheric flight and orbital operations. The EVA space suits developed for Gemini, Apollo, Skylab and the Shuttle Orbiter have all utilized pure oxygen as the breathing atmosphere within the suit. The Shuttle Orbiter space suit is operated at an internal pressure of 29.6 kPa (4.3 psia). Before EVA, the astronaut must prebreathe pure oxygen using one of the sequences shown in the Figures 8.2-2 through 8.2-4 which represent standard, modified, and rapid prebreathing requirements. Each of these prebreathing procedural requirements are designed to minimize the possibility of the astronaut having altitude decompression sickness or the "bends" (Reference 8-3). Figures 8.2-2 and 8.2-3 indicate that a staged depressurization occurs prior to EVA to assure adequate denitrogenation of the crew and EVA astronaut. In the standard and modified prebreathing requirements, the entire crew undergoes a depressurization from 101.3 kPa (14.7 psia) to 70.3 kPa (10.2 psia) by breathing pure oxygen during a one hour cabin depressurization. The reduced pressure cabin atmosphere is enriched to 27 percent oxygen nominal content such that the partial pressure of oxygen would be equivalent to that found on Earth at a 4,000 ft altitude.

The standard prebreathing requirement conditions the Orbiter crew and EVA astronaut in the reduced pressure cabin atmosphere for 24 hours prior to commencing EVA. The EVA astronaut would then don his space suit, enter the air lock and breathe pure oxygen for 40 minutes in the space suit followed by a depressurization to 29.6 kPa (4.3 psia) in 20 minutes. At this point, the astronaut would exit the air lock and perform EVA for a limited time period of 6 to 8 hours before reentering

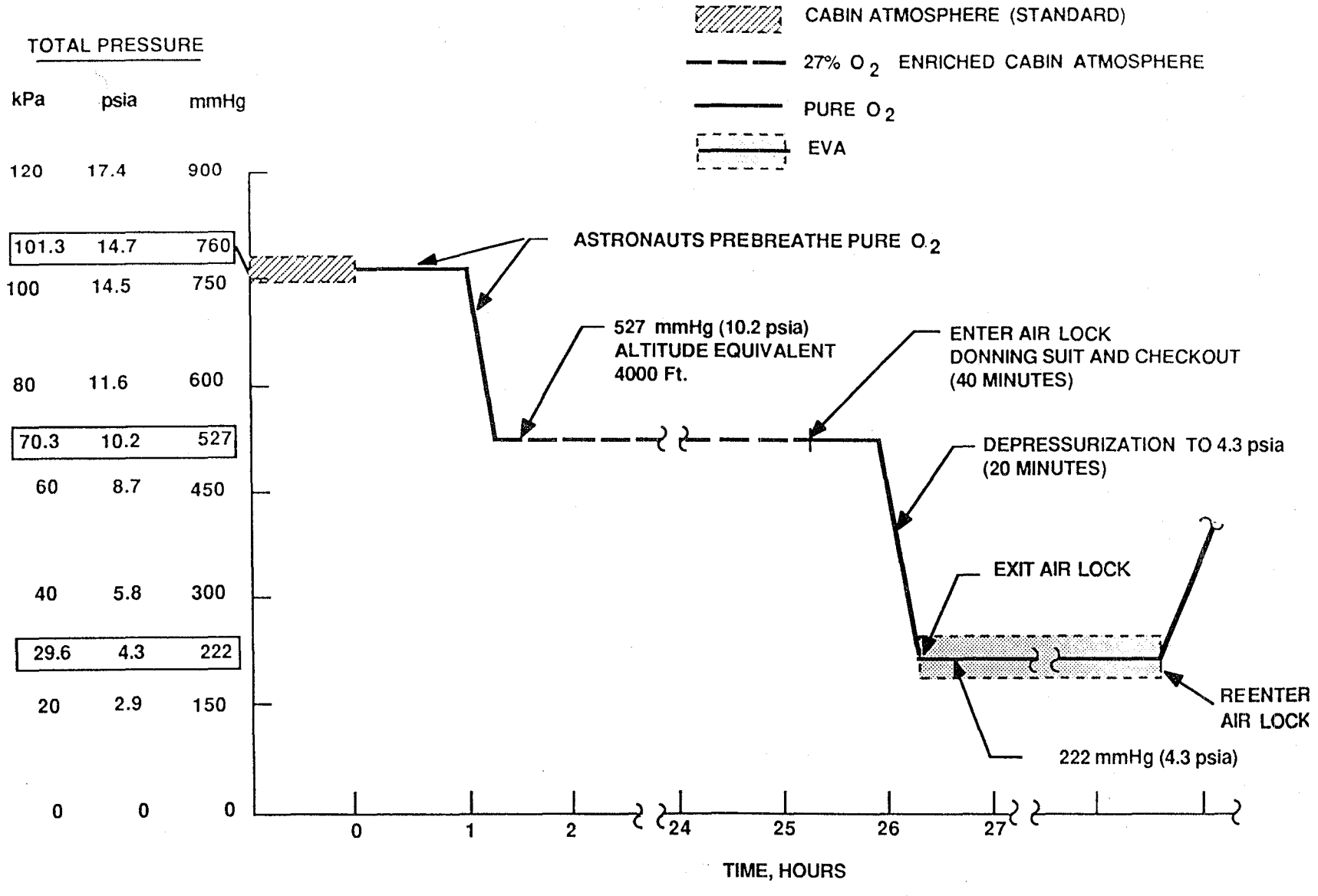

Figure 8.2-2 Standard Prebreathing Requirements for EVA (NSTS Astronaut) (Reference 8-3)

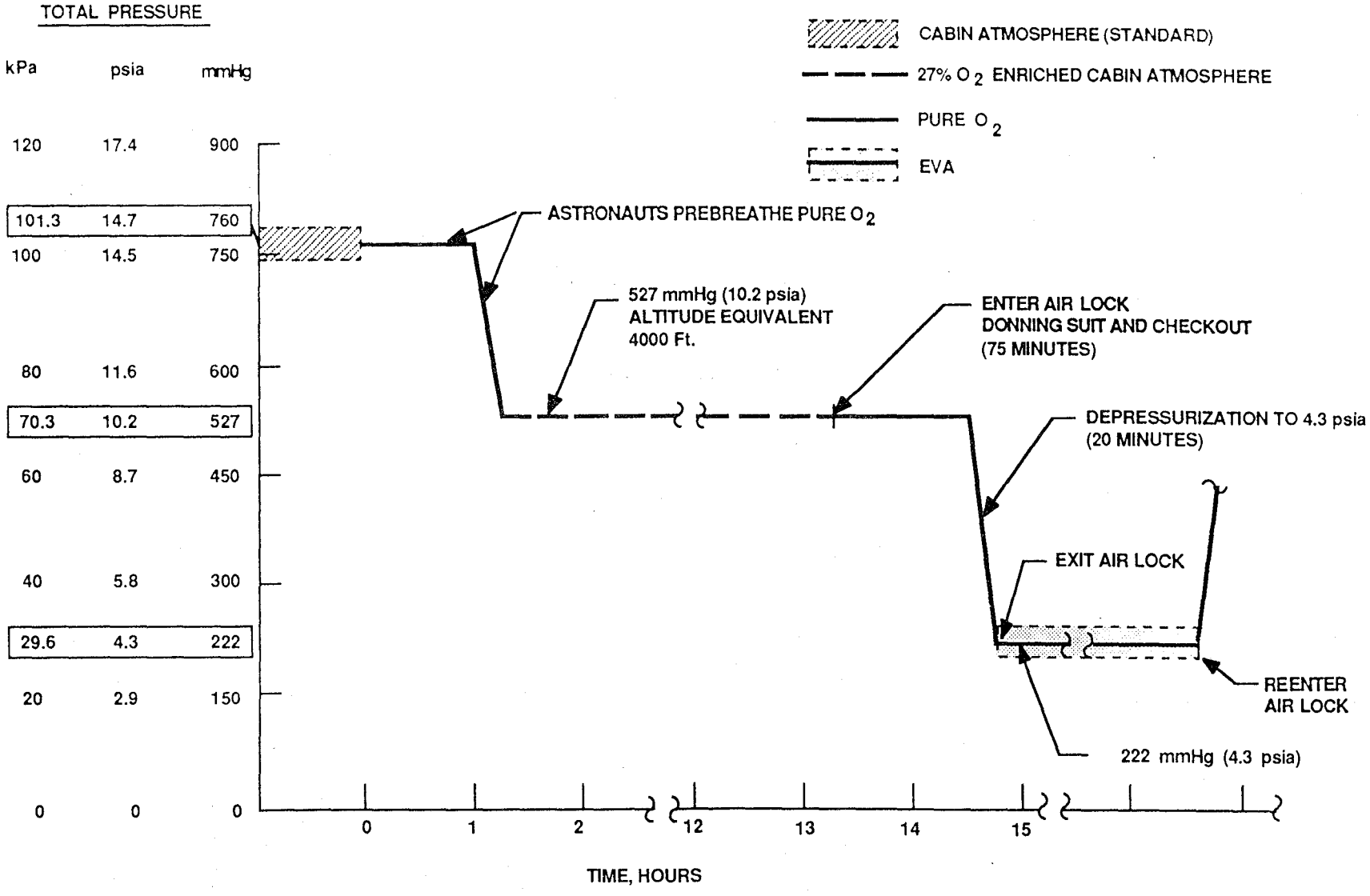

Figure 8.2-3 Modified Prebreathing Requirements for EVA (NSTS Astronaut) (Reference 8-3)

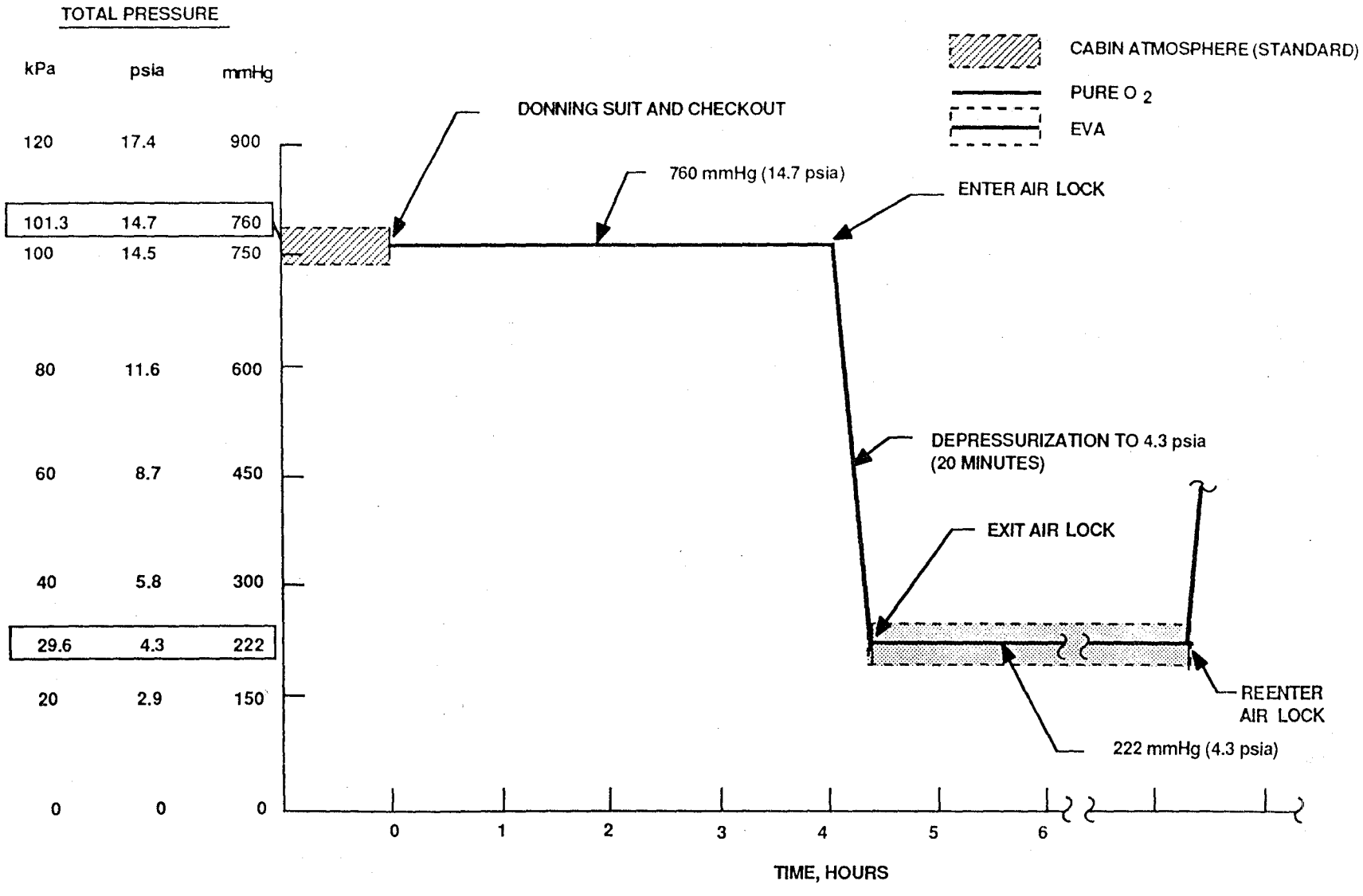

Figure 8.2-4 Rapid Prebreathing Requirements for EVA (NSTS Astronaut)
(Reference 8-3)

the air lock for repressurization to 70.3 kPa (10.2 psia) and reentry into the Orbiter cabin (Figure 8.2-2).

The modified prebreathing procedure requires a reduced dwell time of 12 hours at 70.3 kPa (10.2 psia) in a 27 percent oxygen enriched cabin atmosphere. The astronaut would then don his space suit, enter the air lock and prebreathe pure oxygen for 75 minutes followed by depressurization in 20 minutes to reach 29.6 kPa (4.3 psia) prior to EVA (Figure 8.2-3).

A rapid prebreathing requirement has been developed for the EVA astronaut that permits the crew to remain at the cabin standard atmosphere of 101.3 kPa (14.7 psia). The EVA astronaut dons his suit and breathes pure oxygen for a period of 4 hours at the equivalent pressure of the cabin atmosphere followed by a depressurization to 29.6 kPa (4.3 psia) in 20 minutes prior to air lock exit. Upon reentering the air lock he is repressurized back to 101.3 kPa (14.7 psia), thereby, the crew is not subjected to the cabin depressurization cycle and the astronaut is prepared for EVA in the shortest possible time (Figure 8.2-4).

Russian cosmonauts using the upgraded suits have a much reduced prebreathing period prior to EVA as shown in Figure 8.2-5. Note that the cosmonaut would don his upgraded suit, enter the air lock, and while breathing pure oxygen, undergo a depressurization to 51.7 kPa (7.5 psia). He could then exit the air lock for EVA after a total prebreathing period of one hour. He has the ability to adjust his own suit pressure downward to 22 kPa (3.2 psia) to achieve improved dexterity and tactility for demanding manual tasks. He can remain at 22 kPa (3.2 psia) for a maximum of 20 minutes before repressurizing back to 51.7 kPa (7.5 psia) in order

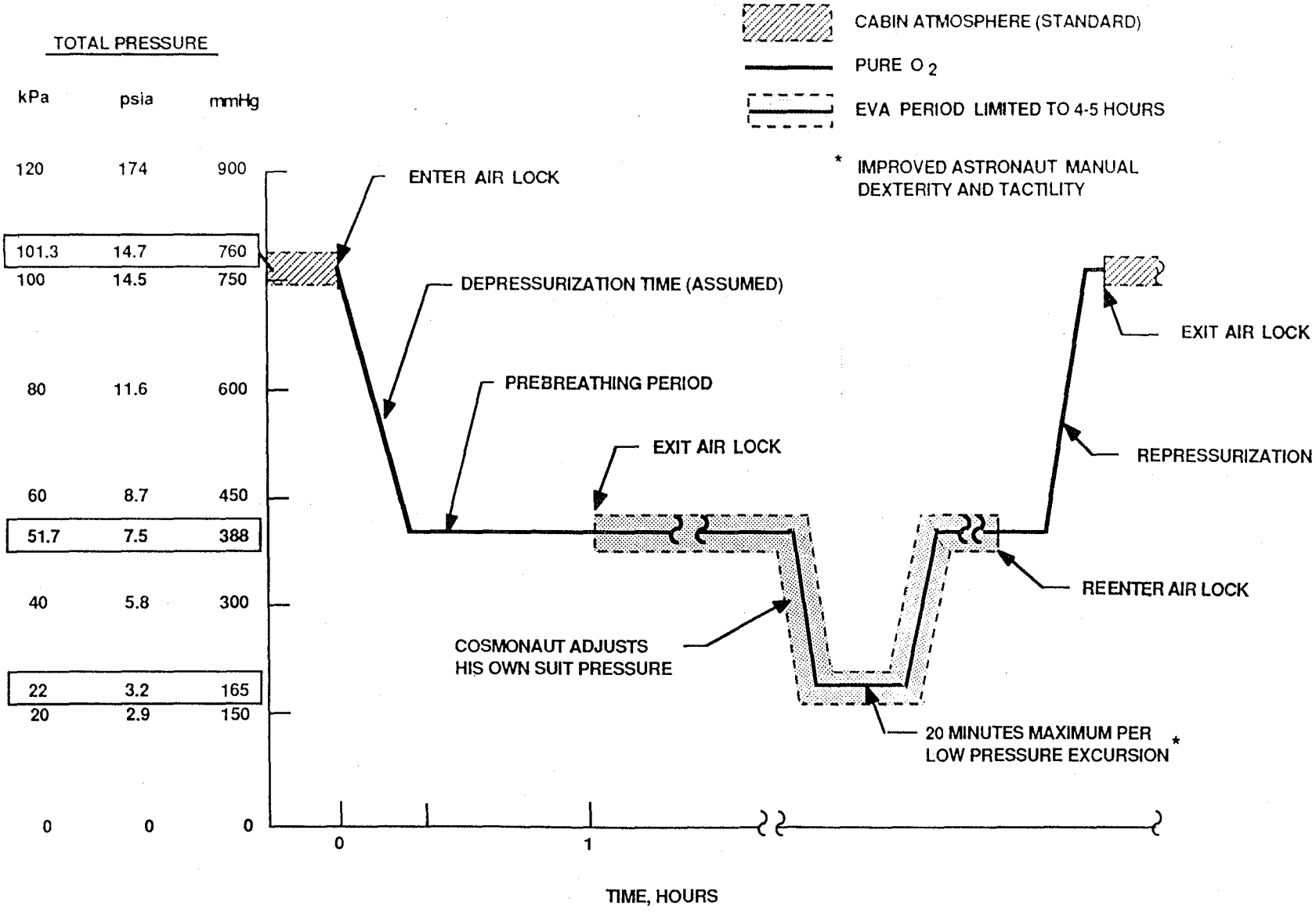

Figure 8.2-5 Prebreathing Requirements for EVA (Russian Cosmonaut Using Upgraded Suit) (Reference 8-4)

to minimize the possibility of decompression sickness and excessive fatigue. The EVA period has limits ranging from 4 to 5 hours before the astronaut has to reenter the air lock for repressurization to 101.3 kPa (14.7 psia) (Reference 8-4).

The United States IOC Space Station has requirements for a high pressure suit to minimize the astronauts' EVA prebreathing requirements and eliminate the need for the crew to undergo a decompression cycle, as shown in the Figure 8.2-6 sequence. The astronaut would don his space suit, enter the air lock, and undergo a depressurization to 57 kPa (8.3 psia) during which the partial pressure of oxygen in the ambient atmosphere is maintained at approximately 21 kPa (3 psia). The space suit total pressure would be maintained at 57 kPa (8.3 psia) by oxygen replenishment as required to compensate for oxygen and nitrogen atmospheric leakage. In the worst-case suit leakage condition, the partial pressure of oxygen could climb to 57 kPa (8.3 psia). The EVA period is limited to 6 hours nominal and 8 hours in an emergency. At the end of the EVA the astronaut would reenter the air lock and repressurize back to 101.3 kPa (14.7 psia) (Reference 8-5).

A high pressure space suit should be perfected and available for use in assembly and operation of the ATSS for the year 2025. This assumption is based on the technological advances to date in development of a high pressure suit to be operated at 57 kPa (8.3 psia) for the IOC Space Station. There are two high pressure space suit versions currently under development, identified as the AX-5 suit and the ZPS Mk.3 suit. These suits will begin their underwater testing during 1988. Three astronauts have commented that each of these two high pressure suits provide the

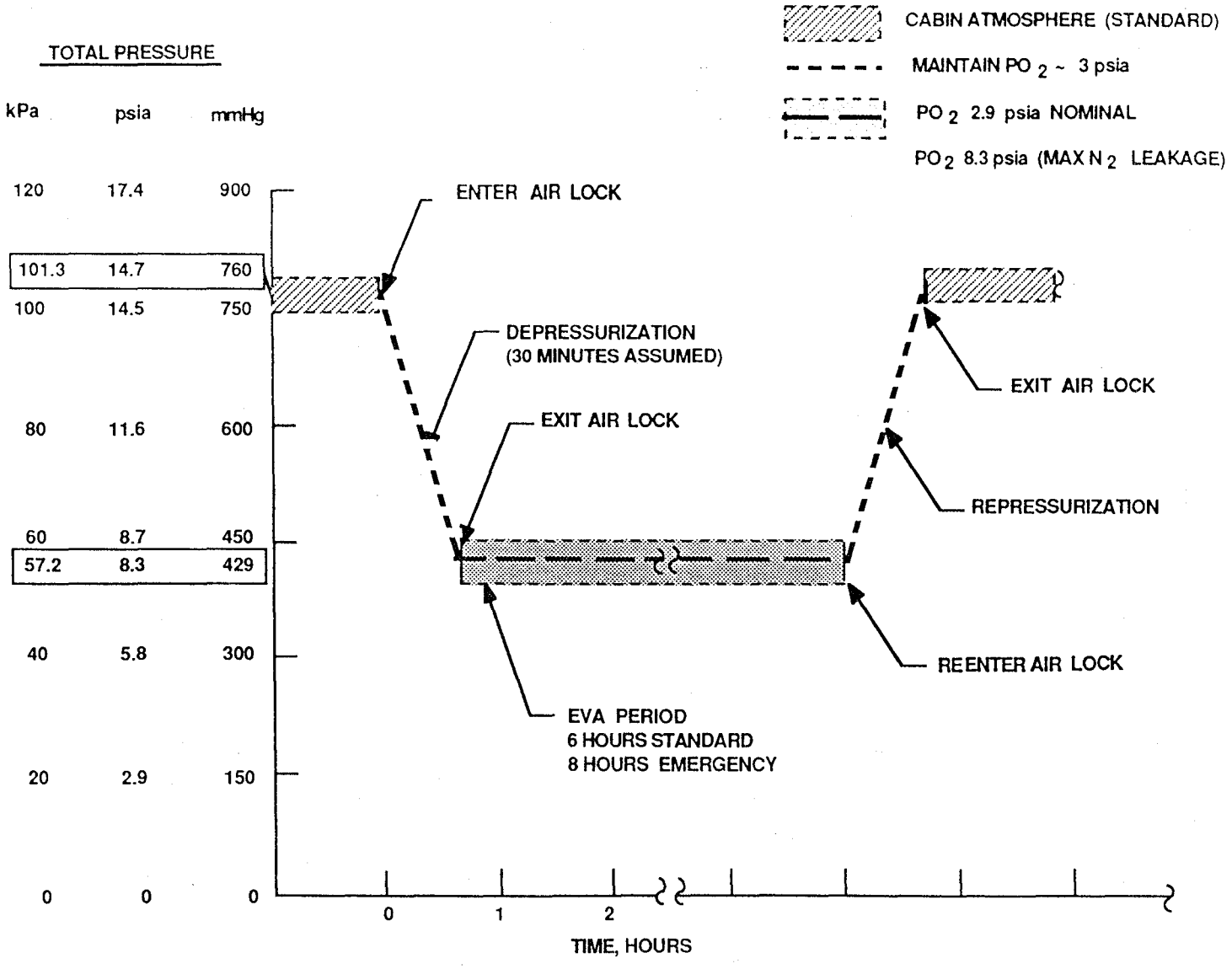

Figure 8.2-6 Prebreathing Requirements for EVA (Extravehicular Mobility Unit for Permanently Manned Space Station Activities) (Reference 8-5)

user with manual dexterity and tactility near equal to that provided by the Shuttle Orbiter EVA space suits operated at 29.6 kPa (4.3 psia).

8.3 Ignition and Flammability Characteristics

As noted in Figures 8.2-2 through 8.2-4 the Shuttle Orbiter astronauts are subjected to varying ambient atmospheric compositions during the pre-EVA protection protocols. Extensive testing has been performed on a variety of materials that would be utilized within the habitable area of the Shuttle Orbiter and the materials of construction of the EVA space suits; Figure 8.3-1 summarizes the overall results. The percentage of oxygen for the total ambient atmospheric composition will determine the flammability characteristics of materials. Note that all of the materials tested will burn in a 100 percent oxygen atmosphere. Extensive data are available on the flammability of materials at approximately 20-percent to 30-percent oxygen and 100-percent oxygen atmospheric content. An upper limit of 30 percent oxygen content in the Shuttle Orbiter cabin atmosphere has been established as a result of the extensive test data (Reference 8-6).

The likelihood of fire within the habitable areas of the Shuttle Orbiter are greatly increased if the cabin atmospheric oxygen content exceeds 30 percent. Materials considered acceptable for standard atmosphere spacecraft construction may become a significant fire hazard in a cabin atmosphere of more than 30 percent oxygen. Examples of material hazards include:

- The Halon fire extinguisher gas becomes significantly less effective at 30 to 33 percent atmospheric oxygen content and requires a much

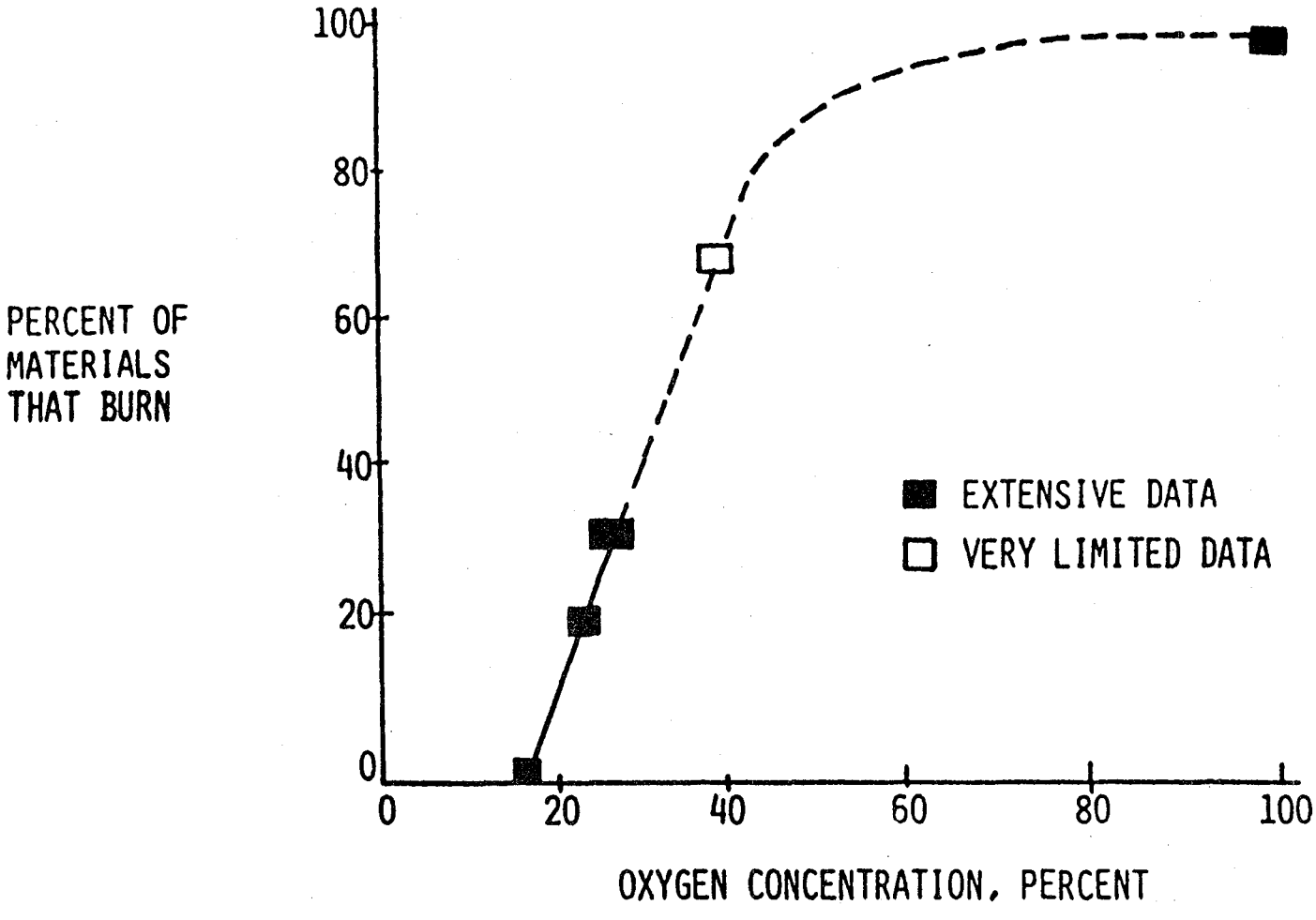

Figure 8.3-1 Materials Flammability versus Oxygen Concentration (Reference 8-6)

larger quantity than normal to extinguish a fire. At a 40 percent oxygen content, it fails to extinguish fire.

- The outer layer of the EVA space suit will burn in a 33 percent atmospheric oxygen content.
- A standard fire barrier conformal coating will burn in a 31 percent atmospheric oxygen content.

8.4 Internal Pressure Versus Pressure Vessel Weight

The ATSS torus, spokes, and central tube will be comprised of cylinders joined at their ends to serve as pressure vessels. The torus is composed of 24 cylinders with mitered ends for assembly. The thickness of a cylindrical stressed skin pressure vessel shell can be determined by the formula (Reference 8-7):

$$t_m = \frac{P_o r}{\sigma_w}$$

t_m = Thickness of the wall
P_o = Internal pressure
r = Radius of the pressure vessel
σ_w = Working stress for the wall material

The mass of an aluminum shell with 10 mm (0.375 in) average thickness for a torus totals 8.62×10^5 kg (1.9×10^6 lb) for construction of a pressure vessel to contain one Earth atmosphere of pressure at 101.3 kPa (14.7 psia). If the torus internal pressure was reduced to one third of an Earth atmosphere, the weight of the torus pressure shell structure would be reduced proportionately, as indicated in Figure 8.4-1. Significant weight savings could be accomplished by reducing the internal pressure within the Space Station.

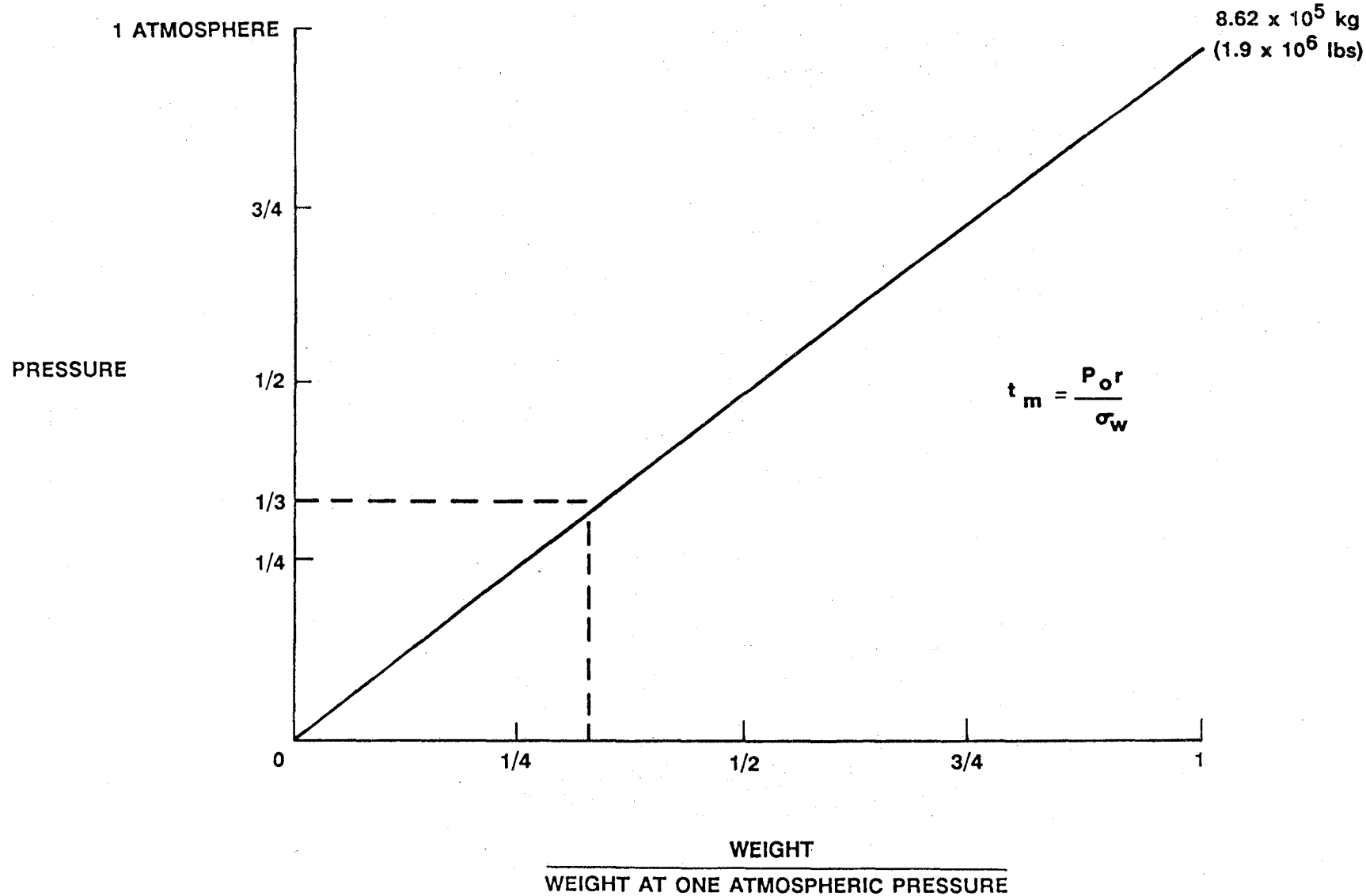

Figure 8.4-1 Torus Weight versus Pressure

8.5 Nitrogen Resupply Requirements for Reduced Atmospheric Pressure in the Space Station

The pressure and composition of the cabin atmosphere for the ATSS are worthy of further evaluations of mass trade-offs related to the resupply benefits of atmospheric nitrogen lost through leakage. The atmosphere of the Earth contains 78 percent by volume of nitrogen and 21 percent by volume of oxygen with 1 percent other gases, excluding water vapor. For resupply evaluation purposes, a two component atmosphere of nitrogen and oxygen may be assumed.

The oxygen constituent of the atmosphere can be generated in the environmental control-life support system through the electrolysis of water or conversion of carbon dioxide. Electrolysis of water is part of the ATSS operational mode; however, atmospheric nitrogen is essentially inert and not the principal output of any operational system on the Space Station. Therefore, any nitrogen losses would have to be satisfied by specific resupply in some form of molecular nitrogen. The use of supercritical wet air oxidation as a waste recovery system will produce a small quantity of GN_2 but not in quantities sufficient for resupply needs (Reference 8-10). The form of the resupply of nitrogen, therefore, must consider the liquid, gas, or solid state. Nitrogen can be provided as a cryogenic liquid given sufficient insulation and tankage. Provision as a gas could require large-volume, high-pressure, storage vessels and could prove to be an undesirable hazard. Nitrogen in chemical combination with other elements offers a resupply source which has greater density than gaseous nitrogen and is more easily stored and transported. Liquid ammonia and solid ammonium nitrate are prospective compounds which could be transported to the ATSS and thermally decomposed to yield nitrogen gas for atmospheric resupply demands. The synergy for combining ammonium

nitrate with emergency propulsion has also been addressed in Reference 8-10. Within a breathing atmosphere, nitrogen is a diluent, and the reduction of both cabin pressure and nitrogen proportion becomes potentially advantageous to the ATSS design from a mass standpoint. The U.S. space program has conducted a long-term project of evaluating nonstandard breathing atmospheres for flight crews. This has included both reduced pressure and reduced nitrogen (increased oxygen) options. Two distinct limits have been determined. One relates to the minimum acceptable partial pressure of oxygen which is present in the respiratory air for the crew. This limit is approximately 21.3 KPa (0.21 atm) for sea level Earth atmosphere equivalency, and this lower limit will be used for the nitrogen resupply and related leakage evaluation. The other limit is less specific and is derived from materials flammability test and evaluation. Nitrogen as a diluent in the atmosphere suppresses ignition and flame spread. At oxygen mole fractions greater than 0.30, within the range of pressures of interest for crew operations, the list of acceptable materials becomes quite limited. At oxygen fractions above about 0.30, such common items as the crew uniform fabric and even the fire suppressant (Halon) become fire hazards. Therefore, the upper limit on oxygen concentration is taken as a 0.30-mole fraction. Using the above limits on the cabin composition, it is possible to define the coincident range of composition for nitrogen and proceed to the evaluation of the nitrogen leakage and resupply problem.

For the purposes of this evaluation, the cabin atmosphere is assumed to have: a) an ideal gas mixture, b) a composition of nitrogen and oxygen only, and c) have constant specific heat properties. These assumptions apply within 1 percent in the range of the values that are

under evaluation. The assumptions permit simple analytical solutions and parametric trend analysis. The above assumptions permit the total pressure to be expressed as follows:

$$P(total) = P(oxygen) + P(nitrogen) \qquad P_T = P_O + P_N$$

where P_T = total pressure (atm)
P_O = oxygen partial pressure (atm)
P_N = nitrogen partial pressure (atm)

The ratio of nitrogen pressure to total pressure is the mole fraction of nitrogen. This must exceed or equal 0.70 to meet the flammability limit. The partial pressure of oxygen must equal or exceed 0.21 atm to meet the crew breathing requirement. Using the above relationship, the following Table 8.5-1 was computed to determine the acceptable range of cabin atmosphere mixtures.

Table 8.5-1 Cabin Atmosphere Nitrogen Prevalence at Constant Oxygen Partial Pressure

P_T	P_N/P_T	P_O	P_O/P_T
1.0	0.79	0.21	0.21
0.9	0.76	0.21	0.24
0.8	0.74	0.21	0.26
0.7	0.70	0.21	0.30
0.6	0.65	0.21	0.35

Examination of Table 8.5-1 reveals that the limit of 0.30 for oxygen mole fraction occurs at an atmospheric pressure of 0.7 atm or 72.5 KPa (10.3 psia). (See also Figure 8.5-1.) Therefore, the range of evaluation of nitrogen resupply/leakage will be limited to 0.7 to 1.0 atmosphere total pressure, and nitrogen fraction from 0.7 to 0.79. Although this appears to be a small range, the partial pressure and, the mass of nitrogen vary more significantly, namely from partial pressure of 0.79 atm to partial pressure of 0.49 atm. This represents a potential reduction in the mass of nitrogen in the cabin atmosphere by 38 percent.

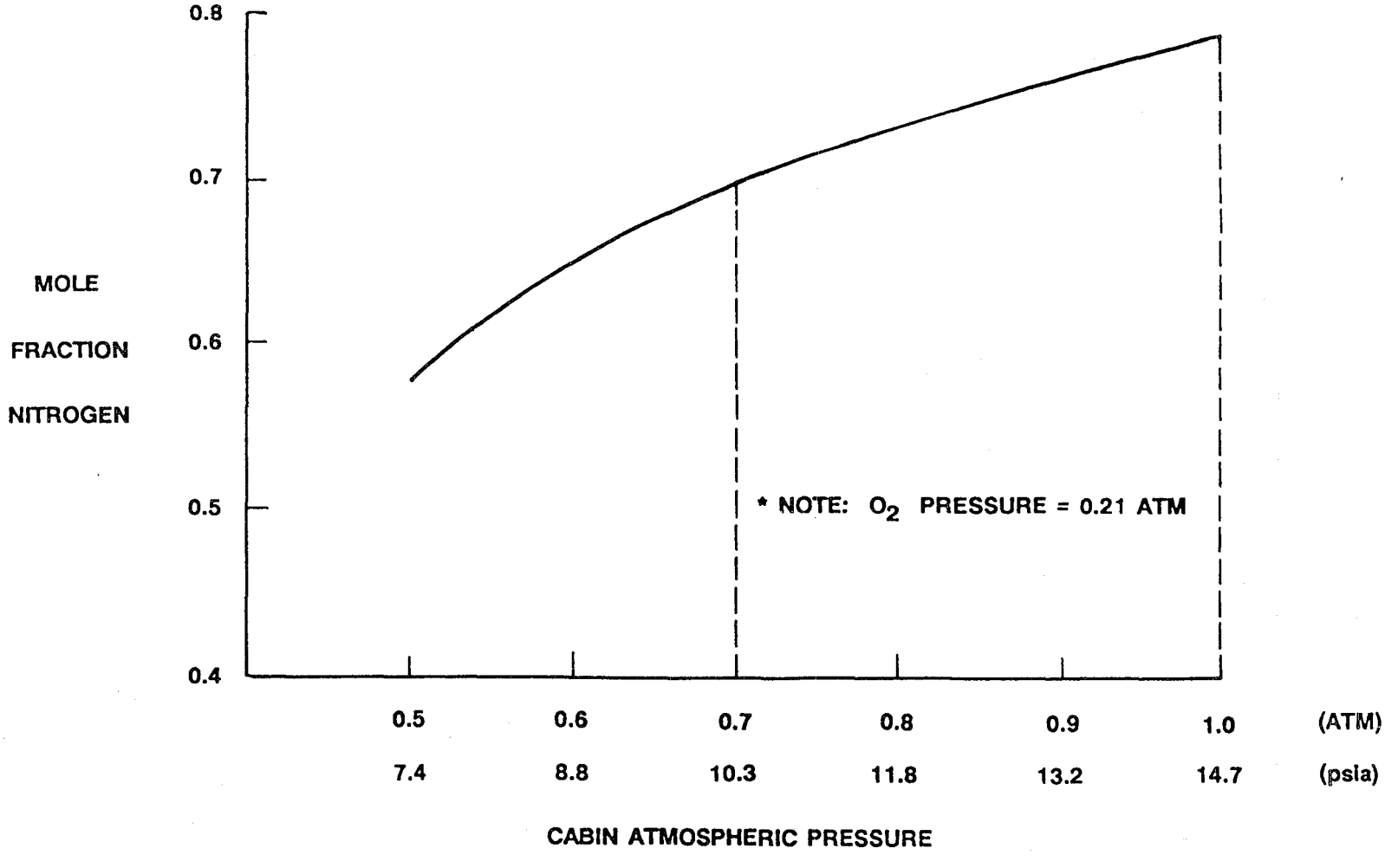

Figure 8.5-1 Nitrogen Mole Fraction for Cabin Air Mixtures with Constant O_2*

There are two distinct pathways for nitrogen loss from the cabin atmosphere. One is through leakage from joints, seals, and other minor defects in the pressure shell. The second results from air lock venting. Some residual air is lost from the air lock when it is finally vented to space. These two paths influence the nitrogen loss differently.

Consider the air lock venting loss first. The initial condition is an air lock cavity at cabin pressure. The air lock is pumped down to some low pressure and the air retained in a reservoir tank. The composition of the residual is unchanged. Therefore, the mass of gas loss can be determined by use of the ideal gas relationship:

$$\tau = \frac{MPV}{RT}$$

where τ = mass of nitrogen gas (grams)
M = molecular weight of nitrogen (grams/mol)
P = partial pressure of nitrogen (atm)
V = volume of the air lock (liters)
T = absolute temperature (K)
R = ideal gas constant 0.0821 $\frac{\text{atm (liters)}}{\text{g mol (K)}}$

The partial pressure of nitrogen is given as the mole fraction multiplied by the final pump down pressure P_O.

$$P = P_O \frac{P_N}{P_T}$$

All of the parameters are constant and independent of the atmospheric mixture except for τ and P. The total gas loss will be the total of all of the air lock operations over a given time. Therefore, to determine the ratio of the mass of nitrogen loss in air lock operations at a specified nitrogen mixture to the mass of nitrogen loss at the standard mixture, i.e., Earth ambient proportion is given as:

$$\frac{\tau}{\tau_O} = \frac{P_N}{P_T}\left(\frac{1}{0.79}\right)$$

where τ = mass loss at reduced pressure
τ_O = mass loss for standard atmosphere

Where 0.79 is the standard mole fraction of nitrogen used in the analysis.

The mass of nitrogen lost at reduced pressure conditions as a ratio to that lost for the standard mixture condition is given in Table 8.5-2 for these assumptions. Figure 8.5-2 illustrates the trend at various total atmospheric pressure conditions.

Table 8.5-2 Resupply Ratio for Air Lock Operations

P TOTAL (atm)	P_N/P_T	τ/τ_O
1.0	0.79	1.0
0.9	0.76	0.96
0.8	0.74	0.94
0.7	0.70	0.89

At the limiting condition of 0.7 atm pressure and 0.7 nitrogen fraction, the nitrogen resupply is 89 percent when compared to the 1 atm condition or a savings in resupply of 11 percent of the nitrogen compared to a standard one atmosphere mission condition. These results indicate that the 30 percent reduction in ambient pressure only reduces the nitrogen resupply by 11 percent for the air lock operations. This may not be a significant savings in the resupply when compared with the potential requirement for qualifying equipment to operate in a 30 percent oxygen, 70 percent nitrogen mixture at 0.7 atmosphere pressure.

The operation at 0.7 atmosphere and 70 percent nitrogen does require flammability qualification of materials and will limit the options available when compared with the standard Earth ambient atmosphere. At this reduced pressure, convective heat transfer from the electronic equipment will be reduced and require design accommodation from the standard configuration. For example, fans may be required to convect heat from specific sources. Also, the transmission of voice

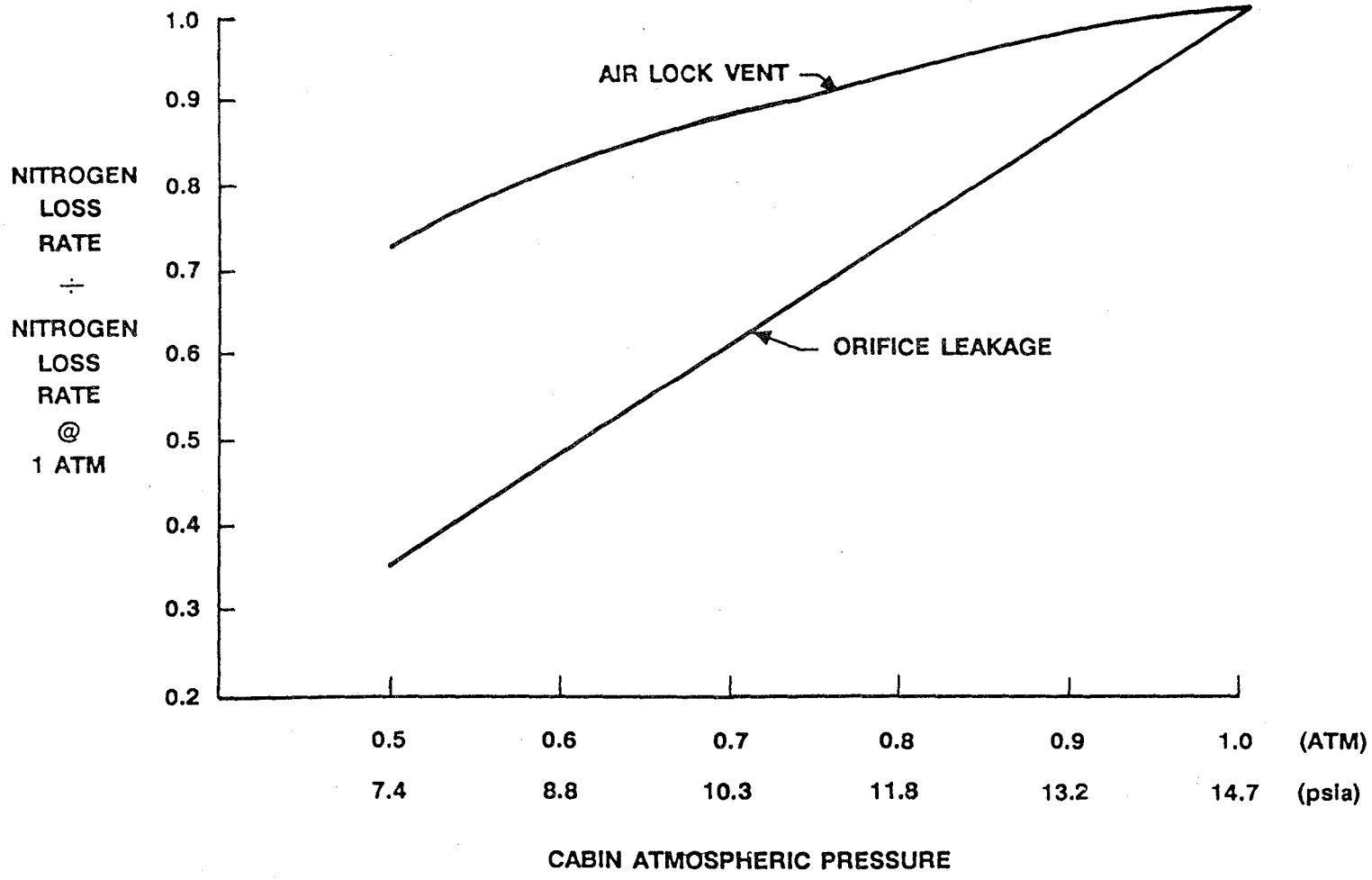

Figure 8.5-2 Nitrogen Loss Rate versus Cabin Pressure for Air Mixtures of Constant O_2 Pressure

sounds is diminished at this pressure. Previous flight crews operating at approximately this pressure have noted this vocal inconvenience. The cabin communications would have to rely more heavily on electronic amplification for transmission of speech. Therefore, the minor advantages in resupply do not appear to warrant the reduced pressure operation when considering routine number of air lock operations. For example, if the standard pressure air lock operations result in a 5 percent loss of total atmosphere in a month of operations, then the total mass saved by the reduced pressure operation is 0.05 x 0.11 or about 0.5 percent of the ambient atmosphere in the same period of time.

The other loss is leakage from joints, seals and holes. This occurs continuously as opposed to the discrete events of air lock operations. In leakage, the flow from a small orifice or seal will be in the critical, or sonic flow regime because the downstream end is at the space vacuum. For an ideal gas, the sonic velocity at the exit orifice is given as:

$$c = \sqrt{\frac{\gamma R T}{M}}$$

where c = sonic speed (m/sec)
γ = ratio of specific heats (1.4 for N2)
R = ideal gas constant (kg $m^2/sec^2\ ^oK$)
T = absolute temperature (K)
M = molecular weight (kg/mol)

The specific heat ratio is a constant 1.4 for both nitrogen and for oxygen. The absolute temperature at the sonic point is given from the energy conservation relationship as:

$$T = \frac{T_o}{1 + \frac{\gamma - 1}{2}}$$

where T_o is the stagnation or ambient temperature which is a constant for all of the gas mixtures considered. The mass outflow is given as the product:

$$\dot{m}(\text{outflow}) = \frac{PMA}{RT}\sqrt{\frac{\gamma RT}{M}}$$

where $\dot{m}$ (outflow) is the composite mass loss (kg/sec) and where A (m^2) is the cumulative area of leakage orifices over the Space Station.

In critical, or sonic flow, an ideal gas such as air, which is composed of diatomic constituents, has a sonic pressure P which is 0.528 P_T. Substituting the preceding into the leakage relation yields the following:

$$\dot{m} = 0.528\ P_T\sqrt{\frac{\gamma MA}{RT}\left(1 + \frac{\gamma - 1}{2}\right)}$$

In this relationship all of the terms are fixed for the various mixtures except for M and P_T. Therefore, it is possible to ratio the mass flow from orifices with a given pressure and mixture to the flow at standard Earth ambient conditions to result in:

$$\frac{\dot{m}}{\dot{m}_o} = P_T\sqrt{\frac{M}{M_o}}$$

where M is the mixture molecular weight and M_o is the standard mixture molecular weight. Within the range of interest, namely with the nitrogen fraction varying from 0.7 to 0.79, the average molecular weight variation is from 29.2 to 28.8. The variation of the ratio of the square root of the molecular weight for the range is 0.993. Therefore, for the purpose of the present analysis, the effect of molecular weight variation is

negligible. Only the total pressure effect is significant. The combined loss of oxygen and nitrogen is proportional to the cabin total pressure. The orifice leakage loss ratio becomes:

$$\tau/\tau_O = P_T$$

where P_T is in atmospheres. The fraction of the total mass flow which is nitrogen may be computed from this relation and the ideal gas mixture relation:

$$\frac{\tau_N}{\tau} = \frac{\text{Mass of nitrogen}}{\text{Total mass of mixture}}$$

$$\frac{\tau_N}{\tau} = \frac{(P_N/P_T)28}{(P_O/P_T)32 + (P_N/P_T)28}$$

Substituting into the prior relationship:

$$\frac{\tau_N}{\tau_{NO}} = P_T \frac{(P_N/P_T)28}{(P_O/P_T)32 + (P_N/P_T)28} \Bigg/ \frac{(0.79)28}{(0.21)32 + (0.79)28}$$

Table 8.5-3 has been computed for the conditions of interest for the Space Station.

Table 8.5-3 Nitrogen Leakage Loss Ratio at Various Cabin Pressure Conditions

P_T	τ_N/τ_{NO}
1.0	1.0
0.9	0.86
0.8	0.74
0.7	0.61

where τ_N/τ_{NO} is the mass of nitrogen lost at cabin conditions ratioed to the mass of nitrogen lost at 1 atmosphere cabin pressure.

The results of Table 8.5-3 appear in Figure 8.5-2 and illustrate that the orifice leakage of nitrogen has a greater effect than does the air lock operation at the same pressure. There is a compounding effect; as pressure is reduced, the overall loss rate also reduces. Also, while pressure is reduced, the nitrogen prevalence is also reduced in fraction from 0.79 to 0.70. Therefore, the resupply of nitrogen due to leakage can be reduced by 39 percent for Station operation at 0.7 atmosphere. The total mass of nitrogen saved will depend upon the leakage rate. It has been previously estimated (Reference 8-10) that the total daily nitrogen leakage was of the order of 26 kg (57 lbs) per day. A savings of 39 percent represents a 10 kg (22 lbs) per day reduction in resupply requirement for nitrogen. This savings includes the 30 percent overall reduction in leakage due to operation at reduced pressure (since the oxygen partial pressure remains constant,) the oxygen resupply rate is essentially unchanged for low pressure operation.

In summary, the criteria for material flammability and crew oxygen requirements limits the potential reduction to pressures of 0.7 atmosphere and oxygen concentration less than 30 percent. Within this permissible range, the effect of pressure on nitrogen resupply was shown to have as much as an 11-percent reduction for air lock type operation and a 39-percent reduction for orifice leakage type loss. For both the air lock and leakage instances, the resupply of oxygen is essentially unchanged. Therefore, only the nitrogen resupply is affected by the option to reduce cabin pressure. The proportion of losses due to air lock operations as compared with losses due to orifice leakage will depend the operational sequence and design approach for leakage control.

REFERENCES

8-1 Bioastronautics Data Book. Second Edition NASA SP-3006, 1973.

8-2 Space Resources and Space Settlements. NASA SP-428, 1979.

8-3 STS Operational Flight Rules, All flights. NASA-JSC 12820, Final March 16, 1987, Update PCN3 July 10, 1987.

8-4 Telephone Conversation: Dr. A. Nicogossian, NASA-Headquarters, to Dr. I. Taback, The Bionetics Corporation. September 15, 1987.

8-5 NASA/USAF EVA Suit Technology Interchange, Human Systems Division (AFSC) Brook AFB, San Antonio, Texas, July 8-9, 1987.

8-6 Space Station Advanced Development Program Review, NASA-Johnson Space Center, October 20-November 6, 1986.

8-7 LeDoux, Paul W.: Spacecraft Material Flammability Testing and Configuration, Proceedings of Spacecraft Fire Safety Workshop, NASA-Lewis Research Center, August 20, 1986.

8-8 Johnson, Richard, D., Editor: Space Settlements, A Design Review, NASA SP-413, 1977.

8-9 M. J. Queijo, et al: Analyses of a Rotating Advanced-Technology Space Station for the Year 2025, Study and Concepts, NASA CR 178345, January 1988.

8-10 M. J. Queijo, et al: An Advanced-Technology Space Station for the Year 2025, Study and Concepts, NASA CR 178208, March 1987.

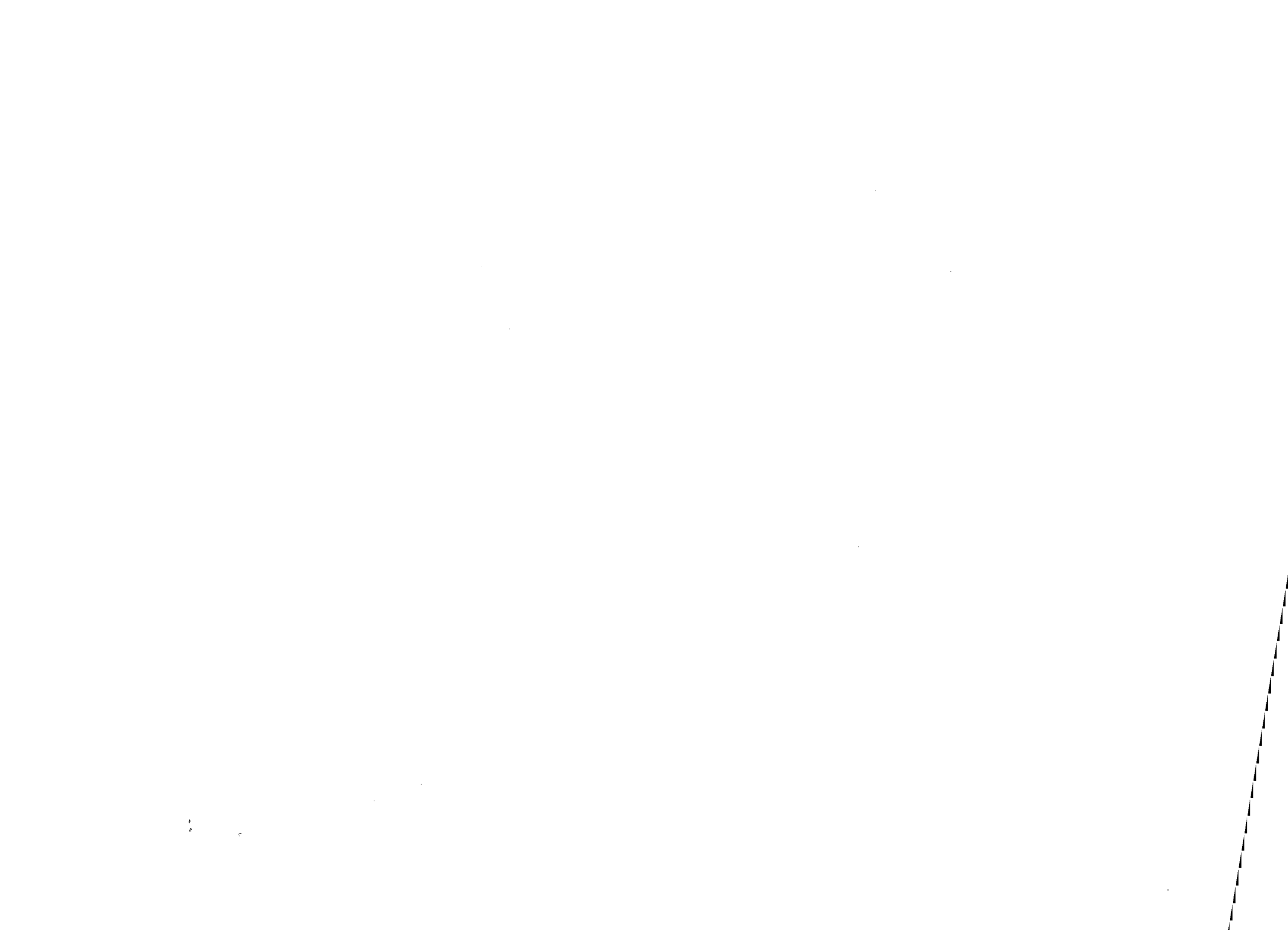

9.0 MANNED MISSION TO MARS SUPPORT BY THE SPACE STATION

9.1 Reference Manned Mars Missions

The Advanced-Technology Space Station (ATSS) is intended to support the ongoing planetary explorations undertaken by the United States and other participating nations. The discussions which follow address the impact on the ATSS design due to the requirement to support specific manned missions to Mars. Three mission studies were identified by NASA to be used as inputs. These Mars missions were the output of studies conducted by: (1) The Space Station Office at Langley Research Center, (2) An MIT Advanced Space Systems Design Course, and (3) A summer intern team from University of Texas at Austin (UTA) and Texas A & M University (TAMU) (References 9-1 to 9-3). A 1985 workshop at Marshall Space Flight Center (Reference 9-4) is an additional source of information on trade-offs for Mars mission requirements. A number of the concepts for the three reference missions were covered during this workshop.

After reviewing the different approaches of these studies, it was found that the required support functions for the Space Station were quite similar for all three of the missions and the ATSS was capable of providing the support. The major differences as viewed from the Space Station were the number of HLLV's required from Earth to Space Station, the number and type of vehicles to be assembled at the Space Station, fuel requirements for these vehicles, and the number of OTV support missions needed. Each of the referenced Mars missions are briefly described as follows and the requirements are compared in Table 9.1-1.

9.1.1 Humans to Mars: A Space Leadership Program, Space Station Office, LaRC.

An on-going LaRC study provided the inputs used here. The final version of this LaRC study (Reference 9-1) will differ in some details from the values used in this report. The study requires Space Station based research related to effects of long duration space flight on humans, robotic missions to Mars, manned roundtrips to Mars, and eventually, permanent manned Martian outposts. The manned roundtrips included a number of options for types of trajectories, number of vehicles, and method of propulsion. A mission utilizing a cargo vehicle and a manned vehicle was designated for the purpose of comparing Space Station support requirements imposed by a Mars mission.

9.1.2 Mars: A Program for its Exploration and Development. MIT Advanced Space Systems Design Course.

This mission concept uses an Interplanetary Vehicle (IPV) assembled in LEO and transferred to HEO in an unmanned condition. The crew of ten would board the IPV from an OTV for an eight month cruise to Mars in an artificial 1-g environment (Reference 9-2). Propulsion power is nuclear electric for an ion engine using mercury (Hg) as the propellant. Reverse thrusting is utilized both for Mars approach and for Earth return to HEO. From Mars orbit, an unmanned cargo lander is first sent to the surface, then followed by a manned landing and return vehicle. The fuel combination for both of these vehicles is specified as monomethyl-hydrazine (MMH) and nitrogen tetroxide (N_2O_4). A Martian moon excursion vehicle is also included for exploration of Phobos and Deimos using the same fuel combination.

TABLE 9.1-1 SUMMARY OF MANNED MARS MISSION FEATURES

MARS MISSION	DELIVERY TO LEO			VEHICLES	VEHICLE MASS kg x 10^4	PROPULSION	FUEL-OXIDIZER OR Hg PROPELLANT MASS kg x 10^4	AEROBRAKING		ARTIFICIAL GRAVITY
	MASS kg x 10^6	HLLV FLIGHTS						AT MARS	EARTH RETURN	
		9.1 x 10^4 kg EACH	2.7 x 10^5 kg EACH							
LANGLEY RESEARCH CENTER SPACE STATION OFFICE "SPLIT-OPTION MISSION"	1.1	12	4	INTERPLANETARY VEHICLE	22	$H_2 - O_2$	72	yes	yes	3/8 g
				MARS CARGO VEHICLE	8.8	$H_2 - O_2$		yes	---	---
				MARS EXCURSION MODULE	7.2	$H_2 - O_2$		yes	---	---
MASS. INST. TECH. ADVANCED SPACE SYSTEMS DESIGN COURSE	1.5	17	6	INTERPLANETARY VEHICLE	57	Nuclear - Hg	42	no	no	1 g
				CARGO LANDER	15	MMH - N_2O_4	10	yes	---	---
				MANNED LANDING & RETURN VEH.	12	MMH - N_2O_4	8.8	yes	---	---
				MOON EXCURSION VEHICLE	0.63	MMH - N_2O_4	0.97	---	---	---
				OTV (LEO TO HEO & RETURN)	1.6	$H_2 - O_2$	6.7	---	yes	---
UNIV. OF TEXAS AT AUSTIN TEXAS A&M SUMMER INTERN TEAM	1.1	12	4	INTERPLANETARY VEHICLE	37	Nuclear - Hg	28	no	no	1 g
				CARGO LANDERS (3 Vehicles)	2.2 ea	$CH_4 - O_2$	Included in IPV Allocation	yes	---	---
				MARS ASCENT/DESCENT VEH. (2 Vehicles)	4.0 ea	$CH_4 - O_2$ & Strap- on	8.9 4.5	yes	---	---
				TAXI (LEO TO HEO & RETURN)	1.6	$H_2 - O_2$	6.7	---	yes	---

On return to HEO, an OTV is again utilized for rapid return of the crew to the Space Station while the IPV is slowly decelerated to LEO for refurbishment.

9.1.3 A Manned Mission to Mars. 1986 Summer Intern Team, UTA and TAMU.

This mission uses an unmanned IPV to HEO which is then boarded by a crew from a manned taxi, probably an OTV. At Mars, three cargo landers and two ascent-descent vehicles are used for exploration (Reference 9-3).

The IPV provides 1 g artificial gravity and propulsion power is also nuclear electric with mercury (Hg). The ascent-descent vehicle uses methane and LO_2 plus strap-on solid or liquid motors. After a return by the IPV to HEO, the taxi vehicle is used for rapid return to the LEO Space Station.

9.2 Requirements and Design Considerations for Mars Mission Support

9.2.1 Delivery to LEO

The total masses to be delivered to the ATSS for the specified missions vary from 1.1 to 1.5 x 10^6 kg (2.4 to 3.3 x 10^6 lb). The variation is not significant, and a growth factor, larger than the variation, could be added.

In Section 7.0 of this study, a payload lift capability of 2.7 x 10^5 kg (6 x 10^5 lb) is assumed for HLLV's to be used in ATSS component delivery to LEO. Using the same type HLLV's for Mars mission spacecraft component delivery to LEO, it might require seven flights for a growth mass of 1.8 x 10^6 kg (4 x 10^6 lb). Volume and packing efficiency may be controlling factors which would increase the number of HLLV flights.

In addition to the spacecraft and equipment delivered to LEO by HLLV's, there will be a number of shuttle or aero-space plane support flights to rotate work crews, provide logistic support, and to deliver flight crews for simulations, checkout, and the actual mission. Post mission flights related to quarantine, storage of Mars spacecraft, and refurbishment will also be required.

9.2.2 Nuclear Engines

The MIT and TAMU/UTA missions both call for nuclear propulsion systems. This could require careful planning in delivery and assembly in the vicinity of the manned Space Station. Both of these missions require the interplanetary vehicle to be boosted by ion thrusters from LEO to HEO in an unmanned condition. This study assumes that techniques will exist for final loading of nuclear fuel at LEO under conditions which do not impact the ATSS operation.

9.2.3 Assembly at LEO

Each of the specified study missions calls for a variety of vehicles to be assembled into either one or two cruise spacecraft for the Mars transit. The TAMU/UTA mission requires the largest assembly area and calls for a 200 by 172 m (656 by 564 ft) structure with tension cables. The Langley SSO proposed spacecraft includes two large aeroshields as part of the assembly.

The ATSS was designed with a 61 m (200 ft) per side cube berthing and assembly bay. This assembly area contains six (or more) cranes that will support assembly of the spacecraft. The Langley and MIT vehicles could be assembled with portions inside the cube, but the TAMU/UTA

vehicle would have to be assembled outside, perhaps attached to one cube face and extending beyond the ATSS in an axial direction with the nuclear unit end of the Mars IPV at the greatest distance. Figures 9.2-1 through 9.2-3 show possible assembly locations and also serve to illustrate the relative sizes of the Mars spacecraft in comparison to the ATSS.

Considerations during the spacecraft assemblies are docking accessibility for shuttle or other vehicles; air lock to air lock transitions to allow shirtsleeve access between Space Station and Mars spacecraft; assembly of component parts of the Mars spacecraft; temporary storage of subassemblies on the docking bay; and station keeping after separation during the final checkout.

9.2.4 Space Station Controllability Effects

Assembly of a structure with a mass of perhaps 1.8×10^6 kg (4×10^6 lb) at one end of the ATSS with a mass of 8.2×10^6 kg (1.8×10^7 lb) will shift the moments of inertia and the structural resonances. In addition these masses will have an effect on the orbital decay rate and re-boost requirements. These factors have not been included in the present dynamic analyses. The results of the Langley SSO mission study indicate the effects will be relatively small. The Langley SSO study addressed a 1.1×10^6 kg (2.4×10^6 lb) mass attached to the IOC Space Station which has a mass of approximately 3×10^5 kg (6.6×10^5 lb) and operates in alignment with the gravity gradient. The Langley SSO study concluded that the impacts would be:

- Slight adverse impact on attitude secular momentum accumulation and orbit-keeping propellant requirements.
- Slight positive impact on orbit lifetime.

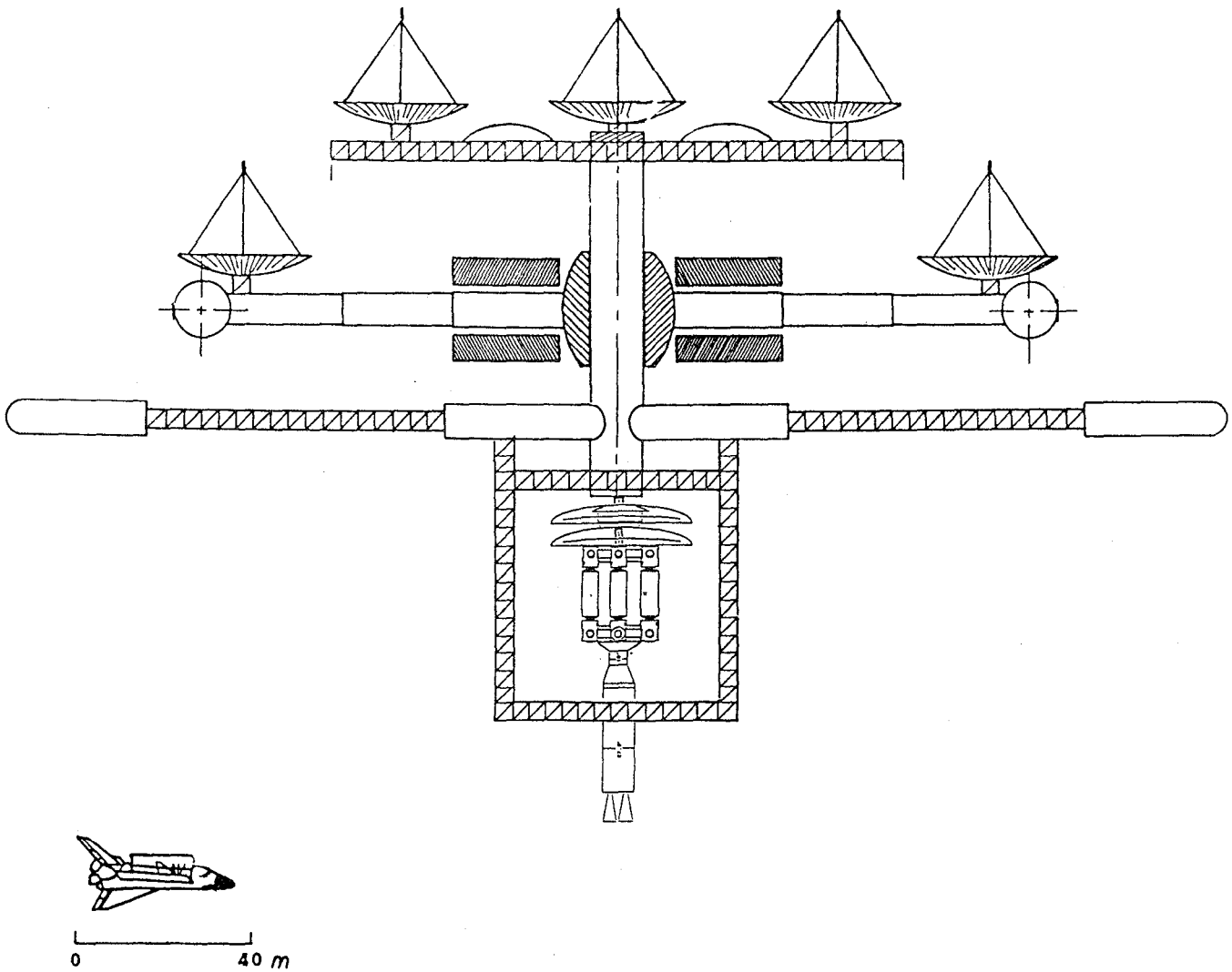

Figure 9.2-1 LaRC-SSO Manned Mars Mission Spacecraft Assembled at Advanced-Technology Space Station

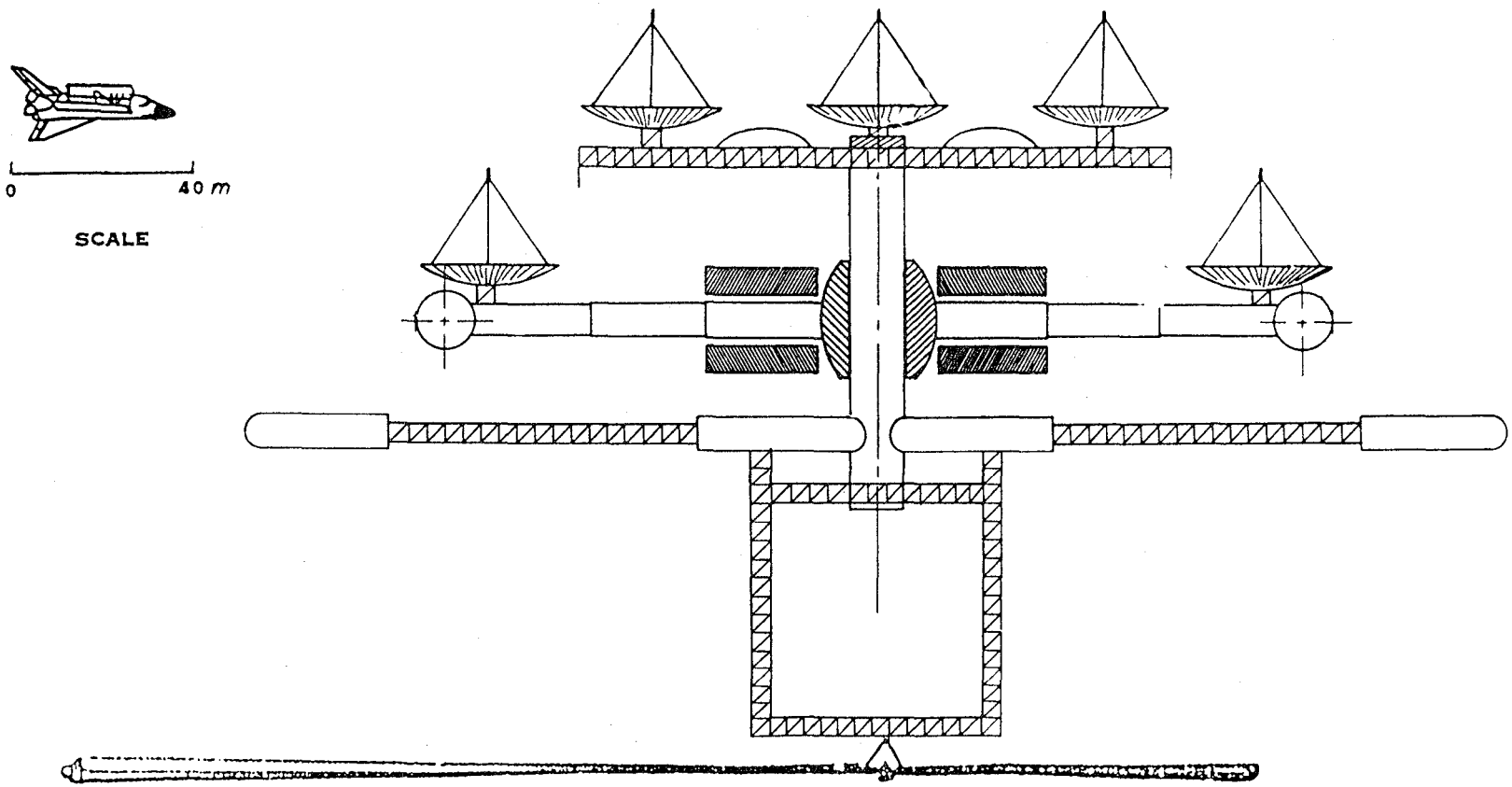

Figure 9.2-2 MIT Manned Mars Mission Spacecraft Assembled at Advanced-Technology Space Station

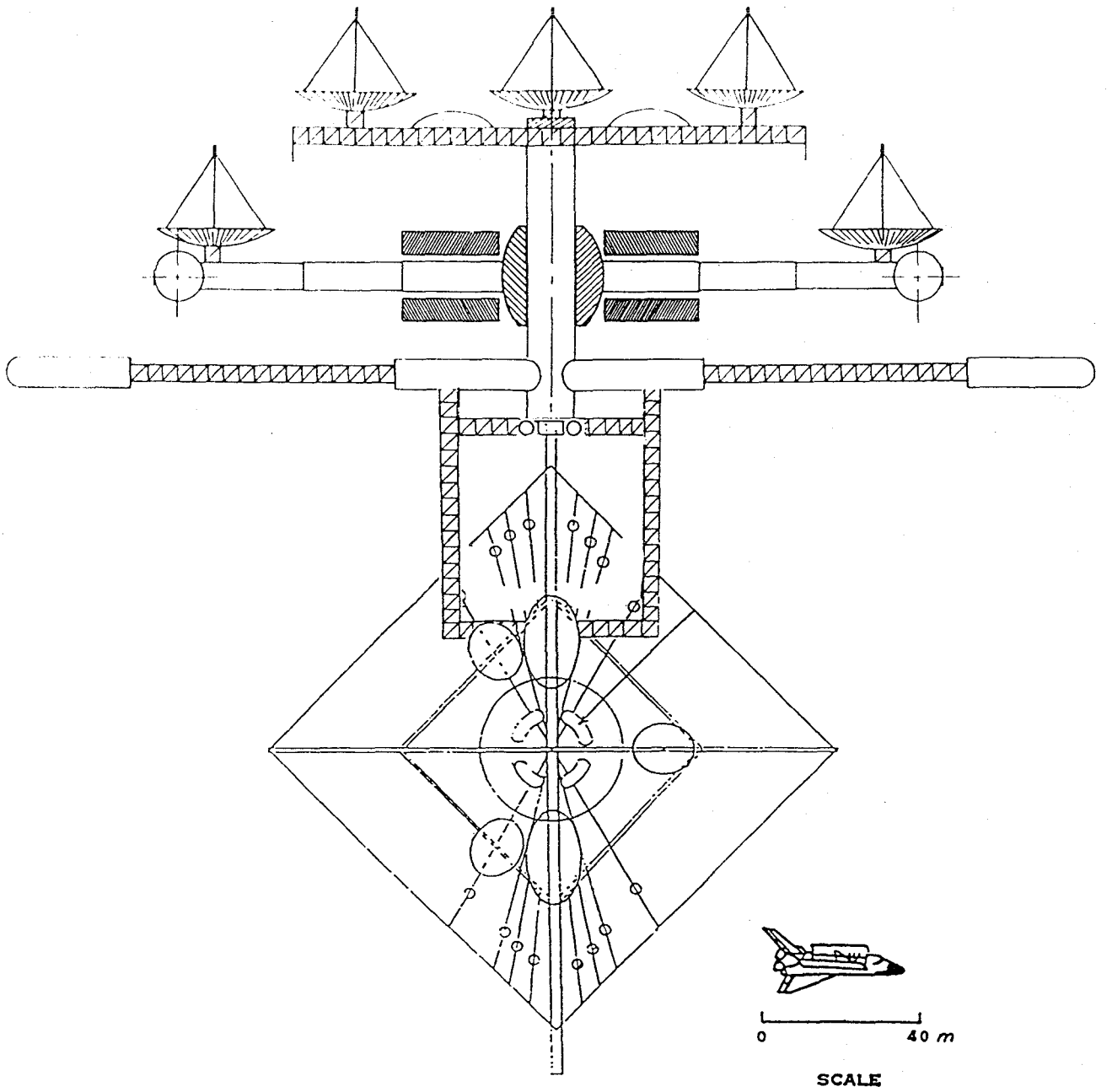

Figure 9.2-3 Texas A&M/UTA Manned Mars Mission Spacecraft Assembled at Advanced-Technology Space Station

- Insignificant impact on microgravity accommodation, CMG sizing and passive attitude stability.

9.2.5 Fuel Requirement Effects

The reference missions specify a variety of propulsion systems. The propulsion methods listed in Table 9.1-1 include: Nuclear fuel with mercury propellant, H_2-O_2, CH_4-O_2, MMH-N_2O_4, and strap-on solid rockets.

The handling techniques and safety precautions associated with some of these systems for receiving, storing, and loading could significantly increase the complexity, manpower or robotic requirements, and auxiliary equipment required at the Space Station.

The ATSS is designed to derive the maximum synergy from an all H_2-O_2 system. It is expected that this concept could be extended to a Mars mission based at the ATSS. The Langley SSO study has all H_2-O_2 propulsion systems for its three different vehicles. It is recommended that as designs for a Mars mission mature, the overall impact of exotic fuels versus a common base fueled H_2-O_2 fuel system be reviewed. The availability of large HLLV's and the H_2-O_2 fuel production capability of the ATSS may tip the balance in favor of H_2-O_2 over the higher specific impulse fuels. These considerations are based on today's technology and it is likely that in the 2025 time frame, new technologies, such as fusion power or super-conducting energy storage, could make them obsolete.

9.2.6 On-board Fuel Production

For H_2-O_2 based propulsion systems, the cryogenic fuel could be delivered from Earth to LEO. An alternate method would be to deliver

water to the ATSS and convert it to fuel using some of the 2.5 MW energy capability and the on-board electrolysis conversion and storage systems.

A more detailed trade would be needed to ascertain the best choice, however, overview calculations can show the scope for the trade.

Assume that 10^6 kg (2.2×10^6 lb) fuel is needed and that one-half the ATSS available energy is devoted to fuel conversion. Also, assume that radiators are available for cooling the gasses to liquid and 20 percent more energy is needed for pumping, control, etc.

If the energy is 4 kW-hr per kg of water converted, 160 days would be required. The fuel production would most likely serve as an energy use leveler and would be programmed to complement other on-board high energy applications such that the actual rate of production and time required might be different.

A rough idea of water transport versus cryogen transport costs can be gained by using the masses and volumes of the individual tanks within the Shuttle Orbiter external tank and assuming that the mass of the water transport tank is the same as the LO_2 tank using Figure 7.2.3-6 from Section 7 as a reference. The calculations show:

	Tank mass kg (lb) $\times 10^4$	Tank volume liters (ft^3) $\times 10^5$	Content mass kg (lb) $\times 10^5$
LH_2 tank and intertank	1.9 (4.1)	15 (0.54)	1.06 (2.3)
LO_2 tank	0.57 (1.2)	5.5 (0.2)	6.3 (14)
Tankage for LH_2-LO_2	2.4 (5.3)	21 (0.73)	7.4 (16)
Water tank	0.57 (1.2)	5.7 (0.2)	5.7 (12)

$$\frac{\text{Cryogen tank Mass}}{\text{Cryogen Mass}} = \frac{2.4 \times 10^4}{7.4 \times 10^5} = 3.3\%$$

$$\frac{LO_2 \text{ tank Mass}}{\text{Water Mass}} = \frac{5.7 \times 10^3}{5.7 \times 10^5} = 1\%$$

Using these same percentages to determine tank masses for 10^6 kg (2.2×10^6 lb) of water versus cryogen payload, the mass decrease would be 2.3×10^4 kg (5.1×10^4 lb). If the cost were $1000 per kg to LEO, the savings would be $23 million plus the simplifications inherent in a water payload. These savings are to be compared with the use of on-board resources to electrolyze water for 160 days.

9.2.7 OTV Support

Two of the three reference missions depart for Mars from a HEO and require the use of OTV's to transport the crews rapidly through the Van Allen radiation belt. OTV flights would also be needed for checkout or last minute updates to the Mars spacecraft while in HEO although possibly the Mars spacecraft could be completely prepared at the ATSS before the slow unmanned spiral to HEO; in such a case only the flights necessary for crew transport and return at end of mission would be needed. In any event, the ATSS is capable of berthing and fueling the OTV's for the Mars mission support required. A Mars mission using H_2-O_2 propulsion has the advantage of departing directly from LEO and avoiding the use of OTV's. On return from Mars, there might be an advantage in leaving a Mars IPV at HEO for refurbishment by OTV's although any extensive rework would most easily be accomplished by return to the ATSS. The ATSS was designed to provide the space for hangers and the capability to fuel OTV's. Reference 9-5 discusses the impact on the IOC Space Station that would be produced by the extensive use of OTV's to support lunar and planetary missions.

REFERENCES

9-1 Cirillo, William M. et al.: Manned Mars Mission Accommodation-Sprint Mission. NASA TM 100598, April 1988.

9-2 1986 Space Systems Engineering class, MIT: Mars, A Program for its Exploration and Development.

9-3 George, Jeff; Groves, Alison; Mahoney, R.J.; Monroe, Darrel: NASA/Universities Space Research Association Texas AMU/UT. 1986 Summer Intern Design Team Final Report, August 8, 1986.

9-4 Manned Mars Missions Working Group Papers: NASA NASA TM-89320/ TM-89321 June 1986.

9-5 Impact of Lunar and Planetary Missions on the Space Station. NASA CR-171832, November 1984.

10.0 IDENTIFICATION AND ASSESSMENT OF TECHNOLOGY DEVELOPMENT REQUIRED FOR THE ADVANCED-TECHNOLOGY SPACE STATION

The Advanced-Technology Space Station (ATSS), as its name implies, is based on the assumption that new and emerging technologies will have advanced to the point of being viable for use in the ATSS. The purpose of this section is to identify these pacing technologies and to assess their need or criticality relative to the ATSS.

10.1 ATSS Configuration and Functions

The conceptual configuration of the ATSS was based largely on three major premises:

1) The human habitat would rotate to provide artificial gravity.

2) The Space Station would support 17 functions identified in Reference 10-1 and repeated herein as Table 10.1-1.

3) Technology trends would be reviewed, and new technology deemed available around the year 2025 would be used where feasible.

10.2 Ranking Criteria for Technical Need or Criticality

A ranking criteria was developed for indicating the technical need or criticality of technology areas felt necessary to make the ATSS feasible by 2025. This criteria assigns a number from one to ten to each technology area, with the higher numbers indicating the greater need. The ranking criteria are listed in Table 10.2-1. The criteria and ranking are somewhat arbitrary, but are felt to be reasonably valid based on state of the art and the requirements for the ATSS.

TABLE 10.1-1 POTENTIAL FUNCTIONS TO BE SUPPORTED BY THE ADVANCED-TECHNOLOGY SPACE STATION

1. A permanent observatory to look down upon the Earth and out into the universe.
2. An orbiting science, medical, materials, and new technologies laboratory.
3. A service and repair facility for payloads, spacecraft, and platforms.
4. An assembly facility where large structures or spacecraft components are manufactured and/or assembled and tested for operation.
5. A transportation node where payloads and vehicles are collected, stationed, processed, and launched and where fuel is manufactured.
6. A safe habitat for space crews.
7. A communications and/or relay station for manned or unmanned spacecraft.
8. An adaptation area (in variable "g") in preparation for long space flights.
9. A storage node for food, fuel, spare parts, etc.
10. A variable "g" research facility.
11. A commercial manufacturing facility (drugs, crystals, etc.)
12. An energy collection and relay station.
13. A diagnostic, medical, and convalescent facility.
14. A tourism attraction.
15. A horticultural research and food growth facility.
16. A technology demonstration facility.
17. A control center for manned and unmanned spacecraft.

TABLE 10.2-1 RANKING CRITERIA FOR TECHNICAL NEED OR CRITICALITY RELATIVE TO THE ADVANCED-TECHNOLOGY SPACE STATION

CRITICALITY ASSESSMENT	CRITICALITY RANKING
The technical advance will enhance the performance of the subsystem or element. Alternate means for accomplishment exist and could be incorporated with a modest compromise in weight, performance, operating complexity, etc.	1 2
The degree of technical advance will define the performance of the subsystem. Alternate means would limit the subsystem performance and compromise other subsystem operations.	3 4
The technical advance is required for subsystem operation. Reduced performances would compromise other subsystems and impact the functioning capability of the ATSS.	5 6
The technical advance has no alternative for accomplishing the subsystem performance and identified synergies.	7 8 9
The ATSS cannot be configured without this technology capability.	10

10.3 Identification and Ranking of Pacing Technologies

A review of the state of the art technology and technology forecast for the NASA Space Systems Technology Model (Reference 10-2) has helped identify technology trends to the year 2000. Literature reviews provided indications of developments and projected developments in many areas of technology. Overall, 23 pacing technology items were identified and ranked. These are listed in Table 10.3-1 in the order of increasing criticality. The table is followed by supplementary material in corresponding order for each technology, organized as:

Technology Title

A. Subsystem and synergies

B. Function performed and particular features

C. Development status and actions

D. Criticality Ranking

10.3.1 Improved Structural Design, Analysis and Assembly Methods

A. Subsystem and Potential Synergies

Structure and mechanism: Synergy throughout the ATSS in that the improved design methods will provide minimum mass structure and mechanisms.

B. Functions Performed and Particular Features

The improved structural design analysis would provide the means for optimizing structural details to minimize mass. The analysis would address filament placement in wound structures in a manner which best accommodates predicted loads. The analysis would address detailed features such as bosses, cutouts, and local reinforcements in a manner that optimizes stress profiles to achieve minimum mass. The improved

TABLE 10.3-1 SUMMARY OF THE TECHNOLOGICAL REQUIREMENTS FOR THE ADVANCED-TECHNOLOGY SPACE STATION

	Technology Item	Technology Area	Criticality Ranking
1.	Improved Structural Design, Analysis and Assembly Methods	Struct/Mechanisms	4
2.	Aft Cargo Carrier for the Shuttle I External Tank	Transportation	4
3.	Use of Shuttle I External Tanks for Cryogenic Fuel Storage	Propulsion	4
4.	Filament Reinforced Structural Composites	Struct/Mechanisms	4
5.	Spent External Tankage as Structural Building Elements of Spacecraft	Struct/Mechanisms	4
6.	Magnetic Torquing with Superconductivity	GN+C	4
7.	Ambient Atmosphere Selection Less Than 1 Atm	Operations	5
8.	Improved Thermal Control Devices and Radiators	Thermal	6
9.	Lightweight Industrial Equipment	Operations	6
10.	High Pressure Space Suit	EVA	6
11.	Expandable and Modular Structural Concepts	Struct/Mechanisms	6
12.	Supercritical Wet Air Oxidation	ECLSS	7
13.	Concentrating Solar Dynamic Power Generators	Electrical Power	7

TABLE 10.3-1 SUMMARY OF THE TECHNOLOGICAL REQUIREMENTS FOR THE ADVANCED-TECHNOLOGY SPACE STATION (concluded)

	Technology Item	Technology Area	Criticality Ranking
14.	Attitude Control and Reboost Thruster System Based on Using H_2-O_2 Fuel	Propulsion	7
15.	Gas Separation by Semipermeable Membranes	ECLSS	7
16.	Predictions of Dynamics and Control of Large Space Vehicles with Flexible, Rotating, and Articulating Components	GN+C	8
17.	Articulated Air Lock Doors and Seals	Struct/Mechanisms	9
18.	Heavy Lift Launch Vehicle	Transportation/ Operations/ Logistics	9
19.	Large Diameter Rotating Joints and Servo Controlled Drives	Struct/Mechanisms	10
20.	Large Diameter Gas Seals for Rotating or Otherwise Moving Joints	Struct/Mechanisms	10
21.	Telerobotic Assembly Machines and Orbital Maneuvering Vehicles	Struct/Mechanisms	10
22.	Artificial Gravity by Rotation, System Operation, and Control	Guid/Navigation	10
23.	Artificial Gravity Technology	Human Factors	10

design analysis would reside in computer aided engineering and design (CAE-CAD-CAM) software and become a fundamental part of the effort to produce hardware. The analysis coupled with materials selection and careful attention to joining techniques compatible with space assembly would achieve the 20 to 50 percent in mass reduction predicted for the advanced design concepts.

C. Development Status and Actions

The structural design and analysis for advanced structures should parallel the development of the data base of advanced materials including structural composites of graphite fiber reinforced resins, ceramics, glasses, and metals.

D. Criticality Ranking: 4

10.3.2 Aft Cargo Carrier for the Shuttle I External Tank

A. Subsystem and Potential Synergies

Launch support and orbit assembly: Synergy with system operation, the Shuttle I external fuel tank is capable of being inserted in low Earth orbit (LEO) but is usually jettisoned just before orbit insertion. The external tank burns up during atmospheric reentry. The addition of an aft cargo carrier (ACC) to the external tank and the use of adequate fuel to accomplish LEO insertion would permit carrying larger experiments and cargo into orbit than can be accommodated in the Shuttle cargo bay.

B. Functions Performed and Particular Features

The addition of an ACC permits transport of a variety of additional experiments and equipment to LEO. The size of the ACC module is 8.4 m (27.5 ft) in diameter by 6.1 m (20 ft) in length. There are conceptual

designs indicating a habitat module of these proportions could be supplied to LEO by using the ACC concept. The external tank, in its present design, contains 2.4 x 10^4 kg (5.3 x 10^4 lb) of aluminum alloy assembled liquid tight and pressure tested to 248 kPa (36 PSI) differential pressure. The value of the external tank delivered to LEO, based on $4,400 per kilogram ($2,000 per pound), equates to $106 M.

C. Development Status and Actions

Studies have been made to achieve maximum utilization of the external tank that is presently jettisoned during each Shuttle launch. Proposed designs indicate that the existing external tank could be used as a habitat, a fuel storage depot, and could extend the Space Transportation System's (STS) payload launch capabilities by adding an ACC. The ACC may well be utilized for additional transport capability of a Shuttle to LEO for assembly of the ATSS for the year 2025.

D. Criticality Ranking: 4

10.3.3 Use of Shuttle I External Tanks for Cryogenic Fuel Storage

A. Subsystem and Potential Synergies

Launch support and orbit assembly: Synergy with system operations

The Shuttle I external tankage has sufficient contingency fuel for insertion into LEO along with the Shuttle vehicle. The external tank could be utilized for storing hydrogen and oxygen in cryogenic liquid form for fueling orbital transfer vehicles and Mars mission and lunar lander spacecraft. Normally, the spent external tank with residual fuel aboard is jettisoned just prior to orbit insertion and is destroyed during atmospheric reentry.

B. Functions performed and particular features

Spacecraft could be fueled with hydrogen and oxygen manufactured aboard the ATSS. A fuel storage depot may best be provided by free flying external tankage co-orbiting with the Space Station. The Shuttle I external tankage could provide the volume necessary to store 6.8×10^5 kg (1.5×10^6 lb) of fuel per unit. The Mars mission may require 1×10^6 kg (2.2×10^6 lb) of fuel depending on the mission design.

The present configured external tank is coated with a cryogenic insulation consisting of polyurethane foam sprayed on the exterior of the tank. There is concern that the foam insulation will outgas in LEO and contaminate the Space Station's critical surfaces such as optics and thermal control coatings.

C. Development, Status and Actions

Suggested modifications to the Shuttle I external tankage would be as follows:

1. Develop a flight-worthy cryogenic insulation which does not outgas in the space environment.

2. Modify the tank construction as required for utilization as a storage tank for receiving and delivery of fuel for supported missions.

3. Develop a flexible cryogenic insulation suitable for use in LEO which can be carried aboard Shuttle I or Shuttle II for application on orbit to the exterior of the external tank. The purpose of this insulation is to augment the previously applied insulation so that long term fuel storage can be achieved with minimum fuel boiloff.

4. Design a station keeping propulsion system to maintain the orbital path of the external tankage so that it may co-orbit with the ATSS.

D. Criticality Ranking: 4

10.3.4 Filament Reinforced Structural Composites

A. Subsystem and Potential Synergies

Structures and mechanisms subsystem: Synergy with all structure elements which can use structural composites of graphite fiber reinforced metals, glasses, and synthetic resins.

B. Functions Performed and Particular Features

Structural composites offer mass savings of 10 to 30 percent over conventional light metals. Pressure vessels can be wound from continuous filament reinforced synthetic resin complete with end dome closures and localized reinforcement. Axially collimated fiber reinforced tubes can be molded to yield high strength truss structure elements with near zero thermal expansion characteristics.

C. Development Status and Actions

Extensive work has been accomplished using carbon or graphite filament reinforced synthetic resins. Graphite epoxy composites require metallic cladding to protect them from solar radiation or atomic oxygen, and to minimize outgassing of the organic resin matrix. Limited laboratory development has indicated the feasibility of producing metal matrix and glass matrix composites which possess near-zero thermal expansivity and minimal outgassing. The ATSS would benefit by manufacture of the following structures from structural composites:

1. Cylindrical sections of the torus; each section 16.4 m (50 ft) in diameter by 30.5 m (100 ft) in length.

2. Mirror support structures.

3. Truss structure.

4. Pressure vessels.

D. Criticality Ranking: 4

10.3.5 Spent External Tankage for Structural Building Elements of Spacecraft

A. Subsystem and Potential Synergies

Structures and mechanisms: Synergy with systems operations.

The NSTS design of the propulsion system could be configured so that the external tank could be inserted in LEO and utilized as a pressurizable, structural building module for space station construction.

B. Functions Performed and Particular Features

The propulsion system tankage for the NSTS could be designed to serve as habitat modules. The tankage would have features such as entry ports, which could be later outfitted with air locks. The internal structure could be scarred to receive fitments, equipment, and controls to serve as a habitation module. The structural ends of the tank could be designed for attachment to other tanks to serve as structural building blocks.

C. Development, Status, and Actions

1. Consideration of a dual purpose tank for the NSTS propulsion system would be beneficial using the tankage as building blocks for future space station applications. The tankage design for personnel access and air lock fitments could be incorporated in the design.

2. Thermal insulation systems that do not outgas in low Earth orbit and could be removed or incorporated into the thermal control of the habitat module would be desirable.

3. Design internal structural attachment locations which are scarred to receive internal fitments.

4. Design the pressure vessel for use at one Earth atmosphere internal pressure.

5. Incorporate within the design of the propulsion system sufficient fuel volume to assure LEO insertion.

D. Criticality Ranking: 4

10.3.6 Magnetic Torquing with Superconductivity

A. Subsystem and Potential Synergies

Guidance and control subsystem: There will be a pervasive synergy throughout all subsystems if predicted "high" temperature superconductivity performance is achieved in addition to the synergy with propulsion and power subsystems for torquing applications.

B. Functions Performed and Particular Features

If "high" temperature practical superconductivity applications are available, they will appear in every future Space Station application where magnetic fields are used including motors, solar dynamic generators, radio transmitters, scientific instruments, and computers. High current superconductions would provide precession torques with torus-circumferential windings or torus rotational torques with ring-circumferential windings. The low losses associated with superconductors would conserve significant energy by reducing the propulsion subsystem fuel usage required to provide the torque or by reducing the power

subsystem energy usage needed to provide I^2R losses in non-superconductivity magnetic coils.

C. Development Status and Actions

The field of "high" temperature superconductivity is moving rapidly. Superconductivity measurements at liquid nitrogen temperatures are reported, and hints of room temperature operation are noted. The extent to which high fields and currents can be produced in practical engineering configurations will determine how rapidly superconductivity can be applied for the ATSS.

D. Criticality Ranking: 4

10.3.7 Ambient Atmosphere Selection Less Than 1 Atm

A. Subsystem and Potential Synergies

Environmental control and life support subsystems: Synergy with structure and life support.

The selection of less than a standard Earth atmosphere interacts with several other functional elements and design features of the ATSS. Reduced internal pressure will proportionally reduce the pressure shell mass and the internal gas atmosphere mass. Leakage and make-up would also be influenced in a positive sense. Reducing the pressure difference between the EVA space suit and the cabin would result in a reduction of the time required for the prebreathing protocol.

B. Functions Performed and Particular Features

The atmosphere provides the shirtsleeve environment in the Station for effective crew operations and the environment for life sciences and other experiments. There are two primary regions of historical

operations that relate to the atmospheric conditions. Those on Earth with ambient air operating at pressure altitudes up to about 3 km (10,000 ft), and prior U.S. space activity at 25 to 35 kPa (3.6 to 5 psia) pressure in pure or high oxygen concentration atmosphere. The trades indicate significant structural mass savings for the pressure shell in proportion to selected pressure. Reducing the torus internal pressure to 0.8 of one Earth atmosphere would reduce the pressure shell weight by 20 percent (Section 8.4).

Lower pressures require higher proportions of oxygen and are intrinsic hazards of ignition and combustion for conventional materials. The potential interest lies in the range of 50.7 to 81 kPa (0.5 to 0.8 atm) pressure at first estimate with oxygen levels at 50 percent or less. Detail selection will be dependent upon the human limits and the combustion hazards.

C. Development Status and Actions

Some EVA suit work is ongoing in the range of pressure cited above. However, the conditions are not common to any other large data base of results. The selection other than an Earth atmosphere air mixture would require a verification program on humans as well as other life science subjects aboard the station.

1. Limits for pressure and oxygen would have to be developed or researched for many materials and processes relative to an ignition or combustion hazard.

2. Human tolerance and influences of various combinations within the safe range would have to be developed.

3. Life science verification studies and projections would have to be researched to determine if separate isolated "Earth atmosphere" zones would be required.

D. Criticality Ranking: 5

10.3.8 Improved Thermal Control Devices and Radiators

A. Subsystem and Potential Synergies

Thermal control: Synergy with electrical power and life support and system operation.

The thermal control subsystem would use waste heat from the electrical power subsystem to maintain thermal control of such areas as the cabin environments, truss mounted experiments, and horticultural domes.

B. Functions Performed and Particular Features

Thermal control systems are currently available to transport heat by pumped fluids or heat pipes that operate on fluid phase change, two phase heat pipe radiators to reject unwanted heat, and capillary pumped loop technology. These systems will perform functions such as environmental thermal control, removal of unwanted heat from manufacturing processes and experiments, and maintaining an internal thermal balance. The ATSS has an identified radiator requirement associated with the generation of 2550 kW electrical power. Much of this power can eventually appear as heat dissipated into the on-board atmosphere from on-board operations such as ventilation, illumination, food preparation, manufacturing, and processing of water. Each area or locale where heat must be extracted will need an appropriate thermal control element. The eventual load applied to the exterior radiators due

to on-board power generation then equates to the 3900 kW (3714 Btu/sec) rejection from the converters plus the 2550 kW from the internal power delivered (Table 3.2-1). There will be an additional increment resulting from the crew consumption of food and the residuals from solar thermal balance.

C. Development Status and Actions

The physical size of the ATSS dictates high efficiency heat pipes, thermal busses, radiators, and capillary pumped loops to transport heat over greater distances with less weight than provided by today's technology.

D. Criticality Ranking: 6

10.3.9 Lightweight Industrial Equipment

A. Subsystem and Synergies

Life support subsystem: synergy with system operations.

B. Functions Performed and Particular Features

Industrial equipment items perform the detail steps in all of the life support, fabrication, and system operating functions. The listing below identifies the generic types of equipment in descending order of criticality for the ATSS:

Listing of Lightweight Industrial Items

1. Electric motors
2. Electric power conditioning
3. Electrolytic cells for H_2-O_2
4. Fluid pumps
5. Gas compressors
6. Air circulating fans
7. Pressure vessels, both liquid and gas
8. Bonding and joining tools
9. Metal-working machine tools
10. Composites forming tools

Within the listing, the items from one through seven are used within the

life support system. The other items provide the required on-board fabrication and spacecraft support functions.

C. Development Status and Actions

Each type of equipment has been well developed for ground operation. Items one through seven have been addressed for space flight applications involving modest power levels and microgravity environments. A recent development in electric motors has resulted in lightweight, high-relative-speed units in the 10 to 20 kW range. The ATSS will require motors in the 50 to 100 kW range. Most of the developments will address the reduction in weight in terms of materials substitutions; the electrical items will be constrained by the requirements for iron in magnetic elements, such as pole pieces, armatures, cores, etc. The developments generalize as:

1. Develop a series of minimum weight equipment items to perform the life support functions (items one through seven).

2. Develop lightweight tool and equipment configurations which can perform the bonding-joining, metal-working, and composite fabrication functions defined for the ATSS.

D. Criticality Ranking: 6

10.3.10 High Pressure Space Suit

A. Subsystems and Potential Synergies

EVA subsystem: Synergy with life support and system operation.

B. Functions Performed and Particular Features

High pressure space suit with associated life support will be required for EVA to assemble the ATSS structure on-orbit, to install experiment modules on the spacecraft's exterior, to inspect and repair

the spacecraft exterior when damaged by debris or other causes, and to perform emergency repairs.

The NSTS Orbiter astronaut currently wears a low pressure space suit (30 kPa or 4.3 psia) for performing EVA. The astronaut must undergo a lengthy prebreathe protocol ranging from four to 26 hours to avoid decompression sickness.

Two high pressure space suits (57 kPa or 8.3 psia) are currently under development by NASA (Reference 10-4). One of the two configurations will be selected for use with the IOC Space Station when permanently manned in approximately 1996. The high pressure space suit will provide the following capabilities:

1. The suit will eliminate the need for prebreathing.

2. The suit will be non-venting.

3. The suit's atmosphere will be recycled by the portable life support system.

4. The manual dexterity and tactile sensing of the astronaut's glove will be upgraded through an evolutionary process. Recently developed high pressure gloves have comparable dexterity and tactile sensing to the NSTS Orbiter low pressure gloves.

5. The high pressure suit will eliminate the decompression sickness (bends) problems associated with the low pressure space suit.

6. The atmosphere of the high pressure suit will not pose an oxygen toxicity problem even in a worst-case suit leakage condition when the suit's atmosphere approaches 100 percent oxygen.

7. The high pressure suit will be rechargeable and maintainable on orbit for repeated use.

C. Development Status and Actions

An advanced high pressure space suit for the year 2000 and beyond should encompass the following features:

1. High pressure gloves would have improved dexterity and tactility with cut and puncture protection qualities.

2. The high pressure suit would be constructed more like a hard-chamber whereby the EVA astronaut could withdraw his hands from the gloves and suit arms to eat lunch or relax, permitting longer EVA excursions. The suit could be self-propelled to minimize the physical effort of self positioning.

3. The operational features of the suit would allow relatively untrained personnel to perform EVA, suggesting civilian visitors could participate in the EVA excursions.

4. On-scene robotics with end effectors could amplify the astronauts manual strength and abilities to perform demanding tasks during EVA.

The ATSS cabin environmental pressure can be selected between 57 kPa (8.3 psia) to 101 kPa (14.7 psia), based on engineering requirements, instead of a prebreathe protocol.

D. Criticality Ranking: 6

10.3.11 Expandable and Modular Structural Concepts

A. Subsystem and Synergies

Structures and mechanisms: Synergy with most other subsystem developments. The use of modular pressure vessels, erectable antennas, solar concentrators and radiators are all potential beneficiaries of this

technology. Each of the subsystems would show weight efficiency benefits or ease of deployment in space.

B. Functions Performed and Particular Features

The function is to provide large size vehicle components which originate in the delivery system as collapsed or otherwise condensed elements. Examples include solar collectors, arrays such as focusing mirrors, antenna forms, and deployable or furlable equipment. There are at least three classes of these concepts: a) nonrigid, which is either flexible or rigidized in space; b) semirigid panels, sections, or modules which change shape or volume in space; and c) rigid modularized components for assembly in space with total weight and volume fixed.

C. Development Status and Actions

1. Nonrigid: These include current smaller scale demonstration efforts such as core foam on command and resin impregnated fabrics rigidized by various environmental modes (ultraviolet, water vapor, or other catalyst). There are also a variety of composite wall structure concepts to be evaluated to generate rigid structures.

2. Semirigid: Furlable and telescoping structures which can be packaged in a condensed state and later extended in space to generate an expandable volume. These include parabolic antenna shapes with rigid but nested petals or gores which deploy to a full shape. Helical bands which uncoil to form tubes are also included in this category.

3. Rigid: These elements include truss assemblies and modules. In general the technology of remote manipulators and assemblers will accompany these developments.

The actions required include the generation of expandable structural concepts and the development of compressed storage geometrics for rigid components.

D. Criticality Ranking: 6

10.3.12 Supercritical Wet Air Oxidation

A. Subsystem and Potential Synergies

Life Support Subsystem: Synergy with propulsion for on-board generation of H_2, O_2, and any on-board processes involving aqueous organic solutions.

B. Functions Performed and Particular Features

Supercritical wet air oxidation will provide the means for a combustion disposal of human wastes together with reclamation of waste water from food processing, bathing, laundry, and housekeeping. The process will oxidize any solution or fine-particle suspension of organic carbonaceous or organic nitrogenous material. A cycle that includes temperatures and pressure above the critical point for water will oxidize carbon to CO_2 and hydrogen to H_2O plus liberating GN_2 and precipitating inorganic compounds as salts (e.g. Na, K, Ca). The process has the capacity to reclaim water for further utilization, extract CO_2 for further reduction, and recover N_2 for atmospheric balance. In addition, the oxidation reactions generate heat energy at conditions which allow further utilization (e.g. in turbo-pumps).

C. Development Status and Actions

Supercritical wet air oxidation has been demonstrated at laboratory scale. Subcritical wet air oxidation is an established industrial

process. The developments required for Space Station applications appear as:

1. Development of an operating sequence for the ATSS which will accommodate the throughput volumes and waste stream contents. The complexity appears in the control of a rapid heat-producing reaction during transitions into and out of the supercritical regime.

2. Development of flight grade pressure vessels, flow passages, and control items. The supercritical regime require operation at pressures above 27.6 MPa (4000 psi) and temperatures above 673 K (1210 ^{o}R). The ongoing chemical reactions require an internal lining which is inert to oxygen under such conditions.

D. Criticality Ranking: 7

10.3.13 Concentrating Solar Dynamic Power Generators

A. Subsystem and Potential Synergies

Electrical Power Subsystem: Synergy with the thermal control subsystem to provide a source of high level heat and synergy with life support in the use of electrolysis cells as load levelers and energy storage.

B. Functions Performed and Particular Features

Concentrating solar dynamic power generators will provide electrical power to the ATSS. Solar-pointed focusing collectors will beam concentrated solar energy on a receiver which serves as the input to a thermodynamic power cycle. Related equipment includes the thermal-mechanical conversion equipment producing electrical energy and the radiator assembly for providing the condensing or cooling function. Subsidiary to these are heat conducting flow loops to transfer the

working fluids. The ATSS concept uses six identical units delivering 425 kW each to supply the electrical power.

C. Development Status and Actions

Component parts of lower power systems have been demonstrated. Developments needed are:

1. Highly reflective full-spectrum focusing concentrators with improved surface dimensional accuracy. Energy into the aperture is 0.9 of the total solar intercept for concentrators up to 40 m (135 ft) in diameter.

2. Weight and power efficient long life dynamic converter components. The converters deliver 40 percent of the solar input energy as electrical power to the ATSS.

3. Improved radiator emissivity and working fluid transport such that the radiator areas and concentrator area are the same.

D. Criticality Ranking: 7

10.3.14 Attitude Control and Reboost Thruster System, in the Range 400 to 5500 N (100 to 1200 lb), using H_2-O_2 On-board Generated Fuel

A. Subsystems and Potential Synergy

Propulsion: Synergy with life support subsystem in the on-board generation of H_2-O_2 and synergy with logistic resupply as relief from the transport of cryogenic fuels.

B. Functions Performed and Particular Features

Attitude control and reboost thrust from H_2-O_2 fuels at a specific impulse of 4315 N-sec/kg (440 sec) provides the combination of energy efficiency and the clean exhaust necessary for continuous operation of the ATSS in orbit. The utilization of excess electrical power to produce H_2 and O_2 from water will provide the life support needs with a

surplus sufficient for all station-keeping propulsion fuel requirements and in addition, provide fuel for the OMV and OTV. Resupply for the ATSS then becomes potable water which eventually enters electrolysis after reclamation from crew wastewater.

C. Development Status and Actions

The main engines for the shuttle are large H_2-O_2 engines with lift-off specific impulse values in the 3400 to 3500 N-sec/kg (350 to 380 sec) range and operate with chamber pressures at 20 MPa (3000 psi). Small H_2-O_2 engines in the 450 to 5500 N (100 to 1200 lb) thrust range do not presently exist. The development actions are:

1. Develop a series of combustors and nozzles covering the thrust range from 450 to 5500 N (100 to 1200 lb) capable of operating with chamber pressures in the 20 to 35 MPa (3000 to 5000 psi) range. The minimum operating life would be 1000 burns of 20 sec each.

2. Develop the tankage, supply lines, flow control valves and control techniques to support the thrusters.

3. Develop the compressors and fuel transfer techniques to support the system.

D. Criticality Ranking: 7

10.3.15 Gas Separation by Semipermeable Membranes

A. Subsystem and Potential Synergies

Life support: Synergy with propulsion in the on-board storage of O_2-H_2 fuels and synergy with any on-board process that generates volatiles which must be removed from a gas stream.

B. Functions Performed and Particular Features

Semipermeable membranes for gas separations will provide the means for scrubbing or selective separation of gaseous constituents. Membranes-in-series, each with a controlled porosity, have the potential for separating CO_2 from N_2 and the removal of large molecule trace contaminants from the cabin atmosphere. The membranes would offer particular advantages in scrubbing the residuals from galleys, on board laboratories, and some fabrication operations. The microgravity environment has been recognized as a means for producing films and polymeric materials with uniform controlled porosities tailorable to the passage of specific molecules.

C. Development Status and Actions

Semipermeable membranes are well established commercial items with applications that include renal dialysis filters, reverse osmosis separators, and gas purification. Present research involving microgravity is addressing ultra-thin films and optical quality polymers which will transmit molecular oxygen as a material for long wear contact lenses. The developments would extend the techniques to provide a high-flow separation capability for:

1. Extracting CO_2 directly from the cabin air streams.
2. Separating CO_2 from N_2 at the exit of the wet air oxidizers.
3. Separating O_2 and N_2 from other gasses evolved from on-board operations.
4. Separating trace quantities of H_2 from the ullage gases used during on-board storage of gaseous fuels.

The principal development focus will become improved flow at lower driving pressures. Microgravity processing may be a requirement, and the

development of a microgravity facility could pace the availability of these materials.

D. Criticality Ranking: 7

10.3.16 Predictions of Dynamics and Control of Large Space Vehicles with Flexible, Rotating, and Articulating Components

A. Subsystem and Potential Synergies

Guidance, navigation, and control subsystem: Synergies exist with most other subsystems.

B. Functions Performed and Particular Features

The analytical tools will perform structural dynamic evaluations as well as engineering mechanics evaluations to obtain the effects of flexible body dynamics. Features will include a rotating disc for simulating gravity and articulations. The predictions must address mass motions from within and from outside the rotating vehicle as personnel, fluids, and equipment are transferred about the vehicle.

C. Development Status and Actions

Current design tools will have to be expanded in capability to accept large rotating components and very large flexible components. Precession torquing and angular momentum management of the large rotational components will have to be modeled. Response to various impulse conditions, such as berthing of large vehicles and relative movement within the vehicle of substantial masses, i.e., personnel, working fluids, and general materials transfer, will have to be incorporated.

D. Criticality Ranking: 8

10.3.17 Articulated Air Lock Doors and Seals

A. Subsystem and Synergies

Structure: Synergy with system operations

B. Functions Performed and Particular Features

The articulated air lock doors seal the berthing and assembly bay end of the central tube and provide the internal pressure bulkheads needed to divide the central tube into working segments. These become air locks in support of station resupply or in support of assembly and repair of other spacecraft. Effective utilization of the central tube requires an air lock door system which can accommodate near full-tube diameter dimensions for equipment serviced. Articulated doors with seals appear as the candidate for the application. The smae concept used for the central tube would also apply to pressure doors in the smaller diameter tubular sections such as the docking bay, observation tube, the spokes and in the torus.

C. Development Status and Actions

One-piece movable pressure doors for air lock and autoclaves are well established items for both spaceflight and industry. The ATSS represents an expansion in size plus the need for segmentation which complicates the sealing technique. The axial load imposed upon a central tube air lock approaches 1.8×10^7 N (4×10^6 lb) for a one atmosphere pressure difference. The development activities indicated appear as:

1. Develop a minimum weight configuration for a segmented air lock door which will accommodate equipment packages or spacecraft elements up to diameters approximately equal to the central tube.

2. Develop a seal configuration and sealing technique for segmented air lock doors.

D. Criticality Ranking: 9

10.3.18 Heavy Lift Launch Vehicle

A. Subsystem and Potential Synergies

Launch vehicle: Synergy with all large structural elements.

B. Functions Performed and Particular Features

The launch vehicle delivers the station component parts to LEO for assembly. The current baseline design concept requires a capability of net payload of 2.7×10^5 kg (6×10^5 lb) to LEO, with a shroud envelope diameter of 33.5 m (110 ft) and length of 60.9 m (200 ft). This capacity is currently driven by the plan to deliver the rotating hub assembly as a one piece payload. This assembly contains the rotating bearings and seals for the torus and spokes.

C. Development Status and Actions

The ongoing NASA HLLV studies and evaluations for future launch vehicle remain somewhat parametric for multiple missions. The ATSS planning must be incorporated into the NASA-wide planning. Specific areas include the following:

1. Evaluations of large volume shroud envelopes of the capacity presented above. This includes the entire design evaluation of the various loads and configurations which are generic to the delivery of the large scale station components.

2. Shroud deployment methods to allow access to the payload by auxiliary equipment for transport to the vicinity of the on-orbit ATSS assembly area.

D. Criticality Ranking: 9

10.3.19 Large Diameter Rotating Joints and Servo Controlled Drives

A. Subsystem and Synergies

Structure: Synergy with systems operations

B. Functions Performed and Particular Features

The rotating joints provide the relative movement capabilities between sections of the ATSS. A continuous rotating joint at 16 m (52 ft) diameter operates at speeds up to 3 rpm and controls the relative motion between the nonrotating central tube and the rotating torus. This joint must accept up to 0.15 m (6 in) center offset between the central tube and torus and include a sensing technique for that offset which becomes an input to the torus trim-balance system. The drive system will provide sufficient torque to eliminate the drag reactions into the central tube. Similar joints at diameters of 25 m (82 ft) operate under the counterrotators; these joints will maintain relative motion between the counterrotators and the torus, in addition they transmit the torques that null the angular momentum of the system. The concentric joints within the end sections of the observation tube move to follow a tracking, communication, or Earth viewing operation. Motions can be either continuous or intermittent and can include reversals of direction. Those reversals must be accomplished without loss of tracking or beam lock during a communication sequence.

C. Development Status and Actions

These joints are generically related to camera mounts and gun turrets. The concepts for tracking motions and sensing of position have been developed for other applications. The developments for the ATSS are adaptations to the particular size and mission functions. The specific requirements appear as:

1. Configure a rotating joint which incorporates the requirements for the central tube to hub joints and the hub to counterrotator joints.

2. Configure a general rotating joint which incorporates requirements associated with the end elements of the observation tube.

D. Criticality Ranking: 10

10.3.20 Large Diameter Gas Seals for Rotating or Otherwise Moving Joints

A. Subsystem and Synergies

Structure: Synergy with systems operation.

B. Functions Performed and Particular Features

The large diameter, 16 m (52 ft), rotating seals operate between the central tube and the torus under continuous rotation up to 3 rpm with some center offset and a one atmosphere pressure differential. The friction drag will be countered by a servo drive. The seals must be capable of indefinite continuous operation which implies a means for replacement of any wearing surfaces while running. The seals at other locations, 9 m (30 ft) diameter, must accommodate motions in both directions, including changes in the direction-of-motion without disturbing a tracking function (e.g., bumpless) and accept extended periods of no relative motion. For the smaller seals, the change out of wearing surfaces must be performed without violation of the pressure

integrity; however, the change out could occur under conditions of no relative motion.

C. Development Status and Actions

Pressure sealing of joints with intermittent motion has been addressed in the development of the "8 psia Astronaut Suit" and shows leakage rates compatible with the IOC Space Station requirements for less than 4.5 kg/day (10 lb/day). Leakage establishes the major portion of the nitrogen resupply requirement. A projected leakage rate for the ATSS at ten times the IOC Space Station levels would require an annual GN_2 resupply of 10,000 kg (22,000 lb), which appears excessive. As a development goal, the total leakage from the 12 seals on the ATSS should be less than 10 percent of that projected value and be equal to the present IOC Space Station cabin leakage prediction of 2.3 kg (5 lb) per day. Rotating joints on the scale required do not exist and are not included in any of the presently defined missions. The development actions become:

1. Develop and configure pressure seals for the two continuous rotating joints at the central tube-hub interface. The estimates of the requirements for each joint seal are:

   a) Diameter, 16 m (52.5 ft) with up to 0.15 m (6 in) offset between rotating and nonrotating centers.

   b) Rotation up to 3 rpm.

   c) Pressure of one atmosphere.

   d) Leakage less than 0.22 kg/day (0.5 lb/day).

   e) Life 5 years minimum with change outer repair while running.

2. Develop and configure pressure seals for the ten joints and interfaces in the observation tube. The estimates of requirements for each joint seal appear as:

a) Diameters of 9 m (30 ft) up to 10 mm (0.5 in) center offsets.

b) Rotations up to 2 rpm either direction with a smooth reversal of direction.

c) Pressure of one atmosphere.

d) Leakage of 0.2 kg/day (0.5 lb/day) maximum.

e) Life five years minimum with change out or repair without loss of pressure integrity.

D. Criticality Ranking: 10

10.3.21 Telerobotic Assembly Machines and Orbital Maneuvering Vehicles

A. Subsystems and Potential Synergies

Structures and mechanisms: Synergy with system operation.

B. Functions Performed and Particular Features

The telerobotic assembly machines will perform the major operations throughout the on-orbit assembly of the ATSS. The machines will include mobile remote manipulation systems and truss assembly machines. Orbital maneuvering vehicles will provide the transport of the large components into the near-mating position. These elements will become part of the remote assembly and docking support manipulators within the assembly and docking bay.

The class of equipment including teleoperators, robotic assembly machines, and orbital maneuvering vehicles all perform amplification of

the crew capability in assembly of the ATSS. The specific features of the equipment will include the following capabilities:

1. Orbit maneuvering vehicles capable of taking the large mass components from the launch vehicle shroud and transferring them to the joining position on the ATSS.

2. Telerobotic machines that would perform the assembly of the torus and spoke segments once brought to proximity for assembly.

3. Truss assembly machines capable of joining the truss elements at the joints to perform the junction assemblies required in the ATSS.

C. Development Status and Actions

The entire technology of teleoperators and robotics is in active development. The several types of equipment required have industrial counterparts in concept. The principal new features will be the size of the large assembly teleoperators and the uniqueness of the orbit maneuvering vehicle. The assembly machines will work on an equipment scale of tens of meters and therefore will require booms and arms of commensurate size. This introduces the requirement for accurate placement controls over a large span of action.

D. Criticality Ranking: 10

10.3.22 Artificial Gravity by Rotation, System Operation, and Control

A. Subsystem and Synergy

Guidance, navigation, and control: Synergy with structural dynamics, life support, and system operation.

B. Functions Performed and Particular Features

The system operating control for the rotating portions of a space station has to provide a continuous monitor with corrective action over:

1. Center of rotation (out of round tolerance)
2. Plane of rotation (wobble tolerance)
3. Center of gravity
4. Rotating velocity and moment of inertia

These parameters include a sensing followed by a trimming ballast. The trimming will occur while the rotating section accommodates:

a. Movement of equipment and personnel circumferentially
b. Movement of equipment and personnel radially
c. Movement of equipment and personnel between the rotating and nonrotating portions of the ATSS.

These functions will involve the controlled transfer of ballast as a continuing motion. The function will occur while the control system recognizes structural dynamic effects, disturbances from rotating machinery, or structural coupling. Water will be the principal ballast medium and in addition provide for crew related functions as well as the input to fuel generation. All rotating systems will require the continuous control. The level of artificial gravity will determine the magnitude of the forces required and quantities of ballast transferred.

C. Development Status and Actions

The control system would be developed in conjunction with elements of structure, structural analysis, and predictive techniques. The principal effort will continue the predictive efforts and include:

1. Development of a control algorithm which can actively predict and accommodate the conditions listed above

2. Validate the control algorithm in a series of experiments and simulations of a rotating system. The initial validations will require

scale models operating on Earth followed by some degree of validation in space (e.g., a centrifuge or a platform in space).

D. Criticality Ranking: 10

10.3.23 Artificial Gravity Technology

A. Subsystem and Potential Synergies

Life support, crew operations: Synergy with all man tended operations.

The rotating system, the torus and spokes, provide "weight" to the human musculoskeletal system in the space environment. Reduction of the artificial "weight" will synergistically impact the structural load and mass of the vehicle, the counterrotation system, the rotating seal technology, and the control of the ATSS as complicated by the rotational elements. There will be a direct influence on human performance in the rotating areas.

B. Functions Performed and Particular Features

Reference 10-4 discusses the influences of weightlessness on human physiology and performance. The evidence of space flight experience indicates serious physiological problems and a degradation of the musculoskeletal system of humans. With the expectation of extended space missions, artificial gravity becomes a primary countermeasure for the degrading effects of weightlessness. Section 5 of this report and Reference 10-4 discuss the effects of artificial gravity and its attendant rotation on the human and his performance.

Spacecraft rotation is a complex problem regarding energy use, precession, general control, and center of mass location maintenance as well as rotating seals, and the movement of materials, fluids, and humans

between rotating and nonrotating environments. The least amount of rotation and the least amount of artificial gravity, or "weight", for the adequate maintenance of human physiology needs to be established.

C. Development Status and Actions

As the human is the critical element involved in the need for artificial gravity, reduced gravity studies with humans seem essential. Ideally, such experiments should be done in space. Experiments performed in the ATSS could attain 1 g at 2.8 rpm, 0.5 g at 2 rpm, and 0.25 g at 1.4 rpm. However, it seems essential to attain ground based knowledge of the effects of partial gravity at the earliest opportunity. A minimum of two levels of partial gravity seems necessary to attain information between the known 1-g condition and the partly-known weightless condition.

Studies of the response to partial gravity in the Earth's gravitational field seems an improbability. However, the 20 year-old studies of weightlessness in bed rest and water immersion attained great success and are still being held today. These experiments predicted man's performance in the moon's gravity by using sling supports at angles such that only one-sixth g was felt on the feet. Similarly, performance in artificial gravity was studied on rotating devices with slings supporting Earth's weight while the artificial gravity due to rotation was weighted on the feet (Reference 10-5).

Special studies could be performed with inclined platforms and slings where the long body axis is exposed only to partial g much as weightlessness is studied on Earth in bed rest. The test regime should encompass work stations, exercise and mobility stations, rest and recreation stations and sleep stations in a normal flat bed. With

sufficient subjects and an appropriate duration of testing, the loss of bone minerals, muscle mass, etc., may be stabilized for each partial gravity level while under a space simulted regime, including work, exercise, rest, and sleep.

D. Criticality Ranking: 10

10.4 Conclusions

Advancements in technology are required to make the ATSS feasible. These technologies have been reviewed and a criticality number from one to ten assigned for each technology. The criticality factor of ten indicates a technology vital to the station and may require extensive development.

REFERENCES

10-1 Queijo, M. J. et al.: An Advanced-Technology Space Station for the Year 2025, Study and Concepts, NASA CR-178208, March 1987.

10-2 NASA Space Systems Technology Model. NASA TM 88174, June 1985.

10-3 NASA Space Systems Technology Model. Vol. 1, Data Base, Part A, Technology Forecasts; Vol. 1, Data Base, Part B, Technology Forecasts; Vol. 2, Data Base, Technology Analysis; Vol. 3, Data Base, Future Mission Payloads; NASA TM 88176, 1985.

10-4 Shifrin, Carole A. et al.: NASA to Evaluate Two Suit Designs for Space Station, Aviation Week and Space Technology, January 11, 1988.

10-5 Queijo, M. J. et al.: Analyses of a Rotating Advanced-Technology Space Station for the Year 2025, NASA CR-178345, January 1988.

NASA

Report Documentation Page

1. Report No.	2. Government Accession No.	3. Recipient's Catalog No.
NASA CR 181617		

4. Title and Subtitle

Some Operational Aspects of a Rotating Advanced-Technology Space Station for the Year 2025

5. Report Date

June 1988

6. Performing Organization Code

7. Author(s)

M. J. Queijo, A. J. Butterfield, W. F. Cuddihy, C. B. King, R. W. Stone, J. R. Wrobel, and P. A. Garn

8. Performing Organization Report No.

10. Work Unit No.

506-49-31-01

9. Performing Organization Name and Address

The Bionetics Corporation
20 Research Drive
Hampton, VA 23666

11. Contract or Grant No.

NAS1-18267

13. Type of Report and Period Covered

Contractor report
5/87-11/87

12. Sponsoring Agency Name and Address

National Aeronautics and Space Administration
Langley Research Center
Hampton, VA 23665-5225

14. Sponsoring Agency Code

15. Supplementary Notes

Langley Technical Monitor, Melvin J. Ferebee Jr.

16. Abstract

This report continues the study of an Advanced-Technology Space Station which would utilize the capabilities of subsystems projected for the time frame of the years 2000 to 2025. The particular studies include trade-offs of nuclear versus solar dynamic power systems that produce power outputs of 2.5 megawatts and analyses of the dynamics of the spacecraft of which portions are rotated for artificial gravity. The design considerations for the support of a manned Mars mission from low Earth orbit are addressed. The studies extend to on-board manufacturing, internal gas composition effects, and locomotion and material transfer under artificial gravity forces. The report concludes with an assessment of technology requirements for the Advanced-Technology Space Station.

17. Key Words (Suggested by Author(s))	18. Distribution Statement
Space Station Artificial Gravity Advanced Systems	Unclassified Unlimted Subject Categories 18 and 54

19. Security Classif. (of this report)	20. Security Classif. (of this page)	21. No. of pages	22. Price
Unclassified	Unclassified	312	A14

End of Document